12 Central Nervous System

12.1 Supratentorial Anomalies

Beth M. Kline-Fath

The central nervous system (CNS) is frequently abnormal in prenatal malformations. Up to 1 out of 100 neonates are born with a CNS anomaly.[1] CNS malformations vary from minor with little symptomatology to extremely complex causing high morbidity and mortality. Prenatal diagnosis is essential to guide counseling and direct pregnancy decisions including continuation, mode of delivery, and perinatal and postnatal care.

In this chapter, brain malformations are listed in the order of expected embryonic insult. Despite best attempts to understand the timing of insult, classification of the defect can be difficult. Occasionally, the primary event is linked to other pathologies which may make it challenging to define the embryonic stage. In addition, many structures in the brain are developing at the same time, so it is not unusual for multiple malformations to occur simultaneously, thus limiting the ability to classify an anomaly as primary. CNS disorders can also be of different severity, likely because of genetic and environmental factors. Therefore, in general, it is usually best to describe the abnormalities present individually unless the findings reflect a known syndrome. More importantly, when imaging the fetal brain, it is imperative that all anomalies, particularly extra cranial, are identified. When one organ is abnormal, often many body parts are involved. Being able to identify all anomalies may give clues to an underlying genetic syndrome, which can be significant for fetal outcome.

EMBRYOLOGY/PATHOPHYSIOLOGY

The embryology of the brain is covered in detail in normal imaging of the fetal brain. The stages of development are provided in Table 6.2-2 in Chapter 6.2. Human development is dependent on correct chromosomal complement and organization. Thus, many disorders are related to genetic disorganization. Environmental factors can have an adverse, disruptive effect on the embryo or fetus. Common teratogens include drugs, radiation, and infection, especially viruses. Maternal conditions, especially diabetes mellitus type I, often have an impact on genetic or acquired defects in the fetus. Mechanical disruptions can result from trauma, vascular, amniotic, or extraneous effects.

IMAGING TECHNIQUES

Sonography has significant advantages over other imaging. There is no radiation, images have high anatomical resolution, real-time capabilities allow dynamic assessment of the fetus, and color Doppler provides excellent interrogation of blood flow. Prenatal sonography is sensitive at detecting the vast majority of primary CNS anomalies through careful examination of the cranium and spine.[2] Ninety-seven percent of CNS anomalies can be identified on one or more of the three standard cranial views.[3] Eighty-eight percent of CNS anomalies are identified on the transventricular view by diagnosis of enlarged cerebral ventricles.[3] Evaluation of the lateral cerebral ventricles is thus very important, especially in the second trimester when head size may be normal or even decreased.[2] Inadequacies of the technique include limited soft tissue contrast and loss in cerebral detail in the near field due to reverberation artifact. In addition, fetal head position, maternal body habitus, the presence of oligohydramnios, and ossification of the fetal skull can degrade cerebral detail. Importantly, ultrasound (US) is dependent on the ability of the person to correctly display anatomy on the imaging and the skill of the reader to diagnose the abnormality.[4]

Fetal magnetic resonance imaging (MRI) is an excellent adjunct to prenatal US. It has multiple advantages, including large field of view that allows evaluation of the fetus in multiple planes and high soft tissue contrast and resolution, both of which allow depiction of the complex normal and abnormal maturation of the developing brain. Neuronal migration, gyration, sulcation, and myelination are accurately depicted. MRI does not suffer from acoustic shadowing of the fetal skull. The posterior fossa, brainstem, and corpus callosum can be easily evaluated, and injury from hemorrhage and ischemia is accurately defined. Multiple authors have demonstrated that fetal MRI is a valuable adjunct to US in the evaluation of fetal brain.[1,4–8] Levine et al found that MRI led to a change in diagnosis in 32% of cases of US detected fetal brain abnormalities, and changed counseling in 50%, and patient management in 19%.[6] MRI also increases confidence in diagnosis, thus reducing patient anxiety.[5] There are, however, limitations to the technique. Fetal MRI is not widely available and high in cost. The study is also operator dependent, and imaging can be suboptimum in the presence of significant fetal and maternal motion and claustrophobia. Imaging early in gestation can be difficult to interpret and less diagnostic because of primitive brain architecture.[6] This may have significant implications if termination of pregnancy is being considered. At this time, restricted sequences and coils are available. Higher MR imaging techniques, such as spectroscopy, functional and diffusion tractography, are more difficult as longer acquisition times are required.

Kline9781451175837-ch012.1.indd 345 08/08/14 9:58 AM

VENTRICULOMEGALY

Ventriculomegaly (VM) is a descriptive term indicating the presence of excess cerebrospinal fluid (CSF) in the ventricles of the brain. Hydrocephalus is present when there is increased CSF pressure in the ventricles, usually in association with increased head circumference. VM can be isolated (IVM) or associated with other anomalies (AVM). It is important to recognize VM because it may be an indicator or manifestation of additional significant CNS defects.

Incidence: The incidence for fetal VM ranges from 1 to 2 cases per 1,000 births.[9–11] It is the most common CNS anomaly identified by prenatal sonography.[12–14] Lateral ventricular enlargement represents the tip of the iceberg in fetal CNS imaging, as it is sensitive for the detection of a wide variety of fetal CNS abnormalities.[15] Reportedly, 70% to 85% of cases with VM have associated anomalies.[10,16–18] IVM is cited in up to 20% of cases VM with an incidence of 0.4 to 0.9 per 1,000.[10,18]

Pathogenesis: The pathophysiology underlying the dynamics of normal and abnormal CSF flow is still incompletely understood. The major portion of the CSF is produced by the choroid plexus in the lateral and to a lesser extent third and fourth ventricles.[19] Normal CSF flow is from the lateral ventricles, through the foramen of Monro into the third ventricle, and then by way of the aqueduct of Sylvius to the fourth ventricle, out the foramen of Magendie and Luschka into the subarachnoid space (see Fig. 6.2-5 in Chapter 6.2). The major pathway for CSF reabsorption postnatal is via arachnoid granulations into the blood capillaries and then the cerebral venous sinuses. Minor CSF absorption also occurs via the lymphatic system, at the level of cribriform plate and nasal submucosa, the interstitial and perivascular space and the choroid plexus which drain via capillaries to the vein of Galen.[19,20] In the immature brain, it is favored that the minor pathways are the primary route for CSF reabsorption as the arachnoid granulations are not developed prenatal.[20]

The mechanisms for development of VM are varied (Table 12.1-1). In obstructive VM, there is an imbalance between production and absorption of CSF. Noncommunicating VM does not allow communication between the ventricular system and the subarachnoid space. The lesion can occur internal to the ventricular system, as in maldevelopment of the aqueduct of Sylvius, or external to the ventricular system, such as in Chiari II malformation, or in the presence of an intraparenchymal abnormality effacing ventricle (tumor, mass). Communicating obstructive VM is rare in the fetus but occurs when there is abnormal absorption of the CSF by the cerebral venous sinuses or lymphatics.[21] In the presence of obstructive VM, in which there is increased pressure, there is potential for the ventricular dilatation to cause progressive brain injury. Nonobstructive disorders include ex vacuo dilatation, due to brain injury or dilatation due to abnormal neuronal development. Rarely, increased CSF production can occur in the presence of a choroid plexus papilloma.

The natural history of VM can be difficult to predict. Prenatal, the dilatation can resolve, stabilize, or progress. In a review of nearly 300 cases of IVM, 29% resolved, 57% stabilized, and 14% progressed.[22]

Etiology: Given the multiple mechanisms responsible for the development of VM, many etiologies are possible. Chromosomal anomalies are associated in 2% to 12% of IVM and 10% to 36% of AVM cases.[18] Intrauterine infection is noted in 2% to 5% of all VM cases.[16] Infections, mainly TORCH, are the cause of severe IVM in 10% to 20% of cases.[21] Rarely, intraventricular hemorrhage due to alloiummune thrombocytopenia is the underlying cause.

Table 12.1-1 Mechanisms for Development of Ventriculomegaly

Obstructive

Noncommunicating
- *Intrinsic—ventricular*
  - Aqueductal stenosis
  - Posterior fossa malformation
  - Posthemorrhagic obstruction
  - Postinfectious obstruction
- *Extrinsic—parenchymal or mass*
  - Tumor or arachnoid cyst
  - Hemorrhage or edema
  - Malformation (Chiari II)

Communicating
- Lack of resorption of CSF by venous sinuses

Nonobstructive

Overproduction of CSF
- Choroid plexus lesion

Malformation of cerebral development
- Holoprosencephaly
- Lissencephaly/schizencephaly
- Agenesis of corpus callosum
- Disorder of proliferation and neuronal migration
- Disorder of organogenesis
  - Genetic etiology
    - Trisomy 13, 18, 21, and many others

Destructive-ex vacuo dilatation
- Vascular
- Infection
- Ischemic

Modified from Levine D, Feldman HA, Kazam Tannus JF, et al. Frequency and cause of disagreements in diagnoses for fetuses referred for ventriculomegaly. *Radiology*. 2008;247:515–527.

Diagnosis: When VM is identified, a detailed prenatal US should be performed to exclude other anomalies. Fetal echocardiography and MRI may be helpful, especially in the verification of the diagnosis and depiction of associated anomalies. Karyotype testing and TORCH screening is highly recommended.[23] A feto-maternal alloimmune thrombocytopenia screen for anti-HPA (human platelet antigen) antibodies may be considered.[21,24]

Ultrasound: The fourth ventricle can be detected earliest on sonograms at 9 menstrual weeks, initially a large anechoic ellipsoid structure compared with the total brain.[15] After brief visibility, the fourth ventricle becomes small. The third ventricle is identified slightly later and demonstrates adult slit-like linear hypoechoic configuration, lying between the thalami.[15] The lateral ventricles are apparent at 13 to 14 menstrual weeks and change dramatically with development of the cerebral hemispheres.[15] Although the volume of the ventricles increases with gestational age (GA), the CSF spaces of the lateral ventricles become less

Kline9781451175837-ch012.1.indd 346 08/08/14 9:58 AM

conspicuous during the pregnancy. The choroid plexus can be a helpful landmark, extending from the foramen of Monro to fill the posterior horn of a normal lateral ventricle.[15]

Normal technique and measurements of the lateral ventricles are imperative to avoid false negative and positive diagnosis of VM. The atrium of the lateral ventricle is preferred as a measurable landmark since the size and configuration is essentially stable during the second and the third trimesters, in contrast to the frontal horn, which changes in configuration with gestational age.[25–27] In addition, since the trigone and occipital horn are typically the first areas to dilate in VM, this area of investigation is most important in the diagnosis.[25,26] As the wall of the atrium is perpendicular to the beam in the axial plane, it can be identified easily, and the presence of the choroid plexus aids in localization of the most lateral ventricular wall (Fig. 12.1-1).[3,25,26] VM is one of the most common false positive diagnoses at US screening.[21] Care must be taken to obtain the measurement on a true transventricular plane at the level of the glomus of the choroid.[28] Since the choroid plexus fills the ventricular atrium with only 1 to 2 mm of CSF separating the choroid from the adjacent lateral ventricular wall, the choroid can be utilized as a marker for the most distant ventricular wall.[15,26] The measurement is obtained by placing calipers in the largest part of the lateral ventricles inside the echogenic interface defining the lateral ventricular walls (Fig. 12.1-1). [15,27] Ventricle asymmetry of at least 2 mm without dilatation can be present physiologically as a normal variant.[29,30]

Measurements are subject to error because of off-axis image plane, angled measurement, or improper choice of ventricular boundary.[31] In an attempt to decrease these possible deficiencies, it has been further suggested that the axial view should be strictly assessed by demonstrating that the proximal and distal calvarial margins are equidistant, that anterior landmarks include the cavum septi pellucidi or fornix and posterior landmark, the fluid-filled V shape of the ambient cistern (Fig. 12.1-2). The measurement should be opposite the internal parieto-occipital sulcus and placed at the junction of the ventricular lumen and wall perpendicular to the inner and outer border of the ventricle.[31]

Limitations of the technique include visualization of only one lateral ventricle in the distal hemisphere because of near field artifacts. Angled views through the brain may be helpful to overcome this shortcoming.[32] In addition, it can be difficult to visualize the entire ventricle because of fetal position or calvarial ossification. If the true transverse axial plane cannot be obtained, then a coronal image at the level of the atria should be utilized for the measurement (Fig. 12.1-3).[27]

The normal mean diameter of the atrium of the lateral ventricle midgestation is 7.6 ± 0.6 mm from 14 to 38 weeks with excellent interobserver reliability.[25] The atrial width of one or both ventricles >10 mm is more than 2.5 to 4 standard deviations above the mean and is thus considered VM midgestation irrespective of gender.[12,25–27] When the ventricle enlarges, the choroid hangs in a dependent location and separates from the nondependent wall. This appearance of a "dangling choroid" will often provide clues to the presence of VM (Fig. 12.1-4).[33]

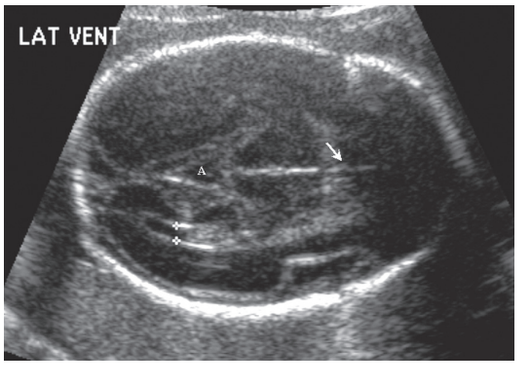

FIGURE 12.1-2: Transventricular plane with atrial measurements at the level of the cavum septi pellucidi *(arrow)* and ambient *(A)* cistern.

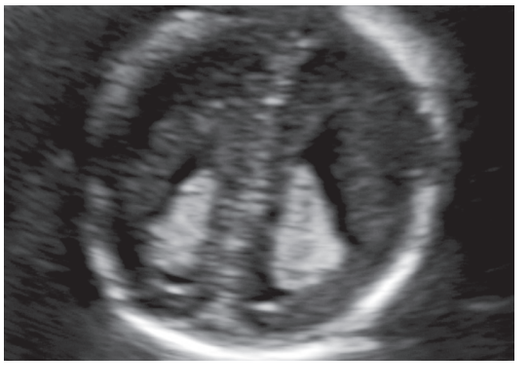

FIGURE 12.1-3: Coronal plane of both atria with echogenic choroid.

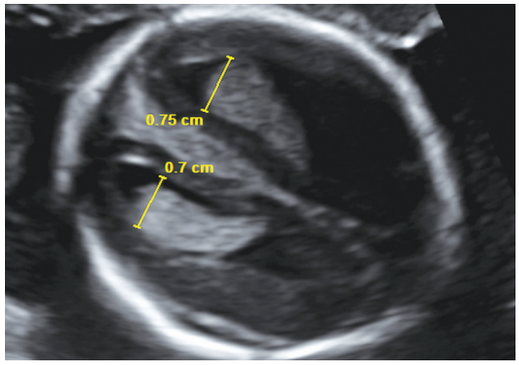

FIGURE: 12.1-1: Measurements of the atrium of the lateral ventricles. Note echogenic choroid plexus. Ventricular measurements are also obtained inside the echogenic interface.

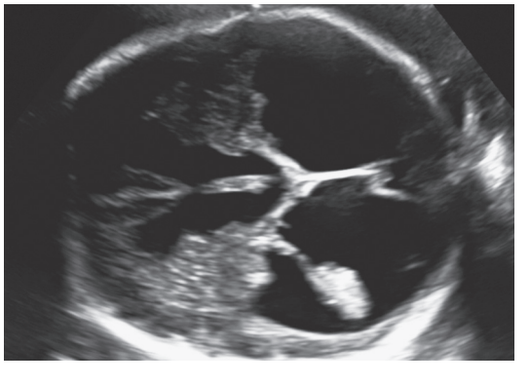

FIGURE 12.1-4: Axial transventricular view with dangling choroid in a fetus with ventriculomegaly because of aqueductal stenosis.

VM can also be diagnosed when there is choroid plexus separation from the medial ventricular wall of >3 mm.[34]

In the past, borderline or mild VM has been defined as atrial measurements of 10 to 15 mm, and severe VM when atrial width is >15 mm. Recently, VM has been further segregated such that mild represents measurements between 10 and 12 mm, moderate >12 to 15 mm, and severe >15 mm.[21,35]

Sensitivity of diagnosis is controversial. Previous studies have reported a sensitivity of 88% to 93.5% in the presence of a ventricular dilatation to or greater than 10 mm.[3,36] However, before 24 weeks, the sensitivity drops to 35%.[9] In fact, a recent study noted that only 57% of cases of severe VM were diagnosed prior to 24 weeks.[35] False positive diagnosis has been reported between 10% and 33%, with the most common disagreement being in the diagnosis of mild VM.[4,37,38] Causes for the false positive prenatal diagnosis include regression of VM during fetal life, measurement variability, and difference in criteria with regard to the presence of VM close to 10 mm.[4,21]

Although diagnosis of lateral VM is extremely important, the third and fourth ventricles should also be closely assessed as they may provide clues to the underlying diagnosis. Enlarged third and fourth ventricles are documented when the transverse dimensions are ≥3.5 and ≥4.8 mm, respectively.[10] This may be possible on routine axial imaging, but a complete neurosonographic examination should include both coronal and sagittal views through the fetal brain (Fig. 12.1-5).[39,40] A midsagittal image can be very helpful with a positive predictive value of 93%, improving detection of anomalies of the posterior fossa and corpus callosum.[41] If these planes are difficult to perform because of fetal positioning, transvaginal, and/or 3D imaging can assist with fetal anatomy.[39–41] Transvaginal imaging, especially if the head is in cephalic positioning, uses the fetal fontanelles as an acoustic window allowing visualization of both hemispheres and ventricles without artifact related to fetal skull or maternal obesity.[42]

It is very important to determine whether the VM is isolated or associated with other CNS or non-CNS anomalies. Evaluation of the morphology and borders of the lateral ventricle can provide important clues. In the presence of angular lateral ventricles, a neural tube defect should be sought (see Fig. 15.2-3C in Chapter 15.2). With a pattern of colpocephaly, agenesis of the corpus callosum (ACC) may be suggested (Fig. 12.1-20A).[43] Evaluation of the ventricular wall for increased echogenicity, thickening or irregularity should be performed to exclude hemorrhage or periventricular heterotopia. Internal ventricular debris, fluid–fluid level, or enlargement of a heterogeneous choroid plexus would indicate hemorrhage. Septation of the ventricles raise the suspicion of infection. The septum pellucidum, germinal matrix area, and cerebral parenchyma should be closely examined. Head circumference and biparietal diameter should be assessed to evaluate for volume loss versus hydrocephalus; however, early in gestation, these measurements may not be helpful. Finally, the entire fetus should be evaluated for extra-CNS anomalies. Most studies indicate that it matters little whether the associated anomaly is CNS or of another organ system in predicting an unfavorable outcome.[15] Up to 30% may develop polyhydramnios, and 33% will be breech presentation at birth.[44] Although a high-quality ultrasound is essential, even in the most experienced hands, anomalies can be difficult to detect on US with a false negative rate reported between 10% and 40%.[14,15,33]

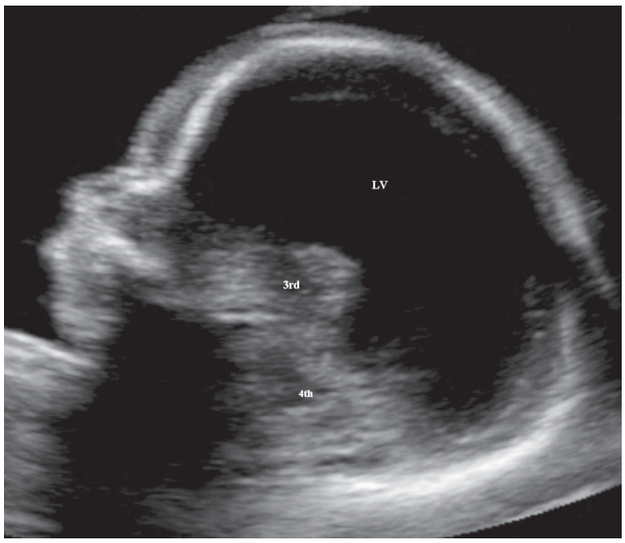

FIGURE 12.1-5: Sagittal US in a fetus with aqueductal stenosis. There is severe lateral ventriculomegaly *(LV)*. The third *(3rd)* is mildly enlarged and the fourth *(4th)* is normal.

MRI: Fetal MRI can be a helpful adjunct to US and has been shown to improve the detection of additional abnormalities in up to 50% of US diagnosed VM.[45] MRI when performed because of abnormal CNS findings on US, may change the referral diagnosis in as high as 35% of cases.[6] Aside from the technical limitations of US, some anomalies in cortical migration, hemorrhage, and parenchymal damage have been noted to be too subtle to be defined by US.[46] In addition, even when an US anomaly is confirmed on MR, many times additional anomalies are seen that are important in determining prognosis.[47] As it is important to separate cases of IVM from AVM, additional imaging with MRI may be considered.

On fetal MRI, precise measurements of the lateral, third, aqueduct of Sylvius, and fourth ventricles can be defined (see Chapter 6.2). Some authors have found that measurements of the lateral ventricles on MRI are slightly larger than on US by an average of 0.6 mm.[4] However, most conclude that there is a 90% agreement between the atrial dimensions on US when compared with MRI.[48] Rarely, measurements defined as VM on US are found to be normal on fetal MRI.[48]

With fetal MRI, many prefer measuring the lateral ventricles on a coronal plane parallel to the brainstem, including the choroid, as it is more reliable than the axial.[10] On a coronal plane, the third ventricle should be below 4 mm, and on sagittal imaging, the fourth below 7 mm.[10]

Below 24 weeks and sometimes beyond, the ventricles may demonstrate a primitive configuration in which the occipital horns are mildly disproportionate to the frontal horns (see Chapter 6.2).[49] If the ventricles are angular, a neural tube defect is almost always present (see Fig. 15.2-2C in Chapter 15.2).[43,49] Colpocephaly, marked dilatation of the posterior horn with abnormal frontal horns, should raise concern for a corpus callosum abnormality (Fig. 12.1-24C).[43,49] The ventricular wall should be evaluated for irregularity, thickening or nodularity that would suggest heterotopia. Septations would support infection. The germinal matrix should be symmetric and of appropriate size for gestational age. T1-weighted imaging and gradient echo may be helpful to confirm hemorrhage. Cystic lesions in the germinal matrix may suggest old insult. The septum pellucidum, corpus callosum, posterior fossa, and aqueduct of Sylvius should

Kline9781451175837-ch012.1.indd 348 08/08/14 9:58 AM

be closely examined. Parenchymal signal and sulcation should be correlated with gestational age. Measurements of the frontooccipital and biparietal diameter and evaluation of the subarachnoid spaces may be clues to hydrocephalus or volume loss. The entire fetus should be examined for extracranial anomalies.

Fetal MRI in the presence of VM has been shown to demonstrate a higher percentage of associated anomalies (43%) versus US (32%).[50] However, it is important to remember that migrational abnormalities may not be apparent early in gestation. MRI has been shown to be more likely to find additional anomalies at GA >25 weeks when brain development is more advanced.[48] It should also be remembered that there is often a lag in development of the sulci and gyri when a fetus has VM or other CNS abnormalities.[51]

Associated Anomalies: VM is often the tip of the iceberg, representing the first and only sign of associated multisystem fetal abnormalities.[15,25,28] Associated anomalies are present in 70% to 85% of fetuses with VM, and 60% of those malformations may be extracranial.[15,17] In AVM, the most common CNS anomalies include aqueductal stenosis (AS) (30% to 40%), Chiari II malformation (25% to 30%), dysgenesis of corpus callosum (20% to 30%), and posterior fossa defects (7% to 10%).[10,16,17] There is a clear relationship between the degree of VM and the risk of other brain abnormalities.[48] Severe VM is 10 times more likely to be associated with a brain anomaly than mild or moderate VM.[48] Those cases with borderline or mild VM have structural anomalies in 41% whereas the moderate VM group cite anomalies in 75%[35]

The overall frequency of chromosomal anomalies in the presence of VM has been quoted from 2% to 29%.[35,52] The incidence of chromosomal anomalies is strongly related to the presence of multisystem malformations.[52] In a fetus with AVM, chromosomal anomalies are higher at 25% to 36% whereas in IVM, the risk falls to 3% to 6%.[17,21,52]

Differential Diagnosis: Misinterpretation of the anechoic brain can sometimes result in incorrect atrial measurements leading to the false diagnosis of VM. A cystic lesion, such as arachnoid or dermoid cyst, or an enlarged extraaxial fluid space can be misinterpreted as VM.

Prognosis: Review of the literature suggests that fetal VM is not associated with outcome in a simple or consistent way. VM has many causes and can evolve during gestation. Therefore, counseling should always be performed with a certain degree of caution.[53] Although many studies have been performed in an attempt to improve counseling, one should review the literature carefully. There are variations in outcome and standards between many studies, and this, unfortunately, is because of small sample sizes, variable techniques in the evaluation of VM, variable ages at assessment of development, and lack of standardized methods to assess development. Therefore, prognosticators of outcome are sometimes inconsistent.

The prognosis of VM overall has been stated to be guarded with mortality of 70% to 80% and only half of surviving children developing normally.[15,54] When attempting to determine which VM cases will have a worse outcome, there is agreement in the literature that some factors can guide prognosis. The cause of VM plays an important role in the prognosis for the fetus.[17] The presence of associated intracranial and extracranial malformations decreases the likelihood of a good outcome.[17,55] There is a 56% increased morbidity and mortality in AVM versus 6% with IVM.[56] Neurologic delay in IVM ranges from 9% to 36% as compared with 84% with AVM.[22,57]

The association of chromosomal abnormality is another negative prognostic indicator.[17] In the presence of VM due to chromosomal/genetic defects, a normal outcome is present in 28% of cases with severe VM and 87% in fetus with VM between 10 and 15 mm.[21] Those cases in which VM is present with viral infection tend to have poor outcomes.[23]

Most support that the severity of the VM is another negative indicator for outcome.[16,17,58,59] In the presence of mild VM, normal outcome has been noted in 93% versus 75% in those with moderate VM and 62.5% in severe.[35] Survival greater than 24 months in fetuses with IVM is 98% when mild, 80% with moderate, and 33.3% with severe VM.[35] Most confirm progression of VM in utero as a poor prognosticator with 80% demonstrating neurodevelopmental delay.[10,16] When VM improves or resolves, 70% to 80% of fetuses have a good outcome.[21] Stable or nonprogressive IVM tends to have a favorable prognosis.[16]

Multiple debated patterns have been described. The early appearance of the VM in pregnancy is controversial but has been associated with a poor prognosis.[10,23,59] It is questioned whether unilateral VM has a better outcome than bilateral VM.[10,59] Asymmetrical VM has been most commonly described with severe VM, which tends to have a worse prognosis.[16,54,60,61] Controversial data suggest that a male fetus with VM has a better outcome than female.[10,21]

Management: Depending on gestational age at identification, management options include termination or expectant management at delivery.[62] Counseling should be directed to known findings and potential outcomes. If continuation of the pregnancy is decided, cesarean delivery is recommended for those fetuses with enlarged cranium.[62] In this case, delivery must be delayed until the fetus is mature enough to survive. Dilemma occurs in the presence of progressive hydrocephalus, as increasing ventricular dilatation can result in brain damage.[62] The current recommendation is early shunt placement after induced delivery as soon as lung maturity permits.[53]

Postnatal treatment is directed to cause. In cases of VM due to cerebral malformation or destruction, no surgical intervention is typically warranted. Neurologic consultation and directed neurodevelopmental therapy should be considered to improve outcome. In the presence of open neural tube defect or hydrocephalus, surgical intervention is often necessary. With increased intracranial pressure, ventricular peritoneal shunt is the first line of therapy.

Recurrence: Recurrence risk depends on the etiology. The overall recurrence risk for VM without associated anomalies is less than 2%.[63] In the presence of a chromosomal syndrome, the risk may increase.

MILD, MODERATE, AND UNILATERAL VENTRICULOMEGALY

In the literature, there is lack of standardization in the terms mild and borderline VM. In the past, mild or borderline VM has been described as lateral ventricular dilatation between 10 and 15 mm and a choroid lateral ventricular separation of greater than or equal to 3 mm and less than or equal to 8 mm. However, more recently, VM has been further refined into borderline or mild VM when ventricle dilatation is between 10 and 12 mm and moderate

when dilatation is noted between >12 and 15 mm. This section will utilize these new standards, and it is hoped that subsequent research will apply this methodology to homogenize terminology to allow improved counseling.

Incidence: Mild-to-moderate VM (10 to 15 mm) represents 15% to 20% of all VM and occurs bilaterally in 0.15% to 0.7% and unilaterally in 0.07% of pregnancies.[14,15,55,56,64]

Pathogenesis: Mild-to-moderate IVM is overall less well defined probably because it can be a dynamic process in utero.[22] It typically is not associated with increased intracranial pressure as most cases are nonprogressive. The head circumference is usually normal. Mild-to-moderate IVM may resolve in 41%, remain stable in 43%, and progress in 16%.[57] Progression of VM may suggest underlying disorder that can prevent normal development.[65]

Mild or borderline IVM is a diagnostic dilemma as there is research that suggests it may represent a variation of normal.[25,48] Prior US imaging studies have shown that atrial diameters above 10 mm can include fetuses that are healthy.[66] Studies have suggested that the lateral ventricles are larger in boys than in girls, with a difference of approximately 0.4 to 0.6 mm.[10,66,67] Because of the difference in gender ventricular size, 0.28% of males and 0.06% of healthy girls will have measurements equal to or above 10 mm atrial size.[66] These authors, however, still support that the 10-mm value should be maintained regardless of gender.[66–68]

Other studies have questioned the 10-mm value. Salomon et al.[12] noted that a ventricular width greater than 10 mm can be found in 1% of normal fetuses throughout gestation. In the third trimester, the mean diameter of the lateral ventricles has been found slightly larger, with upper range at 10.2 mm, representing 2 SD at term, and another study demonstrated that the 95% confidence interval exceeded 10 mm from 34 weeks to term.[26,69] Additional research has demonstrated that isolated choroid plexus separation in the presence of normal-sized ventricles is usually temporary, resolving in 70% within 4 weeks of diagnosis, with 80% to 94% normal outcome postnatal.[70] The lesion in these cases may represent an alteration in size or configuration of the choroid plexus or ventricle owing to a variation in the shape of the fetal head.[70]

In support of these findings, some studies have shown that the rate of male fetuses with ventricular size <12 mm is higher than that in the case of females and correlates with a good prognosis, probably because of inclusion of normal fetuses.[58,59,71] This type of VM also tends to be present in large for gestational age fetuses and those near term.[72] Unilateral ventriculomegaly (UVM) has also demonstrated a higher incidence in males or fetuses with birth weight of >90 percentile.[73]

UVM is uncommon and has been hypothesized to result from atresia, maldevelopment, or obstruction of the foramen of Monro by neoplasm, infection, or vascular anomaly or unilateral degenerative changes of the adjacent hemisphere.[73] UVM may also represent a normal variant when mild and nonprogressive.[64]

Etiology: Chromosomal anomalies for mild-to-moderate VM are reported between 3% and 12.6% with mean of 9%.[22] The majority of fetuses with mild-to-moderate VM and abnormal karyotype will have additional sonographic abnormalities.[22] With IVM between 10 and 15 mm, positive chromosomal anomaly is defined in 3% to 5%, and in mild IVM, aneuploidy is detected in 3%.[24,61,72] Therefore, karyotype testing is recommended.

Fetal infection is found in 1% to 5% of cases of mild-to-moderate VM.[58,74] If the VM is isolated and between 10 and 15 mm and between 10 and 12 mm, positive infection is 1.5% and 0.4%, respectively.[24,61,72] Cerebral VM is one of the more common prenatal US abnormalities in fetuses with cytomegalovirus (CMV), present in 18% of cases, half of which are isolated.[24] TORCH screen would thus also be prudent.[24]

Diagnosis

Ultrasound: When VM is identified, the opposite ventricle should be evaluated to exclude unilateral VM (Fig. 12.1-6). Detailed neurosonography with multiplanar imaging should be obtained to exclude additional anomalies.[24] Transvaginal with high-resolution probe usually results in the greatest detail. However, if this is not possible, 3D imaging should be attempted.[24] The false negative rate in detection of anomalies with IVM is equivalent to 11%.[56] IVM is a diagnosis of exclusion.

As progression is possible and 13% of anomalies are detected on sequential ultrasound, follow-up US examination is

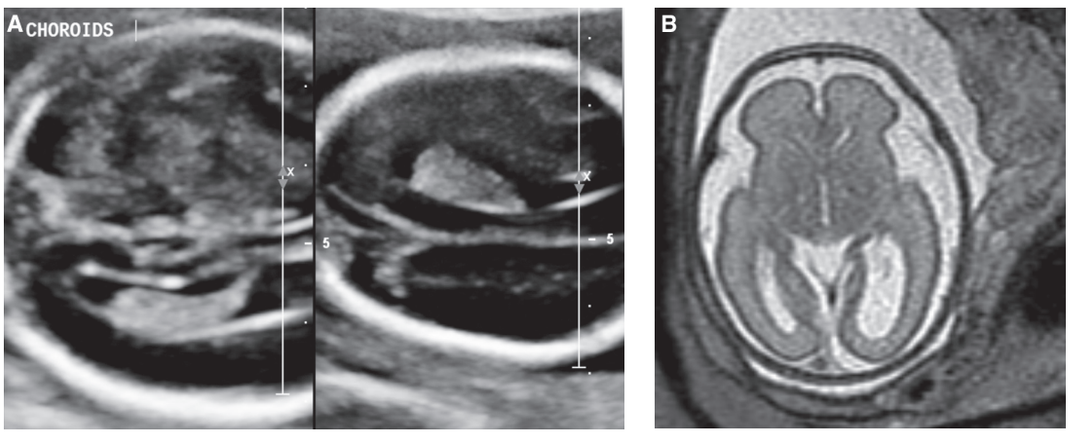

FIGURE 12.1-6: Unilateral ventriculomegaly in a fetus at 25 weeks, gestation. **A:** Axial ultrasound of both right and left ventricles demonstrating asymmetric enlargement of the left lateral ventricle. **B:** Axial SSFSE T2 image from same fetus demonstrating asymmetric ventricles without associated anomalies.

suggested.[24] At least one additional detailed US should be performed between 28 and 34 weeks to search for other cerebral and extracerebral anomalies.[24] Some advocate for monthly US to determine whether the ventricles return to normal, remain stable, or progress.[74]

MRI: Fetal MRI is helpful in cases in which US is inadequate. Many also support the modality when there is suspicion of cerebral anomaly or in the case of moderate VM or AVM (Fig. 12.1-7). In the presence of IVM, fetal MRI can improve detection in 17%.[75] This leads to an improvement in counseling, as another recent study demonstrated that fetuses with MRI confirmed IVM had normal developmental outcome in 94% of mild and 85% of moderate VM.[59]

However, the contribution of fetal MRI in cases of mild isolated VM remains controversial.[76] MRI performed in the presence of mild IVM provided information that modified obstetric management in 6% of cases and was reassuring to families in the presence of isolation.[77] Another study suggested that in fetuses with mild IVM, MRI diagnosed major cerebral anomalies in 9%.[54] However, a recent study found additional findings on MRI in 20%, but noted that the imaging only changed clinical diagnosis in 1.1% of cases, raising the question of the need for the additional test.[76] There is also no consensus on the optimal time for imaging; but most suggest that later gestation imaging, particularly after 25 weeks, will provide better detail of cortical development.

Associated Anomalies: The rate of associated anomalies in mild-to-moderate VM ranged between 10% and 76% with an average of 41%.[9,56] Those with mild VM had a lower rate of associated anomalies than those with moderate VM.

Differential Diagnosis: False positive diagnosis may occur with incorrect imaging plane, incorrect placement of calipers, and differences in measurement interpretation for the presence of VM.

Prognosis: Outcome in mild-to-moderate VM is also dependent on the presence of associated anomalies, genetic/chromosomal anomalies, or positive titers. Being able to prove that VM is isolated is therefore important for prognosis.[55,56] Moderate VM, when compared with mild VM, is more likely to demonstrate associated anomalies, 56% versus 6%.[24,56] Mild-to-moderate IVM has a reported survival of 85% with normal outcome in 85%.[54] In those with mild-to-moderate AVM, perinatal or early childhood death increased to an average of 37%.[55] Fetuses with mild-to-moderate IVM have abnormal neurologic outcome in 10% to 20%, while those with AVM are abnormal in up to 40% to 50%.[1,56]

The degree of VM is also an important prognosticator, with neurodevelopmental delay being an average of 14% to 17% when the IVM is moderate versus 3% to 11.8% when mild.[9] Therefore, fetuses with mild IVM approach the general population in which neurodevelopmental delay has been noted in 2.5%.[24,56] These numbers have also been supported by a recent study that utilized fetal MRI, in which mild IVM had 94% excellent outcome and those with moderate IVM had 85% good outcome.[59] It is also interesting that fetuses with mild IVM have higher rates of stable or even regressive diameters of the ventricular system, with 90% of cases resolving, decreasing, or stable, but less than 10% increasing over the course of pregnancy.[55]

The overall risk of neurologic sequelae in stable VM is significantly lower than in progressive VM.[54–56,61] Sixteen percent of fetuses with mild to moderate VM have progression, and the neurodevelopmental outcome is worse, 44% versus 7% without progression.[24] There is also a higher incidence of chromosomal anomalies in progressive VM, 22% compared to 1% without progression.[24] Cases of mild to moderate IVM that resolve before birth tend to have a normal outcome.[15]

Because males have a more generous ventricular size, mild IVM is more commonly depicted in males.[56] In support of normal larger ventricles in males, some have found that the risk for abnormal outcome in male fetuses with IVM and normal karyoptype is 5% versus 23% for female.[55,56,72] However, several studies have demonstrated that there is no difference in outcome when comparing male and female fetuses.[24,59] Signorelli et al.[78] have shown that all cases of mild VM had a normal outcome up to 10 years after birth. Therefore, many believe that mild IVM may be a variation of normal.[72,78,79]

There is a controversy in the literature as to whether UVM has a better prognosis than bilateral.[59,72] It is most important to understand that UVM follows the same rules as bilateral in determining outcome. Although many believe UVM tends to be

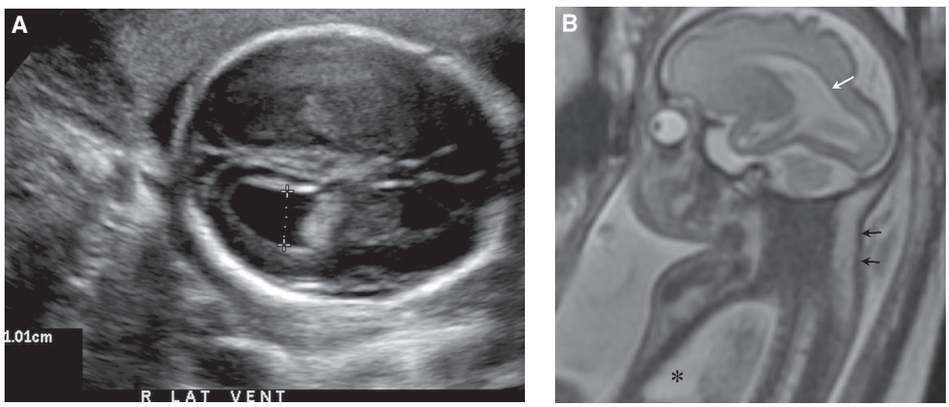

FIGURE 12.1-7: Fetus with trisomy 21 at 29 weeks. **A:** Axial ultrasound demonstrating mild VM. **B:** Sagittal T2 MR of the same fetus demonstrating mild lateral ventriculomegaly *(white arrow),* but also moderate pleural effusion *(asterisk)* and nuchal thickening *(black arrows)*. Imaging was performed to assess lung compression and exclude mediastinal mass.

benign as it is less likely to have a clinically significant associated anomaly, there is still a 3% risk for chromosomal aberration, with risk for developmental delay ranging from 6% to 15%.[30,55] In a review of 366 cases, 97% had normal development with unilateral VM versus 90% with mild bilateral IVM.[54] Another study reported developmental delay in mild bilateral IVM and unilateral as being very similar at 6% and 7.4%, respectively.[24] Good neurologic outcome has been noted in UVM when it is isolated without genetic disorder or infectious etiology.[10,80] The prognosis is also excellent in the presence of dilatation that is nonprogressive and less than 12 mm.[55,79]

Finally, sometimes although the diagnosis of IVM is made, the VM is in fact not really isolated.[24] Current evidence suggests that even with prenatal workup and fetal MRI, additional anomalies can be discovered at birth, including white matter signal abnormalities, which may not be detected until after birth, some of which were not visible on MRI until 1 year of age.[59] Recent data have shown that prenatal VM is associated with postnatal VM.[81] Neonates with prenatal mild VM have higher cortical volume and reduced white matter volume, suggesting altered cortical development and either delayed or abnormal white matter development.[81] Bloom found a significant linear relationship between ventricle width and decreased mental development index.[82] In recent studies, fetuses with mild VM and postnatal neurologic follow-up showed abnormal, mostly motor disabilities in 12% to 28% of cases and intellective retardation in 5%.[24,83] In addition, studies have demonstrated that up to one-third of cases of moderate IVM have additional findings detected later in pregnancy or postnatally that had a negative impact on neurologic outcome.[66] Therefore, IVM may not be normal, and the physiologic development of the brain should be taken into account.

Management: Counseling should be performed after all testing has been obtained with knowledge of associated anomalies, genetic abnormalities, and positive infection titers. In the presence of IVM, the counseling can still be difficult. A physician should advise the family that nonprogressive IVM can be confidently diagnosed only after birth. And, although some children appear normal at birth, a 10-point deficit when compared with normal controls can be documented.[82] There is also limited developmental follow-up of children with prenatal diagnosis of IVM beyond 30 months to guide counseling for long-term outcome.[61]

Most cases of isolated mild VM can be delivered vaginally. Postnatal management includes confirming the diagnosis and checking for associated disorders that were undetected prenatally. Long-term postnatal follow-up may be helpful.[24] Follow-up should continue until development is established as normal. If delay occurs, neurologic consultation and therapeutic intervention should be considered as this can improve outcome.[73] MRI, especially after 1 year of life, may be helpful to evaluate for white matter lesions.[59,81]

Recurrence: Recurrence is rare in isolation but is dependent on the cause and the presence of a genetic or chromosomal aberration.

AQUEDUCTAL STENOSIS/ SEVERE VENTRICULOMEGALY

Incidence: The overall incidence of aqueductal stenosis (AS) is 0.5 to 1 per 1,000 births.[84] After Chiari malformation, AS is the second most common cause for fetal VM, accounting for 20% to 40% of cases.[17] X-linked hydrocephalus is the most common hereditary hydrocephalus with an incidence of 1 in 30,000, accounting for 2% to 25% of primary idiopathic hydrocephalus in newborn males.[84–86]

Pathogenesis: There is evidence that suggests AS may develop because of early fetal hydrocephalus. In the presence of massive lateral ventricular enlargement, the midbrain may be compressed laterally, resulting in aqueductal narrowing.[87] Others suggest that the aqueduct may inherently become narrowed, particularly at the superior colliculus or intercollicular sulcus. In some cases, the aqueduct can be "forked," with branching dorsal and ventral channels.[17] Less commonly, a web can develop along the most inferior recess of the aqueduct. Acquired AS has many etiologies, including infection, bleeding, or other pathologies that cause gliosis and then obliterate the aqueduct.[17]

Recent research has found that rhombencephalosynapsis (RES), which is fusion of the cerebellar hemispheres in conjunction with absence of the cerebellar vermis, is identified in 9% of patients with AS.[88] In those patients with RES, up to 50% of cases have associated AS.[88] The anomaly may be related to a defect in dorsal midline signaling leading to malformation of the brainstem and cerebellum.[88] The correlation makes sense as both the aqueduct and the vermis originate from the mesencephalon.

In the presence of AS, increased CSF pressure occurs consistent with hydrocephalus. When hydrocephalus develops, there is pressure on the developing brain from the ventricular system, but there is also uterine amniotic pressure restraining the expansion of the overlying skull.[11] This increased pressure causes alteration in neuronal proliferation, migration, and delayed maturation.[89] With pressure in the ventricles, there is flattening of the ependyma and interruption of the CSF–brain barrier with ependymal rupture, edema in the periventricular white matter, and axonal swelling. In the late phase, destruction of nerve fibers, demyelinization, gliosis, and volume loss in the white matter and corpus callosum occur.[62]

Etiology: A multifactorial pattern of inheritance or postinflammatory insult is probably likely in most cases. Increased risk of congenital hydrocephalus has been described in males, primogeniture, older maternal age, maternal insulin-dependent diabetes, maternal alcohol abuse, and lower social class of the father.[58,84,90]

In 5% of all cases, an X-linked transmission, known as Bickers–Adams syndrome may be the etiology. This genetic disorder, which is also known as X-linked hydrocephalus and hereditary stenosis of the aqueduct of Sylvius (HSAS), is related to mutation of the *L1CAM* gene on chromosome Xq28.[86] The gene encodes a neural cell adhesion molecule L1, which is involved in neuronal migration, fasciculation, outgrowth, and regeneration. L1 is essential to the formation of the pyramids and corticospinal tracts. Because many diseases have been associated with this gene mutation, the syndrome is now known as CRASH, representing *c*orpus callosum hypoplasia, *r*etardation, *a*dducted thumbs, *s*pastic paraplegia, and *h*ydrocephalus.[86] The mutation primarily affects males, but females are carriers, and there is a 5% risk for a female to develop mild manifestations of the disorder.[44] In X-linked AS, the aqueduct is stenosed in only 40% of cases, and thus some suggest that the aqueduct is narrowed by lateral ventricular compression rather than primary maldevelopment.[85,91]

Kline9781451175837-ch012.1.indd 352 08/08/14 9:58 AM

Diagnosis: In the presence of severe VM, it is important to perform karyotype and infectious testing for TORCH. If X-linked AS is suspected, screening should be performed for *L1CAM* gene mutations, as the detection rate can be as high as 93%.[15,86]

Ultrasound: There is often moderate to severe lateral VM and typically a mild-to-moderately dilated third ventricle with disruption of the septum pellucidum (Fig. 12.1-8A,B). Measurements are usually not necessary to define the lateral VM, but can be useful to monitor the progression of ventricular dilatation. The aqueduct of Sylvius obstruction is typically difficult to identify via US. The fourth ventricle should be normal in size. At 18 to 20 weeks, the subarachnoid spaces are large, and with increasing gestation, there is progressive decrease in their size. In the presence of severe VM, the supratentorial parenchyma may be compressed between the skull and the dilated ventricles (Fig. 12.1-9A). With increasing ventricular dilatation, disruption of the cortical mantle can occur due to damage from the intraventricular pressure.[11] Evaluation of the brain and extracranial structures is essential to exclude other anomalies. A search of the hands for adducted thumbs may support X-linked AS.

MRI: On fetal MRI, the aqueduct of Sylvius is well depicted. With obstruction to CSF flow, there can be complete or partial obliteration of the CSF space in the aqueduct (Fig. 12.1-8C,D).[90] The tectum may be deformed or thickened (Fig. 12.1-9B). The lateral and third ventricles are dilated. Ventricular disruption is sometimes depicted in the posterior mesial aspects of the brain, the location of the choroidal fissure and weakest part of the ventricular wall (Fig. 12.1-9C).[87] This results in a focal ventricular diverticulum and thinning of the adjacent brain parenchymal mantle. Most disruptions are lined with white matter and are thus not consistent with schizencephaly. The septum pellucidum can be partially or completely absent. Although MRI can visualize the corpus callosum, in the presence of severe VM, it is often displaced, severely stretched, or partially absent (Fig. 12.1-8C). The subarachnoid spaces may be normal or absent depending on gestational age, and sulcation is typically delayed. The posterior fossa may be small owing to mass effect.

Other anomalies, such as RES or Z-shaped brainstem in the presence of congenital muscular dystrophy, are seen in association with AS (Fig. 12.1-8).[88] In the presence of X-lined AS, corpus callosum agenesis, absent septum pellucidum, fusion of

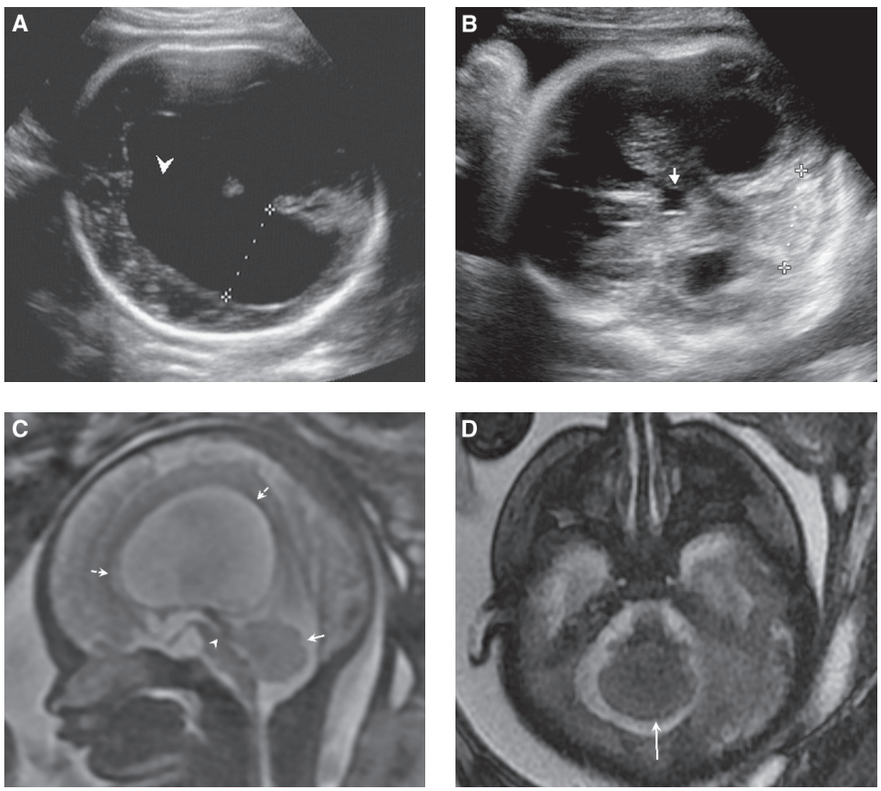

FIGURE 12.1-8: Fetus at 36 weeks with aqueductal stenosis and rhomboencephalosynapsis. **A:** Axial US demonstrates severe ventriculomegaly with atrium measuring 34 mm and septum pellucidum absent *(arrowhead)*. **B:** Axial US demonstrating dilated third ventricle *(arrow)*. The cerebellum measured small, appropriate for a 28-week fetus. Notice the continuous foliation of the superior cerebellum. **C:** Sagittal SSFSE T2 image demonstrates obstruction of the aqueduct of Sylvius distally *(arrowhead)*. Notice that the vermis does not appear normal as the deepest fissure is the horizontal fissure *(solid arrow)*, typical for the cerebellar hemispheres. The corpus callosum is thin *(dashed arrows)* due to the hydrocephalus. **D:** Axial SSFP image confirms absence of cerebellar vermis with continuous foliation across midline (*arrow*) consistent with fusion of the cerebellar hemispheres in rhomboencephalosynapsis.

FIGURE 12.1-9: Fetus at 34 weeks with AS secondary to TORCH. **A:** Axial US demonstrates severely dilated ventricles and subtle suggestion of brain parenchyma *(arrows)* compressed along the calvarium. It would be difficult to exclude hydranencephaly. **B:** Axial SSFSE T2 image demonstrates heart-shaped midbrain and deformity of tectum *(arrow)*, typical of AS. **C:** Coronal SSFSE T2 image demonstrates ventricular rupture of the left lateral ventricle with destruction of adjacent brain parenchyma *(solid arrow)*. The ventricular wall is ballooned on the right with thinning of the adjacent brain *(dotted arrow)*. The sulcation is significantly delayed for age of 34 weeks.

thalami, small brainstem, hypoplasia of the corticospinal tracts, and absence of the pyramidal tract may be present.[85,86] Fifty percent of fetuses with X-lined AS demonstrate adduction of the thumbs.[44]

Associated Anomalies: Associated abnormalities have been diagnosed in approximately 60% to 65% of severe VM.[14,45,92] Chromosomal anomalies are reported to be as high as 15%.[9] The rate of associated infection in severe VM is 10% to 20%.[14]

In a study directed at AS, 60-87% of the cases were associated with a genetic syndrome, chromosomal anomaly or maternal exposure.[90] Chromosomal abnormalities were detected in 8%. The most common genetic syndromes were Walker–Warburg, VATER, and Peter Plus.[90] RES was a common associated anomaly. Environmental exposures, including insulin-dependent maternal diabetes, fetal alcohol and TORCH, were present in 16%.[90]

Differential Diagnosis: Severe VM can be seen in association with other known anomalies, such as holoprosencephaly (HPE), hydranencephaly, agenesis of the corpus callosum, Chiari II, or other posterior fossa malformations.

Prognosis: Outcome in fetuses with AS is guarded. Overall mortality is 40%, perinatal mortality of 23% and of those that survive only 10% have normal development.[90,93] Normal development in severe AS with associated anomalies is only 5% but increases to 50% when isolated[90]. Although IVM in AS carries the least severe prognosis, it is not common, accounting for only 10% of cases.[90] Those patients with X-linked hydrocephalus have variable clinical symptomatology.[94] Some die in utero or early infancy. If a child with X-linked AS survives, severe mental retardation and spastic diplegia can occur; however, some live into adulthood.[44,94]

A recent study of nonspecific severe IVM showed major morbidity in 50%, minor in 40%, and normal outcome in 10%.[95] Prognosis has been shown to depend on age at diagnosis as progressive increased intracranial pressure can result in further insult to the brain.[91,95] The presence of additional anomalies, karyotype abnormality, and in utero progression result in a negative outcome.[91] When additional anomalies were present, only 23.5% survived and only 15% of the survivors were normal, with the majority having cerebral palsy, seizures, and impaired motor capabilities.[16,17]

Management: In the presence of AS or severe VM, termination may be considered, depending on severity of dilatation and presence of associated anomalies. As it is known that progressive injury can occur to the brain throughout the gestational period, in the past, decompression of the ventricular system was attempted by performing cephalocentesis and/or the placement of in-utero shunts.[62,96] However, the ventriculo-amniotic shunts, due to high pressure in the amniotic cavity, sometimes did not allow drainage of fetal CSF and often the catheters migrated or obstructed.[88] The main problem, more importantly, became overall case selection as many of these fetuses had associated anomalies. Because of controversial results and the lack of the ability to define a group of fetuses that would benefit, the procedure was mostly abandoned in 1986.[96] With improved understanding of the natural history of the disease in utero and improved shunt technology, revisitation of the intervention may be entertained.[62]

In the past when the prognosis was poor, cephalocentesis with 90% rate of perinatal death or vaginal delivery with fetal sacrifice was performed.[95] However, this has been virtually abandoned in the United States. Most fetuses with enlarged cranium require delivery by C-section. Postnatally, most infants require ventricular shunting.

Recurrence: The recurrence risk for sporadic cases in subsequent siblings is 0.5% to 4%.[77] However, in the presence of X-linked AS, the risk of recurrence is 50% in a male fetus and in the case of a girl, 50% risk for carrier with low (<5%) risk for manifesting clinical features.[28,44]

DISORDERS OF VENTRAL INDUCTION

Holoprosencephaly

Holoprosencephaly is a group of complex congenital malformations of the brain and face in which there is impaired or incomplete cleavage of the prosencephalon.

Incidence: HPE is considered the most frequent CNS defect in humans, occurring at a prevalence of 1:250 conceptions.[97] However, as only 3% of fetuses with HPE survive to delivery, the incidence decreases to 1 in 10,000 to 20,000 live newborns.[97] There is a female preponderance, being 3:1 in the alobar type.[97,98]

Pathogenesis: HPE occurs due to failed diverticulation of the embryonic prosencephalon in the first 4 weeks of embryogenesis. The primary disorder results from failure of migration of the prechordal mesoderm, which is responsible for induction of ventral forebrain, nasofrontal process, and median facial structures.[99] HPE represents a defect in dorsoventral patterning, beginning in the area of the hypothalamus but contiguous along cortex, striatum, midline ventricles, thalamus, and mesencephalon.[100]

HPE is subdivided based on site and degree of failed cleavage; however, no precise boundaries are present and intermediate cases may occur.[101,102] Classically, DeMyer divided HPE into three subcategories from severe to mild including alobar, semilobar, and lobar; however, a milder form known as middle interhemispheric fusion has recently been described (Fig. 12.1-10).[100] Of the three classic forms, alobar is the most frequent type, occurring between 40% and 75% of cases, with semilobar second, followed by lobar.[97]

In classic HPE, the ventral forebrain or embryonic floor plate, in the region of the hypothalamus and subcallosal cortex, is most severely affected. Common possible associated midline anomalies include undivided hypothalamus and thalami, undivided deep gray structures, absent or dysgenetic corpus callosum, absent septum pellucidum, and absent or hypoplastic olfactory bulbs and tracts, and optic bulbs and tracts (Table 12.1-2).

In *alobar* HPE, there is a single midline forebrain ventricle and cerebral holosphere with absent midline structures and thalamic fusion. The monoventricle is continuous with a cyst, hypothesized to represent remnant third ventricle, velum interpositum, or primitive prosencephalic vesicle, demarcated from the ventricular cavity by ridge of cerebral tissue representing hippocampal fornix.[103,104] In *semilobar*, the defect is localized anteriorly with some posterior interhemispheric fissure, rudimentary lateral ventricles but absent frontal horns, partial fusion of thalami, and variable corpus callosum, usually splenium. The *lobar* type has noncleavage of the frontal basal lobes and separation of most of the cerebral hemisphere, rudimentary frontal horns, and absent anterior corpus callosum. A mild variation of the lobar type with fusion of the septal and preoptic area has been termed *septopreoptic HPE*. In the *middle interhemispheric variant (MIH) or syntelencephaly*, there is a defect of the dorsal mesenchyme or the roof plate resulting in failure of separation of the posterior frontal and parietal lobes with the poles of the frontal and occipital well separated.[105,106] The genu and splenium of the corpus callosum are present, but the body is poorly defined. Classification is not well defined in less severe ends of the phenotypic spectrum which include absent olfactory tracts and bulbs (arrhinencephaly) and hypopituitarism.[107] In addition, with recent molecular data, it has been found that the HPE phenotypic spectrum is very large, including a "microform" variety, encompassing facial malformation but normal brain.[107]

HPE is associated with a number of midline anomalies of the face (Table 12.1-3).[108–110] There is an 80% correlation with the severity of the HPE and the extent of the facial malformation; thus in these cases, the "face may predict the brain."[107,111] However, in 10% to 20% of cases, there is no clear correlation between face and brain anomaly subtypes.[97]

Etiology: Genetic, environmental, multifactorial, and unknown causes appear to be involved in the development of HPE (Table 12.1-4).[97] Chromosomal anomalies account for 25% to 50% of HPE cases.[108,112] The most common association is trisomy 13, representing 75% of cases, followed by triploidy at 20% and trisomy 18 at 1% to 2%.[113] The incidence of chromosomal abnormalities is strongly related to the presence of multisystem anomalies.[114] About 18% to 25% of HPE are syndromic with a single gene mutation.[102,111]

The nonsyndromic or isolated HPE can be inherited autosomal dominant, autosomal recessive, and X-linked inheritance.[113] In the cases with normal karyotype, genetic mutations

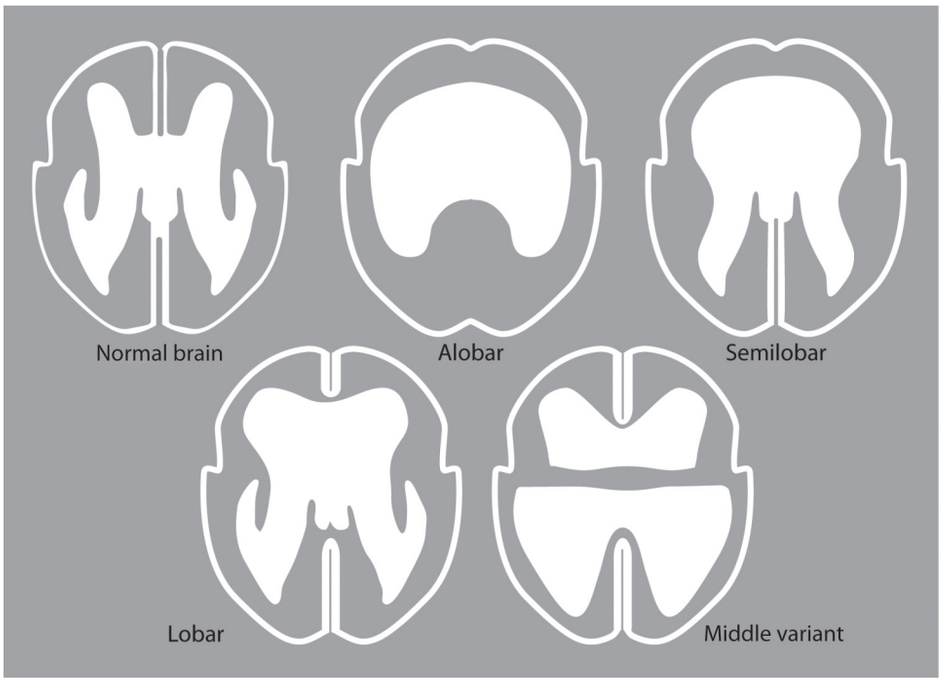

FIGURE 12.1-10: Diagram of the four major types of holoprosencephaly. (Modified from Volpe P, Campobasso G, De Robertis V, Rembouskos G. Disorders of prosencephalic development. Prenatal Diagnosis 2009;29:340-354.)

Table 12.1-2 Findings in HPE

Types	Alobar	Semilobar	Lobar	MHF	Septopreoptic
IHF/falx absent	All	Anterior	Hypoplastic anterior	Midportion	Deep
Cerebral nonseparation	All	Frontal	Basal frontal/ cingulate	Posterior frontal/ anterior parietal	Preoptic/ subcallosal
Lateral ventricles	Single	Absent anterior	Rudimentary anterior	Fused mid lateral	N/small
		Rudimentary occipital	Normal posterior	N/hypoplastic anterior	frontal
Dorsal cyst	Yes	Variable	Rare	Present 25%	No
Third ventricle	Absent	Small	Present	Present	N
Septum pellucidum	Absent	Absent	Absent/hypoplastic	Absent/hypoplastic	N/hypoplastic/ absent
Thalami	Fused	Partial fusion	Divided	Fused 30%–50%	N
Deep gray	Fused	Partial/caudate	Variable	Caudate fused	N
Corpus callosum absent	All	Rostrum, genu, body	Rostrum, genu	Body	Rostrum/genu
Hypothalamus	Fused	Often fused	Likely fused	Separated	Anterior fused
Hippocampal fornix	Fused	Often fused	Fused	Separated	N
Olfactory bulbs and neurohypophysis	Absent	Absent/hypoplastic	Absent/hypoplastic/N	N	N
Optic tracts	N/fused/absent	Absent/hypoplastic	Present	Present	N
Slyvian fissures	Absent	Anterior medial	Anterior medial	Connected over midline	N
Cortical dysplasia/ Heterotopia	Broad gyri	Occasional broad gyri	Rare midline/ frontal	Very common	N
Cerebral vasculature	No ACA MCA Rete vessels	Azygous ACA	Azygous ACA	Azygous ACA	N/azygous ACA
Craniofacial	Severe/mild	Severe/mild	Mild	Hypertelorism	Mild

Modified from Hahn JS, Plawner LL. Evaluation and management of children with holoprosencephaly. *Pediatr Neurol*. 2004;31:79–88. N, normal; ACA, anterior cerebral artery; MCA, middle cerebral artery

Table 12.1-3 Facial Anomalies in Association with HPE

Facial Defect	Features/Associations	Brain HPE
Cyclopia	Single eye, arhinia, possible proboscis	Alobar
Synophthamia	Partially fused eyes in single eye fissure	Alobar
An or micoophthamia	Absent or small eye	Alobar or semilobar
Ahrinia	Absent nose	Alobar or semilobar
Ethmocephaly	Hypotelorism proboscis between eyes	Alobar or semilobar
Cebocephaly	Hypotelorism, single nostril	Alobar or semilobar
Median cleft lip/palate (premaxillary agenesis)	Hypotelorism, flat nose	Alobar or semilobar
Bilateral cleft lip	Philtrum-premaxillary anlage	Alobar/semilobar/lobar
Hypotelorism		All types/microform
Hypertelorism		All types/microform
Eye abnormalities	Iris or retinal coloboma	All types/microform
Flat nose		All types/microform
Mild palate	Lateral cleft, high arch, bifid uvula	All types/microform
Single central incisor	Hypoplasia piriform aperture	All types/microform

Modified from Dubourg C, Bendavid C, Pasquier L, et al. Holoprosencephaly. *Orphanet J Rare Dis*. 2007;2:1–14.

Kline9781451175837-ch012.1.indd 356 08/08/14 9:58 AM

Table 12.1-4 Causes and Conditions Associated with HPE

Chromosomal
- Trisomy 13
- Trisomy 18
- Triploidy
- Other genetic mutations
  - Deletions, duplications, partial monosomy 14q, unbalanced aberrations

Syndromic-monogenetic
- Autosomal dominant
  - Dysgnathia complex
  - Pallister–Hall
  - Kallmann
  - Rubinstein–Taybi
  - Steinfeld
  - Martin
  - Thanatophoric dysplasia type II
- Autosomal recessive
  - Spinocerebellar ataxia
  - Ivemark (heterotaxy)
  - Lambotte
  - Meckel
  - Genoa
  - Hydrolethalus
  - Pseudotrisomy 13
  - Smith–Lemli–Opitz
  - XK aprosencephaly
- X-linked
  - Aicardi
  - Ectrodactyly
  - Fetal hypokinesia/akinesia

Nonsyndromic
- Familial
  - Inherited autosomal dominant
  - Gene mutations, such as *SHH* or *ZIC2*

Environmental
- Retinoic acid
- Ethyl alcohol
- Salicylates
- Estrogen/progestin
- Anticonvulsants
- CMV
- Rubella
- Toxoplasma
- Maternal diabetes
- Maternal hypocholesterolemia

Modified from Simon EM, Barkovich AJ. Holoprosencephaly: new concepts. *Magn Reson Imaging Clin N Am*. 2001;9:149–164.

have been identified in 15% to 20% cases.[102] To date, more than 13 genes and mutations thereof have been shown to cause HPE.[113] The four main genes involved in HPE include *SHH*, *ZIC2*, *SIX3*, and *TGIF*. Many of the genes in HPE are linked to sonic hedgehop (*SHH*) signal networks. *SHH* protein appears to be a developmental regulator of the ventral neural tube and thus important for induction and differentiation. The second most common HPE gene is *ZIC2*, which is associated with variable CNS malformations, including MIH and mild facial anomalies.[107,109] This gene may have a role in editing the response to *SHH* protein signaling but affects the roof plate and dorsal brain structures.[109]

About 10% of individuals with HPE have defects in cholesterol biosynthesis, as cholesterol is required for activation of the *SHH* molecule.[102,112] Environmental factors, most commonly infection (especially cytomegalovirus) and maternal diabetes, are reported in HPE.[108] Infants of diabetic mothers have a 1% risk (200-fold increase) for HPE.[112] Despite these known associations, 70% of HPE have no known molecular basis, and therefore a "multiple hit" from both environment and genetics is likely.[101]

Diagnosis: When HPE is identified, karyotyping should always be performed. If karyotype is normal, genetic counseling with molecular testing may be considered. Prenatal history, detailed family history, and focused examination of the parents may help identify microforms of HPE.[102,112] A search for additional anomalies with US, MRI, and echocardiogram should be considered.

Ultrasound: Tranabdominal or transvaginal US can confirm severe HPE as early as 10 weeks.[101,103,115] Coronal and axial imaging of the brain should be performed to verify fusion of hemispheres and thalami and lack of interhemispheric fissure. A helpful marker of alobar HPE is the featuresless configuration of the monoventicle and dorsal cyst lacking occipital, temporal, and frontal horns (Fig. 12.1-11).[103] The choroid is prominent at this age, and absence of the normal choroidal "butterfly" configuration may also be a helpful clue[116]

In *alobar HPE*, the cortex of the prosencephalon is displaced rostrally and assumes the shape of a pankcake with the posterior aspect appearing as a horseshoe (Fig. 12.1-12A). When the dorsal cyst is small, the holophere may have a cup- or ball-like appearance.[117] There is complete absence of midline structures and fusion of deep basal ganglia and thalami. If there is absent cleavage of anterior hemisphere with single anterior ventricle, cleavage of the posterior hemispheres with rudimentary occipital horns, partial falx, and incomplete fusion of the thalami, the diagnosis of *semilobar HPE* should be considered (Fig. 12.1-13A,B).[103,118]

Milder degrees of HPE, including *lobar* or *MIH HPE,* are more difficult to detect and differentiate from other anomalies by US.[112,119] In lobar HPE, a midcoronal US image demonstrates

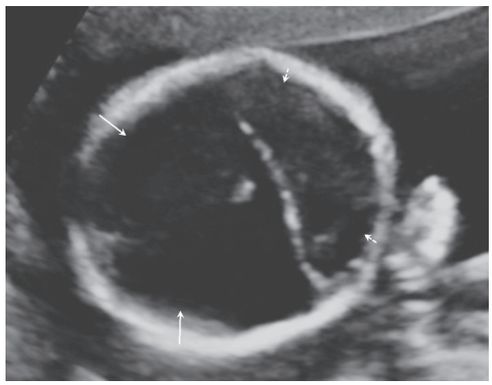

FIGURE 12.1-11: Axial US demonstrating large monoventricle *(long arrows)* and pancake mantle of fused brain anteriorly *(short arrows)* in a fetus with alobar HPE.

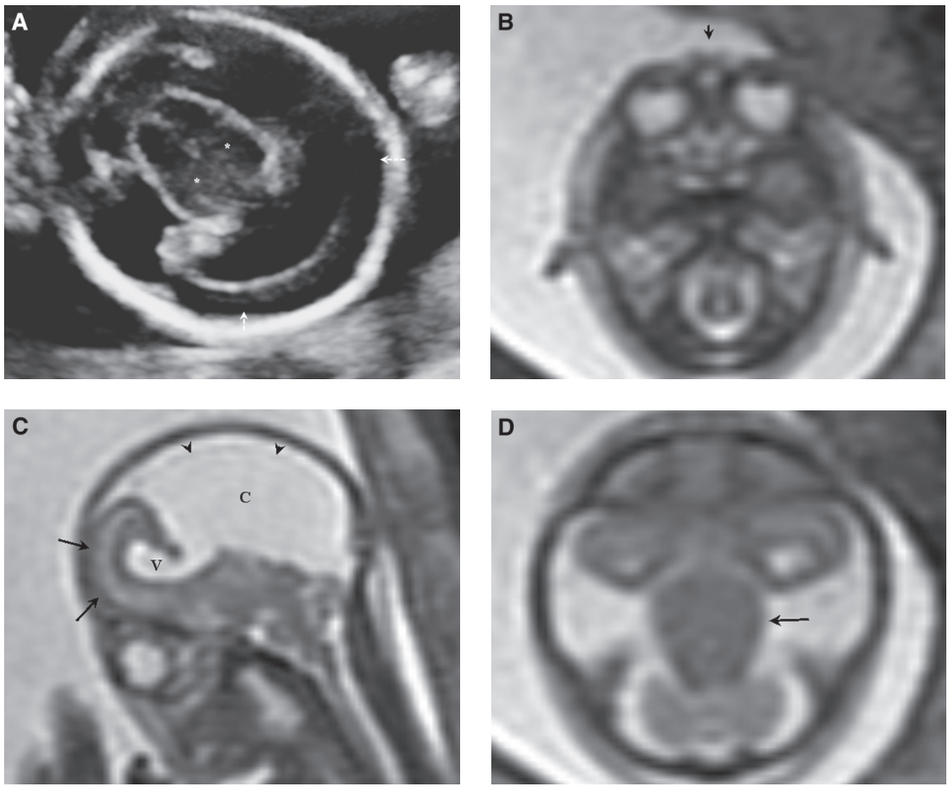

FIGURE 12.1-12: Fetus at 21 weeks with alobar HPE. **A:** Axial US demonstrates distorted choroid plexus and cuplike brain *(arrows)*. The thalami *(asterisks)* are fused. **B:** Axial T2 MR image demonstrates hypotelorism and single nostril *(arrow)*. **C:** Sagittal MR image demonstrates cuplike fused cerebral mantle *(arrows)* and monoventricle *(V)* contiguous with dorsal cyst *(C)*. *Arrowheads* denote wall of the cyst. **D:** Axial image demonstrates fused mass of deep gray nuclei, thalami, and midbrain *(arrow)*.

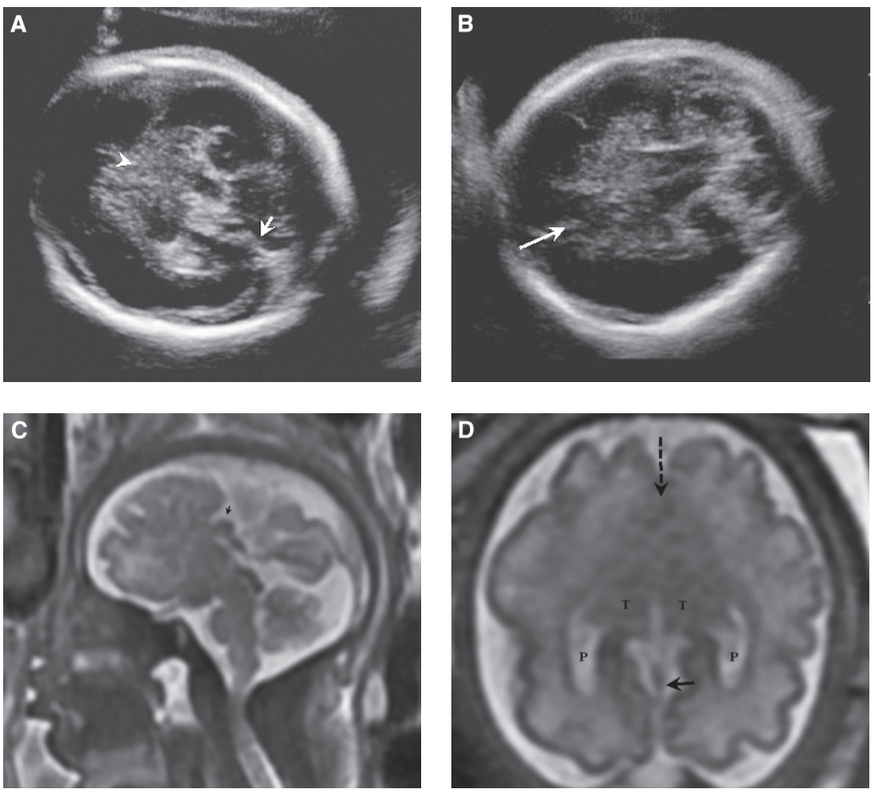

FIGURE 12.1-13: Fetus at 34 weeks with semilobar HPE. **A:** Axial image demonstrates falx posteriorly *(arrow)*. There is poor separation of the brain tissue anteriorly *(arrowhead)*. **B:** More inferior axial image verifies fusion of the anterior hemisphere *(arrow)* and partial fusion of thalami. **C:** Sagittal MR image demonstrates fused cerebral hemispheres anterior and small splenium of the corpus callosum *(arrow)*. **D:** Axial T2 image demonstrates separation of hemispheres posteriorly *(arrow)*. The posterior *(P)* horns of the lateral ventricles are normal but frontal horns and septum pellucidum absent owing to fusion of the anterior hemispheres across midline *(dotted arrow)*. The thalami *(T)* are partially fused, and there is fusion of the deep gray nuclei.

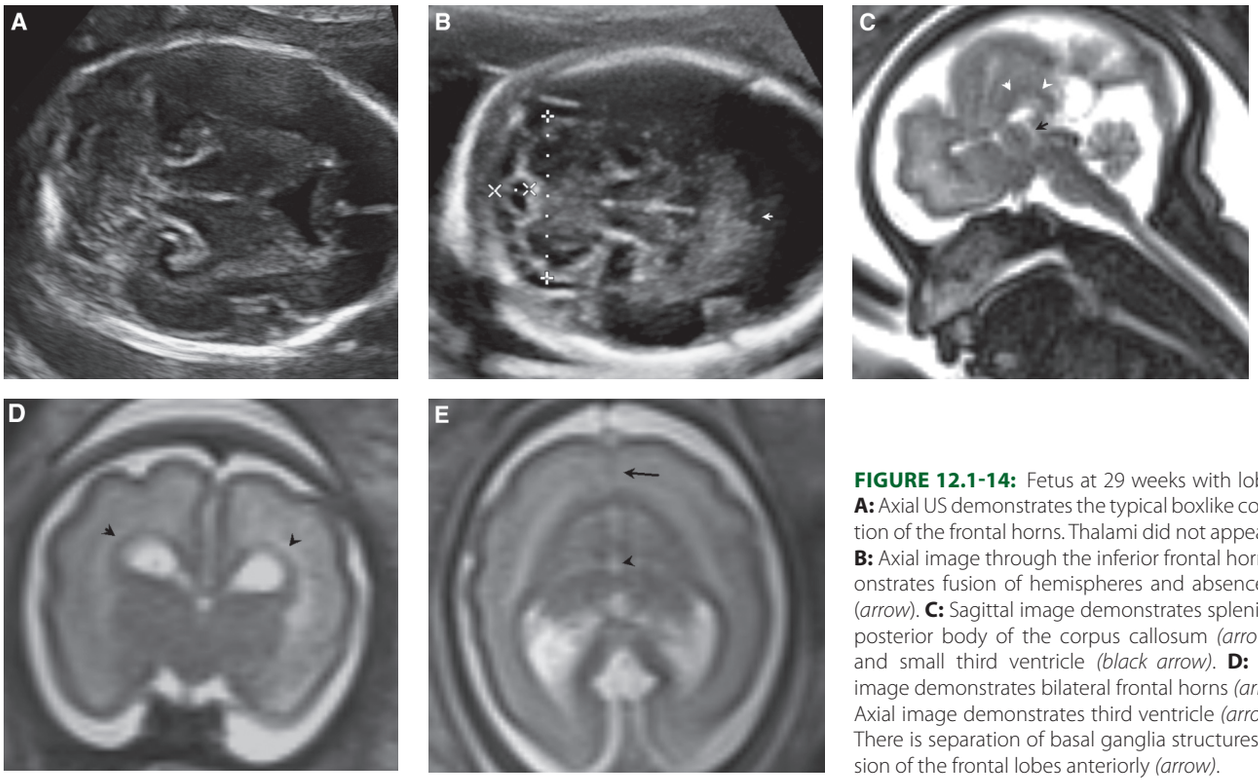

FIGURE 12.1-14: Fetus at 29 weeks with lobar HPE. **A:** Axial US demonstrates the typical boxlike configuration of the frontal horns. Thalami did not appear fused. **B:** Axial image through the inferior frontal horns demonstrates fusion of hemispheres and absence of falx (*arrow*). **C:** Sagittal image demonstrates splenium and posterior body of the corpus callosum *(arrowheads)* and small third ventricle *(black arrow)*. **D:** Coronal image demonstrates bilateral frontal horns *(arrows)*. **E:** Axial image demonstrates third ventricle *(arrowhead)*. There is separation of basal ganglia structures, but fusion of the frontal lobes anteriorly *(arrow)*.

absence of the cavum septum pellucidum (CSP) and central fusion of the frontal horn appearing as a boxlike squared shape with flattened roof in communication with the third ventricle (Fig. 12.1-14). Absence of the falx can be difficult to identify via US. However, the presence of an echogenic rounded structure variably identified within the third ventricle, representing fused fornices traveling from the anterior to posterior commissure, may help secure diagnosis.[120] An additional sonographic sign on midsagittal view is known as the "snake under the skull," representing a single (azygous) anterior cerebral artery displaced by the abnormal bridging frontal tissue.[121] In MIH, mild-to-moderate ventriculomegaly without CSP is common, but basal ganglia and thalami are normal (Fig. 12.1-15A). Fusion of hemispheres across the convexity can confirm this variant of HPE (Fig. 12.1-15B).

US is limited in diagnosing the HPE type, being inconsistent in 41% of cases.[98] Prenatal diagnosis detection rate of HPE by US has been noted to be as high as 71% but also as low as 22%.[108,117]

Early diagnosis of facial abnormalities may assist in confirmation of HPE.[122,123] Sonographic assessment of the fetal face, especially midline structures, is imperative.[124] The orbits should always be visualized and measured to exclude hypotelorism.[115] Three-dimensional/four-dimensional imaging is extremely helpful in further depiction of these anomalies and facilitates parent's understanding of the abnormality (Fig. 12.1-16).[125,126]

Growth restriction is found in higher than 50% of fetuses with HPE.[98] Microcephaly is noted in 75% of classic HPE and 50% with MIH.[102] As the pregnancy progresses, macrocephaly can develop because of disturbances in CSF dynamics.[114] A fetus with alobar HPE with dorsal cyst and severely nonseparated thalami are the most likely to develop hydrocephalus because of blockage at the third ventricle and aqueduct of Sylvius.[102,127] Exclusion of extracranial anomalies is imperative. In HPE, there is a high incidence of polyhydramnios.[99]

MRI: It is important to define the grade of HPE, as the image predicts the function.[102] MRI can identify all forms of HPE by demonstrating areas of cerebral nonseparation, abnormalities of the corpus callosum, and deep gray matter fusion.[128] In addition, MRI may help define subtle but significant facial anomalies (Fig. 12.1-12B).[129] On MRI, the severity of noncleavage of the cerebral hemispheres (grade) correlates with the severity of nonseparation of the deep gray nuclei.[130] The hypothalamus and caudate nuclei, 99% and 96%, respectively, are the most commonly nonseparated deep gray structures.[102,131] The thalami are noncleaved in 67% of HPE, and the degree of thalamic fusion correlates strongly with the presence of dorsal cyst.[100,117]

MR imaging is not typically necessary to diagnose the severe forms of HPE, but fused cerebral mass, monoventricle and dorsal cyst, and absence of septum pellucidum, corpus callosum, and interhemispheric fissure are well delineated (Fig. 12.1-12C). If MRI is obtained for *alobar*, approximately 27% will show nonseparation of the mesencephalon and 11% will demonstrate a single deep gray nuclear mass replacing basal ganglia, thalami, and midbrain (Fig. 12.1-12D).[117]

Differentiation from semilobar and lobar can be difficult as there is no clear boundary between the two types. In *semilobar* HPE, there is fusion anteriorly, presence of falx posteriorly, and partial fusion of the thalami. The splenium of the corpus callosum is present, and deep gray is incompletely separated. The septum pellucidum is absent with poor formation of the frontal horns (Fig. 12.1-13C,D). If the third ventricle is present, thalami are separate, and some frontal horn formation and splenium/posterior body corpus callosum are complete, then HPE variant is considered *lobar* (Fig. 12.1-14C,D). Fusion of the fornices in lobar HPE is better depicted on MRI than on US.[101] In septopreoptic HPE in which there is fusion in the septal (subcallosal) or preoptic region, the septum pellucidum may

Kline9781451175837-ch012.1.indd 359 08/08/14 9:58 AM

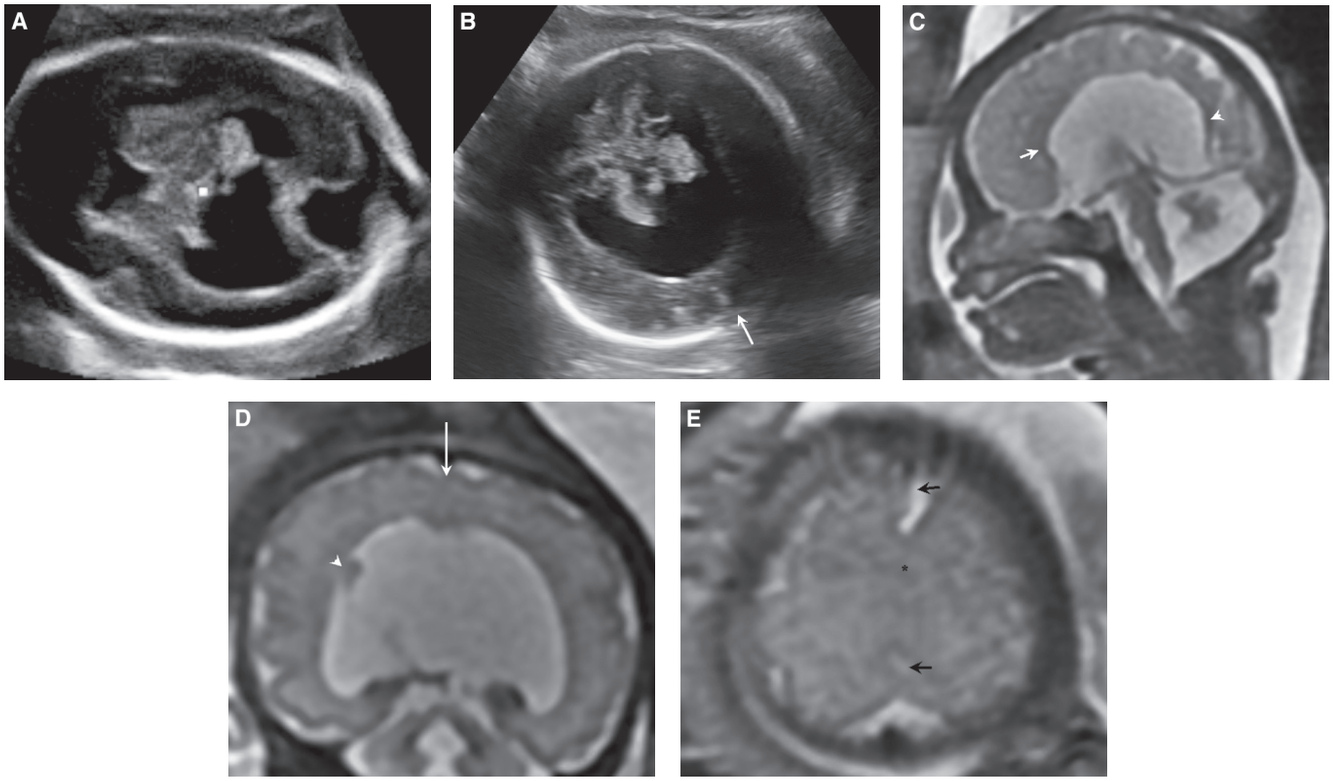

FIGURE 12.1-15: Fetus at 34 weeks with middle interhemispheric fusion. **A:** Axial image demonstrates moderate ventriculomegaly and absence of the septum pellucidum. **B:** Coronal image shows absence of interhemispheric fissure and fusion of cerebral hemispheres *(arrow)* at convexity of the brain. **C:** Sagittal T2 MR image demonstrates presence of the genu *(arrow)* and splenium *(arrowhead)*, but lack of visualization of the body. The vermis and brainstem are incidentally small. **D:** Coronal T2 MR image demonstrates fusion across midline *(arrow)*. There is gray matter heterotopia along the right lateral ventricle *(arrowhead)*. **E:** Axial MR T2 image demonstrates interhemispheric fissure anteriorly and posteriorly *(arrows)*, but fusion *(asterisk)* in the posterior frontal anterior parietal area.

be variably abnormal, fornix is dysplastic or thickened, corpus callosum may be thickened or hypoplastic, and azygous artery is usually present.[132,133] In *MIH*, the sylvian fissures are vertical, connected across the midline vertex of the brain in the posterior frontal anterior parietal lobe (Fig. 12.1-15C–E).[134] There is lack of visualization of the body of the corpus callosum, absence of the septum pellucidum with normal basal ganglia and thalami. In MIH, many have mild anomalies of the face, the most common being hypertelorism.[102]

In most forms of HPE, there is a low incidence of sulcation or cortical migrational abnormalities, with broad gyri being seen in severe forms, absent sylvian fissures alobar, vertical wide sylvian fissures semilobar and lobar, and rarely cortical abnormalities medial frontal in lobar HPE.[135] The exception is MIH, in which two-third have subcortical heterotopic gray or cortical dysplasia (Fig. 12.1-15D).

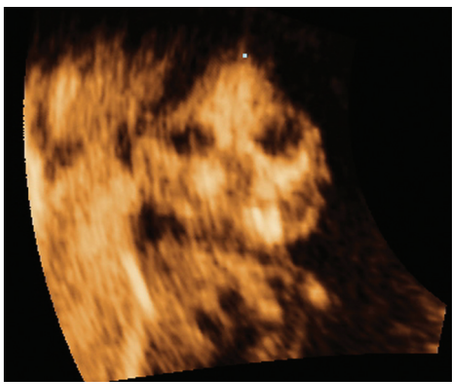

FIGURE 12.1-16: 3D reformat in a fetus with semilobar HPE and median cleft, hypotelorism, and trigonencephaly.

Associated Anomalies: About 51% to 55% of nonsyndromic HPE have multiple congenital defects.[97] HPE is typically associated with anomalies of the CNS, heart, skeleton, and gastrointestinal tract.[101] Of the CNS, HPE is associated most with neural tube defects and posterior fossa anomalies, including rhombencephalosynapsis.[136] Of noncraniofacial anomalies, 24% of HPE cases can demonstrate genitourinary defects, 8% postaxial polydactyly, 5% vertebral anomalies, 4% limb reduction, and 4% transposition of the great arteries.[97] Rarely, HPE is seen in the presence of heterotaxy syndromes.[133]

Differential Diagnosis: The main differential includes hydrocephalus, midline cerebral defects such as agenesis of corpus callosum (ACC), septo-optic dysplasia (SOD), hydranencephaly, and porencephalic cysts. Hydrocephalus can be differentiated by demonstrating persistence of the interhemipheric fissure, distinct separate ventricles, and splaying of the thalami. In hydranencephaly and porencephaly, thin cerebral cortex, partially present or deviated falx, and lack of fused thalami are noted. HPE is also differentiated from posterior fossa malformations by normal falx, supratentorial structures, and unfused thalami. ACC with interhemispheric cyst is often difficult to

distinguish but can be best discriminated by normal cleavage of the brain. Differentiation of lobar HPE from SOD is by identifying the presence of fused fornices and absence of abnormally developed interhemispheric fissure between the anterior hemispheres. MRI in the third trimester may be helpful to exclude optic nerve hypoplasia.[101]

Prognosis: There is a natural loss of fetuses with HPE, being as high as 40%, mostly during the first trimester.[108] For the most part, there is a direct correlation with severity of HPE and outcome.[102] The prognosis at birth is much worse for those with severe facial disorders and cytogenetic anomalies, with only 2% surviving beyond 1 year, compared with 30% to 54% with normal karyotype.[102] In those with normal karyotype, an inverse relationship between survival and severity of HPE and facial anomalies is noted.[101] Most with alobar HPE will not survive beyond infancy with 89% perinatal mortality rate.[101,115] Those with milder forms can survive into childhood and beyond, and may only have mild cognitive impairment.[102]

Children with HPE have multiple neurological problems, including mental retardation, motor dysfunction, seizure disorder, and endocrine abnormalities. Motor dysfunction including hypotonia, dystonia, and spasticity are present in all types of HPE, with the classic forms only having involuntary movements.[102] The severity of the brain malformation and the higher degree of nonseparation of gray nuclei correlate with the severity of developmental delay and neurologic deficit.[107,127] Approximately 50% will develop seizure, but only 25% will have chronic epilepsy.[107,127] Feeding problems are common, and the severity of dysfunction correlates with the grade of HPE.[101,107] Seventy-five percent of children with classic HPE have diabetes insipidus correlating with the degree of hypothalamic nonseparation rather than defects of the pituitary gland.[102,127] Dysautonomic dysfunction can also be present with instability of temperature, heart, and/or respiratory rate.[107] Frequent causes of demise include infection, dehydration due to uncontrolled diabetes insipidus, intractable seizures, and brainstem malfunction.[137]

Management: Genetic counseling is imperative. In the presence of severe HPE, elective termination of the pregnancy may be considered. Cesarean delivery should be considered only for maternal indications in the absence of fetal macrocephaly.[115] Cephalocentesis may be considered in the presence of macrocephaly. After birth, treatment is based on symptoms and usually requires a multidisciplinary approach. Medical management should focus on endocrine dysfunction, motor and developmental impairments, respiratory issues, seizures, and hydrocephalus. Feeding difficulties are common in neonates with HPE, and about two-thirds of those with lobar and semilobar HPE require gastrostomy tubes.[107] Neurologic management is not specific but may require anticonvulsive, physical, and occupational therapies. Surgery is typically performed to treat hydrocephalus and repair cleft lip and/or palate.[107,112]

Recurrence: HPE has a higher recurrence risk than other major malformations, being 6% to 20% after an isolated case, in a fetus with normal karyotype and no syndrome.[108,138] If inherited, the risk is 50% in the dominant form or 25% with recessive transmission.[112] Overall risk to the subsequent child with dominant transmission is 37% for HPE, 27% for HPE microform, and 36% for normal phenotype.[139]

COMMISSURES/MIDLINE

Agenesis of Corpus Callosum

The corpus callosum may be completely absent (agenesis), partially lacking (hypogenesis), or globally or partially thin (hypoplastic). Agenesis of the corpus callosum (ACC) can also be associated with meningeal dysplasias such as interhemispheric cysts and lipomas.

Incidence: ACC or hypoplasia of the corpus callosum is reported in 2 per 10,000 live births and is seen in approximately 13% of cases referred for VM.[140–142] There is a male preponderance.[141,142] With regard to race, the order of risk is higher for blacks, then whites, and finally Asian descent.[141] Postnatally, the incidence of complete ACC (CACC) and partial ACC (PACC) is equivalent. ACC is isolated in 30% of cases, with the remaining associated with other cerebral or extracranial anomalies.[143]

Pathogenesis: The corpus callosum is the largest and most significant of the five midline forebrain commissures, composed of axons which facilitate communication between the cerebral hemispheres. It contains five sections, anterior to posterior: rostrum, genu, body, isthmus, and splenium (see Fig. 6.2-25 in Chapter 6.2). The corpus callosum arises from the lamina terminalis, originates in the area of the massa commisuralis between 7 and 20 weeks of gestation, and reaches adult size by 2 years of age (see section on normal corpus callosum Chapter 6.2).

There are many inciting factors that may result in its absence, with three possible mechanisms described: missing or defective development of the massa commissuralis, failure of the axons to form in the cerebral cortex, or inhibited cellular migration due to the absence of normal chemical attractants or repellants or an interhemispheric lesion. It is suspected that CACC is mostly a primary embryologic disorder with failure of development of the termina laminalis or massa commissuralis, whereas PACC is a malformation or destructive event in which there is partial absence of the commissural plate or lack of normal growth.[144,145] Hypoplasia is likely secondary to a developmental error or insult later in fetal development.

If the axons develop but are unable to cross the midline because of the absence of the massa commisuralis or a lesion in the interhemispheric space, large heterotopic axons that were destined to cross the corpus callosum lie parallel to the interhemispheric fissure along the medial walls of the lateral ventricles, forming the bundles of Probst. If there is a defect in the commissural axons or their parent cell bodies fail to form in the cerebral cortex, the commissures are absent, Probst bundles are absent, and white matter volume is decreased.[146] When the corpus callosum is completely absent, there is associated absence of the hippocampal commissure, and 50% of the time, the anterior commissure is also missing.[146] If the corpus callosum is partially absent, usually the posterior aspect is deficient. ACC is primary when it is the main pathology; however, it can be secondary if it is due to destructive events or when associated with other major malformations, such as encephaloceles and HPE.[146]

In the presence of ACC, there is associated distortion of the intracranial architecture. The cingulate gyrus remains everted, and the sulci of the medial brain extend into the third ventricle, creating a radial or sunburst pattern.[147] When callosal bundles of Probst are present, the lateral ventricles, especially in the frontal area, have a crescentic "steer horn" appearance.[147] The third ventricle is large and high-riding, communicating with the interhemispheric fissure (Fig. 12.1-17). The foramen

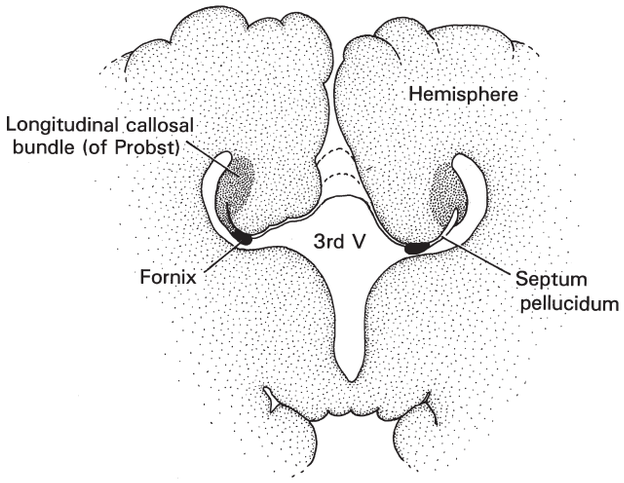

FIGURE 12.1-17: Schematic drawing of ACC. The lateral ventricles demonstrate a crescentic shape due to the presence of Probst bundles. The third ventricle is large, extending upward into the interhemispheric fissure. The cingulate gyri are everted, and sulci do not form. (From Barkovich AJ. Apparent atypical callosal dysgenesis: analysis of MR findings in six cases and their relationship to holoprosencephaly. *AJNR Am J Neuroradiol*. 1990;11:333–340, with permission.)

of Monro is enlarged. White matter volume loss is nearly uniform, likely representing a primary dysplasia or hypogenesis. In the case of complete absence, the lateral ventricles maintain a straight parallel configuration with focal dilatation of the temporal, atrial, and occipital horn due to hypogenetic and loose white matter tracts.[148] This ventricular dilatation posteriorly is known as colpocephaly. Abnormalities of the anterior and hippocampal commissures, either being absent or abnormal in size, are common.[149] The hippocampal formations are often incompletely rotated.[148] Malformations in cortical development and delay in sulcation are common, with gray matter heterotopias identified in approximately 29% of cases.[149]

Meningeal dysplasias include cysts and lipomas. Interhemispheric cysts are associated with ACC in 14% to 30% of cases.[149] The cyst can communicate with the ventricles (type 1) or lack ventricular continuity (type 2). *Type 1* lesions represent a single ventricular diverticulation of CSF attenuation which is not typically associated with hemispheric malformations.[145,150] In *type II* cysts, multilocular complex cysts are present, and these children are more likely to be born with hydrocephalus. Associated brain malformations are more common with type II, and in the presence of hemispheric asymmetry and polymicrogyria, Aicardi syndrome should be considered.

Up to 3% of patients with ACC will have interhemispheric lipomas.[149] Pathogenesis of pericallosal lipomas are believed to be because of abnormal resorption of the menix primitiva.[151] Two types are described including the *tubulonodular*, which are round and measuring >2 cm, and the *curvilinear*, which is thin and elongated, measuring <1 cm in diameter. The tubulonodular type is more common, seen with major, usually anterior callosal malformation, often have internal calcification, and may be associated with frontofacial anomalies. The curvilinear is posterior with less severe callosal abnormalities.[145,151] Goldenhar and trisomies have been associated with ACC with lipoma.[151]

Etiology: There are innumerable causes of ACC including chromosomal, genetic, infectious, vascular, inborn errors of metabolism, or toxic causes (Table 12.1-5), but the etiology is unknown in more than 50% of defined cases.[152] For 30% to 45% of individuals with CACC and PACC, the cause is chromosomal (10%) or genetic syndromes (20% to 35%).[153] If only CACC is considered, recognizable syndromes drop to 10% to 15%, with 75% lacking identifiable cause. Aneuploidy is identified in 1 in 10 ACC cases, the most common being trisomy 8, 13, 18, and 21.[154] In the presence of additional structural abnormalities and/or advanced maternal age, ACC is seen at a higher frequency with chromosomal disorders.[141,143]

There are over 175 syndromes in which ACC is a significant finding. A well-known disorder associated with ACC is Aicardi. This X-linked dominant condition seen primarily in females and in males with Klinefelter syndrome (XXY) is due to a balanced translocation of the X chromosome and is characterized by infantile spasms, ACC, and chorioretinal lacunae. The presence of ACC with polymicrogyria, periventricular hetertopia, cysts of the choroid plexus, pineal, and/or interhemispheric region, micropthalmia, asymmetry of the hemispheres, and abnormal EEG is highly suggestive of Aicardia.[155] Another syndrome to consider is CRASH (ACC, retardation, adducted thumbs, spastic paraplegia, and hydrocephalus), which is caused by mutations in the L1 cell adhesion molecule (L1CAM).

Metabolic disorders, fetal infections, or in utero exposure to teratogens, such as fetal alcohol syndrome and maternal diabetes, have been described with ACC. Infants born prematurely have an almost four-fold higher prevalence.[141]

Table 12.1-5 Common Etiologies for Agenesis of Corpus Callosum (ACC)

Genetic Disorders

Consistently associated with ACC
- Aicardi syndrome—chorioretinal lacunae, infantile spasms
- Andermann syndrome—peripheral neuropathy, dementia
- Acrocallosal syndrome—hallux duplication, polydactyly, craniofacial
- Calloso-genital dysplasia—coloboma, amenorrhoea
- Shapiro syndrome—ataxia, drowsiness
- CRASH/L1CAM—hydrocephalus, adducted thumbs

Inconsistently associated with ACC
- Meckel–Gruber—encephalocele, polydactyly, polycystic kidneys
- Rubinstein–Taybi—broad thumbs and great toes, microcephaly
- Sotos syndrome—physical overgrowth, craniofacial
- Fryns—congenital diaphragmatic hernia, pulmonary hypoplasia, craniofacial changes

Inborn errors of metabolism
- Glutaric aciduria Type II
- Neonatal adrenoleukodystrophy
- Nonketotic hyperglycinemia
- Pyruvate dehydrogenase deficiency

Chromosomal disorders
- Trisomy 18, 13, 8

Teratogens
- Fetal alcohol syndrome
- Cocaine

Data from Bedeschi MF, Bonaglia MC, Grasso R, et al. Agenesis of corpus callosum: clinical and genetic study in 63 young patients. *Pediatr Neurol*. 2006;34(3):186–193.

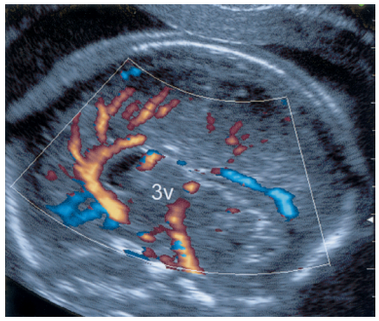

FIGURE 12.1-18: Partial agenesis of the corpus callosum. The corpus callosum appears thin but can be positively identified by the pericallosal artery anteriorly.

Diagnosis: Fetal karyotyping should be performed to exclude chromosomal anomaly.

Ultrasound: In the first trimester, early ultrasound examination at 11 to 14 weeks can provide clues to the existence of ACC. Normal anatomy of the pericollosal arteries on the sagittal plane demonstrates the vessels arising from the anterior cerebral arteries to curve posteriorly following the normal anatomy of the corpus callosum.[156] Lack of visualization of the normal pericallosal artery raises the suspicion of ACC (Fig. 12.1-18).[156] With ACC, the midbrain diameter is typically increased and falx diameter decreased, yielding a high midbrain-to-falx diameter ratio.[157] These findings are, however, not 100% sensitive or specific and should be confirmed with second-trimester imaging.

In the second trimester, the diagnosis of a callosal abnormality is typically suggested by the presence of mild-to-moderate ventriculomegaly.[158] Direct visualization of the corpus callosum is best via coronal or sagittal imaging but can be difficult prior to 22 weeks (Fig. 12.1-19).[159,160] The sensitivity in identifying ACC by direct visualization is variable in the literature, ranging from 28% to 85%.[161] Three-dimensional reformats of axial images in the sagittal plane are helpful, or in the presence of a cephalic fetus, transvaginal US can increase visualization.

When the corpus callosum cannot be directly visualized, high suspicion for the diagnosis is via indirect signs (Fig. 12.1-20). The indirect signs of ACC include the following[154,158,159,162]:

- Absent septum pellucidum identified as early as 17 to 18 weeks
- Ventriculomegaly with disproportionate dilatation of the occipital horns creating a teardrop configuration (colpocephaly)
- Increased distension of the interhemispheric fissure with separation of the lateral ventricles and both medial and lateral walls aligned parallel to the midline
- Concave appearance of the medial, especially anterior horns of the lateral ventricles, due to protrusion of the cingulate gyrus and Probst bundles
- Upward displacement of a variably dilated third ventricle
- Radial arrangement of medial cerebral sulci
- Abnormal appearance of the pericallosal artery

However, these indirect findings may be absent early in the second trimester with colpocephaly often not apparent until 26 weeks and radial arrangement of the medial sulci until third trimester.[159,160]

Direct diagnosis of CACC can be difficult, and PACC may be technically more difficult because of inconsistent indirect signs.[163,164] In the presence of PACC, the most common finding is colpocephaly, although sometimes a small or absent cavum septi

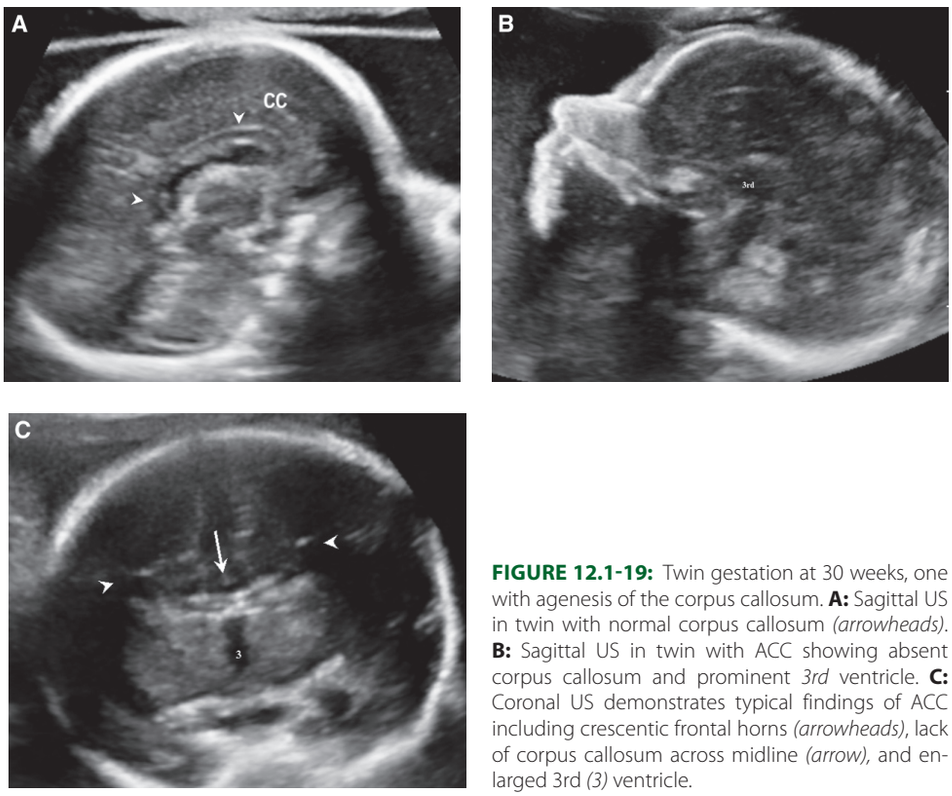

FIGURE 12.1-19: Twin gestation at 30 weeks, one with agenesis of the corpus callosum. **A:** Sagittal US in twin with normal corpus callosum *(arrowheads)*. **B:** Sagittal US in twin with ACC showing absent corpus callosum and prominent *3rd* ventricle. **C:** Coronal US demonstrates typical findings of ACC including crescentic frontal horns *(arrowheads)*, lack of corpus callosum across midline *(arrow)*, and enlarged 3rd *(3)* ventricle.

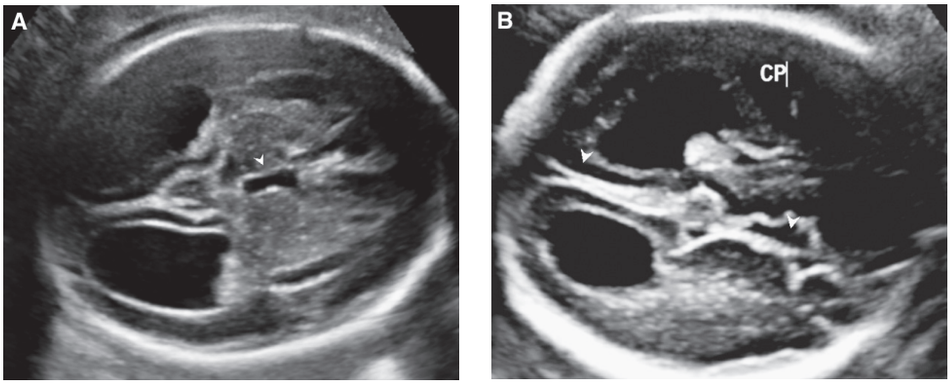

FIGURE 12.1-20: Indirect signs of ACC. **A:** Axial image demonstrates colpocephaly and dilatation of the third ventricle *(arrowhead)*. No septum pellucidum was identified. **B:** Axial image through dilated posterior ventricular horns with prominent interhemispheric fluid *(arrows)*. CP represents choroid plexus.

pellucidi is noted. An important pitfall in sonography is that in PACC or CACC, dysplastic or displaced leaflets of the septum pellucidum and fornix may simulate a normal cavum septum pellucidum, and therefore direct visualization of the corpus callosum with sagittal imaging in conjunction with pericallosal color Doppler may be required.[164–166] Using expert sonography with 3D reformation and comparison with normative callosal values, hypogenesis and hypoplasia have been diagnosed.[166,167]

In the presence of interhemispheric cyst, the third ventricle can be mildly dilated or significantly enlarged. The cyst may be simple and communicate with the third or lateral ventricles (Fig. 12.1-21A) or may be complex mulitlocular without ventricular communication (Fig. 12.1-22A). Lipomas are nodular or curvilinear echogenic masses within the interhemispheric fissure. Some large lipomas have spiculated margins with or without extension into the frontal horns or the choroid plexus (Fig. 12.1-23A).[151]

MRI: Fetal MRI is useful in evaluation of the corpus callosum and has high sensitivity in confirming presence or absence as the structure is well defined on axial, sagittal, and coronal images.[161,163] In prior studies, fetal MRI has identified an intact corpus callosum in about 20% of cases referred for ACC.[168,169] Prenatal MRI easily depicts the common intracranial direct and indirect signs that are present with this pathology (Fig. 12.1-24). MRI has also been shown to identify additional brain anomalies, especially migration anomalies, in 63% to 93% fetuses with ACC that were not apparent on US (Fig. 12.1-25).[168–170]

In a recent study, nearly all cases of ACC have been noted to have abnormalities of sulcation, 50% with disorders of the cerebellum and 33% of the brainstem.[170] Most brainstem abnormalities are present in conjunction with cerebellar anomalies (Fig. 12.1-26).[170] Sulcation delay can be associated with good neurodevelopmental outcome and may reflect white matter dysgenesis. In fact, a recent study notes that sulcation delay is seen at a high frequency in fetuses with ACC in the third trimester, likely because of failed commiseration and not because of additional brain malformations.[171] If delay in sulcation is excluded, only 69% of ACC cases have additional anomalies via fetal MRI.

In the presence of focal abnormal sulcation morphology, 42% of cases of ACC on prenatal MRI have been found to be associated with multiple brain anomalies and a syndrome.[170] In 25% of ACC cases, additional findings identified by fetal MR imaging led to a diagnosis of a specific disorder or syndrome.[169] In 10% of ACC cases, destructive changes suggested acquired injury.[170]

MRI easily defines the presence of associated interhemipheric cyst or lipoma and extent of the lesion. In type 1, the cysts are isotense to CSF and communicate with the ventricle (Fig. 12.1-21B); whereas type II cysts present as multiple cysts demonstrating higher signal than CSF on T1 and heterogeneous

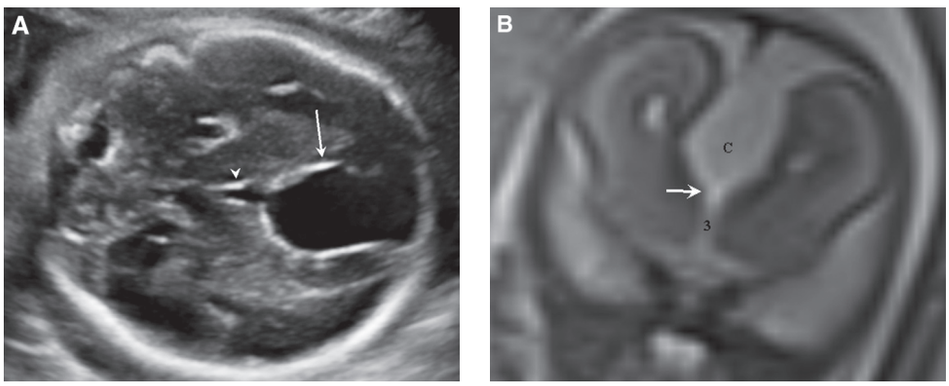

FIGURE 12.1-21: Type I interhemispheric cyst in a 20 week-fetus with ACC. **A:** Coronal oblique US image demonstrates simple interhemispheric cyst *(arrow)* in continuity with third ventricle *(arrowhead)*. **B:** Coronal T2 MR image verifies cyst *(C)* and confirms communication *(arrow)* with third ventricle (*3*).

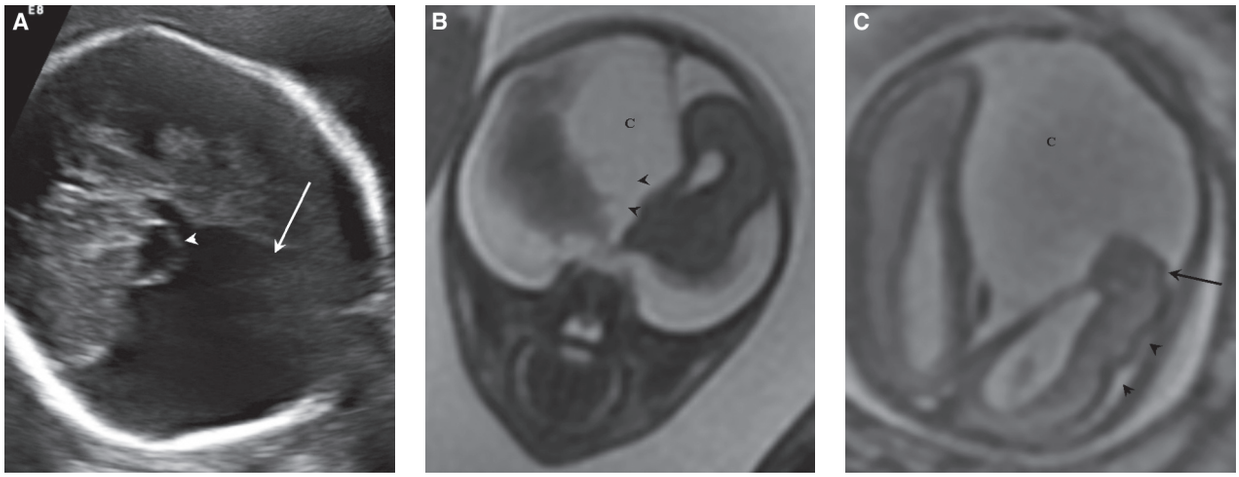

FIGURE 12.1-22: Fetus at 23 weeks with ACC and type II interhemispheric cyst. **A:** Axial US demonstrates a large interhemispheric cyst *(arrow)* with septation *(arrowhead)* midline. **B:** Coronal MR SSFP image demonstrates small septated areas (*arrowheads*) deep in the interhemispheric cyst (*C*). No communication with ventricular system was noted. **C:** Axial T2 image demonstrates large cyst (*C*). The left hemisphere was abnormally small, and abnormal dark parenchymal signal *(arrow)* and unusual cortical lobulation *(arrowheads)* along the hemisphere were consistent with migrational abnormality.

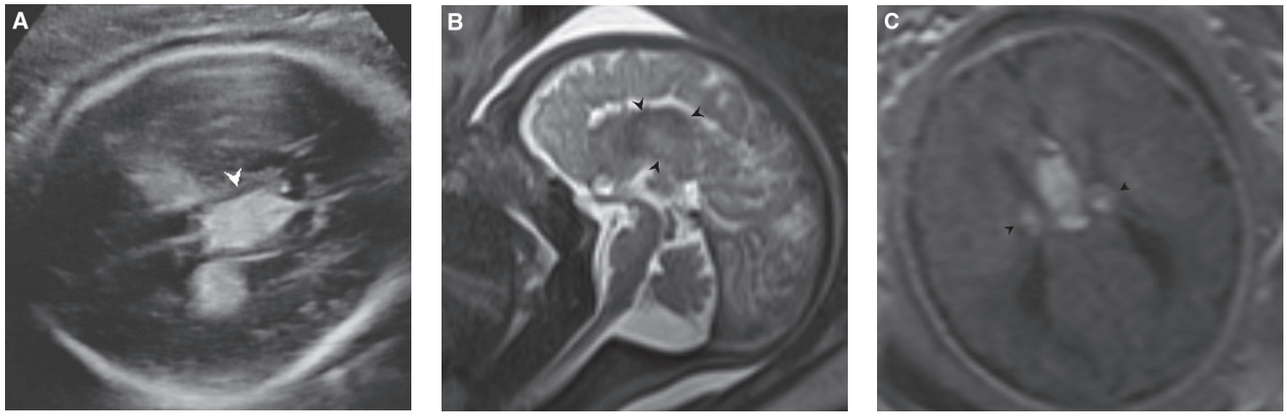

FIGURE 12.1-23: ACC and tubulonodular lipoma in a fetus at 35 weeks. **A:** Axial US demonstrates echogenic midline mass *(arrowhead)* with prominent choroid plexus. **B:** Sagittal T2 MR image demonstrates ACC with heterogeneous hypointense *(arrowheads)* mass in the midline. **C:** Axial T1 image demonstrates hyperintense mass in midline and small nodules extending into the choroid *(arrowheads)*.

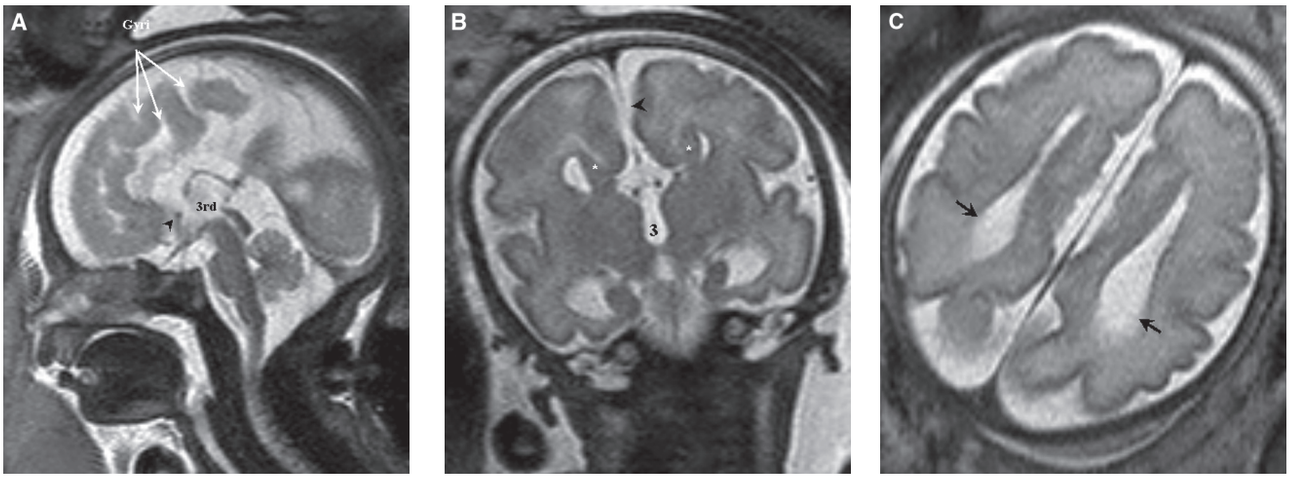

FIGURE 12.1-24: MR imaging of fetus at 30 weeks with ACC. **A:** Sagittal T2 shows absence of the corpus callosum and missing hippocampal commissure and fornix. Anterior commissure is present *(arrowhead)*. Notice radial arrangement of gyri and prominent *3rd* ventricle. **B:** Coronal image demonstrates prominent *3*rd ventricle and interhemispheric fluid *(arrowhead)*. Probst bundles are noted *(asterisks)* adjacent to crescentic frontal horns. No cavum septum pellucidum. Hippocampi are incompletely rotated. **C:** Axial image demonstrates parallel configuration of the lateral ventricles consistent with colpocephaly *(arrows)*.

Kline9781451175837-ch012.1.indd 365 08/08/14 9:58 AM

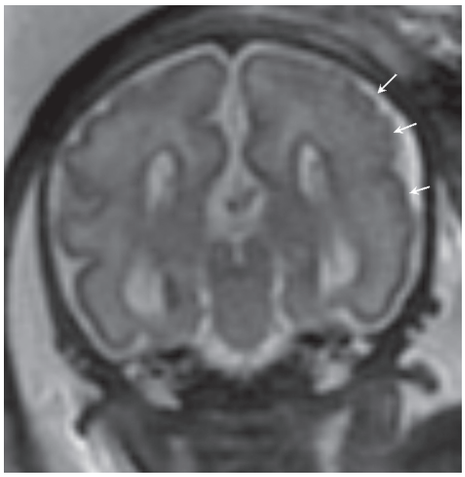

FIGURE 12.1-25: Migrational anomaly in fetus at 30 weeks with ACC. Coronal T2 image demonstrates irregularity and poor gray white differentiation left opercula area *(arrows)* consistent with polymicrogyria. Compare with the opposite normal right side.

signal on T2 imaging and do not communicate with the ventricular system (Fig. 12.1-22B,C). Lipomas demonstrate hyperintense signal on T1 and hypointense signal on T2 and when tubulonodular may extend into the choroid plexus (Fig. 12.1-23B,C). Fetal US and MRI are helpful in suggesting the diagnosis of Aicardi by evaluating for choroid plexus cysts (CPCs), microphthamia, asymmetric hemsipheres, and cortical malformations (Fig. 12.1-27).

Associated Anomalies: Both intracranial and extracranial anomalies are seen in corpus callosum disorders (Table 12.1-6). Because the corpus callosum development overlaps with complex processes involving neuronal proliferation and migration, common associated CNS anomalies include disorders of neuronal organization, posterior fossa malformations, and neural tube defects.[140,141] The incidence of CNS anomalies in ACC ranges from 50% to 85% in some series.[172] Extra-CNS anomalies are present in approximately 65% of ACC patients.[153] Common organ systems include eyes, heart, and kidneys.[173]

Differential Diagnosis: ACC should be differentiated from other causes of VM. In the presence of ACC with an interhemispheric cyst, differential would include enlarged cavum septum pellucidum et vergae, arachnoid cyst, porencephaly, ventricular rupture in obstructive hydrocephalus, and vein of Galen malformation. Interhemipheric cysts may be confused with the dorsal sac of HPE but the morphology of the separated frontal horns helps in differentiation. In the presence of a lipoma, differential diagnosis includes hemorrhage or rare tumor such as craniopharyngioma or choroid plexus papilloma.

Prognosis: Outcome is dependent on multiple factors including presence of microcephaly, genetic abnormality, and/or associated anomalies.[152] In the presence of ACC with syndrome or chromosomal abnormalities, the outcome is typically poor.[144] Children with Aicardi have significant developmental delay, seizures, and shortened life span with survival of 76% at 6 years and 40% at 14 years, demise most commonly due to respiratory infection.[155,172] Children with ACC and associated migrational disorder are more likely to have moderate-to-severe developmental delay.[174] It is controversial whether PACC versus CACC has better outcome.[144,164,171,175] When reviewing all patients with ACC, moderate-to-severe developmental delay is described in 80%, epilepsy in 35% to 45.8%, cerebral palsy in 37.5%, microcephaly in 33.3%, and visual and hearing defects and behavioral disorders in many.[152,175,176]

Most believe that an asymptomatic outcome in isolated agenesis can occur; however, it is more likely the exception rather than the rule.[152] Isolated ACC has been shown to have outcomes ranging from normal to severe delay.[142] In addition, even though 5% to 20% of cases have prenatal diagnosis of isolated ACC, additional anomalies have been detected postnatally.[173,177]

Although some research suggests better prognosis in those fetuses with isolated CACC, with small studies quoting 100% normalcy and larger studies noting normal developmental outcomes in two-thirds of cases and literature citing rates between 45% and 85%, the information is still incomplete as these studies include variable number of cases, isolation diagnosed only via fetal MRI and limited follow-up ranging only between 2 and 6 years of age.[140,144,154,178] It has been demonstrated that as age

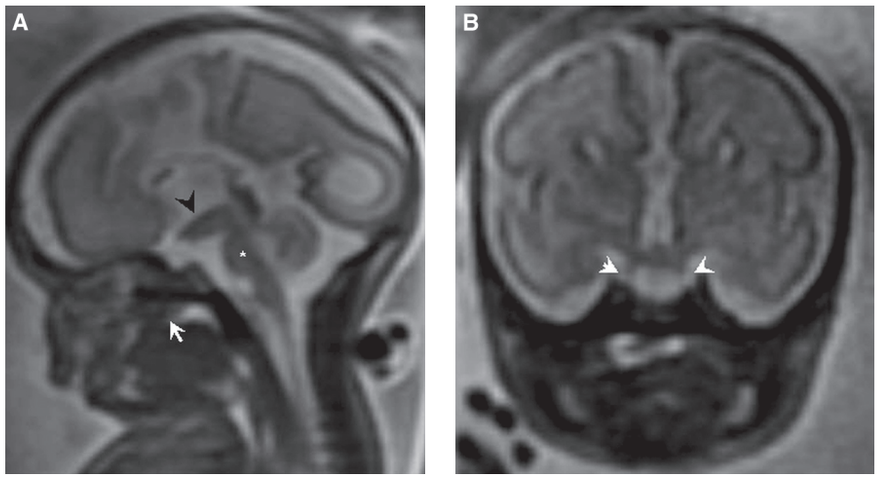

FIGURE 12.1-26: Fetus at 30 weeks with ACC and epignathus. **A:** Sagittal T2 image shows ACC with small brainstem *(asterisk)*. Cerebellar vermis also measured small. The hypothalamus is thick *(arrowhead)*. There is heterogeneous tissue in the area of the palate *(white arrow)*. **B:** Coronal T2 image demonstrates two infundibula *(arrowheads)* consistent with duplicated pituitary.

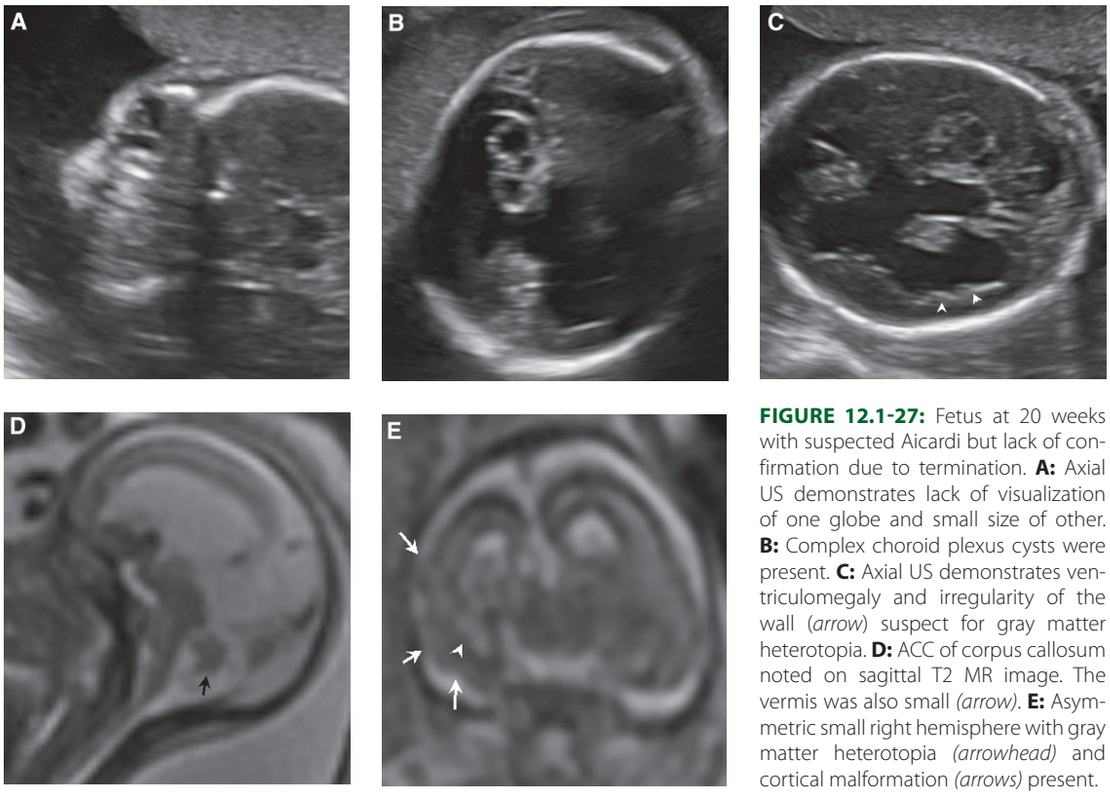

FIGURE 12.1-27: Fetus at 20 weeks with suspected Aicardi but lack of confirmation due to termination. **A:** Axial US demonstrates lack of visualization of one globe and small size of other. **B:** Complex choroid plexus cysts were present. **C:** Axial US demonstrates ventriculomegaly and irregularity of the wall (*arrow*) suspect for gray matter heterotopia. **D:** ACC of corpus callosum noted on sagittal T2 MR image. The vermis was also small *(arrow)*. **E:** Asymmetric small right hemisphere with gray matter heterotopia *(arrowhead)* and cortical malformation *(arrows)* present.

increases, more delays often become apparent.[178] For example, a recent study demonstrated lower than normal IQ of 19% at 2 years, 33.5% at 4 years, and 43% at 6 years in a series of 17 children with isolated ACC.[178] Another recent study demonstrated that children with isolated ACC may have normal cognitive and neurologic outcome, but lower than expected based on family history and sometimes other subtle to severe defects identified later childhood, including difficulties at school, intellectual impairment, verbal communication defects, sleep disorders, and seizures.[174,178] Prediction of outcome even still must be cautious as some individuals with isolated ACC have deficits in the social and behavioral domain, which may place them in the spectrum of autism, attention deficit disorder, and schizophrenia that usually do not become evident until preteenage years.[174] Recent epidemiology studies have documented that there is only 27% normal outcome in the presence of isolated ACC.[142]

In ACC with interhemispheric cyst, seizures are noted in less than half of patients. It has been suggested that Type 1 cysts tend to have more developmental delay and neurologic deficits than type II; however, outcome is likely dependent on associated anomalies and the development of hydrocephalus.[150] In the presence of associated lipoma, neurologic status is variable depending on type of lipoma, associated callosal anomalies, and other malformations; however, overall 50% of children with ACC and lipoma have seizures and psychological disorders.[151]

Management: Termination of the pregnancy may be considered after complete prenatal workup. At birth, close evaluation for

Table 12.1-6 CNS and Extra-CNS Abnormalities with Agenesis of Corpus Callosum

CNS Abnormalities	*Extra-CNS Abnormalities*
Periventricular nodular heterotopia	Cranio facial
Pachygyria	Skeletal
Hypothalamic, pituitary, and optic hypoplasia	Cardiac
Polymicrogyria	Ocular
Dandy Walker malformation	Genital
Cerebellar vermis agenesis	Renal
Pontine hypoplasia	

Data from Bedeschi MF, Bonaglia MC, Grasso R, et al. Agenesis of corpus callosum: clinical and genetic study in 63 young patients. *Pediatr Neurol*. 2006;34(3):186–193.

extracerebral malformations should be performed to exclude underlying genetic syndrome. If no other abnormalities are detected and the ACC is isolated, close clinical follow-up is suggested. If anomalies are present, postnatal MRI and evaluation by a multidisciplinary team including neonatologists, neuroradiologistis, neurologist, and geneticist is indicated. Comorbidities including epilepsy and feeding problems should be addressed.

Recurrence: In most cases of ACC, recurrence is moderately increased at 5% to 10%.[160] If the etiology is syndromic, recurrence is dependent on the type of transmission. Risk is high in a family with previous child diagnosed with Aicardi syndrome.

Septo-optic Dysplasia

Septo-optic dysplasia (SOD), or De Morsier syndrome, is a disorder of midline anomalies that include a triad of findings of complete or partial absence of the septum pellucidum, optic nerve hypoplasia, and hypothalamic pituitary abnormalities.

Incidence: SOD is fairly rare with an incidence of 1 per 10,000 live births with equal prevalence in males and females.[179] The disorder is noted at a higher incidence when there is bleeding early in pregnancy or in children born to younger, especially teenage, mothers.[179,180]

Pathogenesis: The septum pellucidum is intimately associated with the corpus callosum and is also formed from the lamina terminalis. The structure is bounded by the corpus callosum anteriorly and superiorly, and by the fornix inferiorly and posteriorly. The septum pellucidum forms the medial border of the frontal horns of the lateral ventricles, the posterior margin defined by the foramen Monro. Each leaflet from lateral to medial has a ventricular ependymal lining, thin layer of gray matter, thin layer of white matter, and inner pial layer.

Prosencephalic maldevelopment or destructive insults between 4 and 6 weeks of gestation are suspected to give rise to SOD. This is the time when the septum pellucidum is linked to development of the commissures (see corpus callosum Chapter 6.2). Optic nerve defects are also possible as this is when the optic vesicles and retinal ganglion cells differentiate. Pituitary disorders, particularly in the presence of ectopic posterior lobe, may occur because of ischemic injury to the hypophysis causing necrosis of the infundibulum.[181]

The phenotype of SOD is variable, with the diagnosis obtained by identifying two or more of the triad of findings. Usually, the diagnosis is confirmed by ophthalmology postnatally when hypoplasia of the optic discs is present in conjunction with partial or complete absence of the septum pellucidum. Pituitary dysfunction, commonly in association with structural abnormalities such as ectopic or absent posterior pituitary, truncated or absent infundibulum, and hypoplastic anterior lobe, may be present.[182] Approximately 30% of patients have the triad of findings, 62% have hypopituitarism, and 60% to 75% demonstrate absent septum.[183,184] About 75% to 80% of patients with SOD have optic nerve hypoplasia, which may be unilateral (12%) or more commonly bilateral (88%).[183] SOD can also be associated with absence, hypogenesis, or hypoplasia of the corpus callosum.[185] Isolated absence of the septum pellucidum is rare.

Two distinct groups of SOD are noted. One group has complete or partial absence of the septum pellucidum in conjunction with malformations of cortical development, usually schizencephaly in the frontal lobe area.[186] The term SOD-plus is sometimes utilized to describe these complex cases.[187] The second group has complete absence of the septum, hypoplasia of the cerebral white matter, normal cortex, and often pituitary dysfunction.[188] These findings overlap with HPE, possibly representing a milder form of lobar HPE.

Etiology: The etiology of the syndrome is likely multifactorial, related to multiple genetic disorders and environmental factors that result in intrauterine vascular disruption.[184] The condition is primarily sporadic, but rare autosomal recessive and dominant familial cases have been cited.[5] A gene found to cause SOD, documented in familial cases, is the *HESX1* gene, which is produced by tissue adjacent to the developing prosencephalon and is suggested to be important for proper induction of the forebrain and midline.[183] The *HESX1* gene is also one of the earliest markers of the pituitary primordium and may explain the associated hypopituitarism. *SOX2* and *SOX3* genes are also necessary for development of the pituitary, and these genes have been implicated in pituitary anomalies seen in SOD.[183,189] In utero injury causing SOD may be due to viral infections, teratogens such as exposure to alcohol or drugs, or degenerative damage.[183,184]

Diagnosis

Ultrasound: On US, the leaves of the septum pellucidum and interposed cavum can be visualized sonographically as a rectangular or triangular fluid-filled space between the frontal horns in 100% of normal fetuses from at least 18 to 37 weeks.[190] At midgestation, however, if only axial imaging is obtained, an artifact created by US beam crossing, can mimic the septum pellucidum and result in misdiagnosis.[191] Two other causes of false positive include an enlarged cavum septum pellucidum with displaced leaflets laterally and imaging slightly below the plane of the septum pellucidum in which the columns of the fornix, defined as two hypoechoic tubular structures separated by three echogenic interfaces, can be misinterpreted as the cavum.[192] Coronal and sagittal planes either 2D or 3D should be attempted. Transvaginal imaging may also prove helpful.

On US, absence of the septum pellucidum can be diagnosed after 20 weeks and causes the frontal horns to appear fused and squared (Fig. 12.1-28).[187,193] Mild-to-moderate ventriculomegaly

FIGURE 12.1-28: Axial image in fetus at 30 weeks with SOD. Note absence of the septum pellucidum, squared frontal horns and mild ventriculomegaly.

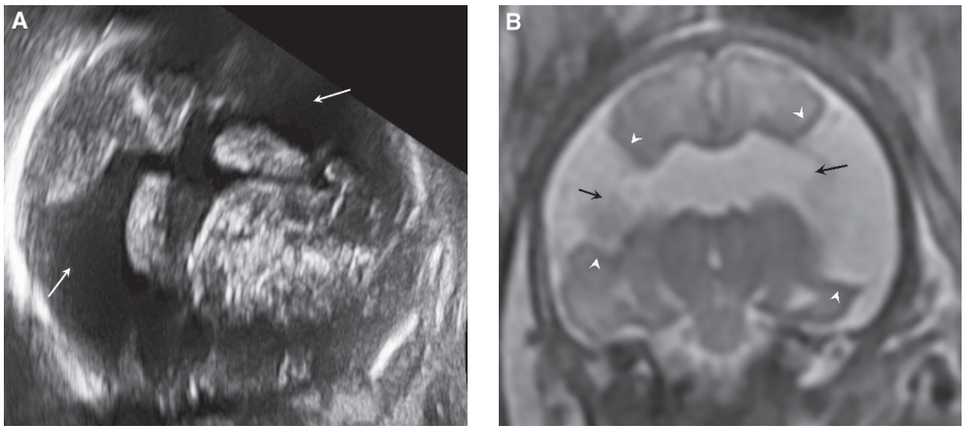

FIGURE 12.1-29: Fetus at 36 weeks with SOD with bilateral open-lipped schizencephaly. **A:** Axial oblique US demonstrates absence of the septum pellucidum and large bilateral frontal defects *(arrows)*. **B:** Coronal T2 MR demonstrates open-lipped schizencephaly defects *(arrows)* lined with gray matter *(arrowheads)*. Notice absence of the septum pellucidum. This fetus would be considered in the spectrum of SOD-plus.

may be present, likely because of white matter volume loss. Defects in the brain parenchyma extending from the lateral ventricles to the arachnoid space, especially when bilateral and frontal, are typical findings of open-lipped schizencephaly (Fig. 12.1-29A).

Three-dimensional axial reconstruction of the brain at the level of the circle of Willis can be helpful in confirming normal pituitary tissue and evaluating the optic nerve/tracts.[194,195] Although measurement of the optic tract can be difficult to obtain, recent US data have shown a linear increase in optic tract diameter with gestational age (Table 25B of Appendix A1).[195] Comparing these standards with optic tract diameter, hypoplasia can be diagnosed.[195]

MRI: MRI has been shown to be 100% accurate when identifying absence of the septum pellucidum, whereas US has been noted to detect only 70%.[196] On MRI, excellent thin sagittal and coronal view of the midline is important. Similar to US, when the septum pellucidum is absent, the frontal horns will appear square, bat wing, or boxlike (Fig. 12.1-30A). There is usually low position of the fornices, which may be fused, and mild dilatation of the suprasellar cistern and anterior recess of the third ventricle (Fig. 12.1-30B).[197] In the presence of severe hypoplasia of the optic nerves, the imaging may be suggestive, but mild optic nerve hypoplasia is usually difficult to diagnose prenatally, owing to the small size of the nerve, slice thickness, and angle of the chiasm with regard to the imaging plane.[196] Clinical postnatal opthalmalogic exam remains the standard reference. The pituitary gland can be identified on T2 and T1weighted imaging. In the fetus, both the anterior and the posterior lobe are hyperintense on T1-weighted sequences; therefore, no distinction is typically possible between the anterior and the posterior lobes, unless the posterior is ectopic.[194] Schizencephaly, usually in the frontal lobe area, should be excluded (Fig. 12.1-29B).

Associated Anomalies: Up to 75% of patients with SOD have associated brain anomalies, the most common being bilateral polymicrogyria with or without clefting (schizencephaly), followed by cortical heterotopias.[181,185] Fusion of the fornices and thinning or absence of the corpus callosum is often present.[181] Cerebellar hypoplasia, encephaloceles, and cortical dysplasias are frequent. Absence of the olfactory bulbs and tracts is also rarely identified.[198] Dysmorphic features, especially of the head (macrocephaly/microcephaly) and face, are often noted.[185] Genital anomalies and delayed skeletal maturation are usually attributed to pituitary dysfunction.[185] Limb abnormalities such as constriction rings, syndactyly, and reduction deformity of the digits are not uncommonly described.[184,189]

Differential Diagnosis: Absence of the septum pellucidum is associated with various malformations, including HPE, ACC,

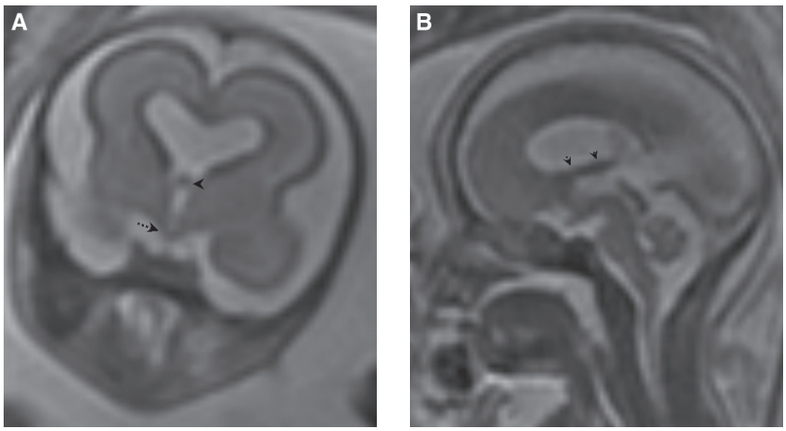

FIGURE 12.1-30: Fetus at 23 weeks with SOD. **A:** Coronal T2 image demonstrates absence of the septum pellucidum. The fornix is fused *(arrowhead)*. The optic nerves are identified *(dotted arrow)* but it is difficult to exclude hypoplasia. **B:** Sagittal T2 image from same fetus again demonstrates low position of fused fornix *(arrows)*. No pituitary abnormality was detected despite T1 imaging. The morphology in this fetus may be considered to be in the spectrum of lobar HPE. Note also absence of the secondary palate.

and predominately basilar encephaloceles.[197] Fusion of the hemispheres and basal ganglia, especially in the presence of facial anomalies, support the diagnosis of HPE. However, some cases of lobar holoprosencephaly overlap and may be difficult to separate from SOD.[199] In ACC, typical findings should be sought, including separated ventricles, colpocephaly, and radial array of medial sulci. Disruption of the septum can occur because of hydrocephalus from AS or Chiari malformations and in an encephaloclastic event, such as hydranencephaly and porencephaly.

Prognosis: The outcome for patients with SOD ranges from mild-to-severe endocrine and neurologic dysfunction. Isolated absence of septum is rare and even when present, most if not all have neurologic deficits.[196,200] Patients with complete absence of the septum pellucidum have worse neurological and developmental outcome than those with partial absence. Those with isolated optic nerve findings have good developmental prognosis.[200] However, in the presence of hemisphere abnormalities and posterior pituitary ectopia, the prognosis is more guarded.[200]

Endocrine abnormalities are variable, and 22% with abnormal septum and normal pituitary have endocrine dysfunction, versus 25% with normal septum and abnormal pituitary, and 56% with abnormal septum and pituitary. Overall, in 50% to 90% of patients with SOD, there is associated early or delayed hypothalamic–pituitary dysfunction, usually manifesting at a mean age of 4 to 5 years as growth retardation secondary to decreased levels of growth hormone and thyroid-stimulating hormone.[182,193,201] Rarely, individuals with SOD may exhibit precocious puberty.[201] Diabetes insipidus and hypoglycemia are less commonly associated.[183,201]

Visual symptoms include normal vision, decreased acuity or nystagmus. Neurologic deficits range from global retardation (55% to 78%) to focal deficits such as epilepsy (22%) or hemiparesis.[182,189,201] In addition, over half have behavioral disorders, nearly one-third diagnosed with autism.[189]

Management: Prenatal management includes possible termination of the pregnancy or no alteration of standard obstetrical care.[187] Early recognition of pituitary dysfunction is important. Low maternal serum and urinary estriol levels can suggest fetal adrenal insufficiency and aid in the diagnosis of SOD.[193] Hypopituitarism is a serious problem, and failure to recognize carries a risk of adrenal crisis, hypoglycemia, and death.[182] Given the possibility for later development of hormonal deficiencies, long-term follow-up is necessary.[189] Neurologic consultation is important in the presence of seizures or neurologic delay.

Recurrence: Most cases are sporadic with low recurrence risk at 2% to 3%.[202] The risk may be increased in the presence of familial transmission.

DISORDERS OF CORTICAL/CNS DEVELOPMENT

Cortical disorders are classified by the pattern of development, which includes the overlapping phases of cell lineage, proliferation, differentiation, migration, and organization (Table 12.1-7). In humans, cell lineage defines the basic cell type, and then proliferation takes place from 5 - 6 weeks in the ventricular zone after the neural tube is complete. Neuron and glial cells arise from neuroblast precursors primarily to 15 - 20 weeks (finished 30 weeks) through approximately 35 divisions. Differentiation of the neurons and glial cell into a refined cell type is followed by migration between 6 - 7 weeks to 20 - 24 weeks. Cortical organization starts at 22 weeks and continues until 2 years of age. It should be stressed that disorders of cortical development often present with multiple coexisting anomalies of neuronal transition. In these instances, the cortical disorder is described by the earliest disturbed developmental process.[203]

Table 12.1-7 Disorders of Cortical (CNS) Formation

Cell Lineage	*Abnormal*	Hemimegalencephaly Tuberous sclerosis
Proliferation	*Decreased*	Microcephaly/ microlissencephaly/ simplified gyral
	Increased	Macrocephaly/ megalencephaly
Differentiation	*Abnormal*	Cortical dysplasia CNS tumors
	Leptomeningeal	Arachnoid cyst
	Choroid	Choroid plexus cyst
	Neuroepithelial	Glioependymal cyst
	Vascular	Vein of Galen
Migration	*Undermigration*	Lissencephaly Heterotopia
	Overmigration	Congenital muscular dystrophy
Organization	*Deranged*	Polymicrogyria Schizencephaly

Pathology related to cortical development is caused by lack of normal gene expression, production of an abnormal gene, or interruption of gene function via infection or ischemia.[204] Unfortunately, the etiology is unknown in about 50% of cases.[203] At the same time as cortical development, differentiation and evolution of the leptomeninges, choroid, and intracranial vasculature is occurring. CNS pathologies in these areas will be inserted for completeness.

Disorders of Cellular Lineage

Hemimegalencephaly

Incidence: Hemimegalencephaly (HME) is a rare sporadic disorder. It is cited in 1 to 3 cases per 1,000 epileptic children and is equal in sex distribution.[205,206]

Pathogenesis: Hemimegalencephaly is a hamartomatous brain malformation characterized by overdevelopment and enlargement of all or part of one cerebral hemisphere (Fig. 12.1-31). In this disorder, cells are altered in their growth and/or differentiation with disorganization of the tissue architecture such that there is an abnormal gyral pattern in the affected hemisphere that may manifest as agyria, pachygyria, polygyria, and polymicrogryia. Hemimegalencephaly is isolated in approximately 53% to 66% of cases. In the remaining, it is seen in

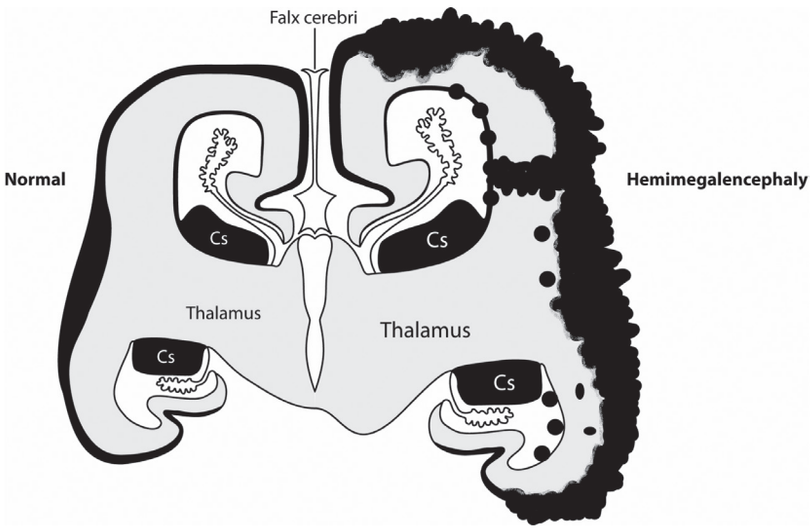

FIGURE 12.1-31: Hemimegalencephaly of the left hemisphere showing overgrowth with abnormal migration of gray matter and cortical development.

conjunction with neurocutaneous syndromes including epidermal nevus, Proteus, neurofibromatosis type I, hypomelanosis of Ito, Klippel–Weber–Trenaunay, and tuberous sclerosis.[206,305] In these syndromes, hemicorporal hypertrophy may be present. Total hemimegalencephaly is a rare form described in the presence of ipsilateral enlargement of the cerebral hemisphere, brainstem, and cerebellum.[207]

Current studies suggest that hemimegalencephaly occurs at 3 to 4 weeks' gestation because of a primary disturbance in cellular lineage and cell growth, with secondary effects being disturbed cell migration and organization.[205,208] A recent fetal pathologic evaluation of hemimegalencephaly found a normal number of cells in the proliferative zone.[205] Microscopically, the cells are immature or abnormal with mixed lineage and disturbed morphology, and there is a complete disorganization of the cytoarchitecture and loss of normal lamination with giant immature neurons and glial cells within the cortex and white matter.[205,208] Bizarre glial cells, or balloon cells, myelination delay, and white matter gliosis have been described postnatally.

Etiology: It has been hypothesized that genes involving neuraxis or body left right symmetry are involved in the disorder.[209] Advances in recent genetics have shown de novo somatic mutations in components of the phosphatidylinositol 3-kinase (P13K)-AKT mammalian target of rapamycin (mTOR) pathway in HME cases.[210] These genes, which include *AKT3, PIK3CA, PIK3R2,* and *MTOR,* are critical for regulation of cellular proliferation, size, and metabolism.[210] Several of these genes are also linked to overgrowth syndromes and tumors.

Diagnosis

Ultrasound: Prenatal diagnosis should be suspected in the presence of UVM, with the most commonly dilated area being the posterior horn of the lateral ventricle (Fig. 12.1-32A). The head circumference is increased, usually in the 90th percentile. In conjunction, midline shift, usually in the occipital area, is noted due to asymmetry of the cerebral hemispheres.[211] Three-dimensional multiplanar reconstruction may be helpful in detecting subtle asymmetry.[212] Sometimes, especially with 3D and transvaginal imaging, abnormal sulcation and cortical thickening along the affected hemisphere can be noted (Fig. 12.1-32B).

MRI: The enlarged hemisphere will have deformity of the lateral ventricle with diffuse dilatation and/or straightening or collapse of the frontal horn and/or disproportionate dilatation of the occipital horn (colpocephaly) (Fig. 12.1-32C,D).[207] The midline is straight or displaced contralaterally, especially in the occipital area. The white matter may be increased in volume and may demonstrate abnormal decreased signal because of heterotopia, gliosis, or abnormal myelination (Fig. 12.1-32D).[213] Sulcation is abnormal for gestational age, demonstrating thick cortex with too many lobulations or not enough, which later will manifest as polymicrogryria, pacygyria, and agyria. The dysplastic gray and white matter is typically heterogeneous, demonstrating increased and decreased T1 and T2 signals, respectively (Fig. 12.1-32E).[214] There typically is loss of normal fetal brain layering and blurring of gray white matter interfaces.[207] The corpus callosum, particularly on the affected side, may be thick (Fig. 12.1-32F).[207] Restricted diffusion can be present, likely owing to increased cellularity in the affected hemisphere.[215] In the presence of a mild case, the distribution may be primarily lobar. In 40% of cases of HME, enlarged deep and/or superficial veins can be seen along the enlarged hemisphere (Fig. 12.1-33).[207,216] The ipsilateral cerebellar hemisphere can be enlarged in 47%, although only 7% will demonstrate ipsilateral brainstem hypertrophy. Abnormal folia of the cerebellum may be identified bilaterally.[216] In 26% of cases, ipsilateral olfactory and in 3% optic nerve enlargement can accompany HME.[216] The opposite hemisphere may be smaller than normal and distorted due to midline shift.

Associated Anomalies: Of the neurocutaneous syndromes, epidermal nevus syndrome is the most commonly associated and typically presents with linear nevus, sebaceous nevus, and facial lipoma and hypertrophy typically on the affected

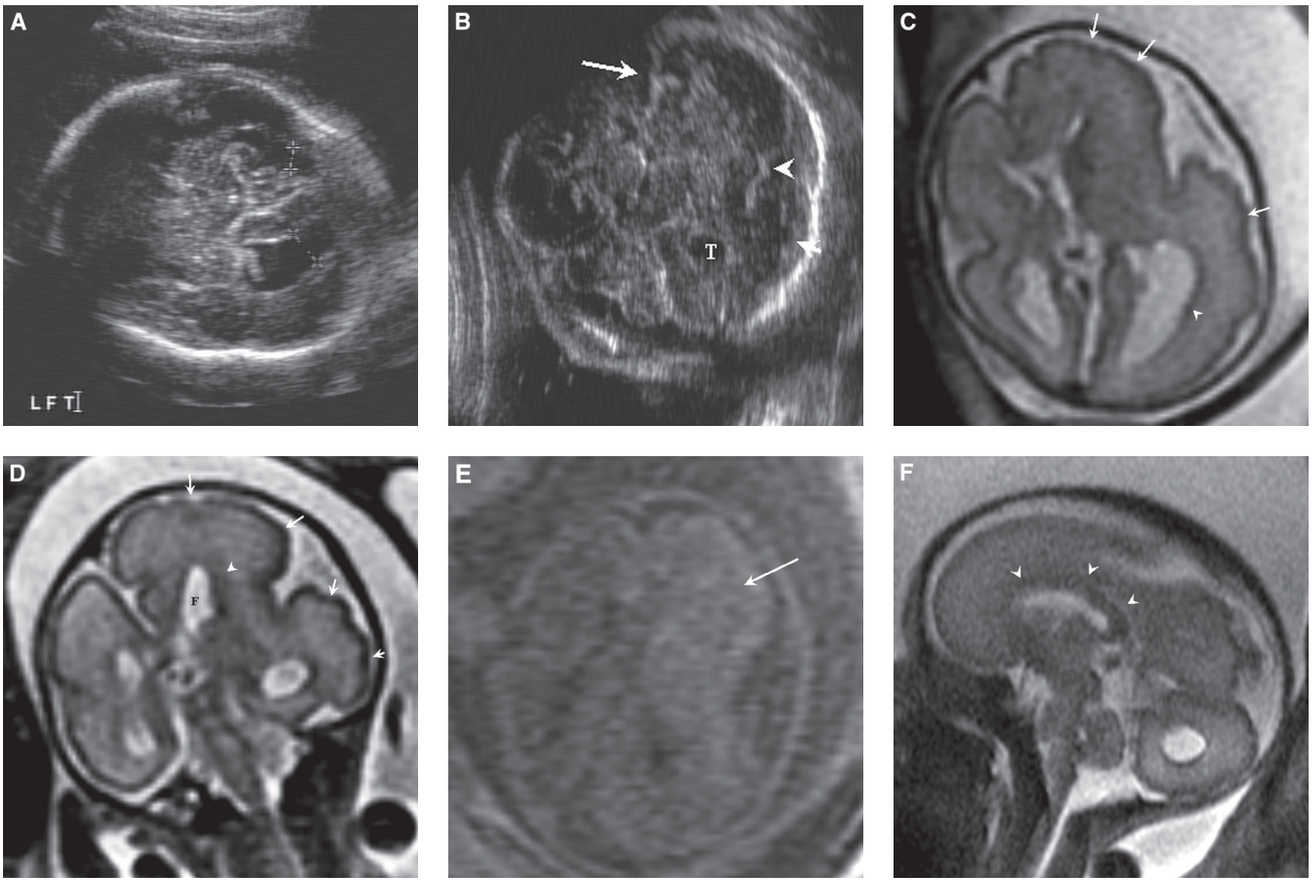

FIGURE 12.1-32: Hemimegalencephaly in a 29-week fetus. **A:** Axial US demonstrates mild dilatation of the left lateral ventricle at 11 m versus opposite of 7 mm. Note slight shift of the left occipital lobe across midline. Head circumference was increased. **B:** Coronal US demonstrates subtle asymmetry of sizes of the hemisphere with left larger than right and shift of midline falx *(arrow)*. The left temporal horn *(T)* is prominent. *Arrowheads* point to subtle lobulation along the cortex. **C:** Axial T2 MR demonstrates enlargement of the left hemisphere and dilated occipital horn. Note nodularity *(arrowhead)* along ventricle consistent with heterotopia. The cortex (*arrows*) demonstrates abnormal sulcation (compare with normal opposite side). **D:** Coronal image demonstrates straightened frontal *(F)* horn with abnormal dark signal *(arrowhead)* in the white matter consistent with disorganized neurons. There is again abnormal sulcation with blurring of normal gray white interface *(arrows)*. **E:** Axial T1-weighted image demonstrates increased T1 signal *(arrow)* in the abnormal hemisphere. **F:** Sagittal T2 demonstrates thickening of the corpus callosum *(arrowheads)*.

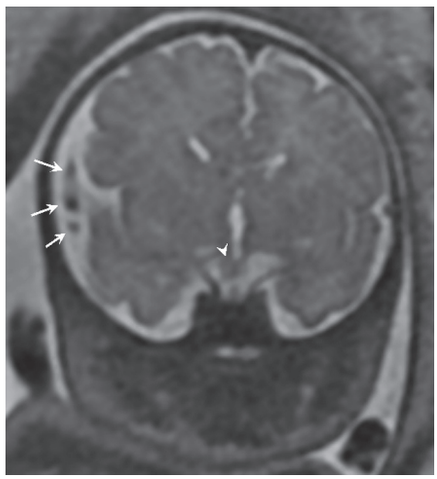

FIGURE 12.1-33: Subtle case of right HME in a fetus at 34 weeks. Notice prominent extra-axial space along the abnormal right hemisphere with large dilated veins *(arrows)*. The right optic chiasm is also enlarged *(arrowhead)*.

hemispheric side.[209] Abnormal vascular shunting over the enlarged hemisphere can lead to congestive heart failure.[213]

Differential Diagnosis: The main differential is cerebral hemisphere enlargement due to tumor or hemorrhage. Shift of midline structure also may be related to volume loss in one hemisphere.

Prognosis: Symptoms are similar in the isolated and syndromic children.[209] The worse developmental outcome has been correlated with the most severe cerebral asymmetry.[210,213] Those with severe HME are at risk of mortality in the first year of life.[207] However, most patients demonstrate developmental delay, psychomotor deficits, progressive hemiparesis, and intractable seizures.[205] The marked hyperexcitability of the dysplastic cortex results in catastrophic epilepsy, with seizures typically beginning in the first 6 months of life.[211] It has been found that the earlier the onset of seizures, the more severe motor and intellectual deficit in children with HME.[209]

Management: Therapy is directed to seizure control. Although anticonvulsant drug therapy may be utilized in mild cases, the

most common treatment option is surgery. In the past, anatomical total or partial hemispherectomy was performed but at a high morbidity secondary to development of hydrocephalus, intracranial hematomas, and infection.[205,206] Because of fewer complications, the most common surgical approach is now a functional hemispherectomy, a technique which involves disrupting internal capsule and corona radiata with resection and interruption of the mesial temporal structures, section of the corpus callosum, and frontal horizontal fibers.[214] After surgery, approximately 60% to 85% of children have control of their seizures.[210,214] With control of the seizures, there is improved intellectual and physical development.[211,214] For this reason, most advocate surgery as early as possible to preserve neurologic development.[214]

Recurrence: Hemimegalencephaly is mostly sporadic with low recurrence risk.

Tuberous Sclerosis

Tuberous Sclerosis, or Bourneville disease, is the second most common phakomatosis (after neurofibromatosis type 1), representing a neurocutaneous syndrome characterized by the formation of benign hamartomas and low-grade neoplasms in multiple organ systems, most notably the brain, heart, kidneys, and skin.

Incidence: Tuberous sclerosis (TS) has an autosomal dominant inheritance with variable expression and incomplete penetrance. The incidence is 1 in 10,000, and prevalence is 1 per 6,000 to 10,000 live births.[217] The disorder occurs equally in all races and both genders.

Pathogenesis: TS is characterized by widespread development of hamartomas in many different tissues owing to a disorder of cell lineage. TS is similar to hemimegalencephaly but has pathologically more cellular and nuclear pleomorphism and a potential for neoplastic formation.[208] Almost all patients with TS have cutaneous stigmata, with the most common and earliest being multiple hypopigmented macules known as ashleaf spots. Adenoma sebaceum, a misnomer, is present in 70% of TS patients, representing angiofibromas on the malar region of the face.[218] Brain lesions include subependymal nodules and cortical tubers, seen in infants in 93% and 88%, respectively, and, less commonly, white matter abnormalities and subependymal giant cell astrocytomas.[219] Tubers are hamartomas that exhibit disorganized cortical lamination with atypical giant astrocytes, maloriented neurons, and bizarre giant cells. Subependymal nodules represent dysplastic astrocytic and neuronal cells. White matter lesions are heterotopic neuronal and glial elements arrested in migration. Subependymal giant cell tumors develop in 10% to 15% of patients with TS but are rare prenatal.[220]

Cardiac rhabdomyomas are the most common cardiac tumors prenatally, with 39% to 80% associated with TS.[221,222] Rhabdomyomas usually present during the second or third trimester and are the most common fetal finding in TS.[219] Renal findings, which include cysts and angiomyolipomas (tumors composed of abnormal blood vessels, smooth muscle, and fat) are rare prenatally, usually developing during childhood and adolescence in approximately 61% of patients.[223] Diagnosis of TS is dependent on identification of two major or one major and two minor features in the complex (Table 12.1-8).

Table 12.1-8 Criteria for Diagnosis of Tuberous Sclerosis

Major Features	*Minor Features*
Facial angiofibroma or forehead plaque	Dental pits
Ungual/periungual fibroma	Hamartomatous rectal polyps
Hypomelanotic macules (>3)	Bone cysts
Shagreen patch	Cerebral white matter migratory tracts
Cortical tuber	Gingival fibromas
Subependymal nodule	Nonrenal hamartoma
Subependymal giant cell astrocytoma	Retinal achromic patch
Multiple retinal nodular hamartomas	"Confetti" skin lesions
Cardiac rhabdomyoma	Multiple renal cysts
Lymphangiomyomatosis	
Renal angiomyolipoma	

Diagnosis

Definitive: 2 major or 1 major plus 2 minor
Probable: 1 major plus 1 minor
Possible: 1 major or 2 or more minor

Etiology: TS is caused by mutations of either the *TSC1* or the *TSC2* gene located on chromosomes 9q34 and 16p13, respectively.[220] The gene products hamartin (*TSC1*) and tuberin (*TSC2*) act as tumor suppressors by negative feedback of the mTOR kinase cascade, whose activity is important in regulating cell growth and proliferation. There is high penetrance of the genetic abnormality, but phenotype expression is variable. Approximately 70% to 80% of TS cases are sporadic, resulting from de novo genetic mutations.[220,224] However, there are cases of recurrence in families of unaffected parents, suggesting a germline mosaicism.[225] *TSC2* mutations are more common, lead to a more severe phenotype, and tend to be spontaneous, while, the *TSC1* are less common and more likely to be familial.[218] Polycystic kidney disease is sometimes associated with TS as the gene responsible for this disorder lies adjacent to the *TSC2* gene.[220]

Diagnosis: Genetic testing for the *TSC1* and *TSC2* genes from amniotic fluid or chorionic villus sampling can be definitive in about 80% of mutations.[217] However, because of genetic heterogeneity, testing can have a false negative rate of 10% to 20%.[225] Imaging is often helpful for detection and diagnosis.

Ultrasound: About 80% of fetuses with TS have rhabdomyomas, usually presenting during the second or third trimester, as early as 20 weeks.[225] Rhabdomyomas are typically round, homogeneous echogenic intraluminal and sometimes intramural masses, often located in more than one cardiac chamber but usually along ventricular walls or septum (Fig. 12.1-34A).[224,226] Brain lesions may be present but can be inconspicuous on prenatal US. If identifiable, brain lesions present as an echogenic mass along the

lateral ventricular wall or a focal area of echogenicity in the brain parenchyma (Fig. 12.1-34B).[227] Renal masses are rarely detected prenatally but include cysts, multiple cysts as in polycystic kidney disease, or focal smooth echogenic lesions in the renal cortex, consistent with angiomyolipomas (Fig. 12.1-34C).[228]

MRI: On prenatal MRI, cortical tubers and subependymal nodules are the most common CNS lesions detected with an incidence of 33% to 62%.[220] Other TS lesions, including white matter abnormalities and subependymal astrocytomas, are less frequent. Prenatal imaging is limited by spatial resolution, and small subtle lesions can be missed.[229] However, both T1 and T2 imaging are important as T1 signal abnormality may be most easily seen.[226,229] In the fetus, the tubers are present in the cortex and/or subcortical white matter of primarily the supratentorial brain and demonstrate wedge-shaped or banded areas of increased T1 and decreased T2 signal, opposite of a myelinated child or adult (Fig. 12.1-34D,E).[229,230] Subependymal nodules can be detected prenatally but may not be evident as many develop through the first decade of life. Subependymal nodules, when present, dot the ependymal surface of the lateral ventricles, especially near the caudate and foramen Monro, and are isointense to gray matter being T1 hyperintense and T2 hypointense (Fig. 12.1-34C,F).[229,230] It is important to verify these lesions in two anatomic planes as motion artifact can mimic a lesion. Ninety percent of subependymal lesions do mineralize, but prenatal diagnosis is unlikely as most do not calcify until 1 year of age.[220,225] Subependymal giant cell astrocystomas are rare prenatally but typically arise near the foramen of Monro, measure greater than 5 mm, grow and can obstruct the ventricular system.[220] Associated rhabdomyomas are isointense to cardiac muscle on T1 and T2 images (Fig. 12.1-34G). Renal lesions may be heterogeneous or follow cystic characteristics (dark T1 and bright T2) (Fig. 12.1-34H).

Associated Anomalies: Retinal hamartomas occur in 40% to 50% of patients, with one-third bilateral.[231] Harmartomatous gastrointestinal polyps and oral gingival fibromas can develop. Patients with TS are at increased risk for arterial aneurysms, including aorta, peripheral and intracranial. Pulmonary manifestations are present in 1% to 26% of patients, with the most common being lymphangiomyomatosis.[231] Sclerotic and cystic bone lesions and ungal fibromas adjacent to or underneath the nail bed are sometimes noted.

Differential Diagnosis: In the presence of a cardiac mass, the most common differential is a fibroma that is typically solitary T2 hypointense and can be seen with orofacial abnormalities and Gorlin syndrome. Intracranial lesions, especially when solitary, should be differentiated from subacute hemorrhage, tumor, congenital infection, ischemia, or cortical dysplasia of other cause. When lesions are defined along the ventricle, germinal matrix hemorrhage or gray matter heterotopia should be considered.

Prognosis: TS increases the risk for adverse maternal and perinatal outcomes; thus close surveillance is indicated.[221] Cardiac rhabdomyomas tend to increase in size in utero and regress after delivery, with 80% resolving in infancy or early childhood.[221,224] Most are well tolerated with only a 4% to 6% risk of fetal demise.[224] In the presence of a large lesion >3 cm, fetal dysrythmia and/or compromised fetal cardiac function due to tumor obstruction, prenatal medication, early delivery, and/or surgery may be indicated. Preterm delivery in TS is as high as 35% and cesarean delivery is reported at 33%.[221]

The clinical triad of TS, *epilepsy*, *mental retardation*, and *facial angiofibromas*, is actually noted in only 30% to 40% of patients.[220] The most common cause of morbidity is neurologic, with seizures in 90%, mental retardation in 50%, developmental delay, behavioral problems, and autism in 25% to 50%.[220] Postnatally, there is a correlation between number, size, and, importantly, volume of cerebral lesions and neurodevelopmental outcome.[232] However, it is more difficult to predict outcome prenatally, given lower resolution in fetal imaging and the possibility of lesions developing later in pregnancy and postnatal.[222] TS-associated renal disease also increases the risk of perinatal complications, including renal failure, polyhydramnios, and oligohydramnios. Postnatal, renal complications are the most common cause of death, with 10% developing renal failure or hypertension.[220] Angiomyolipomas that are present in 60% to 80% of TS patients are benign but can cause morbidity in about 10% of cases because of catastrophic hemorrhage, either spontaneous or in the presence of minimal trauma.[218] Polycystic renal disease is noted in 5% of TS patients and confers a worse prognosis.[220] Renal carcinomas are seen in 2% to 3% of patients.[220] In female patients postmenarchal, lymphangiomyomatosis of the lung can develop because of smooth muscle cell metastasizes, with 5% progressing to end-stage lung disease.[220]

Management: Diagnosis, screening of family members, and appropriate counseling is indicated. Termination may be considered. Close surveillance during the pregnancy is warranted. In the presence of a complicating rhadomyoma, early delivery may be necessary. Brain imaging and abdominal imaging should assess for neoplasm, complicating renal tumors, and vascular malformations, including aneurysms. Anticonvulsants and surgical resection of tubers are treatments for epilepsy. Rapamycin inhibits mTOR pathway and causes regression of giant cell astrocytomas and may be helpful in the treatment of rhabdomyomas, angiomyolipomas, and lymphangiomyomatosis.[218,231] Embolization of symptomatic or large angiomyolipomas may be necessary.

Recurrence: The recurrence risk of an unaffected parent having a child with TS is 2% to 3%.[225] In the presence of an affected parent, transmission is 50%.

Disorders of Cellular Multiplication/Proliferation

Microcephaly

Synonyms: Microcephaly vera, true microcephaly, radial microbrain, microcephaly with simplified gyral pattern, oligogyria, microlissencephaly.

Microcephaly implies a small head size whereas micrencephaly represents a small brain. In the past, microcephaly has been defined when postnatal head circumference was two standard deviations (SD) or more below the mean, being below the third percentile.[233] More recent data suggest that microcephaly should have a cut-off of −3 SD below the mean.[233]

Incidence: Birth incidence is estimated at 1 in 5,400 to 8,500 newborns.[234,235] Higher occurrence is noted with parental consanguinity. Microcephaly may present prenatally; however, a significant number of cases develop postnatal.

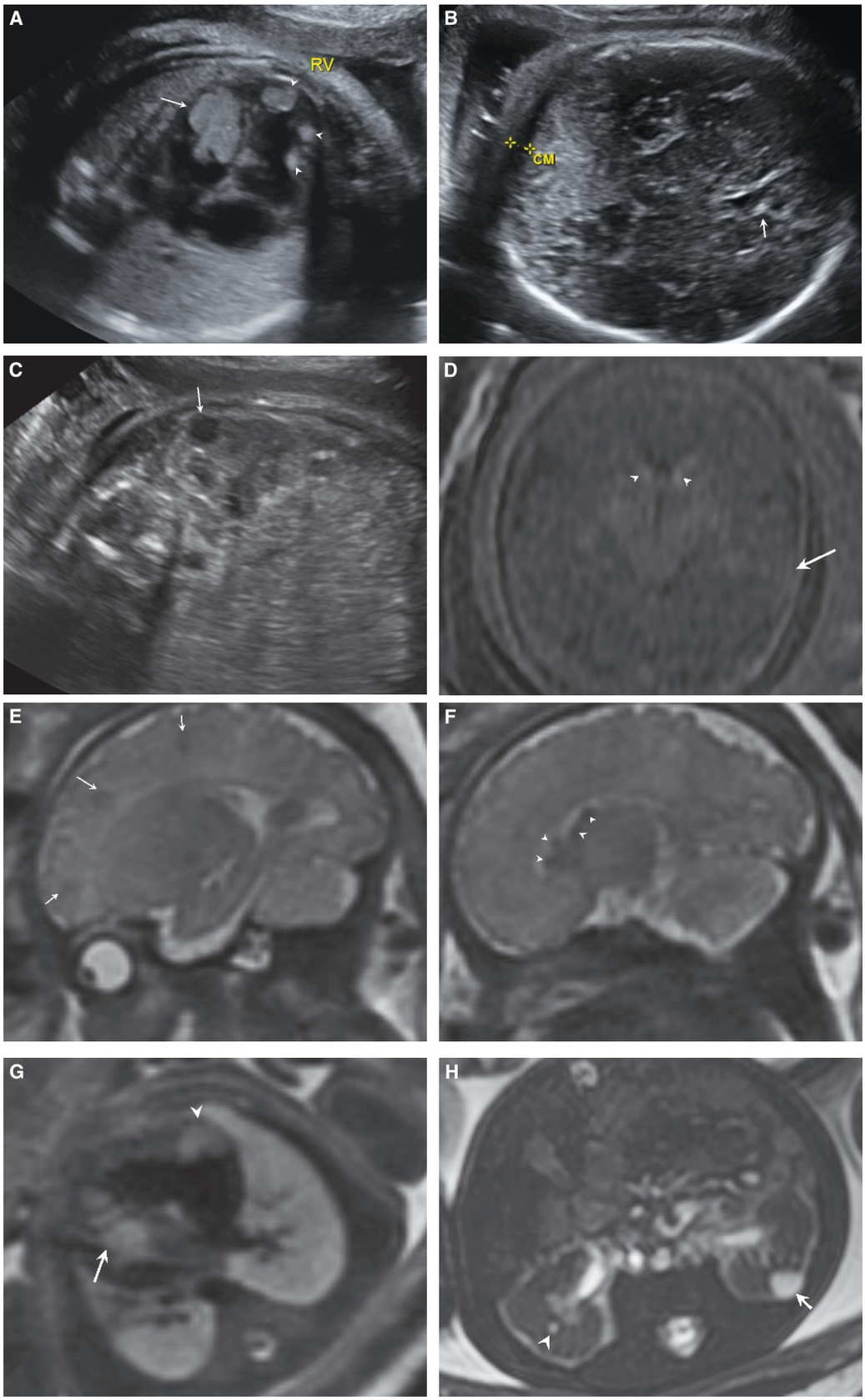

FIGURE 12.1-34: Tuberous sclerosis in a fetus at 35 weeks. **A:** Axial US demonstrates multiple homogeneous echogenic masses in the right ventricle *(arrowheads)* and large mass in the left ventricle *(arrow)*. **B:** Axial cranial image shows the area of the foramen Monro with questionable nodularity *(arrow)*. **C:** Axial image of the left kidney demonstrates the presence of a cyst *(arrow)*. **D:** Axial T1 image in the fetal brain demonstrates a band of T1 signal in the left hemisphere consistent with parenchymal tuber *(arrow)*. Also note small hyperintense lesions at the foramen of Monro *(arrowheads)* consistent with small subependymal tubers. **E:** Sagittal T2 image shows focal areas of dark signal *(arrows)* consistent with tubers. **F:** Sagittal T2 demonstrates dark round nodules *(arrowheads)* near the foramen of Monro consistent with subpendymal tubers. **G:** Axial T2 image shows T2 hyperintense masses in the left *(arrow)* and right ventricles *(arrowhead)* consistent with rhabdomyomas. **H:** Axial SSFP image through the kidneys confirm left renal cyst *(arrow)* but also defines an additional small right renal lesion *(arrowhead)*.

Kline9781451175837-ch012.1.indd 375 08/08/14 9:58 AM

Pathogenesis: Microcephaly results from multiple pathologies that cause either decreased cell production or increased programmed cell death in the germinal zones. Microcephaly can be syndromic, often with other anomalies, or isolated. Primary or congenital microcephaly is typically genetic whereas secondary microcephaly occurs as a result of a destructive insult. Currently, most primary microcephaly pathologies are classified and grouped by the genetic disorder and clinical findings.[203]

In primary or congenital microcephaly, the brain may have a well-preserved gyral pattern or abnormal gyral pattern.[236] Microcephaly without extracerebral malformation in the presence of a small architecturally normal brain and normal gyral pattern is known as true microcephaly or microcephaly vera. Microcephaly with simplified gyral pattern is likely in the continuum of true microcephaly demonstrating reduced gyri, shallow sulci, normal cortical architecture, and normal or reduced thickness cortex. There is a strong correlation between the degree of microcephaly and the presence of a simplified gyral pattern and white matter volume loss.[237] Microlissencephaly is a term that has been utilized previously to describe a brain with abnormal gyration and thickened cortex due to a cortical migrational rather than solely proliferation anomaly. This term is confusing and should be avoided.[237] These pathologies are included here as the earliest insult is abnormal proliferation, which is then associated with disturbed migration. Some currently utilize the term lissencephaly type III to describe a thickened cortex in the presence of severe microcephaly.

Etiology: The cause of microcephaly is heterogeneous. Microcephaly may result from chromosomal or genetic disorders or environmental factors that are destructive (Table 12.1-9). Many new loci are being identified, the most common mode of transmission being autosomal recessive.[238] It has been estimated that 20% to 35% of idiopathic microcephaly is hereditary.[239] Genetic associations with microcephaly cannot be completely listed here as more than 500 associations are described in online Mendelian inheritance in man (OMIM). Excluding HPE, in a group of fetuses with microcephaly, 28% have been shown to have abnormal fetal karyotype, 24% genetic syndrome, 28% with complex anomalies, and 20% isolated.[240] The etiology for microcephaly may be detected in only as high as 57%.[241]

Table 12.1-9 Causes of Microcephaly

Microcephaly with Thin Cortex

Genetic

- *Isolated*
  - Autosomal recessive, dominant, X linked
- *Syndromic*
  - Chromosomal
    - Trisomy 21, 13, 18
    - Gene Deletions
      - Wolf-Hirschhorn
      - Williams
      - Miller-Dieker
  - Others
    - Smith–Lemli–Opitz
    - Cornelia de Lange
    - Feingold
    - Lymphedema, microcephaly, chorioretinopathy

Environmental

- Hypoxic, vascular, intrauterine infection
- Teratogens
  - Alcohol
  - Hydrantoin
  - Radiation
  - Maternal phenylketonuria
  - Maternal diabetes

Microcephaly with Thick Cortex (Lissencephaly III)

- Norman Roberts syndrome
- Barth syndrome
- Seckel syndrome
- Primordial osteodysplastic dwarfism (MOPD 1)

Diagnosis

Ultrasound: Prenatal diagnosis may be challenging, particularly in the second trimester, as head measurements may be normal until the third trimester, usually after 27 to 28 weeks.[242,243] Antenatal diagnosis may be lower than 60%.[235] Most concur that fetal microcephaly should only be diagnosed when the head circumference (HC) is smaller than 3 SD below the gestational mean.[242,244] In a recent study by Malinger, there was no deficit in neuropsychological outcome with isolated microcephaly with head circumference −2 to 3 SD below the mean.[244] A biparietal diameter (BPD) and fronto-occipital diameter −3 SD below the mean has also been utilized but can be falsely positive in the presence of calvarial deformity.[243] Because more than half of fetuses with microcephaly are small for gestational age, more than half of HC/abdominal circumference and one-third of HC/femur length ratios are situated within normal range.[240,241]

Sonographic findings that may be helpful include small frontal lobes, sloping forehead, enlarged subarachnoid spaces, and VM due to neuronal loss (Fig. 12.1-35A,B).[233,245] Frontal lobe dimensions in the plane of the BPD from the posterior margin of the cavum septum pellucidum to the inner midline fetal skull can identify small frontal lobes and help diagnose microcephaly.[235,246] Sometimes, fetuses with microcephaly have narrow sutures and closed fontanelles providing restricted visibility. However, the brain should be imaged through available windows to exclude abnormal morphology, echos, calcification, and hemorrhage. Poor visualization or smaller caliber of the anterior cerebral circulation when compared with the posterior circulation on Doppler may be helpful.[245] Most cases of microcephaly (83%) are complex; therefore, associated anomalies should be excluded.[240]

MRI: A small craniofacial ratio is present, and decreased fronto-occipital and biparietal diameters may be present (Fig. 12.1-35C). In the presence of simplified gyral pattern, MRI early in pregnancy can be diagnostically difficult. Delayed sulcation can be detected after 26 weeks, but confirmation may require imaging after 30 weeks.[247] MRI will identify wide and shallow primary and secondary sulci, especially in the frontal lobes, and absent tertiary fissures (Fig. 12.1-35D).[248,249] The cortex is usually thin (normal 3 to 4 mm), but in some cases can be thick. There is also usually white matter volume loss and mild-to-moderate ventricular dilatation with obliquity of the lateral ventricles. The corpus callosum, brainstem, and cerebellum can be abnormal. Cortical migrational defects should be excluded.

Kline9781451175837-ch012.1.indd 376 08/08/14 9:58 AM

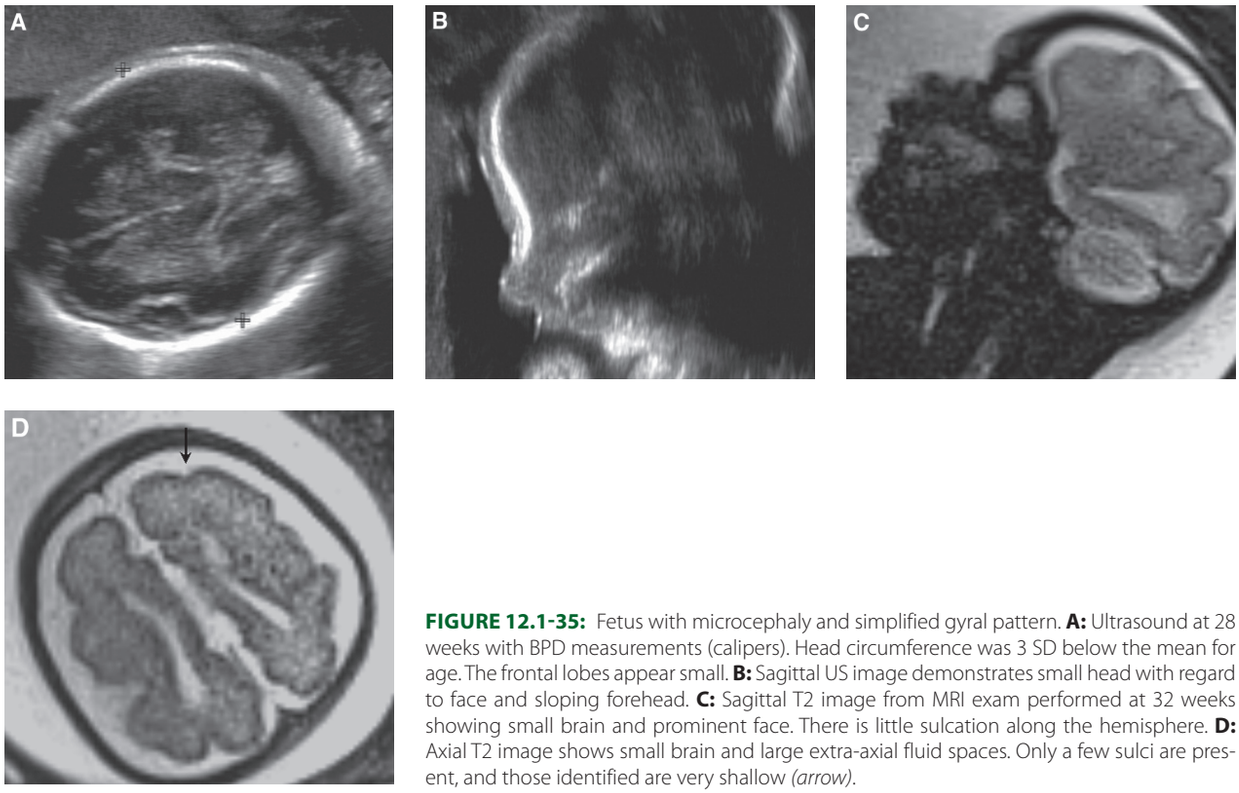

FIGURE 12.1-35: Fetus with microcephaly and simplified gyral pattern. **A:** Ultrasound at 28 weeks with BPD measurements (calipers). Head circumference was 3 SD below the mean for age. The frontal lobes appear small. **B:** Sagittal US image demonstrates small head with regard to face and sloping forehead. **C:** Sagittal T2 image from MRI exam performed at 32 weeks showing small brain and prominent face. There is little sulcation along the hemisphere. **D:** Axial T2 image shows small brain and large extra-axial fluid spaces. Only a few sulci are present, and those identified are very shallow *(arrow)*.

Associated Anomalies: Microcephaly is often associated with other cortical malformations including agyria, pachygyria, polymicrogyria, and gray matter heterotopia. Agenesis/hypogenesis of corpus callosum, delayed myelination, and dysplasia/hypoplasia of the cerebellum and brainstem may be present.[236,238] In Cohen syndrome, a thick corpus callosum is present with microcephaly.

Differential Diagnosis: Holoprosencephaly and lissencephaly have abnormal gyral pattern and often present with microcephaly.[240] Microcephaly can also be seen in conjunction with encephaloceles and craniosynostosis.

Prognosis: Prenatal head circumference −3 SD below the mean correlates with microcephaly postnatally; however, those between 2 and 3 SD below may not correspond.[242,244] An occipitofrontal circumference of more than 2 SD below the mean in the past has been considered microcephaly postnatal; however, this value includes 2% of normal individuals with normal cognitive outcome. Evaluation of family head circumference should be considered as small head size may be a normal developmental variant.[236]

Severity of mental delay is related to the severity of microcephaly with median IQ decreasing linearly with head circumference.[244,250] Microcephaly in the presence of abnormal karyotype or intrauterine infection has a poor outcome.[233] The presence of abnormal gyral pattern and/or associated anomalies has also been shown to have a negative impact on outcome.[34,48] Children with microcephaly and preserved gyral pattern demonstrate mild delay in early development, some difficultly with feeding, and limited language skills.[236,238] Those with a simplified or abnormal gyral pattern have a more severe clinical course, including poor feeding, severe developmental delay, intractable epilepsy, and early death.[238] Perinatal mortality for children with microcephaly has been quoted as high as 70%.[240]

Management: Microcephaly is not treatable. Evaluation of family head circumference is important as similar small head in the fetus may be a developmental variant. Genetic testing should be performed. Termination of the pregnancy may be considered, depending on chromosomal studies and associated anomalies; however, delayed third trimester diagnosis may limit possibility. Postnatally, children with mild microcephaly usually require special schooling, intensive speech therapy, and early psychomotor support.[247] Children with more severe microcephalies require anticonvulsive therapy and nasogastric tube feeding.[247]

Recurrence: Recurrence risk is 25% in the presence of primary microcephaly.[238]

Macrocephaly/Megalencephaly

Macrocephaly is noted when head circumference is above the 98th percentile or more than 2 standard deviations (SD) above the mean. Megalencephaly indicates a large brain with weight or volume greater than 98th percentile or ≥2 SD above the mean.

Incidence: Limited data quote isolated macrocephaly in 0.5% of the population.[251]

Pathogenesis: Macrocephaly occurs because of increased neuronal and glial cell proliferation and/or faulty apoptosis. Most cases do not become apparent until the last trimester of pregnancy or postnatally.[252]

Etiology: Benign familial macrocephaly accounts for approximately 50% of the cases and is transmitted autosomal dominant.[233,253] Megalencephaly may be associated with over 200 genetic syndromes, many of which are difficult to diagnose prenatally.[252,253] Common genetic disorders with enlarged head size include overgrowth, cutaneous, and polymicrogyria syndromes.[236] Rarely, macrocephaly may be related to chromosomal microdeletions.[252]

Diagnosis

Ultrasound: Prenatal US diagnosis of macrocephaly has been detected as early as 18 weeks.[254] However, most fetuses with macrocephaly have a normal second-trimester head circumference, and diagnosis is not made until late in the pregnancy or postnatally.[252] Fetuses with larger head circumference (HC) and associated anomalies due to associated syndromes will tend to be identified earlier (28 weeks) versus those with isolated macrocephaly (32 weeks).[252] When macrocephaly is identified, head circumference growth will be proportional rather than accelerated.[254] Note should be made that enlarged fetal head circumference has low specificity, with only 67% of children diagnosed prenatally having large head circumference postnatally.[251] Some of this variation is technical, related to limitations in accuracy of HC but also inconsistencies between prenatal and postnatal derived HC growth curves.[251] Most fetuses with macrocephaly will be large for gestational age.[252]

MRI: Similar findings are present, including increased craniofacial ratio and head measurements for gestational age. Mild ventriculomegaly and enlarged extra-axial fluid spaces are often present and in isolation are common for benign macrocephaly (Fig. 12.1-36).[252] In syndromic cases, frontal bossing, callosal anomalies, including thick corpus callosum, and cortical migrational abnormalities may be present. A thick corpus callosum has been linked to enlarged white matter, and can be seen in syndromes such as neurofibromatosis type I and macrocephaly–capillary malformation.[255] In the presence of additional white matter signal abnormality and significantly enlarged extraaxial spaces, glutaric aciduria type 1 should be considered.[256]

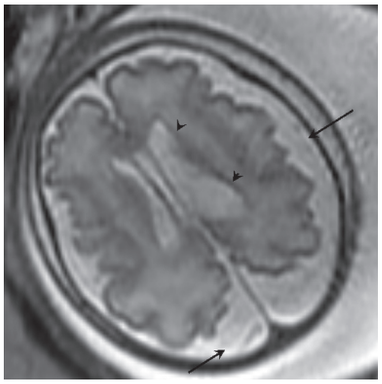

FIGURE 12.1-36: Macrocephaly of unknown origin in a fetus at 33 weeks. Head circumference on US was at 3 SD above the mean. MRI biparietal and fronto-occipital dimensions were increased. Axial T2 image demonstrates enlarged extra-axial fluid spaces *(arrows)* and mild asymmetric left lateral ventricular dilatation *(arrowheads)*.

Associated Anomalies: Macrocephaly is present in the overgrowth syndromes, which include Sotos, Weaver, Simpson–Golabi–Behmel, Gorlin, Macrocephaly-cutis marmorata telangiectatica, and Beckwith Wiedemann. Many of these fetuses are at increased risk for brain, heart, limb, and spine anomalies.[253] Fragile X is also an overgrowth syndrome in white males with facial abnormalities.[257] Cutaneous syndromes, presenting with soft tissue masses, related to mutations in the PTEN (phosphatase and tensin homolog deleted on chromosome TEN) include Bannayan–Riley-Ruvalcaba and Cowden syndrome. Neurofibromatosis type I has cutaneous café au lait lesions and nerve sheath tumors and neuro-cardio-facial-cutaneous syndromes, such as Noonan and LEOPARD, may have heart, face, or soft tissue abnormalities.[257]

Differential Diagnosis: Macrocephaly may be secondary to other pathologies, including hydrocephalus, triploidy, and intracranial neoplasms. Disproportionate head size due to intrauterine growth restriction should also be considered.

Prognosis/Management: Prognosis is dependent on associated anomalies, etiology, and head size.[252] Prenatal head circumference between 2 and 3 SD above the mean is typically isolated and has a good outcome, while a head circumference >3SD is more likely to be syndromic with developmental delay.[251,252] Children with isolated, particularly familial, macrocephaly usually have normal intelligence with enlarged CSF spaces normalizing by 3 to 4 years of age.[233,251,257] Macrocephaly in the presence of a syndrome is often associated with abnormal development. In 3% to 10% of children with overgrowth syndromes, there is risk for neoplasms.[253]

Management: Prenatal evaluation should include family history and parental/sibling head circumference measurements to evaluate for benign familial macrocephaly. Amniocentesis for karyotype and microarray may be considered. Postnatal imaging and evaluation by appropriate pediatrician and clinical geneticist is suggested.[254]

Recurrence: Type of genetic transmission guides recurrence risk.

Disorders of Cellular Differentiation

CNS Tumors

Incidence: The overall incidence of perinatal brain tumors range 1.4 to 3.6 per 100,000.[258] Fetal intracranial tumors are very rare, accounting for approximately 0.5% to 1.9% of intracranial tumors in childhood.[259] Brain tumors represent only 10% of all antenatal tumors.[260]

Pathogenesis: Fetal intracranial tumors are "congenital tumors" that have a different pathophysiology than typical pediatric neoplasms. Normal embryonic cells have a high mitotic rate like neoplasms. Fetal tumor development is believed to be due to lack of normal cellular differentiation and maturation of these embryonic cells. In the presence of high mitotic activity, it is not surprising that many of these lesions, whether benign or malignant, grow rapidly and reach enormous proportions. Fetal tumors are also different in prevalence, location, histologic, and biologic behaviors (Table 12.1-10).[259,260] Unlike pediatric tumors, fetal masses tend to be supratentorial, either cerebral

Table 12.1-10 Types of Fetal Brain Tumors, Prevalence, and Location[259,260]

Type	Prevalence (%)	Location
Teratoma	42	Cerebral hemisphere, suprasellar, pineal
Astryocytoma	25	Cerebral hemisphere, basal nuclei
Craniopharyngioma	11	Suprasellar
Primitive neuroectodermal	10	Cerebral hemisphere, cerebellum
Choroid plexus papilloma	5	Intraventricular
Meningeal	4	Extraaxial
Ependymoma	3	Ventricular

hemisphere, suprasellar, or pineal; however, many are undetermined because of size and extent.[260,261] The type of tumor histology is also different, with teratomas being the most common.[259] Fetal tumors often cause demise because of their size and location, inhibiting normal organ development. Large tumors may result in cardiovascular compromise and hydrops.

Etiology: *Teratomas* represent abnormal development of pluripotent cells of three germ layers and immature neuroglial elements, can be benign or malignant, and often arise along the midline. There are several forms described: large replacing all intracranial contents, small with hydrocephalus, or as bulky lesions with extension into orbit, oropharynx, or neck.[259] Because many are very large, it is difficult to identify site of origin, but when determined most are in cerebral hemispheres, third or lateral ventricles, and the pineal region. The lesions are complex, containing solid and cystic areas with or without calcification.

Astrocytomas are composed of astrocytes of varying degrees of differentiation, from low-grade to high-grade. Unlike pediatric aged tumors, fetal astrocytomas are found supratentorial rather than posterior fossa.[259] Glioblastomas (malignant/high-grade astrocytoma) represent greater than 50% of fetal astrocytomas and are found in the cerebral hemisphere and basal nuclei.[259] Hemorrhage and rapid growth are a common findings.

Craniopharyngiomas are epithelial tumors which arise from Rathke pouch, an ectodermal diverticulum important for development of the pituitary gland. Tumors are usually suprasellar and heterogeneous, frequently containing calcification.

Primitive neuroectodermal tumors (PNET) are a group of small blue cell malignant lesions which are believed to arise from the neural crest cells of the nervous system and soft tissues. There is overlap of this group with atypical teratoid/rhabdoid tumors (ATRT), with cells mimicking a rhabdomyosarcoma. These tumors may arise in the cerebral hemispheres or cerebellum, are very aggressive, and metastasize early to the cerebral spinal fluid and meninges. Extensive hemorrhage and necrosis in a very large mass is common.

Choroid plexus papillomas are composed of mature epithelial cells which line the ventricular choroid plexus. Papillomas are benign and most common prenatally, although carcinomas have rarely been encountered. These lesions are nodular, cauliflower-like lesions typically in the lateral, less likely third or fourth ventricle. The tumor is vascular and secretes CSF, and therefore can cause rapid onset hydrocephalus.

Meningeal are benign or malignant mesenchymal tumors arising from the meninges of primarily the middle and less likely anterior or posterior cranial fossa. Hemangiopericytoma is the main histology. The lesion may create a large bulge in the skull with cranial asymmetry.

Ependymal lesions arise from the ependymal cells lining the ventricles or spinal cord central canal. Most are very cellular, and ependymoblastomas, which overlap with PNET, are described. These lesions also metastasize to the CSF pathways and tend to have extensive necrosis with location in the lateral and fourth ventricles.

Diagnosis

Ultrasound: Most fetal tumors present in the third trimester of pregnancy, with 60% diagnosed later than 30 weeks' gestation.[262] US may be obtained because of a sudden increase in maternal uterine size. Polyhydramnios, owing to decreased fetal swallowing, and macrocephaly are the typical presenting signs.[263]

Initial imaging findings include macrocephaly and intracranial mass (Fig. 12.1-37A). The third most common is hydrocephalus (Table 12.1-11). Masses, in general, displace midline structures and distort normal anatomy. In the presence of an enormous lesion, it may not be possible to identify normal cerebrum, midline structures, or ventricles (Fig. 12.1-37B,C).[258,264] The most common etiology for a large mass and undefined origin is teratoma.

Most tumors are heterogeneous rather than homogeneous echogenic. Heterogeneous lesions often have cystic or necrotic areas and the differential of teratoma, craniopharyngiomas, astrocytomas/glial tumors, PNET, and ependymal mass. In the presence of a primarily cystic lesion, teratoma is the prime consideration, but sometimes the mass may be difficult to discern from benign cystic lesions.[264] Calcification in a heterogeneous mass can point to teratoma or craniopharyngioma. A homogeneous vascular echogenic lesion, especially intraventricular with hydrocephalus, would support choroid plexus papilloma (Fig. 12.1-38A).[265] Doppler typically demonstrates vascularization in a mass, although a minor amount may show no Doppler signal, and thus it can be difficult to exclude hematoma.[265] Location may help with diagnosis. The overall accuracy in diagnosis of cell type by US is approximately 57%.[264]

MRI: MRI is ideally suited in the evaluation of fetal tumors and can confirm diagnosis. The internal architecture and extension of the tumor are better assessed by MRI than US.[265] Identification of tumor location and presence of additional lesions may help in definition of cell type. Most lesions are heterogeneous, being isotense on T1-weighted images and hyperintense on T2-weighted images.[265] Choroid plexus papillomas are lobular homogeneous iso-hyperintense on T1 and hypointense on T2 imaging (Fig. 12.1-38B). The solid tissue in PNET and ependymomas may be T1 and T2 isointense to gray matter (Fig. 12.1-39A,B). The presence of hemorrhage, which is described in 3% to 18% of intracranial masses, is most commonly observed in glioblastoma and PNET.[258] Hemorrhage can be detected on T1 seqeunces as bright signal and gradient echo images with susceptibility artifact (Fig. 12.1-39C).[266] Punctate dark areas on T2, bright areas on T1, or susceptibility artifact on gradient echo may define foci of calcification. Diffusion-weighted

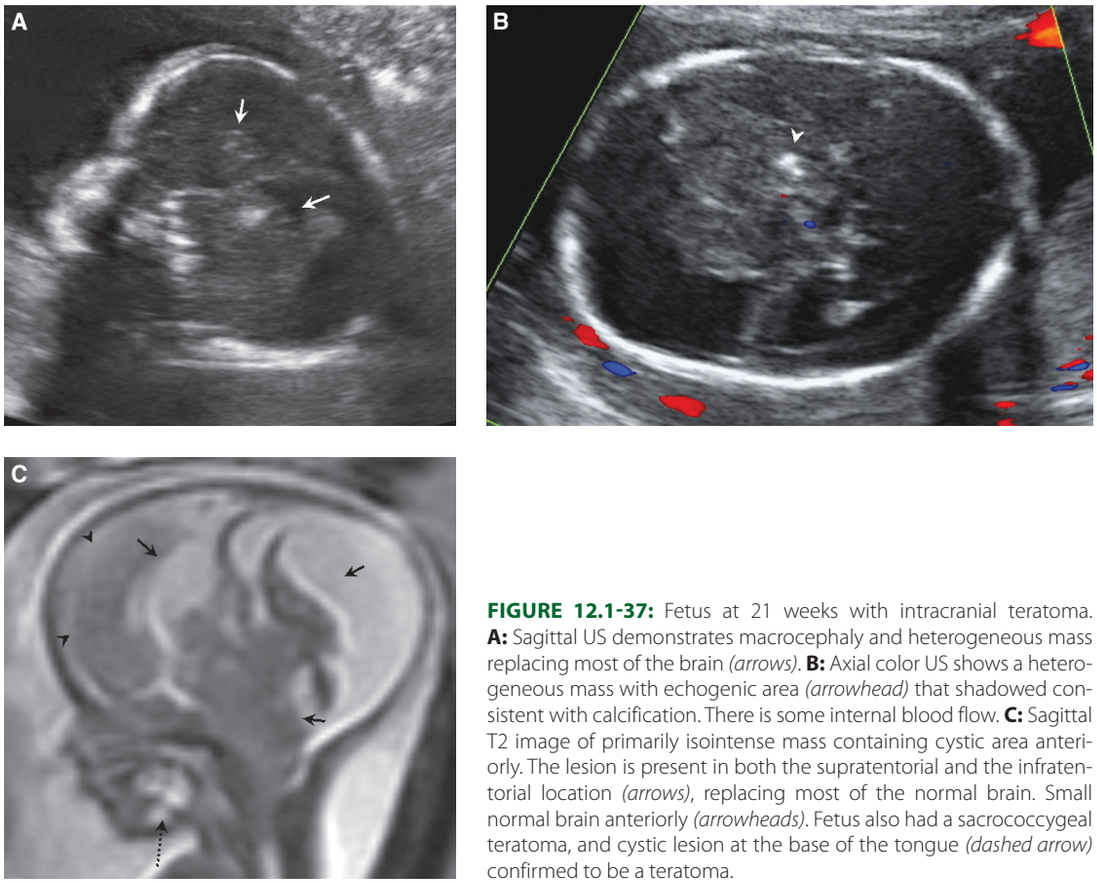

FIGURE 12.1-37: Fetus at 21 weeks with intracranial teratoma. **A:** Sagittal US demonstrates macrocephaly and heterogeneous mass replacing most of the brain *(arrows)*. **B:** Axial color US shows a heterogeneous mass with echogenic area *(arrowhead)* that shadowed consistent with calcification. There is some internal blood flow. **C:** Sagittal T2 image of primarily isointense mass containing cystic area anteriorly. The lesion is present in both the supratentorial and the infratentorial location *(arrows)*, replacing most of the normal brain. Small normal brain anteriorly *(arrowheads)*. Fetus also had a sacrococcygeal teratoma, and cystic lesion at the base of the tongue *(dashed arrow)* confirmed to be a teratoma.

imaging is often positive in the presence of PNET and may be helpful in identification of metastasis (Fig. 12.1-39D).[266]

Associated Anomalies: Approximately 12.5% of fetal brain tumors have associated anomalies.[261] Many are present in the head or face, with cleft lip or palate being the most frequent.[258] Familial syndromes that have higher incidence of tumors include neurofibromatosis type I (optic glioma/astrocytoma), neurofibromatosis type II (schwannoma, meningioma, astrocytoma, ependymoma), TS (giant cell astrocytoma), von Hippel–Lindau (hemangioblastomas) and Li-Fraumeni (PNET, astrocytoma). Chromosomal studies may show karyotype abnormalities.[262]

Table 12.1-11 Prenatal Imaging Findings in Brain Tumors[259,260]

Macrocephaly	58%
Intracranial mass	58%
Hydrocephalus	52%
Intrauterine death	35%
Mass filling intracranial cavity	21%
Brain replaced by tumor	21%
Hydramnios	12%
Cephalopelvic disproportion	11%
Breech	10%
Hemorrhage	8%
Fetal hydrops	6.5%

Differential Diagnosis: Many intracranial masses are missed as they mimic more common conditions such as hemorrhage and hydrocephalus. In the presence of hemorrhage, Doppler shows no flow and MRI may be helpful to exclude mass with or without hemorrhage. Primarily cystic tumors can mimic infarct, porencephaly, arachnoid cyst, or interhemispheric cysts. Other benign lesions to include in the differential are lipomas, hamartomas, intracranial hemangiomas, and vascular malformations. Lipomas are well-defined midline homogeneous echogenic masses often in association with ACC. Hemangiomas are typically extra-axial and appear as a highly vascularized echogenic mass with cysts owing to blood degradation.

Prognosis: A fetus with a brain tumor has a poor prognosis.[259] Approximately 35% are stillborn. Overall survival rate is only 15%. Prognosis worsens with increasing tumor size and decreasing gestational age at diagnosis.[259,262] Death of the child shortly after birth is not uncommon.[259] Intracranial teratomas, glioblastomas, and PNET have the lowest survival rate of brain tumors (6% to 8%).[259] A fetus with meningeal tumor has an overall survival rate of 17%, and those with astrocytoma approximately 21%, usually in the presence of low-grade lesions. Craniopharyngiomas have higher survival at 23% and choroid plexus papillomas the best survival at 37.5%.[207] In those cases in which the tumor is resectable postnatally, overall survival is approximately 67%.[259]

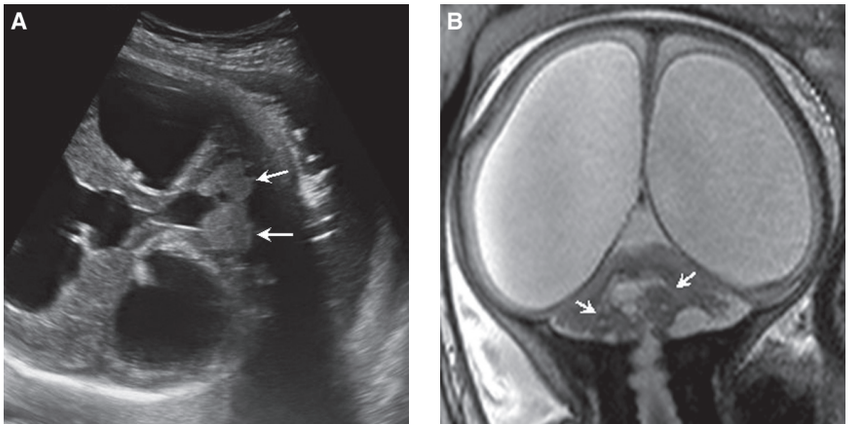

FIGURE 12.1-38: Fetus with choroid plexus papilloma. **A:** Axial ultrasound demonstrates severe lateral and third ventricular dilatation with bilobed echogenic mass *(arrows)* filling the fourth ventricle. **B:** Coronal T2 image in same fetus shows primarily T2 hypointense bilobed mass (*arrows*) in the fourth ventricle. Notice severe ventriculomegaly and compressed supratentorial brain. (Courtesy of Chris Cassady, MD.)

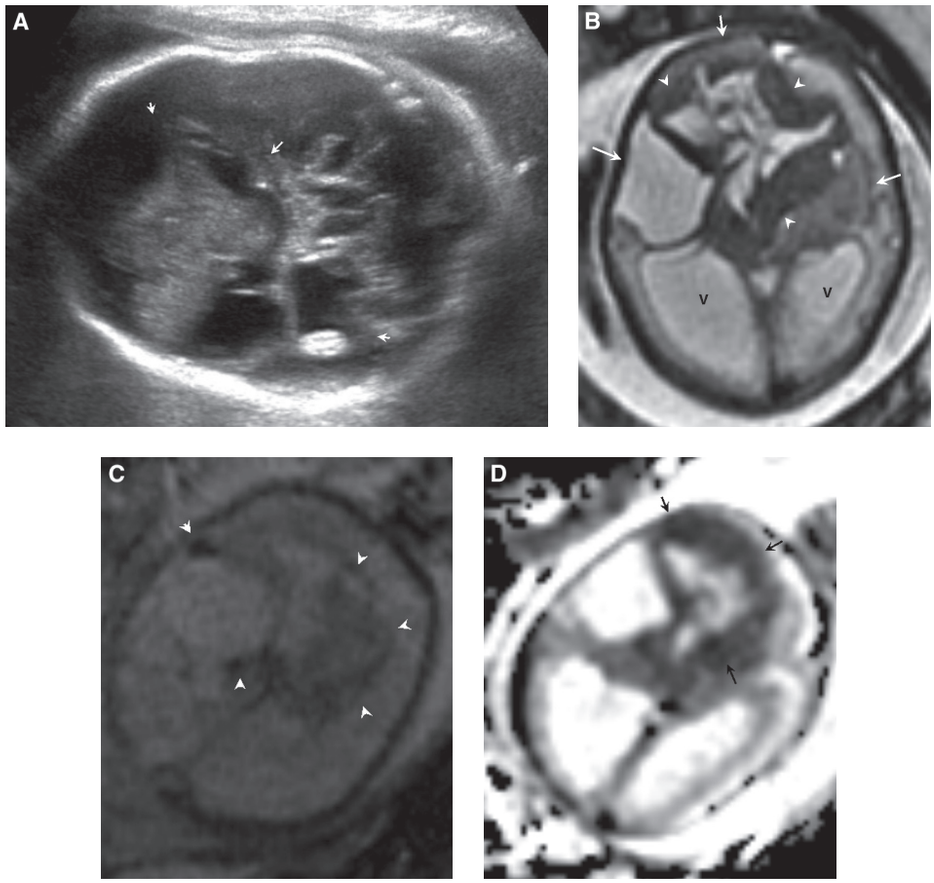

FIGURE 12.1-39: Fetus with suspected PNET at 33 weeks with perinatal demise. **A:** Axial US demonstrates heterogeneous echogenic mass with cystic components centered in frontal lobe distorting anatomy. Ultrasound one month prior was normal. **B:** Axial T2 MR image demonstrates a large heterogeneous solid and cystic lesion centered in frontal lobe *(arrows)*. Note rind of tissue that demonstrates hypointense T2 signal *(arrowheads)*. There is bilateral obstructive ventriculomegaly *(V)*. **C:** Gradient echo axial image demonstrates multiple areas of susceptibility artifact (*arrowheads*), suggesting hemorrhage. **D:** Restricted diffusion *(arrows)* is noted as dark signal on the ADC map. Findings support a high grade cellular lesion.

Management: Imaging to identify site and size of the lesion allows an obstetric plan of management to be made prenatally. Many times, the imaging is nonspecific, and histologic diagnosis is obtained after birth. With hydrocephalus, cephalocentesis may be repeated to decrease mass effect on the developing brain.[263] Early delivery, at or even before 34 weeks, may be considered.[263] In the presence of a large mass, cranial decompression or cephalocentesis may be required for vaginal delivery, but most believe cesarean section should be performed to prevent dystocia.[261,263] Postnatal treatment may be solely supportive care. In the presence of hydrocephalus, a shunt is indicated. Surgical resection of the primary tumor, followed by chemotherapy, is typical therapy. Radiation is contraindicated because of side effects on normal brain development. Survivors often have significant psychomotor deficits.[260,261]

Kline9781451175837-ch012.1.indd 381 08/08/14 9:58 AM

Recurrence: Most are sporadic except in the case of familial or genetic predisposition.[262]

Disorders of Choroid, Leptomeningeal, Neuroepithelial, and Vascular Differentiation

Choroid Plexus Cyst

Incidence: Choroid plexus cysts (CPC) occur in about 0.18% to 3.6% of routine midgestation ultrasounds.[267,268]

Pathogenesis: The choroid plexus (CP) first appears as a lobulated protrusion of ependymal epithelium accompanied by mesenchyme and pia mater in the 6th week of gestation. In the 8th week, the CP becomes wavy because of formation of capillary loops, and in the 9th week, the CP produces CSF.[269] Loose mesenchyme stroma, scattered islets of nucleated blood cells, and poorly defined vascular walls become accentuated by spaces and cysts from 9 to 16 weeks. From 17 to 28 weeks, the loose mesenchymal stroma decreases with increase in connective tissue fibers and fully formed vascular walls. After 29 weeks, the CP contains a mature vascular stroma.

Etiology: The CPC is actually a pseudocyst with a wall of interconnecting angiomatous irregular capillaries.[269] CPCs are believed to occur in the mesenchymal stroma when CSF is entrapped between the intervillous clefts, hypothesized to develop when there is failure in transformation of the lobulated embryonal capillaries into the wavy fetal pattern.[269] Most cysts form from 13 to 18 weeks when the choroid plexus proliferates. The cysts then regress by week 28 when proliferation and reduction in mesenchymal stroma occur. Approximately 95% of CPCs disappear by 26 weeks' gestation.[270]

Diagnosis

Ultrasound: The glomus, a focal thickened bulge along the posterior choroid, develops after 13 weeks and is the most common site for a CPC.[270] A CPC is an echolucent, well-circumscribed structure surrounded by echogenic choroid plexus (Fig. 12.1-40A). A true CPC can be diagnosed when the cyst measures 2.5 mm before 22 weeks and at least 2 mm thereafter.[271] CPC may be multiple or bilateral, can contain septations, and protrude into the ventricle (Fig. 12.1-40B). Approximately 86% are detected in the second trimester in isolation as an incidental finding.[272]

When a CPC is identified, however, a careful anatomic survey with attention to heart, brain, and hands should be performed. In approximately 14% of cases, additional anomalies are noted with CPCs, which raises the risk to as high as 48% for aneuploidy (Fig. 12.1-27).[272,273] CPCs that are bilateral and complex do not increase the risk of aneuploidy.[274] However, a large CPC in excess of 10 mm has been suggested to increase risk.[274] If the cyst is isolated, the risk for aneuoploidy is low at 0.9% to 6.7%; therefore, other factors such as baseline risk should be considered.[272,274,275]

MRI: In the presence of the typical subcentimeter lesion, MRI provides no added advantage, and in fact, most CPCs are not well visualized by MRI. With larger lesions, especially in the presence of complicating factors such as VM, MR imaging can confirm diagnosis of CPC by defining a CSF signal lesion within choroid, evaluating mass effect, and excluding other differentials.[276] In a high-risk pregnancy with CPC or in the presence of multiple other anomalies, MRI may be considered for further information.

Associated Anomalies: About 1% to 2% of infants with isolated cysts will have an underlying chromosomal abnormality, the most common being trisomy 18 followed by trisomy 21.[256] Recent evidence suggests that CPCs may also be associated with congenital heart disease and hydronephrosis.[277]

Differential Diagnosis: Before 22 weeks, the choroid plexus is heterogeneous, and small anechoic areas measuring <2 mm can mimic a cyst.[271] Partial volume averaging of the striatum and choroid and mild ventriculomegaly may falsely suggest CPC.[271] Choroid plexus papillomas are typically differentiated by solid nature and color Doppler flow. Subacute intraventricular clot adherent to choroid plexus may be difficult to discern from CPC in the absence of other findings. Other intraventricular cysts in the differential include colloid or neuroepithelial cysts, which demonstrate a true epithelial wall.

Prognosis: Most CPCs are incidental with no progression of the antenatal cyst after birth.[276] Studies have shown that fetuses with isolated CPC and normal karyotype have normal neurocognitive development after birth.[267,278] In the presence of a large CPC, space-occupying effects can cause obstructive hydrocephalus and/or injury to adjacent tissue that may manifest as focal neurologic deficits or seizure.[276]

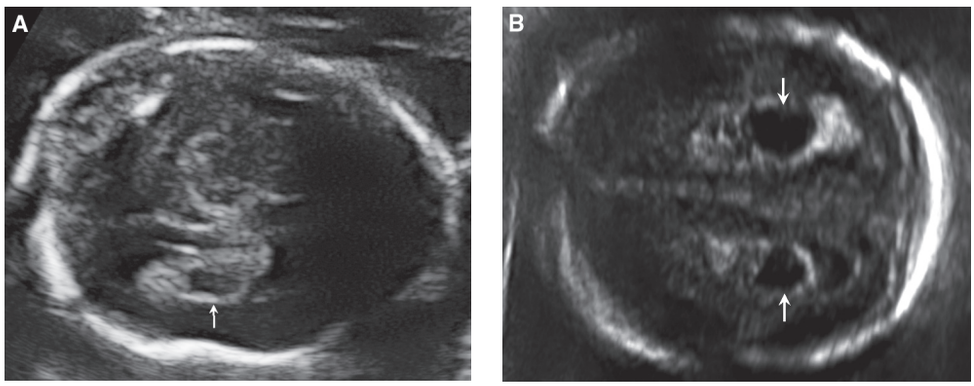

FIGURE 12.1-40: Choroid plexus cyst. **A:** Axial image of a single sonolucent lesion *(arrow)* in the choroid of the lateral ventricle. **B:** Axial US image of bilateral cysts *(arrows)* in the choroid of the lateral ventricles.

Management: Perinatal surveillance is warranted. Counseling is indicated as increased parental anxiety often occurs as some interpret the finding as a brain anomaly.[267] In the presence of CPC and associated anomalies, advanced maternal age, or abnormal triple screen analysis, most recommend amniocentesis or chorionic villus sampling as risk for aneuploidy is 1 in 3.[271–273,279] Although controversial, many believe testing should not be performed in the presence of only isolated CPC as the likelihood of trisomy 18 is low, risk increased by a factor of 7.[275,280] On the other hand, some perform interventional tests solely in the presence of isolated CPC, knowing that 25% to 30% of cases of trisomy 18 have findings undetectable by US and that the risk of aneuoploidy is 0% to 6%, with risk of fetal loss after amniocentesis at 0.5%.[269,271,273] Postnatally, nearly all CPCs resolve, and no further therapy is required. Persistence of a large cyst is extremely rare but could require neurosurgical decompression with fenestration or shunt.[276]

Recurrence: Most CPCs are incidental and sporadic.

Arachnoid Cysts

Incidence: Arachnoid cysts (AC) represent 1% of all intracranial masses in newborns.[281]

Pathogenesis: The most accepted theory for development of an AC is that early first trimester, at the time of evolution of the meninges, there is an abnormal localized splitting of cell layers in the area between the arachnoid and the pia allowing distension of a potential space with CSF. The wall of the AC is usually composed of a thick layer of collagen and hyperplastic arachnoid cells; however, suprasellar cysts may also contain neuroglial elements.[282] The congenital AC does not typically communicate with the subarachnoid space, whereas a secondary or acquired AC, which develops because of CSF entrapment within arachnoid adhesions following in utero hemorrhage, infection, or trauma, is usually patent with the subarachnoid space. Some cysts enlarge, and this is hypothesized to occur secondary to active secretion of CSF from the cyst membrane, osmotic gradients caused by higher protein in the cyst fluid, or cyst communicating with the subarachnoid space via ball-valve mechanism.[282]

Etiology: Intracranial ACs vary in size and location. In the fetus, the majority of ACs are supratentorial (63%), followed by infratentorial (22%), and finally along the incisura (15%).[281,283] Although in children most supratentorial ACs are located in the sylvian fissure or middle cranial fossa, in the fetus the most common location is interhemispheric, followed by skull base, suprasellar, and hemispheric.[281–284]

Diagnosis

Ultrasound: Most cysts are diagnosed in the third trimester, rarely before a gestational age of 20 weeks.[281,284] ACs are present in the extra-axial fluid space and are uniformly sonolucent (Fig. 12.1-41A). An AC will have thin regular walls and posterior acoustic enhancement. The lesion should be devoid of blood flow on color Doppler. Septation within the cyst is possible. A thorough search for additional anomalies with special attention to the corpus callosum is indicated.[284,285] The ventricles and cerebral parenchyma should be assessed for enlargement and mass effect.[281] Three-dimensional US may be helpful to define the nature of the cyst.[285]

MRI: MRI is helpful in confirming diagnosis by identifying the extra-axial location and CSF signal intensity (Fig. 12.1-41B). MRI can also define the extent of the cyst, compression of adjacent structures, communication with the ventricle, and other associated anomalies, especially of the corpus callosum.[283,286] The technique is helpful in excluding other intracranial cysts that may mimic an AC.

Associated Anomalies: ACs are commonly isolated but can be seen with chromosomal abnormalities, especially in the presence of additional anomalies.[281] ACC is the most common association, typically noted in the presence of an interhemispheric cyst. Malformations of the venous system are also possible.[282] Prenatal suprasellar cysts have been seen in association with hypothalamic hamartomas, which are pathologically ectopic benign neural tissue that present as gray matter masses at the floor of the third.[287] Sometimes, ACs are noted in the presence of metabolic diseases such as glutaric aciduria type 1.[285]

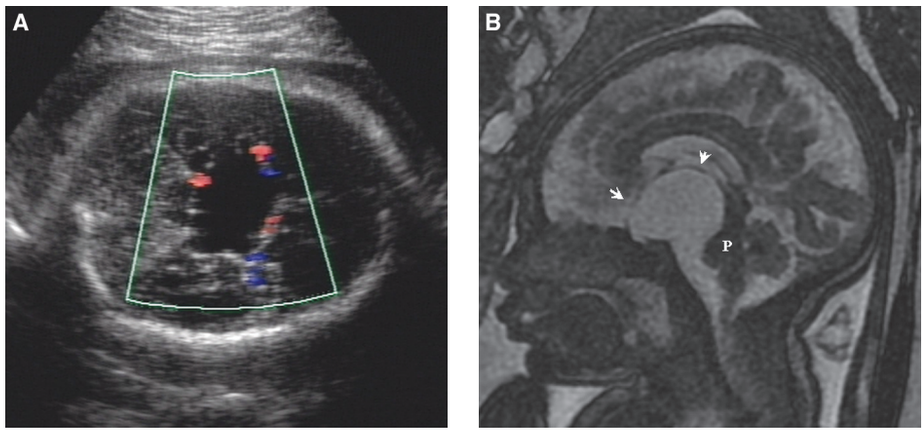

FIGURE 12.1-41: Suprasellar arachnoid cyst in a fetus at 34 weeks. **A:** Axial US demonstrating a sonolucent lesion posterior to the frontal lobes with absence of internal color flow. **B:** Sagittal SSFP MR image in same fetus demonstrates a suprasellar cystic lesion *(arrows)* with thin peripheral wall. There is mass effect on the adjacent pons *(P)*. The cyst continued to grow and postnatal, the child had fenestration of the cyst with good outcome.

Differential Diagnosis: Other "cystic" lesions which should be included in the differential are porencephaly, schizencephaly, cystic neoplasms, subacute intracranial hemorrhage, CPCs, and vein of Galen anomalies. In the presence of porencephaly, the margins may have a jagged contour, and in schizencephaly, clefts are lined by gray matter. In both, volume loss, not mass effect, should be present. Cystic neoplasms typically have associated solid tissue. Vein of Galen is documented in the presence of color flow on Doppler. A prominent cavum velum interpositum is a developmental variant which appears as a triangular CSF space below the splenium of the corpus callous, dorsal to the tectum, and bound laterally by the internal cerebral veins.[288] Enlargement of the septum pellucidum and vergae may mimic an interhemispheric cyst. Lesions that may be difficult to separate from AC include glioependymal cysts, neuroepithelial or colloid cysts, usually present in the third ventricle.

Prognosis: Prognosis is dependent on the presence of other malformations, the rate of cyst growth, and the progression of VM. Early age at diagnosis, growth of the cyst in utero, and a size of more than 15 mm are unfavorable factors.[289]

In general fetal/neonatal AC have a higher risk for growth than the adult population. Cysts increase in volume in 20% to 24% of fetuses and children; however, cyst volume and location do not determine clinical outcome, with some large lesions being asymptomatic.[281,283] Hydrocephalus has been shown to occur in approximately 17% to 25% of cases.[283,284] Hydrocephalus is more likely to occur with midline ACs, including interhemispheric, incisural (quadrigeminal), or suprasellar cysts which obstruct the aqueduct or third ventricle.[283] Suprasellar ACs also have an increased risk for visual disturbances and pituitary dysfunction.[290]

Approximately 28% (or higher) of AC will require postnatal intervention either because of hydrocephalus or symptoms from mass effect.[283,290] There is a slightly higher risk for subdural hematoma with head trauma, which is thought to be due to tearing of more vulnerable bridging veins by the lesions.[290] Overall, though, an AC without associated chromosomal or structural anomaly has a favorable outcome with behavior, neurological development, and intelligence normal in 88% of cases.[283]

Management: Serial prenatal US should be performed to assess the size of the cyst and the ventricles.[281] Close postnatal followup is indicated due to higher risk for growth and secondary complications. In the presence of symptoms from significant mass effect and/or hydrocephalus, current favored therapy is endoscopic cyst fenestration either cystoventriculostomy or cysto-cisternostomy.[281,282] Most do not support shunting of the cyst due to higher risk for secondary complications, including severe CSF overdrainage.[290]

Recurrence: Most are isolated without risk for recurrence.

Cyst of Septum Pellucidum

Incidence: Cysts of the cavum septum pellucidum (SPC) are rare, with an incidence of 0.04%.[291]

Pathogenesis: The septum pellucidum is related to the development of the commissures, with the leaflets containing glial, neuronal, and ependymal cells. The space in between the leaflets, or the cavum, does not communicate with the ventricles. In 85% of cases, the cavum will disappear in the first 3 to 6 months after birth; however, the cavum septum pellucidum has been cited to persist in 15% to 20% of children and adults.[291]

Etiology: Cysts of the septum pellucidum are felt to occur when the septum pellucidum develops the ability to secrete fluid, possibly because of migration of ependymal cells into the leaflets, or as a result of rupture of the cavum, likely secondary to trauma or infection.[292] Increase in intracranial pressure may develop because of obstruction of the interventricular foramina, and the cyst can compress adjacent structures such as the hypothalamus, septal nuclei, and supependymal and internal cerebral veins.[291]

Ultrasound: A cavum septum pellucidum greater than 1 cm is considered abnormal.[293,294] Most cysts of the septum pellucidum range in width from 2 to 5 cm, cause collapse of the frontal horns, and extend posteriorly into vergae, to the splenium of the corpus callosum.[295] US will show a dilated CSF cavity, measuring greater than 1 cm, above the thalami and anterior to the third ventricle in the anatomic location of the septum pellucidum (Fig. 12.1-42A).[296]

MRI: An SPC appears as a CSF cavity greater than 10 mm between the lateral ventricles with different degrees of bowing of the cyst wall, sometimes collapsing the frontal horns (Fig. 12.1-42B).[293] The lateral ventricles appear more parallel, and ventriculomegaly may occur owing to obstruction of the foramen of Monro.[291,293]

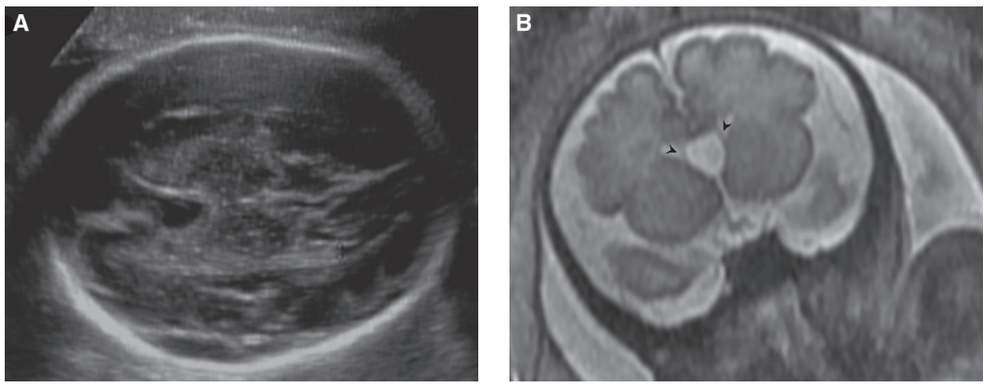

FIGURE 12.1-42: Cyst of the septum pellucidum. **A:** Axial US shows a prominent cavum septum pellucidum that measured 11 mm. **B:** Coronal T2 MRI in the same fetus demonstrates enlarged cavum with lateral bowing of the septal leaflets *(arrowheads)*.

Associated Anomalies: SPCs are typically not associated with intracranial anomalies other than ventriculomegaly.[297]

Differential Diagnosis: Differential for a SPC includes a large third ventricle, aneurysm of the vein of Galen, interhemispheric, arachnoid or neuroglial cyst, and an enlarged cavum velum interpositum. A predominately cystic tumor could also mimic an SPC.

Prognosis: Some SPCs will resolve spontaneously due to rupture into the lateral or third ventricles.[291,297] Hydrocephalus can occur in up to 32% and is more likely to occur under 5 years of age.[291] Children with SPCs have been shown to have focal deficit in 23%, seizures in 10%, and mental status changes in 42%.[291] A large persistent cavum septum pellucidum, but not cavum vergae, has been noted to be a marker of cerebral dysfunction, being associated with increased risk for mental retardation, developmental delay, and neuropsychiatric disturbances such as schizophrenia.[291]

Management: Serial prenatal US should be performed to assess the size of the cyst and ventricles. Symptoms may not be clear, but treatment is usually considered when there are clinical findings from ventricular obstruction or compression of adjacent structures.[291] Neuroendoscopic cyst fenestration is therapy of choice because of high success and low complication rate.[291]

Recurrence: Most are isolated without risk for recurrence.

Glioependymal/Neuroglial Cyst (aka Choroidal, Epithelial, Ependymal)

Incidence: Glioependymal cysts are uncommon, representing fewer than 1% of all intracranial cysts.[298]

Pathogenesis/Etiology: These cysts have a wall composed of neuroepithelium, and are therefore favored to arise from ectopic rests of the primitive neural tube or leptomeningeal neuroglial heterotopy.[299] The wall of the cyst is always lined with epithelium, but the complexing terminology is based on histology, reflecting variable neural, glial, ependymal, and choroidal cells. These cysts can be identified anywhere in the neuroaxis, usually over the cerebral hemisphere but also intraparenchymal.[299] In the fetus, most case reports describe the cyst in the interhemispheric fissure, often in conjunction with ACC.[299–302] Glioependymal cysts have been seen in association with ischemic or hemorrhagic insults.[301]

Diagnosis

Ultrasound: Glioependymal cysts are sonolucent but may be septated or mulitlocular.[300] The lesion will cause mass effect and when interhemispheric is usually associated with agenesis of the corpus callosum. Additional anomalies should be excluded.

MRI: The cystic lesion is often similar to CSF but can be slightly hyperintense to CSF on T1 imaging and hypointense on T2 imaging owing to high protein content.[299,301] The lesion may be unilocular, multilocular, or septated. Since these lesions can occur intra-axial or extra-axial, the glioependymal cyst may or may not communicate with the ventricular system.[301] MRI allows depiction of anatomy of the lesion, mass effect, and exclusion of associated anomalies.

Associated Anomalies: When present with ACC, other anomalies including heterotopic gray matter, cerebellar hypoplasia, and microgyria should be excluded.[299] When present in the posterior fossa, these cysts can cause obstructive hydrocephalus.[303]

Differential Diagnosis: Glioependymal cysts can only be differentiated from an arachnoid cyst by histology. Dorsal cyst with HPE, porencephaly, hydranencephaly, multicystic encephalomalacia, dermoids, epidermoids, and other cystic tumors should be considered.

Prognosis: There is a good prognosis in isolated appropriately treated glioependymal cysts.[300,301] A more guarded prognosis may be seen in the presence of associated anomalies.[301]

Management: Ideal treatment is complete resection, as the cyst not uncommonly recurs likely due to cellular components in the wall that produce CSF.[301,302] Other therapies include fenestration, shunting, and partial resection.

Recurrence: There is no known increased risk for recurrence.

Arteriovenous Malformations/Vein of Galen

Incidence: Most arteriovenous malformations (AVM) in the fetus are vein of Galen malformations (VGM), which represent less than 1% of all intracranial AVM.[304]

Pathogenesis: Early in embryology, a primitive sinusoidal vascular network is present with direct connections between arteries and veins. If there is error in normal differentiation of these vascular connections, the arteries and veins remain in direct communication, resulting in an AVM. As AVMs have no intervening capillaries between the artery and the vein, high-flow arteriovenous (AV) shunting develops that can secondarily result in cardiac failure and brain injury.

A "vein of Galen malformation" is a misnomer as the defect is not truly of the vein of Galen. A true VGM is a persistent communication of the primitive choroidal arterial system and the *median prosencephalic vein of Markowski.*[304] During the 5th week, choroidal and quadrigeminal arteries develop. On the roof of the diencephalon, between 6 and 11 weeks, the lateral choroid plexus expands and is drained via choroidal veins into a central primitive vein known as the median prosencephalic vein. In the 12th week, the vein regresses, with the dorsal remnant developing into the vein of Galen. The straight sinus, developing from fusion of multiple small tentorial veins, appears on the 50th day and drains the lateral choroid plexus. A VGM is hypothesized to occur when there is lack of involution of the prosencephalic vein because of either early occlusion or lack of formation of the straight sinus or due to continuous elevated blood flow through persistent abnormal communication of the choroidal arteries and the median prosencephalic vein. The abnormal angioarchitecture of the VGM also prevents normal development of the intracranial venous drainage, resulting in persistence of other embryologic venous sinuses, most commonly the falcine sinus.

Not surprisingly, choroidal arteries, especially the posterior choroidal, are the most common arterial feeders in VGM.[305] This is followed by subependymal perforators of the posterior cerebral arteries and thalamoperforators.[306] Often branches of the pericallosal artery, a vessel arising from the anterior cerebral and an important supply for the choroid plexus in the third ventricle, also supplies the VGM.[305] In approximately half

of neonates, a persistent limbic arterial arch, which connects the cortical branches of the anterior choroidal artery with the posterior cerebral artery via the pericallosal artery is noted.[307] Supply from the middle cerebral artery is uncommon. Transmesencephalic branches directly from the basilar can supply an AVM; however, in their presence, the AVM is not a true VGM and are otherwise indicative of a tectal not choroidal malformation.[306]

In a VGM, the primitive vein is arterialized, thick walled, and dilated due to high flow and turbulence from either direct or indirect arteriovenous connections. In over half of cases, the straight sinus is absent or thrombosed. The most common finding is a persistent falcine sinus, which extends from the vein of Galen to the sagittal sinus and ascends in the falx cerebri. Maturation of the jugular bulbs occurs peri and postnatal, and in the presence of a VGM, the maturation process, which includes remodeling of torcula, regression of occipital and marginal sinus, and remodeling of jugular bulbs, may not occur.[306] Occlusions and stenosis of the venous channels can develop, especially the jugular bulbs and sigmoid sinuses, which then increase venous pressure but can improve cardiac function by decreasing overload.[306] Anterior venous collateral drainage through the petrous, cavernous, thalamic, lateral mesencephalic, facial, and ophthalmic veins may develop. As the pacchionian granulations do not function until after the first few months of life, CSF must be absorbed at least partly by medullary veins. In the presence of this pathophysiology and with stenosis of veins leading to venous hypertension, the unbalanced hydrovenous state can lead to hydrocephalus.[306] Cerebral maturation is also dependent on a normal venous system. Intracranial venous hypertension likely in conjunction with cardiac dysfunction (steal phenomenon) results in brain injury, which is reflected by subcortical white matter calcification, white matter lesions, and diffuse brain destruction (melting brain), especially with subependymal atrophy (occipital) and ex vacuo ventricular dilatation.[306]

Etiology/Types: VGMs are usually classified by fistula angioarchitecture. The choroidal type is a primitive shunt in the velum interpositum with multiple bilateral feeding arteries, typically choroidal, pericallosal, and thalamoperforators, that converge on a fistula directly into the anterior prosencephalic vein (Fig. 12.1-43).[305,306] This type of VGM leads to a more severe pathology, presenting earlier in life, often with cardiac failure. The mural type is better tolerated and is defined by a single or few feeding typically collicular and posterior choroidal arteries that drain laterally into the wall of the dilated vein. Sometimes, the malformation may be a combination of both types. In all VGMs, the median prosencephalic vein has no connection with the deep venous system.

Although the majority of AVMs in the fetus are VGM, also described antenatally are dural sinus malformations (DSM) and pial arteriovenous fistulas (AVF). DSM are rare, more common in males and represent persistence of an embryonic sinus with or without AV shunt in the wall of a dural lake (see Dural venous thrombosis).[308,309] Pial AVF are typically supratentorial with peripheral pial/cortical feeding arteries draining into an ectatic vein.[106] The pial AVF may secondarily dilate the vein of Galen. Both DSM and pial AVF can result in high-output cardiomegaly and brain injury.[308–310]

Diagnosis

Ultrasound: VGMs are typically diagnosed in the third trimester, with less in the second trimester.[311] The diagnosis is usually suggested when a hypoechogenic less likely heterogeneous

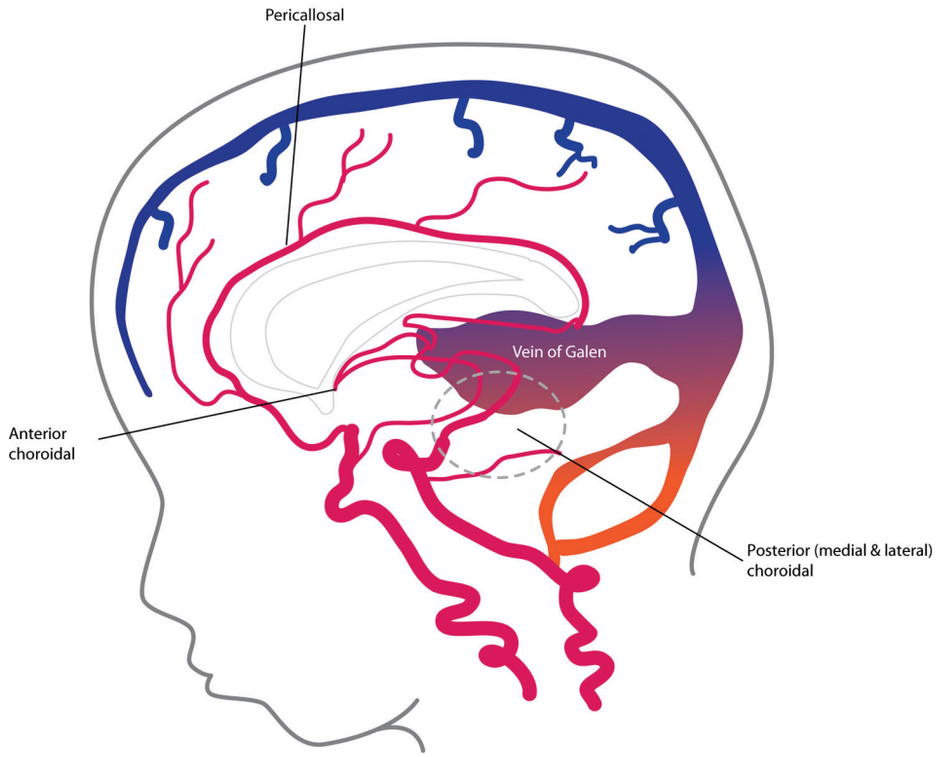

FIGURE 12.1-43: Diagram of choroidal type vein of Galen malformation with feeding vessels from the anterior choroidal, posterior choroidal, and pericallosal vessels forming the so-called limbic arterial arch.

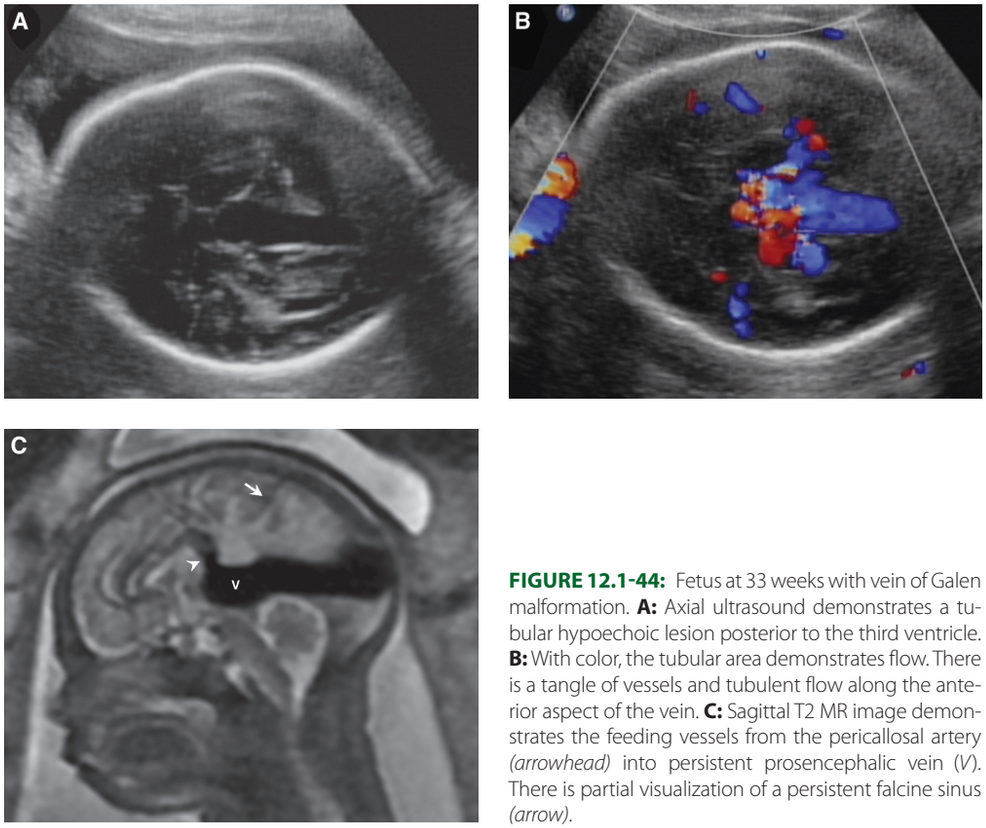

FIGURE 12.1-44: Fetus at 33 weeks with vein of Galen malformation. **A:** Axial ultrasound demonstrates a tubular hypoechoic lesion posterior to the third ventricle. **B:** With color, the tubular area demonstrates flow. There is a tangle of vessels and tubulent flow along the anterior aspect of the vein. **C:** Sagittal T2 MR image demonstrates the feeding vessels from the pericallosal artery *(arrowhead)* into persistent prosencephalic vein (*V*). There is partial visualization of a persistent falcine sinus *(arrow)*.

mass with central color Doppler is identified in the midline of the posterior recess of the third ventricle (Fig. 12.1-44A,B).[304] Doppler will demonstrate bidirectional turbulent flow with very pulsatile "arterialized" veins and high diastolic arterial waveforms (Fig. 12.1-45).[312] If only normal venous Doppler is obtained in the vein of Galen, the dilatation may be related to varicosity or other type of AVM. The sagittal sinus or persistent falcine sinus is often dilated.[312] On 2D US, it can sometimes be difficult to precisely identify the feeders or exclude a parenchymal AVM that drains via the vein of Galen.[305] However, power Doppler, especially with 3D reconstruction, can provide very detailed anatomy of the complex angioarchitecture, allowing depiction of the feeding arteries and venous anatomy (Fig. 12.1-46A,B).[312–314] Limitations of 3D include poor resolution and difficulty in differentiating veins from arteries.[313]

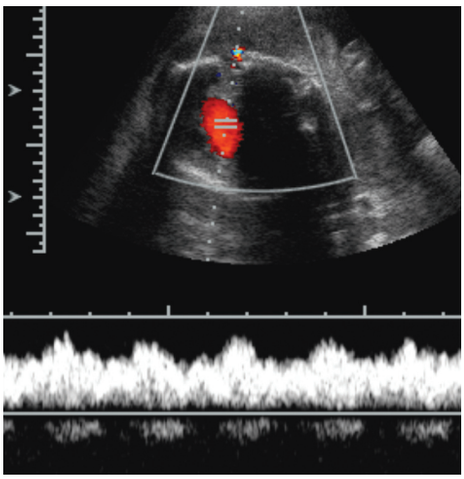

FIGURE 12.1-45: Doppler in a vein of Galen demonstrating arterialized waveform.

Since brain injury is possible, close evaluation for calcification, hemorrhage, volume loss, and hydrocephalus should be obtained (Fig. 12.1-47).[315] Clues to heart failure include cardiomegaly, tricuspid valve insufficiency, dilated inferior vena cava, retrograde aortic diastolic flow, and tachycardia (>200 bpm).[306,315] Enlarged neck vessels, especially the jugular veins, are pathognomonic and can be seen in approximately one-third of cases (Fig. 12.1-48).[311,315] Elevated cardiac output may be measured and has been suggested to correlate with the magnitude of AV shunt.[316] Polyhydramnios, pericardial and pleural effusion, edema and ascites (hydrops) carry a poor prognosis and suggest intractable high flow.[304,315]

MRI: Fetal MRI can aid in confirmation of a VGM and help exclude other arteriovenous anomalies or intracranial anomalies that can mimic a VGM (Figs. 12.1-44C and 12.1-46C). MRI can identify flow void in pathological vessels and can verify the size of the AVM, which may demonstrate flow void or heterogeneous signal due to turbulence.[317] MRI is superior at evaluating for cerebral injury, which may manifest as ventriculomegaly, polymicrogyria, cortical thickening, porencephaly, schizencephaly, periventricular injury, and intraparenchymal hemorrhage in fetuses with VGM (Fig. 12.1-49A).[304,318] T1 imaging is important to exclude acute hemorrhage and/or mineralization

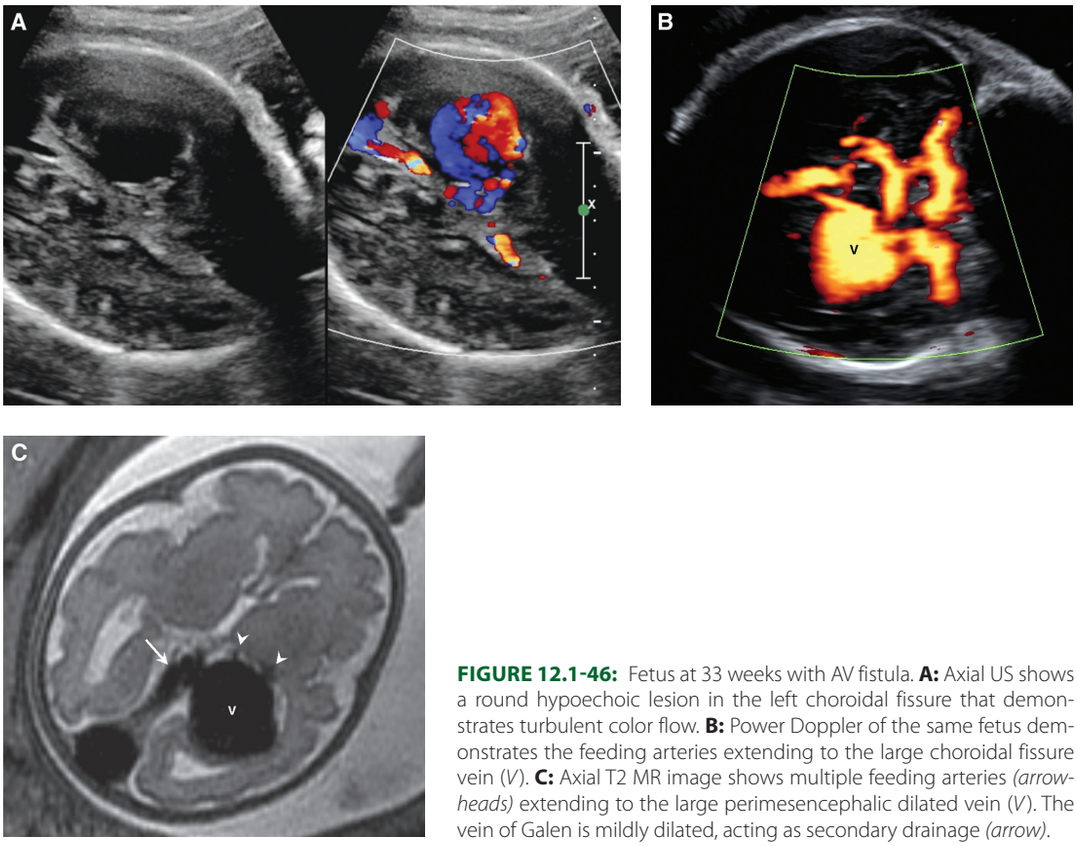

FIGURE 12.1-46: Fetus at 33 weeks with AV fistula. **A:** Axial US shows a round hypoechoic lesion in the left choroidal fissure that demonstrates turbulent color flow. **B:** Power Doppler of the same fetus demonstrates the feeding arteries extending to the large choroidal fissure vein (*V*). **C:** Axial T2 MR image shows multiple feeding arteries *(arrowheads)* extending to the large perimesencephalic dilated vein (*V*). The vein of Galen is mildly dilated, acting as secondary drainage *(arrow)*.

(Fig. 12.1-49B). Diffusion imaging may provide information about acute ischemia, and gradient echo, in the presence of susceptibility artifact, can define hemosiderin or calcification. MRA, especially 2D time of flight (TOF), which is shorter in scan time than 3D TOF, may be helpful in defining the vascular anatomy of the malformation (Fig. 12.1-49C).[319]

Associated Anomalies: VGMs are not associated with chromosomal anomalies. All types of AVM, whether VGM, DVM, or AVF, can cause cardiac failure and brain injury. Sixty to 76% of fetuses with VGMs will have ventriculomegaly, cardiomegaly, and enlarged neck vessels.[311,316]

Differential Diagnosis: Varicose dilatation of the vein of Galen may occur in the absence of AVM. This may be seen in association with heart disease or vascular anomalies that cause venous hypertension.[304] Other differentials include arachnoid cyst, porencephaly, choroid plexus cyst, choroid plexus papilloma, pineal tumor, and intracerebral hematoma. A vascular mass such as hemangioma should also be considered.

Prognosis: Fetuses with prenatal diagnosis of VGM and cardiac failure, hydrops, or cerebral anomalies have a poor outcome.[304,306] These fetuses at birth typically suffer from severe

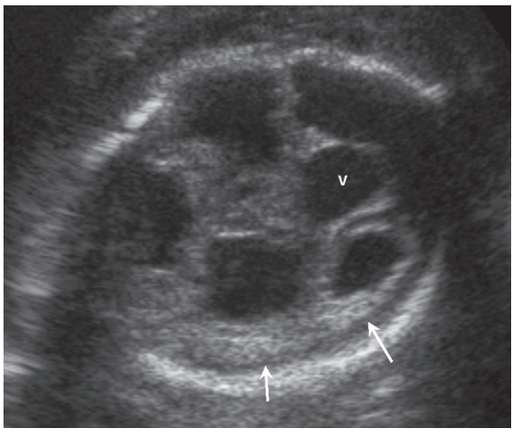

FIGURE 12.1-47: Axial ultrasound in a fetus with VGM *(V)*. The lateral ventricles are enlarged consistent with brain parenchymal volume loss. The thinned brain parenchyma is increased in echogenicity (*arrows*) concerning for brain injury.

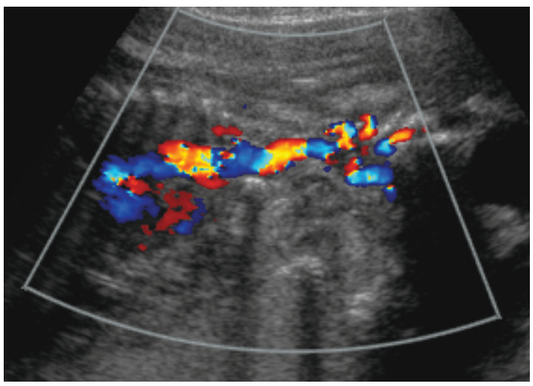

FIGURE 12.1-48: Coronal color ultrasound demonstrating enlarged jugular vein in fetus with VGM.

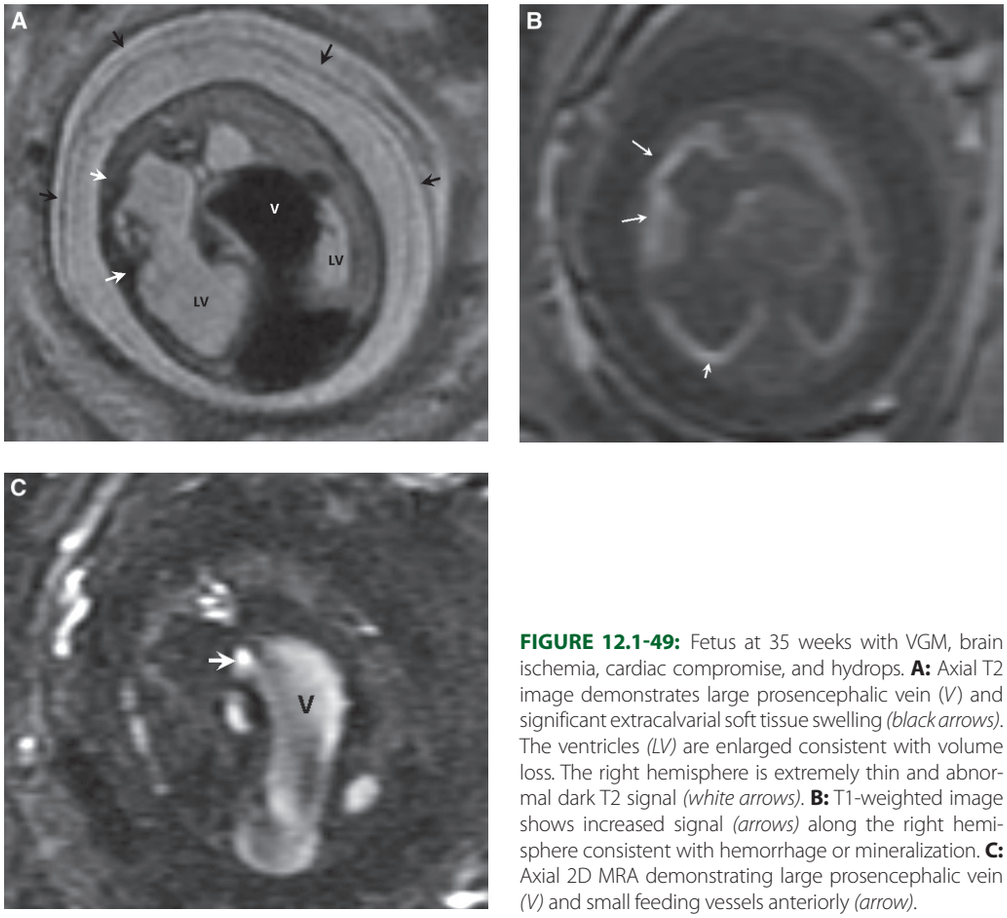

FIGURE 12.1-49: Fetus at 35 weeks with VGM, brain ischemia, cardiac compromise, and hydrops. **A:** Axial T2 image demonstrates large prosencephalic vein (*V*) and significant extracalvarial soft tissue swelling *(black arrows)*. The ventricles *(LV)* are enlarged consistent with volume loss. The right hemisphere is extremely thin and abnormal dark T2 signal *(white arrows)*. **B:** T1-weighted image shows increased signal *(arrows)* along the right hemisphere consistent with hemorrhage or mineralization. **C:** Axial 2D MRA demonstrating large prosencephalic vein *(V)* and small feeding vessels anteriorly *(arrow)*.

irreversible multiorgan failure.[306] Those with isolated VGM have a more favorable prognosis; however, the type of AVM and the number and size of the arterial feeders and draining vein reflect the severity of shunt and have implications for outcome.[304,315] In cases with prenatal diagnosis, overall mortality for VGM has been reported at 22% to 25% with normal neurologic outcome in 67%.[305,320] However, a recent review suggested a much higher perinatal death rate of 54%.[304] In this study, 32% of prenatally diagnosed VGM were alive and well, whereas 14% were alive with mental retardation. Without embolization, mortality in VGM is as high as 90%. With embolization, outcomes for VGM prenatal and postnatal have been recorded at 10% demise, 10% severe disability, 16% moderate delay, and 74% neurologically normal.[306]

Management: Rarely, mirror syndrome can develop in the mother; therefore, close fetal and maternal monitoring is warranted.[321] Patient selection for therapy is usually dependent on the severity of heart failure and degree of brain injury.[305] Termination or no postnatal intervention may be considered on the basis of these factors.[306] Antenatal diagnosis is usually not an indication for early delivery or C-section.[306] Delivery should be performed at tertiary centers with neurosurgical, cardiovascular, and interventional radiology expertise.

At birth, cardiac failure can worsen after delivery because of removal of the low-resistance placenta, facilitating more flow through the foramen ovale. Medical therapy is directed at cardiac dysfunction and includes administration of diuretics to decrease preload. The main intent is to address feeding so that weight gain occurs in the first few months. MRI of the brain should be obtained to assess the degree of brain injury.

In a VGM, clinical and laboratory evaluation regarding cardiac, cerebral, respiratory, renal and liver function are utilized in a scoring system (Bicetre) to determine need and timing for therapy (Table 12.1-12). A score of 8 and below is a decision not to treat, and that between 8 and 12 is considered an emergency endovascular intervention.[307] In the presence of cardiac decompensation or with development of hydrocephalus, immediate embolization therapy is warranted to decrease shunt and venous hypertension in an attempt to reverse pathology.[306,322] If the patient is stable and neonatal score is between 13 and 20, therapy is often scheduled at 5 months of age.

The first line of therapy for VGM is embolization, usually transarterial, with the transvenous (femoral or transtorcular) route being utilized as a second choice because of higher morbidity.[306,322] Surgical treatment is dangerous, difficult, and often incomplete. The goal of therapy is not always to obliterate the AVM, but to balance therapy to allow the brain to mature and develop normally by either improving cardiac status or preventing the development of neurologic symptoms.[306] Several sessions of embolization may be required to safely treat, either completely or incompletely, the vascular anastomosis. Spontaneous thrombosis can occur rarely in VGM (2.5%) and is typically associated with 50% neurologic impairment.[306,307] Complications from the lesion and/or therapy include hemorrhage, stroke, and continued brain injury, which can lead to neurologic deficits and seizures. Macrocrania and

Kline9781451175837-ch012.1.indd 389 08/08/14 9:58 AM

Table 12.1-12 Bicetre Neonatal Evaluation Score

Points	Cardiac Function	Cerebral Function	Respiratory Function	Hepatic Function	Renal Function
5	Normal	Normal	Normal	—	—
4	Overload, no medical treatment	Subclinical isolated EEG abnormalities	Tachypnea, finishes bottle	—	—
3	Failure, stable with medical treatment	Nonconvulsive intermittent neurologic signs	Tachypnea, does not finish bottle	No hepatomegaly, normal function	Normal
2	Failure, not stable with medical treatment	Isolated convulsion	Assisted ventilation, normal saturation $FIO_2 < 25\%$	Hepatomegaly, normal function	Transient anuria
1	Ventilation necessary	Seizures	Assisted ventilation, normal saturation $FIO_2 > 25\%$	Moderate or transient hepatic insufficiency	Unstable diuresis with treatment
0	Resistant to medical treatment	Permanent neurologic signs	Assisted ventilation, desaturation	Abnormal coagulation, elevated enzymes	Anuria

Maximal score = 5 (cardiac) + 5 (cerebral) + 5 (respiratory) + 3 (hepatic) + 3 (renal) = 21.

From Lasjaunias PL, Chng SM, Sachet M, et al. The management of vein of Galen aneurysmal malformation. *Neurosurgery*. 2006;59:S3.184–S3.194.

hydrocephalus that does not respond to therapy can be managed with endoscopic ventriculostomy or shunting.[307] With therapy, venous thrombosis and cerebellar tonsillar herniation due to venous congestion may occur.[103] Facial venous distension can cause epistaxis.

Both DVM and pial AVF have the same complications as VGM.[308–310] Pial AVF, in contradistinction to VGMs, are treated with embolotherapy at birth to prevent brain injury.[310] Spontaneous thrombosis of DVM has been documented; however, close monitoring and embolization may also be required.[308,309]

Recurrence: There is no increased risk of recurrence.

Disorders of Cellular Migration

Lissencephaly: Agyria, Pachygyria, and Subcortical Band Heterotopia (aka Classic or Type I Lissencephaly)

Agyria represents a thick cortex with lack of gyri, also consistent with complete lissencephaly (smooth brain). Incomplete lissencephaly exists in the presence of pachygyria or band heterotopia. Broad, shallow, and flat gyri with thickened cortex are diagnostic of pachygyria. Subcortical band heterotopia represents a band of heterotopic gray matter beneath the cortex, separated by a thin layer of white matter. Often, there is a combination of these anomalies.

Incidence: The estimated incidence of classic or previously denoted type 1 lissencephaly is 1.2 per 100,000 births.[323]

Pathogenesis: Lissencephaly is a severe malformation of the fetal brain that occurs because of impaired neuronal migration during the 3rd to 4th month of gestation.[324] The prime defect is a genetic flaw that results in dysfunctional proteins which are necessary for the normal neural migration.[323] A normal brain contains six cortical layers. In both agyria and pachygyria, the cortex is abnormally thick, remodeled and has only four layers. Despite deficient layers, the cortex is thick as the cells arrested lie in disorganized radial columns.[325] On histology, the two most superficial layers, a cell dense marginal zone and superficial cortical gray zone are formed by neurons that have migrated normal early in gestation. The third layer is cell sparse, with only a few dysplastic neurons. The fourth layer is densely cellular with radial orientated neurons with no lamination (Fig. 12.1-50). Because of the lack of development of axonal and dendritic connections, the subcortical white matter is thin and lacks gray white matter interdigitation.[325] Subcortical band heterotopia demonstrates normal cortical and subcortical white matter architecture with a band of heterotopic columnar neurons.[326]

Etiology: Lissencephaly may be isolated or associated with a syndrome, the most common being Miller–Dieker syndrome (MDS). Miller–Dieker syndrome is seen in the presence of severe lissencephaly and facial dysmorphism that includes prominent forehead, bitemporal hollowing, short upturned nose, thickened upper lip, low set ears, and small jaw. Baraitser–Winter syndrome is characterized by lissencephaly, trigonocephaly, shallow orbits, ptosis, and colobomas.[326] Multiple genes have been associated with lissencephaly (Table 12.1-13).[324,326] *LIS1* and *DCX* account for approximately 85% of isolated lissencephaly, whereas *DCX* is associated with 90% of cases of subcortical heterotopia.[327] The topography of the malformation is dependent on the gene which is affected.

The *LIS1* gene mutation is equally seen in males and females, with gyral abnormalities more severe posteriorly, demonstrating agyria parieto-occipital and pachygyria frontal and temporal.[326,328] Rarely, the *LIS1* gene causes subcortical band heterotopia, mostly in the parieto-occipital area. The *DCX* gene is present on the X chromosome, affects the anterior aspect of the brain more than the posterior and in males causes lissencephaly whereas in females a milder phenotype with subcortical band heterotopia is noted.[329] *ARX* causes an X-linked lissencephaly, and therefore is phenotypically more severe in males than in females, and is seen in association with abnormal genitalia, facial

Kline9781451175837-ch012.1.indd 390 08/08/14 9:58 AM

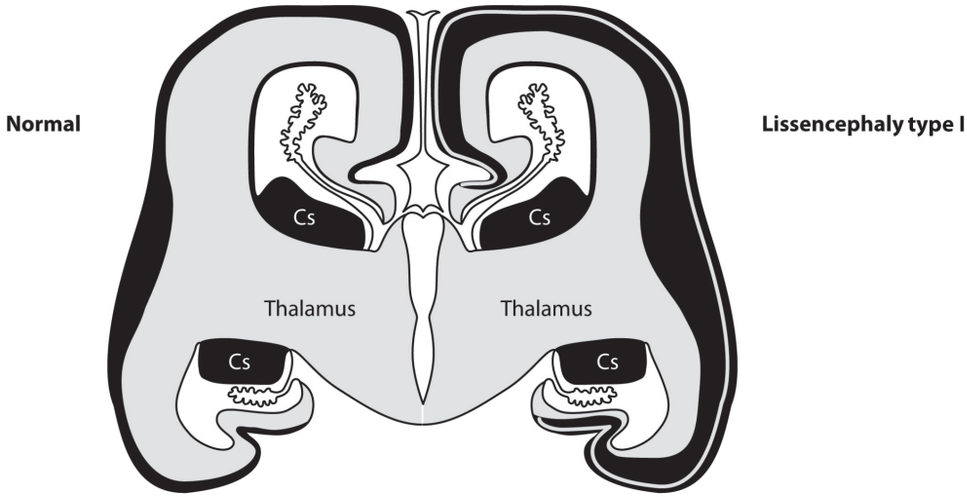

FIGURE 12.1-50: Diagram of the layered pattern in lissencephaly type I.

dysmorphism, and ACC. *RELN* causes lissencephaly in association with cerebellar hypoplasia and often brainstem abnormalities.[323] Both *RELN* and *ARX* demonstrate a thickened cortex but no cell-sparse zone in the area of agyria.

Diagnosis: When there is a concern for lissencephaly by imaging, karyotype is suggested, as FISH analysis of 17p13.3 deletions and sequencing for abnormalities of the *LIS1* and *DCX* genes can be diagnostic.[327]

Ultrasound: Severe forms of lissencephaly are likely to be more easily detected than milder incomplete forms.[330] Agyria/pachygria can be suggested as early as 23 to 24 weeks when there is a smooth thick cerebral surface with absence of parieto-occipital and calcarine fissure and wide sylvian fissures due to abnormal opercular formatin.[330] After 28 weeks, in the presence of a smooth brain, diagnosis of lissencephaly can be confirmed (Fig. 12.1-51A).[330] Three-dimensional imaging may demonstrate sulci better than 2D.[331]

Lamination of the fetal brain can normally be detected as early as 17 weeks, present to 28 weeks' gestation, and disappearing by 34 weeks.[332] The subplate should be anechoic and the intermediate zone homogeneously more echogenic.[332] When lissencephaly is present, no laminar pattern, prominent increased echogenicity in the intermediate zone representing thick disorganized neurons, or persistence of lamination pattern after 33 weeks can be noted.[332] Mild ventriculomegaly and enlarged subarachnoid spaces are often present (Fig. 12.1-52A).[324,333] Immature sulcation with wide and thick gyri is typical.[333] In the presence of other intracranial and extracranial findings, a diagnosis of MDS may be suggested (Table 12.1-14). The most common findings that should raise suspicion of MDS are polyhydramnios (66%), intrauterine growth restriction (62%), and ventriculomegaly (59%).[329] Ultrasound diagnosis for MDS has been noted to be as high as 41% prenatal, mostly third trimester.[329]

MRI: Diagnosis prior to 20 weeks is difficult as the brain is normally smooth at this gestational age. At 23 to 24 weeks, absence of normal parieto-occipital and calcarine sulcus with wide sylvian fissures can be noted.[330] On MRI, the cortex is thick, smooth, or shallow, and the normal ratio of gray to white matter is reversed (Fig. 12.1-51B).[325] A normal cortical thickness is 3 to 4 mm, and in lissencephaly the thickness is often 12 to 20 mm.[326] In the thickened cortex, there is often a band of hypertense T2 signal, usually in the parieto-occipital area, which represents the cell-sparse layer with high water content. This may mimic the normal subplate, which should be disappearing between 25 and 28 weeks. A figure 8 configuration of the brain is due to lack of development of the sylvian fissures, also known as opcular dysplasia. Cavitations in the ganglionic eminences have been described.[334] Mild ventriculomegaly, especially colpocephaly, is often present owing to

Table 12.1-13 Genes/Syndromes in Association with Lissencephaly

Genetics/Type	Gene	Locus
Isolated lissencephaly	*LIS1, TUBA1A, PAFAH1B1*	17p13.3, 12q12–14
Miller-Dieker syndrome	*LIS1, YWHAE, CRK, PAFAH1B1*	17p13.3
X-linked lissencephaly	*DCX*	Xq22.3–q23
Lissencephaly, cerebellum and brainstem abnormal	*RELN, TUBA1A, VLDLR*	7q22, 12q12–14
Lissencephaly, ACC, ambiguous genitalia	*ARX*	Xp22.13
Subcortical heterotopia	*DCX, TUBA1A*	Xq22.3–q23, 12q12–14
Paracentral pachygyria		
Baraitser-Winter syndrome		
Autosomal recessive frontotemporal pachygyria		

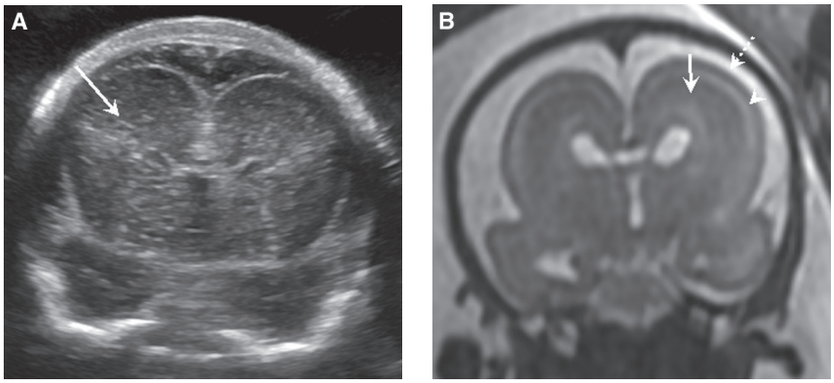

FIGURE 12.1-51: Fetus at 36 weeks gestation with type I lissencephaly. **A:** Coronal US image demonstrates abnormal smooth appearance of the cortex. There is increased echogenicity in the area of the intermediate zone *(arrow)*. **B:** Coronal T2 image in same fetus demonstrates thin peripheral cortex (*dotted arrow*), cell sparse zone *(arrowhead),* and deep thick disorganized neurons *(arrow)*. Notice abnormal smooth architecture of the brain for gestational age. (Courtesy of Dorothy Bulas, MD.)

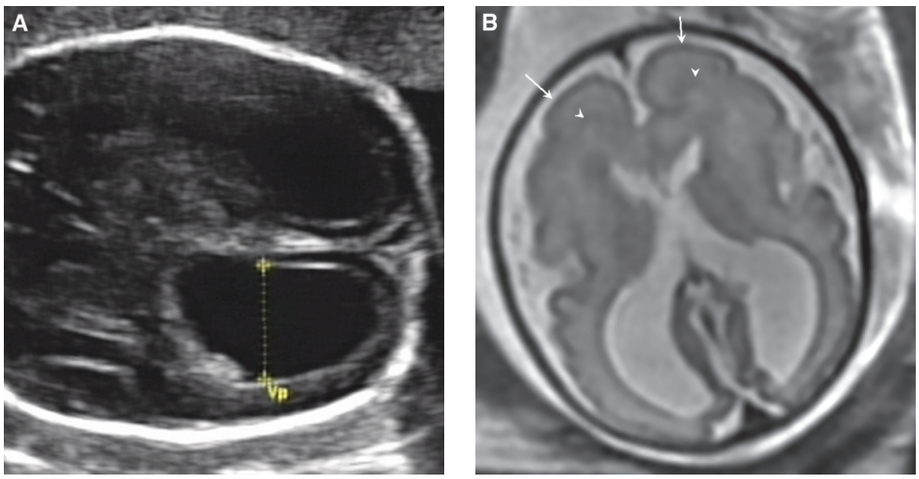

FIGURE 12.1-52: Fetus at 33 weeks with confirmed pachygyria and band heterotopia. **A:** Axial US demonstrates moderate ventriculomegaly. **B:** Axial T2 image shows abnormal lack of sulci (*arrows*) in the frontal lobes bilaterally. Notice dark band of signal in the white matter *(arrowheads),* which is abnormal for gestational age and represented band heterotopia postnatal.

Table 12.1-14 Findings in Miller-Dieker Syndrome

Common
Diffuse agyria
Abnormal sylvian fissure and insula
Ventriculomegaly
Corpus callosum dysgenesis
Microcephaly
Intrauterine growth restriction
Hydramnios

Less common
Micrognathia
Congenital heart disease
Genitourinary anomalies
Omphalocele
Duodenal atresia

lack of development of the calcarine sulcus.[335] Large temporal horns likely represent arrest in hippocampal maturation and invagination.[335]

MRI is more likely to detect subtle areas of pachygyria or band heterotopia.[330] In pachygria, the cortex is thick with a smooth gray white matter junction and deficient sulci that follow a normal pattern of the primary fissures (Fig. 12.1-52B). With subcortical band heterotopia, there is a band of abnormal gray matter separated from the normal cortex by normal white matter. The band tends to be more pronounced and focal than the dark signal of the intermediate zone that is present from 20 to 28 weeks. Beyond 28 weeks, a band of gray matter signal in the white matter is diagnostic of neuronal band heterotopia. MRI is also excellent at excluding associated anomalies of the corpus callosum, brainstem, and cerebellum.

Associated Anomalies: Associated intracranial anomalies are common. The cerebellum, brainstem, and corpus callosum are

often abnormal. Extracerebral anomalies may point to the diagnosis of MDS and other genetic disorders.

Differential Diagnosis: Understanding normal brain development is imperative as early in gestation the brain is normally smooth, and this should not be interpreted as lissencephaly. Diagnosis for delayed sulcation should not be considered until after 20 weeks, and it must be remembered that there can be a 2-week difference in visualization of a fissure.[324] In the presence of other intracranial anomalies, sulcation may be delayed more than 2 weeks owing to the primary CNS abnormality. Abnormal operculization of the Sylvian fissure does not necessarily support a migration abnormality as it may be related to extracortical factors and can be a normal variant, particularly when only the anterior portion is suggested to be abnormal.[336]

Prognosis: In the presence of isolated lissencephaly and MDS, similar neurologic and developmental disabilities are noted.[326] Newborns have hypotonia, poor feeding, and often transient elevations in bilirubin. The head circumference tends to be normal at birth, but is small by 1 year of age. Seizures develop by 6 months in more than 90% of children, and infantile spasms are seen in 80%.[326] With the onset of infantile spasms, there is a rapid decline in function. Most children develop milestones to about 3 to 5 months. Children have poor control of their airway, predisposing to aspiration pneumonia, the most common cause for demise. In children with MDS, death is typically in the first 2 years, whereas in isolated lissencephaly about 50% live to age 10.[326] Milder forms or incomplete lissencephaly tend to have less severe symptomatology. In subcortical heterotopia, the person is predisposed to seizures and intellectual disability, but usually lives into adulthood.[326]

Management: Delayed prenatal US and MR imaging in the third trimester may be necessary to confirm diagnosis. Termination may be considered but may not be possible in all countries, depending on time of diagnosis. With knowledge of the anomaly, decisions can be made with regard to site of delivery and management/support at the time of birth. Genetic counseling is indicated both prenatally and postnatally. Parental testing should be considered as up to 20% of fetuses with MDS will inherit the genetic deletion from a parent.[324] This may have implications for recurrence risk in future pregnancy.[330] In X-linked lissencephaly, genetic testing may be performed in the mother to exclude inherited mutation. Discussion of prognosis with decisions on limitations of care should be communicated.[326]

Most children with lissencephaly require feeding via enteric or gastrostomy tubes. Aggressive management of seizures is imperative to prevent rapid decline in function.[326]

Recurrence: Most cases of isolated lissencephaly and MDS (80% de novo) are sporadic, and the risk of recurrence is negligible.[326,329]

Gray Matter Heterotopia

Incidence: Prevalence in the general population is unknown, but gray matter heterotopias have been described to occur in 11% to 20% of patients with epilepsy.[337]

Pathogenesis: Gray matter heterotopias are normal neurons present in an abnormal location, usually situated anywhere from the subependymal surface to the cerebral cortex (Fig. 12.1-53). Recent evidence suggests that periventricular nodular heterotopia (PVH) is likely due to a disruption in the neuroependyma, which prevents postmitotic neurons from attaching to the radial glial cells, thus impairing migration.[338] Periventricular (subependymal) heterotopias are the most common form of gray matter heterotopia. The heterotopia is located adjacent to the ventricular wall, usually along the trigone or occipital horns of the lateral ventricles.[339] PVH may be nodular or laminar and are commonly described as focal, unilateral, bilateral focal, or bilateral diffuse.[328,340] Histologically, the nodules show rudimentary lamination, similar to that in the cortex.

Subcortical heterotopia (SCH), also due to premature arrest of neurons, is less common but can have many appearances. Some are transmantle, composed of linear columns of neurons continuous from the ependymal surface to cortex. Others may be nodular, curvilinear, or mixed, often solely present in the subcortical white matter.[341] SCH can present as a small, large, sublobar, or regional mass in an otherwise normal hemisphere.

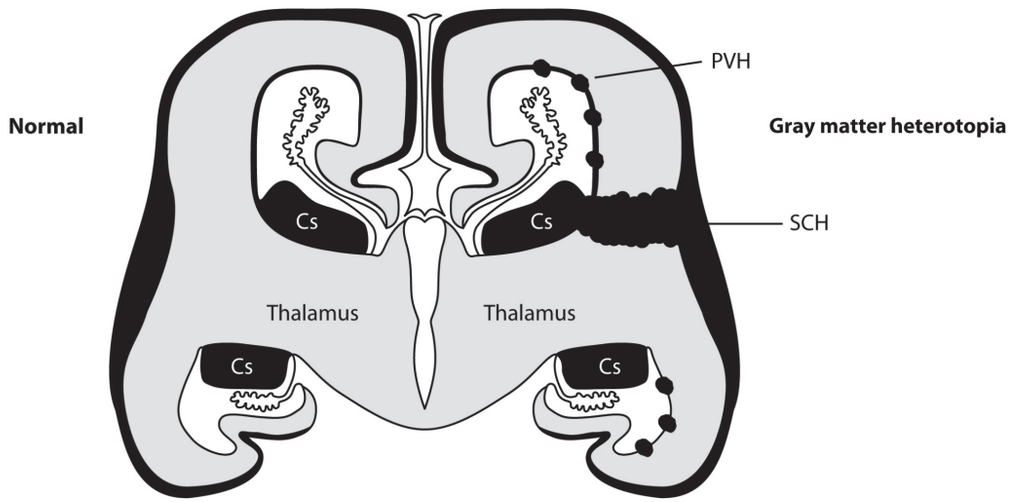

FIGURE 12.1-53: Types of gray matter heterotopia. PVH, periventricular heterotopia; SCH, subcortical heterotopia.

Etiology: Genetic and nongenetic causes for gray matter heterotopia include single gene disorders, chromosomal anomalies, and disruptive events.[338] Unilateral or sparsely scattered PVH is typically sporadic. Bilateral PVH is present in 54% of cases, and in this group, genetic syndromes and associated intracranial anomalies are more likely.[342]

Many cases of PVH are X-linked caused by mutation of the *FLNA* gene localized at the Xq28 loci.[343] Lack of production of the encoding filamin protein arrests neuronal migration. Since the disorder is X-linked, the phenotype in males results in death or severe neurologic deficit, whereas females are only mildly affected with normal or slightly impaired intelligence and late onset seizures in the second or third decade.[343] *FLNA* genetic mutations may be present in up to 49% of all patients with PVH, and as high as 93% of females with PVH.[342] Females with this disorder typically show bilateral symmetric continuous PVH along the walls of the lateral ventricles, sparing the temporal horns. These patients may also have a mega cistern magna and cerebellar hypoplasia.[338] Cardiovascular defects including patent ductus arteriosus and valvular disorders are more common.[339] *FLNA* mutations are also described in patients with Erlos Danlos syndrome and otopalatodigital (OPD) syndromes.[342]

A rare autosomal recessive defect in the *ARFGEF2* gene is characterized by microcephaly and delayed myelination with PVH.[134] Williams syndrome and chromosomal 5p anomalies may demonstrate PVH.[337] Gray matter heterotopia is often seen in association with other CNS malformations, present in up to 19% of cases of ACC.[337] With posterior distributed PVH, cerebral cortical and midbrain/hindbrain anomalies are more common.[338]

Diagnosis

Ultrasound: On ultrasound, PVH tends to be underdiagnosed, with targeted neurosonography missing 36% detected by MRI.[336,337] PVH can be identified as irregular ventricular margins and/or hyperechoic or intermediate echogenic bands or nodules, sometimes bulging along the ventricle surface or in periventricular area (Fig. 12.1-54A; see Fig. 12.1-38).[333,337,344] Dedicated axial and coronal images of the ventricles allow improved detection.[337] Mild ventriculomegaly is often noted, sometimes in association with a squared appearance of the frontal horns and bodies of the lateral ventricles.[337,339]

MRI: Most cases of gray matter heterotopia are detected on a fetal MRI being performed for another indication. On MRI, PVH appears as round or oval nodules which are isointense to the cortex, being dark on T2 and hyperintense on T1 (Fig. 12.1-54B; see Fig. 12.1-38). The nodules are typically within the wall of the ventricle, projecting into the ventricle and/or periventricular area.[328,339] Mild ventricular dilatation, thinning of the overlying cortex, and shallow sulci may be present. In a recent review, fetal MRI was only 67% sensitive for detection of heterotopia, but had 100% specificity when the abnormality was verified on two imaging planes.[345] The detection of heterotopia is often difficult in view of the small size of heterotopia and similar signal to the germinal matrix, and is especially diminished at less than 24 weeks, due to more fetal motion and small size of the brain.[345]

SCH will show gray matter signal extending from the ventricular surface to the cortex or manifest as a focal mass in the white matter (Fig. 12.1-55). The overlying cortex tends to be thin and deficient in sulcation, and the affected area of the brain is small.[340] If large, blood vessels and prominent undulations with CSF signal can be seen in the ectopic gray tissue. Dysgenesis of the corpus callosum is noted in greater than 70% of patients.[340]

Associated Anomalies: Other intracranial anomalies are common with PVH and include pachygyria, polymicrogyria, ACC, Chiari II malformation, posterior fossa anomalies, schizencephaly, encephaloceles, and metabolic disorders such as Zellwegers.[339,340]. Limb and frontonasal disorders can be seen with PVH.[342] SCH is often associated with areas of polymicrogyria and callosal anomalies.[203]

Differential Diagnosis: The normal germinal matrix, especially the area of the ganglionic eminences, is prominent early in gestation and should not be confused with nodular heterotopia. Differential for PVH includes TS and early subacute subependymal hemorrhage. Nodules of TS appear similar to PVH; however, family history and presence of cardiac or renal

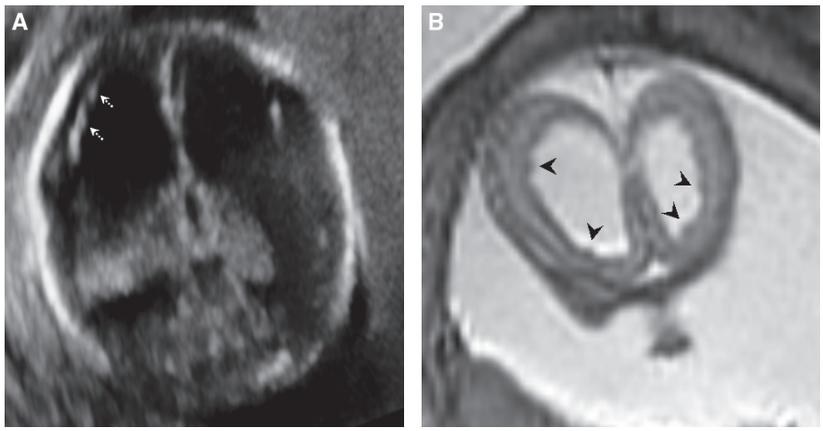

FIGURE 12.1-54: Fetus at 21 weeks with aqueductal stenosis. **A:** Axial ultrasound demonstrates irregularity *(dotted arrows)* of the ventricular wall. **B:** Coronal T2 image in same fetus shows dark nodular areas (*arrowheads*) along the wall of the frontal horns proven postnatal to represent gray matter heterotopia.

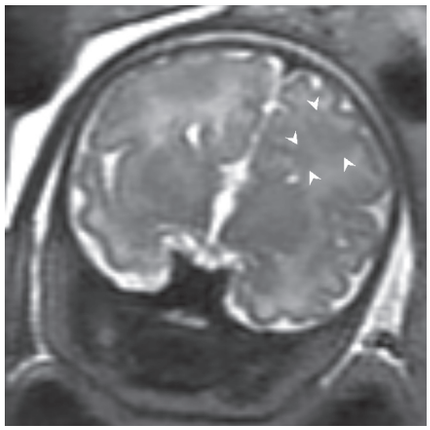

FIGURE 12.1-55: Fetus at 35 weeks with ACC and proven subcortical heterotopia. Coronal T2 image demonstrates a nodular band of gray matter signal (*arrowheads*) extending from the ventricular surface to the cortex.

findings may help differentiate. Subacute hemorrhage usually occurs in the presence of intraventricular hemorrhage and ventriculomegaly, and will evolve over time. SCH should be differentiated from tumor or schizencephaly, which demonstrates a central cleft.

Prognosis: In the presence of associated anomalies, the outcome is worse for both PVH and SCH with developmental delay of variable severity and early seizure onset.[338,339] Males with X-linked PVH have a worse prognosis than females, with high incidence of neurodevelopmental disorders and seizures.[328,339,340] Disorders of cognition are less likely in the unilateral focal PVH group but more likely in those affected with bilateral diffuse PVH.[338,340] In some patients with PVH, the lesion is incidental as no symptoms are present. Approximately 80% of patients with PVH develop epilepsy, usually in the second decade of life.[338,339] Patients with SCH nearly all develop seizures in the second decade of life.[340] Variable motor and intellectual deficiencies occur, depending on the site and size of the SCH.[340]

Management: With epilepsy, treatment with antiepileptic drugs is the first line of therapy. If seizures are refractory, surgical resection of SCH may be considered.[340]

Recurrence: Recurrence is dependent on whether the lesion is sporadic or associated with a syndrome/genetic disorder.

Cobblestone Lissencephaly/Walker-Warburg (aka Lissencephaly Type II; Cerebroocular Dysgenesis; Cerebroocular Dysplasia; Muscular Dystrophy; Chemke, Pagon and HARD Syndrome)

Incidence: Cobblestone or type II lissencephaly is rare with unknown worldwide distribution.[346]

Pathogenesis: For normal neuronal migration, a normal interaction must occur between the radial glial cells and the outermost pial–glial membrane known as the glia limitans.[347] In cobblestone lissencephaly, typically between the 6th to 7th week of gestation, the neurons move too far past the glia limitans into the subpial space. Pathologically, this is caused by impaired linkage of the radial glia to the pial basement membrane leading to a disruption of the pial barrier, which results in lack of normal cortical plate lamination and neuroglial ectopia in the subarachnoid space (Fig. 12.1-56).[203,347] The cerebellum is affected similar to the supratentorial brain; however, in the cerebellum there is disrupted adhesion of the developing granule cells to the pial basement membrane.[347] Cobblestone lissencephaly is most commonly associated with the congenital muscular dystrophies, which are a group of heterogeneous disorders some

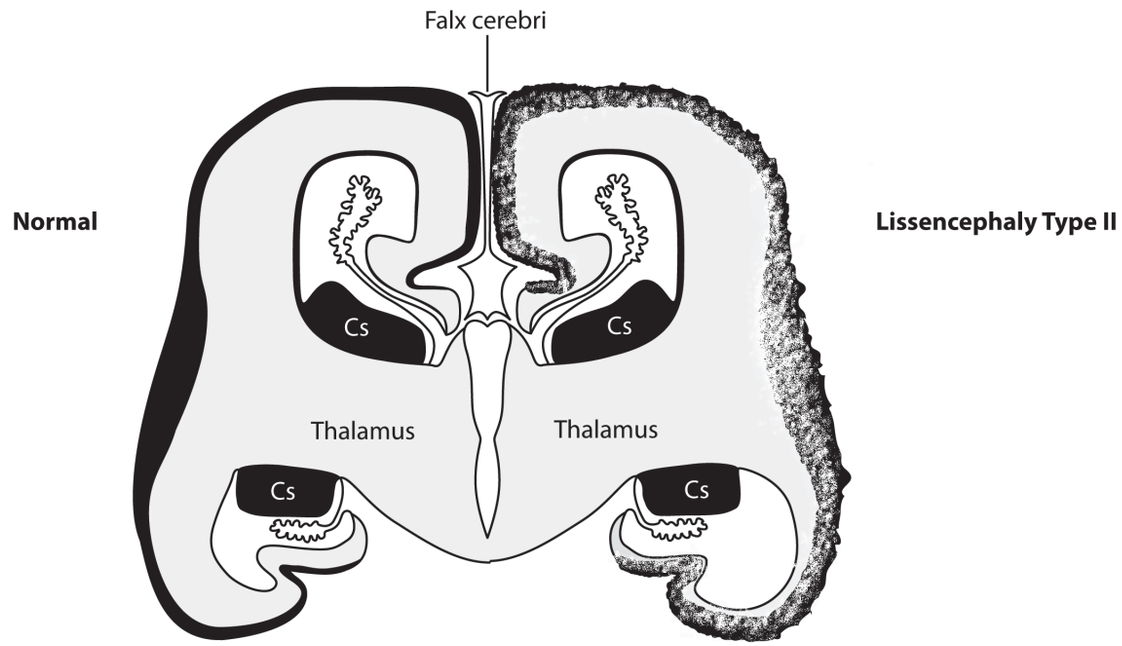

FIGURE 12.1-56: Diagram of imaging findings in lissencephaly type II.

primarily affecting muscle and others with muscle and CNS involvement.[348] Those with CNS abnormalities have abnormal O-glycosylation of α-dystroglycan, which in its absence results in defective formation of the basement membrane of the brain, muscle, and retina.[203]

Etiology: Multiple genes, all thus far inherited autosomal recessive, have been linked to cobblestone lissencephaly. These include *POMT1*, *POMT2*, *FKTN*, *FKRP*, *LARGE*, *POMgnT1*, and *GPR56*.[203,323] The gene type and mutation abnormality have an impact on the severity of the pathology.[203,347] In general, the *POMT1*, *POMT2*, and *FKRP* are associated with severe phenotype, *LARGE* with moderate, and *POMgnT1* with milder disorders.[347] Congenital muscular dystrophies include Walker–Warburg, muscle-eye-brain disease (initially described in the Finnish), and Fukuyama (described in Japanese descent). The most common and severe phenotype is Walker–Warburg syndrome (WWS) also known as hydrocephalus, agyria, retinal dysplasia with or without encephalocele (HARD+E).[324,349] WWS has been associated with multiple identified and many yet unknown genetic abnormalities. The syndrome is typically caused by *POMT2, POMT2, FRKP*, and fukutin genes, but only 10% to 20% of cases have been diagnosed with these genetic markers.[346]

Diagnosis of WWS includes type II lissencephaly, cerebellar malformation, retinal malformation, and congenital muscular dystrophy.[324,350] Ventriculomegaly may be present with or without hydrocephalus. Brainstem abnormalities are common and include fused colliculi, small pons, and dysmorphic mesencephalon with a dorsal pontomedullary kink that is characteristic of primitive hindbrain morphology.[351] Ocular abnormalities may or may not be present and include microophthalmia, anterior and posterior segment anomalies, persistent fetal vasculature, retinal dysplasia, retinal detachment, coloboma, and optic nerve hypoplasia.[349] Muscle changes often do not occur till late fetal period or postnatal. The brain malformations of WWS are most severe, followed by muscle-eye-brain (MEB) and, finally, Fukuyama (FMD) on the milder end of the spectrum.[352] MEB disease findings are similar to WWS, with eye findings milder, including progressive myopia and retinal detachment.[346,352] In FMD, frontal or occipital temporal lissencephaly, cerebellar polymicrogyria and hypogenesis, often in the presence of subcortical cerebellar cysts and simple myopia, are noted.[348,352]

Diagnosis: Amniocentesis with DNA analysis of the *POMT1* gene may be performed.[346]

Ultrasound: In the presence of ventriculomegaly and abnormalities of the posterior fossa, cobblestone lissencephaly should be considered for early prenatal diagnosis.[324,353] Ventriculomegaly is the most common finding, noted in 90% of cases followed by cerebellar abnormalities in 33% (Fig. 12.1-57A).[324,353] Smooth brain, cerebellar, and retinal malformations may be visualized by US in only 25% of cases.[353] Sulcation abnormalities are difficult to diagnose prior to 24 weeks, and this may be even more problematic in the presence of ventriculomegaly, which effaces subarachnoid spaces.[351,353] US may show loss of normal brain parenchymal lamination and/or a thin smooth cortex.[332,333] Transvaginal and 3D imaging may help in evaluation, allowing better detail of the corpus callosum and posterior fossa.[351,353] Ocular anomalies such as bilateral echogenic lenses and conical structures within both globes with apex toward the retina representing primary hyperplastic vitreous with retinal detachment may be detected (Fig. 12.1-57B).[349]

MRI: On MRI, the supratentorial brain may be smooth, but often demonstrates a pebbled appearance of polymicrogyria (Fig. 12.1-57C).[324] There is an irregular gray white matter differentiation, and the white matter can demonstrate increased T2 signal due to edema or dysmyelination.[352] The normal pattern of lamination is absent.[354] The cerebellum, especially vermis, is usually hypoplastic with abnormal foliation.[348] An enlarged superior cerebellar cistern is commonly present.[355] Brainstem hypoplasia with a kink at the pontomesencephalic junction or Z-shaped configuration can be appreciated by MRI (Fig. 12.1-57D).[324,348] The pons may have a central cleft. The tectum may be thick, and aqueductal stenosis can be present, which is often the cause for the ventriculomegaly. The extraaxiaal fluid spaces are small owing to neuronal and glial heterotopia.[352] Ocular abnormalities can also be detected (Fig. 12.1-57E).[324]

Associated Anomalies: Intracranial anomalies of the brainstem, cerebellum, white matter, and corpus callosum are common. Encephaloceles are often present in WWS.[347] Extracranial anomalies are possible and are listed in Table 12.1-15.

Differential Diagnosis: Congenital infection may mimic findings of the cobblestone lissencephaly. Classic lissencephaly will also demonstrate abnormal sulcation but a thick smooth cortex. Chromosomal anomalies such as trisomy 13 and 18 and Fryns syndrome may have ventriculomegaly and other brain anomalies. Meckel Gruber can present with posterior fossa encephalocele but is usually seen in conjunction with large polycystic kidneys.

Prognosis: Children with WWS never reach any developmental milestones, have severe hypotonia, ocular abnormalities, muscle weakness, occasional seizures, and usually die in the first year of life because of respiratory illness.[346] MEB is less severe and children with FMD, although typically with severe mental retardation, can live to 4 to 6 years of age, though usually with progressive myopathy.[352]

Management: With family history of WWS, ultrasound in the first trimester can verify diagnosis.[356] Termination of pregnancy may be considered. Laboratory testing will demonstrate elevated creatine kinase and a muscular dystrophy characterized by hypoglycosylation of α-dystroglycan.[346] No specific treatment is available. Management is supportive.[346] Control of seizures with medication, shunting for hydrocephalus, and surgical repair of encephaloceles may be required.

Recurrence: Most forms are autosomal recessive with a 25% risk for recurrence.[346]

Disorders of Cellular Organization

Polymicrogyria

Incidence: The incidence of polymicrogyria is unknown.[357]

Pathogenesis: Polymicrogyria (PMG) is heterogenous in histology and cause, with a pathogenesis still incompletely

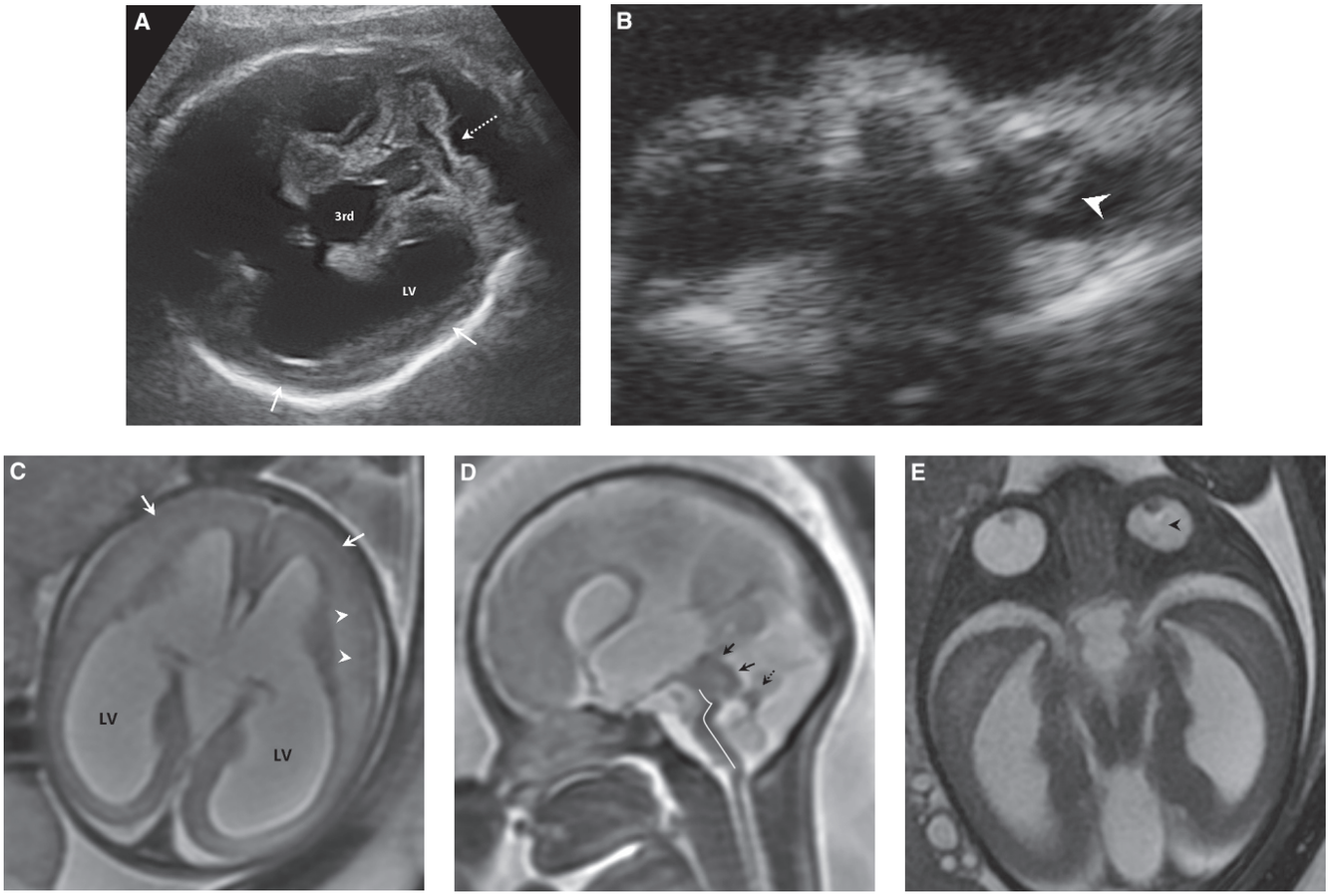

FIGURE 12.1-57: Fetus at 33 weeks with Walker–Warburg syndrome. **A:** Axial US demonstrates moderately severe lateral *(LV)* and third *(3rd)* ventriculomegaly. The visualized cortex is smooth *(solid arrows)*. The cerebellar vermis is small *(dashed arrow)*. **B:** Left globe demonstrates abnormal echogenic tissue extending vertically through the orbit consistent with primary hyperplastic vitreous (*arrowhead*). **C:** Axial T2 MR image demonstrates smooth mildly irregular cortex *(arrow)* with irregular nodular interface with white matter *(arrowheads)*. The white matter appears hyperintense. The lateral ventricles *(LV)*, are enlarged. **D:** Sagittal T2 image demonstrates the Z- or cobra-shaped configuration of the brainstem *(curved line)*. The tecum is thick *(solid arrows)*, and vermis is dysgenetic *(dashed arrow)*. **E:** Axial SSFP image demonstrates small left globe with abnormal tissue *(arrowhead)* extending from the lens to the retina.

Table 12.1-15 Findings of Walker-Warburg Syndrome

Common

Widespread agyria, pachygyria, polymicrogyria
Ventriculomegaly
Cerebellar hypoplasia and dysplasia, especially vermis
Occipital encephalocele
Abnormal brainstem, Z-shaped
Heterotopias
Aqueductal stenosis
Abnormalities of the corpus callosum
Disorganized myelination
Eye abnormalities
Muscular disease

Less common

Cleft lip
Microtia
Genital abnormalities
Intrauterine growth retardation

understood. The current hypothesis is that PMG results from a genetic disorder or injury that occurs between 16 and 24 weeks, toward the end of neuronal migration or early in cortical organization.[357] Histologically, two types are described. The unlayered PMG is believed to represent an early disruption in cortical migration and organization, and demonstrates a continuous external molecular layer covering neurons that have no laminar organization.[357,358] In the second type, the insult is favored to occur later and the PMG histologically appears as a four-layered cortex with a marginal layer, outer cellular zone of cortical layers II, III, and IV, cell sparse layer V due to laminar necrosis, and an inner cellular layer of VI.[357,358] Both types may be present simultaneously, and both result in numerous 2- to 3-mm gyri, some separated by shallow sulci, others with fusion of the molecular layer, excessive cortical folding, and abnormal cortical cellular architecture (Fig. 12.1-58). PMG may be bilateral, unilateral, focal, multifocal, or diffuse. There is a strong tendency for PMG to develop in the sylvian fissures, seen in up to 80% of patients.[358,359] Other areas include frontal lobe (70%), parietal (64%), temporal (38%), and occipital (7%).[359]

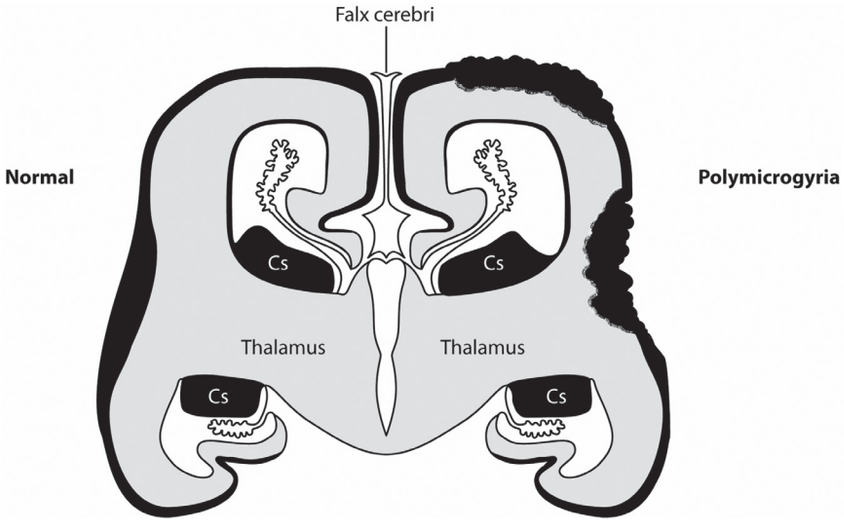

FIGURE 12.1-58: Diagram of polymicrogyria.

Etiology: Cytotoxic, hypoperfusion, or genetic disturbances are possible etiologies for PMG (Table 12.1-16).[357] Bilateral PMG is favored to represent an early insult which may be sporadic but should raise suspicion for genetic abnormalities, many of which are yet defined. Cytotoxic and hypoperfusion injuries typically result in asymmetrical or focal PMG and likely occur later in cortical development.[357] Numerous prenatal insults, including those from infection, toxins, hypoxic ischemic injury, and maternal trauma, can cause PMG.[203,360,361] The etiology is often idiopathic.[221]

Genetic disorders include bilateral frontoparietal PMG, which is an autosomal recessive disorder on chromosome 16q12.2 to 21 with mutations in the *GPR56* gene, and is seen in conjunction with myelination abnormalities and dysplasia of the brainstem and cerebellum.[357] Familial perisylvian bilateral PMG is located primarily at Xq28 with transmission X linked in 75%, the remaining autosomal recessive or dominant.[357] Perisylvian polymicrogyria (unilateral and bilateral) can be seen in chromosomal aneuploidies, the most common being deletion of chromosome 22q11.2 as in velocardiofacial or DiGeorge syndrome.[362] Polymicrogyria with PVH in frontal perisylvian and temporoparietal areas are likely undiagnosed genetic disorders.[363]

Some syndromes have a high association with PMG. Sturge Weber, which is a leptomeningeal vascular dysplasia causing impaired brain perfusion due to blood stasis in abnormal small veins, should be considered when there is PMG along one hemisphere.[364] Temporal lobe enlargement and PMG are present in nearly all cases of thanatophoric dysplasia, identified by multiple deep fissures along the inferomedial temporal and occipital surfaces.[365] Zellweger syndrome or cerebrohepatorenal syndrome is a peroxisomal metabolic disorder caused by a defect of the *PEX* gene family, transmitted autosomal recessive. In Zellwegers, cortical malformations in the perisylvian and perirolandic region occur that appear similar to PMG and pachygyria but actually represent too numerous and too small gyri.[366] Germinolytic cysts, severe hypomyelination, hepatosplenomegaly due to hepatic dysfunction, and renal cystic disease help diagnose this syndrome.[366,367]

Diagnosis: Infectious workup may be considered. FISH analysis for deletions of chromosome 22q11 and 1p35 should be deliberated in the presence of PMG, dysmorphic features, and cardiac defect.[357] *PEX* gene molecular testing or biochemical testing for very long chain fatty acids in the amniotic fluid may be considered if there is concern for Zellwegers.[367]

Ultrasound: Polymicrogyria may be suggested in the presence of abnormal overfolded sulci and gyri, overdeveloped often with respect to the gestational age (Fig. 12.1-59).[333,368] Hyperechogenicity of the cerebral cortex has also been described, representing subcortical necrosis or the excessive infolding (Fig. 12.1-60A).[361,369] Sometimes, the sulcation may be immature.[133] Enlargement of the subarachnoid space overlying the PMG is often present.[368] It is likely easier to diagnose PMG in the second trimester than later in the third due to development of the secondary sulci.[368]

MRI: PMG leads to accelerated development in gyration with patterns including multiple irregular small bulging and invaginating areas, presence of a major sulcus not yet expected for gestational age, sawtooth pattern, or single to multiple bumps (Figs. 12.1-60B and 12.1-61A).[370,371] There is burring and reduced thickness in the subplate and intermediate zone in 80% of cases (Fig. 12.1-61B).[371] Volume loss, especially white matter, and enlarged subarachnoid spaces have been described.[358,369] Venous anomalies in the area of abnormal gyration are present in more than half of cases.[358] Early in gestation, detection may be more difficult, especially less than 24 weeks, but attention to the normal signal of the cortical ribbon, presence of sulci that are not expected for gestational age, and irregular surface of the brain should raise suspicion.[221,344] Fetal MRI has an overall 85% sensitivity and 100% specificity in detection of PMG.[344]

Associated Anomalies: PMG may be isolated but is often present with other intracranial pathologies such as schizencephaly, SOD, periventricular nodular heterotopia, subcortical heterotopia, and ACC.[359] Imaging findings of encephaloclastic insult

Table 12.1-16 Causes of Polymicrogyria

Post insult
Infection
- CMV
- Toxoplasmosis
- Parvovirus

Toxins
- Fetal alcohol
- Maternal drug ingestion

Hypoxic ischemic
- Monochorionic twin pathologies
- Demise of a co-twin
- Twin-to-twin transfusion syndrome
- Maternal hypotension

Trauma

Malformations with PMG
- Schizencephaly
- Septo-optic dysplasia
- Bandlike calcification (pseudo-TORCH)
- Periventricular nodular heterotopia

Genetic
- Velocardiofacial/DiGeorge syndrome—deletion of chromosome 22q11
- Deletion of 1p36
- Bilateral perisylvian PMG—X-linked, autosomal recessive or dominant at Xq28
- Bilateral frontoparietal PMG—autosomal recessive at 16q12.2–21
- Generalized PMG—autosomal recessive

Syndromes
Vascular
- Sturge-Weber
- Megalencephaly, PMG and postaxial polydactyly, midface capillary malformations

Skeletal dysplasias
- Thanatophoric dysplasia
- Osteosclerosis, cleft palate, and bilateral PMG

Metabolic
- Zellwegers
- Neonatal adrenoleukodystrophy
- Congenital muscular dystrophy Walker–Warburg

Others
- Aicardi
- Adams–Oliver
- Delleman (oculo-cerebral-cutaneous syndrome)
- Joubert
- Pena–Shokeir

may be noted. Genetic and chromosomal syndromes that are associated with PMG often present with additional intracranial and extracranial anomalies.

Differential Diagnosis: Normal sulcation anatomy should not be confused with PMG. Encephaloclastic insults such as hemorrhage and ischemia may mimic cortical ribbon abnormalities. Schizencephaly is often associated with PMG, but is present with a central cleft.

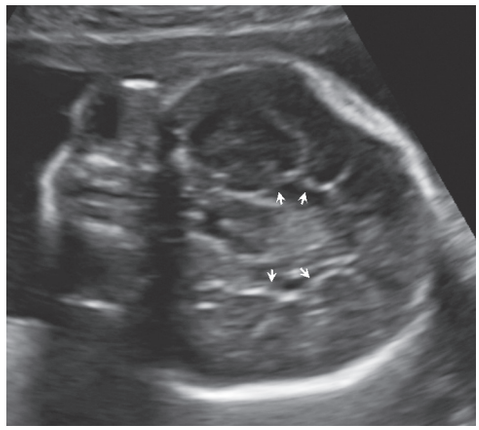

FIGURE 12.1-59: Polymicrogyria in thanatophoric dysplasia at 21 weeks. Axial US demonstrates abnormal advanced sulci along the bilateral medial temporal lobes *(arrows)*.

Prognosis: Outcome depends on the location and extent of the PMG and the presence of associated anomalies.[371,372] Children with PMG may have developmental delay, focal neurologic deficits, and epilepsy. Bilateral or diffuse PMG or PMG of more than half of a single hemisphere are poor prognostic factors, with these children having moderate to severe developmental delay and significant motor dysfunction.[371]

Sporadic cases of bilateral perisylvian polymicrogyria have 100% oropharyngeal dysfunction and dysarthria, epilepsy in 80% to 90%, mental retardation in 50% to 80%, and sometimes congenital arthrogryposis.[371] Familial perisylvian PMG tend to be less symptomatic.[362] Frontoparietal PMG has developmental delay, mild spastic quadriparesis, impaired language, disconjugate gaze, cerebellar signs and epilepsy.[371] Zellwegers has a poor prognosis with death in the 1st month of life.[367]

Management: Depending on the severity of the defect and associated anomalies, termination of the pregnancy may be considered. Postnatal therapy is primarily supportive and includes treatment of epilepsy and physical therapy for neurologic deficits.

Recurrence: In the sporadic form, there is no risk of recurrence. In genetic forms, the recurrence is dependent on type of the transmission.

Schizencephaly

Schizencephaly (SZ), also known as agenetic porencephaly or true porencephaly, represents a transcerebral cleft with a pial ependymal seam, defined as a cleft lined by gray matter from the ependymal lining of the ventricles to the pial covering of the cortex.[373]

Incidence: Prevalence is approximately 1.5 in 100,000 births.[374,375] There is a high association with young maternal age.[374,375]

Pathogenesis: SZ occurs when there is injury of the entire thickness of the hemisphere. Pathologically, there may be a primary insult to the germinal matrix, failure in induction of neuronal migration, or focal ischemic necrosis with destruction of the radial glial fibers during neuronal migration.[374,376,377]

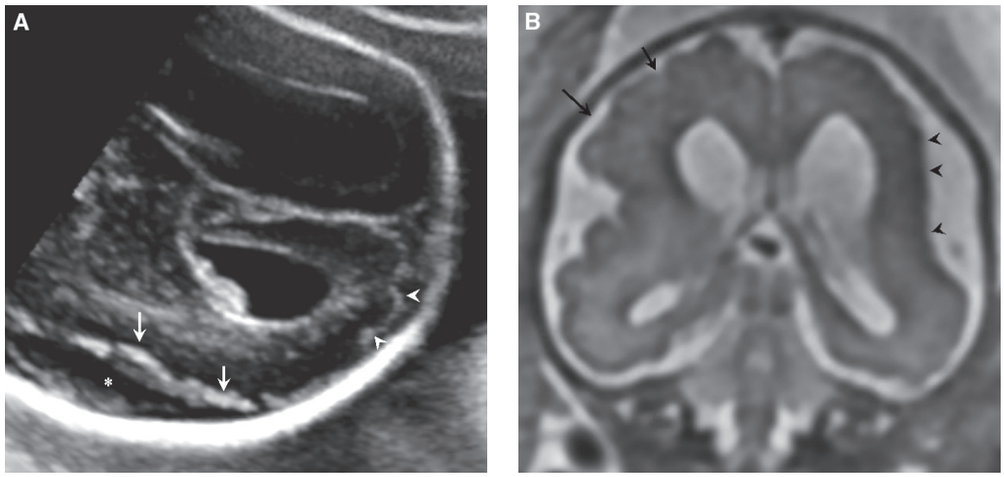

FIGURE 12.1-60: Polymicrogyria in a fetus at 27 weeks. **A:** Axial ultrasound demonstrates increased echogenicity of the cortex *(arrows)*, irregularity of the cortex *(arrowheads),* and enlarged extra-axial fluid space *(asterisk)*. **B:** Coronal T2 MR demonstrates multiple small lobulations along the right hemisphere *(arrows)* and sawtooth pattern along the left *(arrowheads)*. Notice loss of gray white differentiation and lamination with reduced thickness of the brain parenchyma in the left hemisphere.

There has been extensive debate on whether SZ results from a developmental versus destructive insult, though increasing evidence suggests that a vascular disruptive process is likely before 24 weeks' gestation.[374,375] As the perisylvian area is typically abnormal, many believe that SZ may represent a small vessel vascular insult in the watershed zone.

SZ can be bilateral, unilateral, symmetrical, asymmetrical, small, or large. Two type of SZ are described (Fig. 12.1-62). Type I represents a cleft that is closed with gray matter lined lips in contact with each other.[373] Type II is an open defect with CSF separating the gray matter lined clefts. Approximately 49% of SZ are bilateral, 51% unilateral, and 83% are open lipped with remaining fused.[377] Most SZ are frontal or perisylvian with temporal and parietal less likely and occipital least.[377] Approximately 66% of SZ cases are associated with other CNS anomalies.[374]

Etiology: The causes for SZ are heterogeneous. Over half can be attributed to a vascular disruptive event in utero, including infection, teratogen, hypoperfusion injury in twins, inherited thrombophilia or trauma in the first or second trimester.[374] Familial cases are reported.[378] Adams-Oliver syndrome with limb reduction and encephaloclastic changes in the brain, and ectrodactyly are two known genetic associations.[374]

Diagnosis

Ultrasound: There are no US reports of SZ prior to 20 weeks, with most cases identified after 28 weeks gestation.[375,379] It is suggested that the damaging process in SZ may occur early in pregnancy but continue to evolve and not be apparent until la ter.[375,380,381] Therefore, it is possible that an early second-trimester scan will miss the abnormality.[375] Ventriculomegaly is often the first sign detected.[381] Wide clefts of CSF communicating between the lateral ventricles and subarachnoid spaces often lined by echogenic tissue should raise suspicion (Fig. 12.1-63A).[333,382] 3D and transvaginal imaging may prove helpful in characterizing the cleft and demonstrating the connection with the ventricle and subarachnoid space.[380,383]

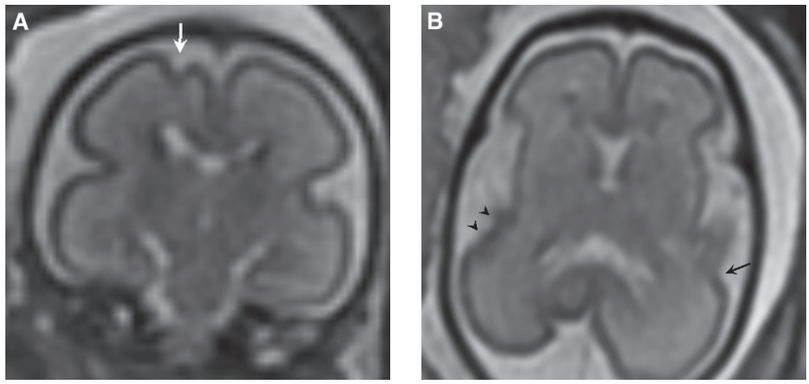

FIGURE 12.1-61: Polymicrogyria in two fetuses. **A:** Fetus at 24 weeks with abnormal bump *(arrow)* focally within the right frontal cortex. **B:** Fetus at 28 weeks with arthrogryposis and focal sawtooth appearance to the right sylvian cortex *(arrowheads)*. The opposite demonstrates abnormal lobulation (*arrow*). Postnatally, the child was proven to have perislyvian syndrome.

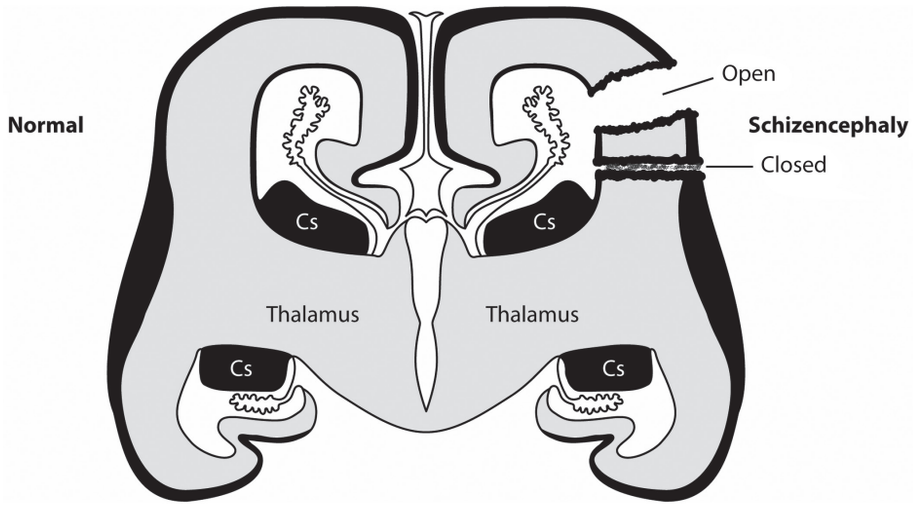

FIGURE 12.1-62: Diagram of types of schizencephaly.

Small open- or closed-lipped cleft can be more difficult to detect with antenatal US but may be suggested in the presence of parallel echogenic tissue extending from the lateral ventricle to extraaxial fluid space (Figs. 12.1-64A).[381] Linear echogenic structures in the white matter may represent normal veins or fetal white matter tracts, so care should be taken not to misinterpret them falsely as clefts.[380]

MRI: Gray matter lining a cleft extending from the ventricular surface to the subarachnoid space is necessary for diagnosing SZ (Fig. 12.1-63B).[376,382] A fine membrane, likely representing remnant of the pia mater or ependyma, can sometimes be detected (Fig. 12.1-63C).[379] A CSF signal tented area may also be identified extending from the wall of the ventricle, pointing to the defect (Fig. 12.1-64B).[378] SSFP imaging is excellent at defining edges of CSF and soft tissue and may be helpful in verifying the CSF cleft.[382] Gradient echo may demonstrate hemosiderin staining along the defect, seen in as high as 83% (Fig. 12.1-65).[379]

Most clefts identified in the prenatal time are open lipped; however, nearly 50% will close postnatally.[379] Sensitivity in detection of SZ on MRI has been cited at 100% sensitivity and 99% specificity.[345] Anomalies can be detected which include absence or partial absence of the cavum septum pellucidum or corpus callosum.[381] PMG tends not to be detected in the cleft prenatally, and PMG and PVH outside the area of SZ are not commonly defined prenatal.[379] Optic hypoplasia is very limited in visualization owing to lower resolution limits of fetal MR.[379]

Cerebellar clefts may be identified prenatally.[384] Some of these clefts extend from the cerebellar surface to the fourth ventricle, often in association with loss of normal architecture, maloriented cerebellar foliation, and irregular gray white matter junction (Fig. 12.1-66). These clefts may also have similar pathogenesis to SZ.[384]

Associated Anomalies: SZ is often associated with PMG (66%), PVH (50%), thin or absent corpus callosum (42%), white matter volume loss, white matter signal abnormalities (20%), optic

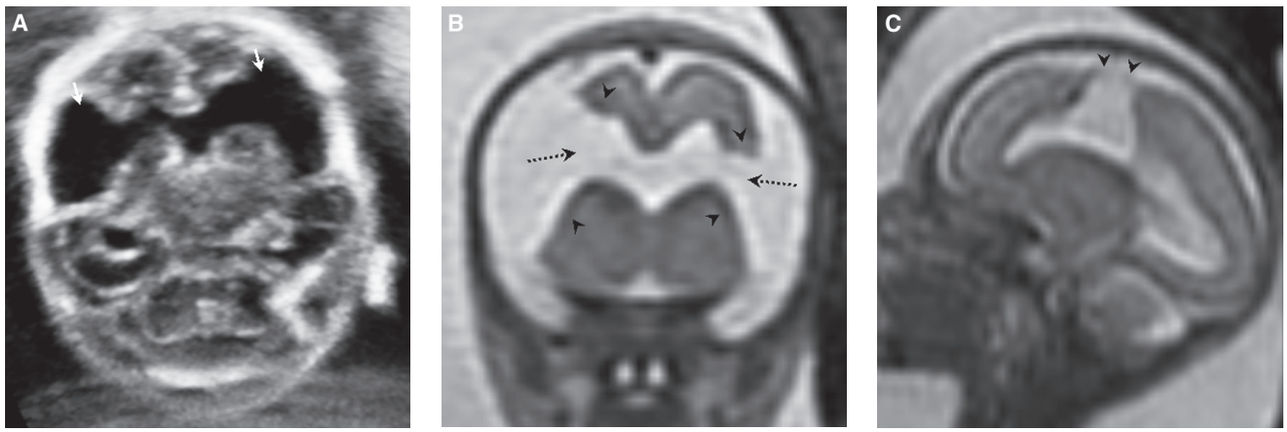

FIGURE 12.1-63: Axial image of fetus at 23 weeks with SOD. **A:** US showing absence of the septum pellucidum and large bilateral frontal defects *(arrows)* proved to represent open-lipped schizencephaly. **B:** Coronal image demonstrates open-lipped schizencephaly defects *(dotted arrows)* lined with gray matter *(arrowheads)*. Notice absence of the septum pellucidum. **C:** Sagittal T2 image of open-lipped defect with thin membrane *(arrowheads)*.

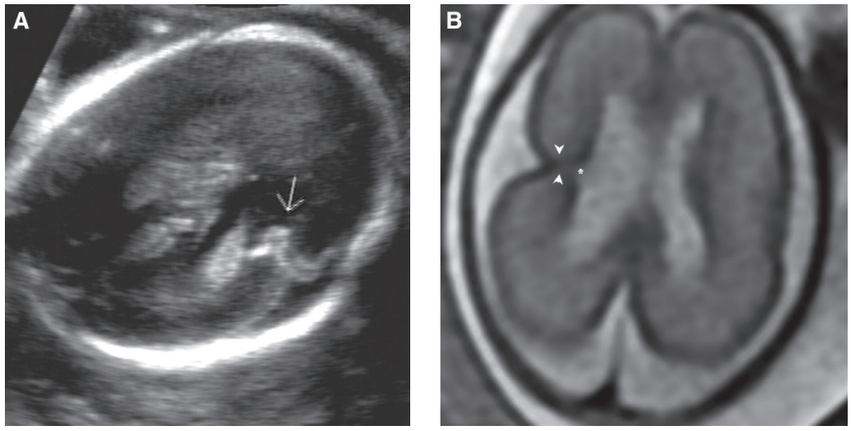

FIGURE 12.1-64: Fetus at 22 weeks with closed-lipped schizencepahly. **A:** Axial ultrasound demonstrates parallel echogenic lines *(arrow)* extending from ventricular to extra-axial fluid space. **B:** Axial T2 MR image shows the closed defect lined with gray matter *(arrowheads)*. Notice tenting or nipple *(asterisk)* extending from the ventricle.

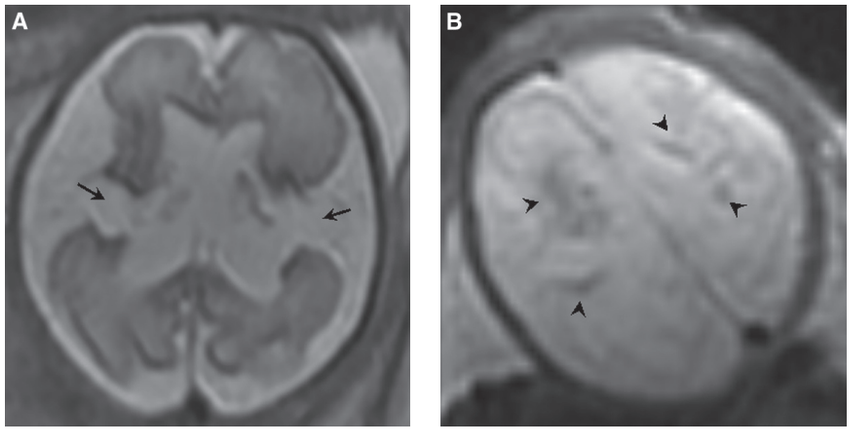

FIGURE 12.1-65: Fetus at 32 weeks with bilateral open-lipped schizencephaly. **A:** Axial T2 image demonstrates the gray matter lined open clefts *(arrows)*. **B:** Gradient echo imaging demonstrates susceptibility artifact along the margins of the cleft *(arrowheads)*.

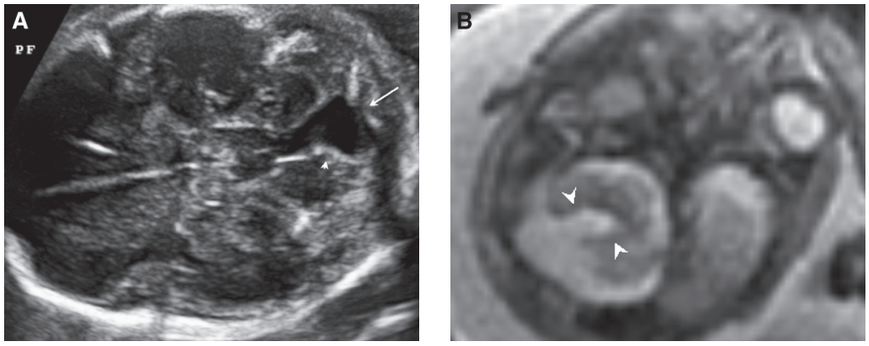

FIGURE 12.1-66: Cerebellar cleft in a fetus at 24 weeks. **A:** Axial US demonstrates a prominent CSF defect in the cerebellum *(arrow)* with mild increased echogenicity of the parenchyma along the defect *(arrowhead)*. Vermian abnormality was questioned. **B:** Axial T2 MR image shows gray matter *(arrowheads)* lined defect through right cerebellar hemisphere. Fetus also had a closed-lipped schizencephaly in the occipital lobe (not shown).

nerve hypoplasia (20%), and absence of the septum pellucidum (35% to 50%).[374,377,385] The septum pellucidum is often absent when the defect is bilateral, open lipped, or in the frontal lobe.[385] Ventriculomegaly is seen in 70% of cases and is more likely to be associated with open defects.[377,383] Posterior fossa anomalies are also reported.[382] SZ can be associated with other extracranial vascular insults including amniotic band, arthrogryposis, gastroschisis, cleft palate and lip.[374]

Differential Diagnosis: Porencephaly, glioependymal cysts, and arachnoid cysts should be considered but are not lined by gray matter. In the presence of large open defects, hydranencephaly and holoprosencephaly can be excluded by detection of normal basal ganglia structures and midline falx.

Prognosis: The size and location of the SZ as well as associated cerebral anomalies have implications on outcome.[376] Bilateral and open clefts as well as SZ with additional anomalies adversely affect outcome.[376] Motor dysfunction tends to correspond to clefts in the frontal lobe. Prenatal diagnosed cases tend to be bilateral, often associated with other CNS anomalies such as absence of the septum pellucidum. These children have a more guarded prognosis.[378] However, when counseling, it should be remembered that an apparently open cleft prenatally may become closed postnatally.[379,380]

Approximately 81% of patients with SZ experience seizures; however, surprisingly, unilateral SZ is more likely than bilateral, but bilateral is more likely to present earlier in life and be more severe.[386] Patients with bilateral SZ have severe developmental delay with language impairment and spastic quadriparesis. Children with unilateral SZ experience variable hemiplegia and mild intellectual deficiencies likely due to the plasticity of the brain at the time of injury.[376]

Management: When counseling, it is important to remember that clefts open prenatally may be closed on postnatal imaging. Termination of the pregnancy may be discussed. Management is supportive with therapy directed at seizure control and rehabilitation of motor deficits.

Recurrence: No increased risk of recurrence is known in the absence of familial history or known syndrome.

DESTRUCTIVE INSULTS

Germinolytic/Subependymal Cysts

Incidence: Subependymal cysts (SC) are found in 0.5% to 5% of all neonates, being more common in the preterm.[387–389] The prevalence of in utero subependymal cysts is not known, but they are described less frequently in the fetal literature.[390]

Pathogenesis: Histologically, SCs are pseudocysts given that the cavities lack an epithelial wall and are instead limited by a pseudocapsule aggregate of germinal cells and glial tissue encircling fluid containing macrophages with rare iron staining.[391] Two types are suggested, one of which is congenital and the other germinolytic due to injury.[392] The congenital is believed to be due to regression of remnant germinal matrix, as an acellular area exists between the germinal zone and the ependyma, which may normally become cystic with growth of the fetus.[387,388] However, the more commonly entertained etiology is that a SC develops from prenatal lysis of undifferentiated germinal matrix cells, likely due to ischemia, inflammation, or hemorrhage.[387,389,392] It is not surprising that these cysts are found most commonly at the caudothalamic groove, inferior frontal by caudate nucleus or, rarely, adjacent to the temporal horn, representing areas of the ganglionic eminences which persist late in gestation.[387,389] When a SC is found in other areas, it may suggest an earlier insult.[393] The cysts are bilateral in 49% of cases, unilateral, simple or complex; however, when unilateral, the left side tends to be more common.[389]

Etiology: Simple pseudocysts are found in up to 50% of cases as isolated cysts, often bilateral and symmetrical in the common locations.[387] In the presence of bilateral simple SC, however, there is still a 20% to 25% chance of the cysts being related to a congenital infection or genetic anomaly.[394] Atypical SCs appear irregular, multilocular, large, along uncommon areas of the ventricle, or different in echotecture or signal from CSF and are very suggestive of an insult.[393,395] A single cyst has lower risk for injury.[394] In the presence of other CNS abnormalities and SC, an insult is more likely.

Subependymal cysts can be caused by vascular disorders, toxic exposures, including cocaine abuse, infection, most notably rubella and CMV, and metabolic, or chromosomal anomalies. Up to 63% of cases of subependymal cysts will have a positive antenatal history predisposing the fetus to hypoperfusion injury.[389] The incidence for infection and SC is as high as 35%.[387] Chromosomal abnormalities associated with SC include DEL q 6 and Del q 4, which impair neuronal migration.[387] Genetic disorders noted with SC include Aicardi-Goutieres transmitted autosomal recessive, with imaging that mimics viral infection.[396] Metabolic disorders associated with SCs include Zellwegers, mitochondrial, Canavans, congenital disorders of glycosylation, organic aciduria, and holocarboxylase synthetase deficiency.[387,390]

Diagnosis

Ultrasound: SCs may be seen as early as 12 weeks.[390] However, most are detected in the third trimester.[390] The type of SC is usually difficult to differentiate sonographically.[6] Most SCs are simple, anechoic well-defined cavities adjacent to the frontal horns, often with a tear-shaped configuration on sagittal imaging (Fig. 12.1-67A).[387,397] The cyst may become increased in echotecture, mimicking hemorrhage.[390] With evolution, SCs can be multiseptated and may increase or decrease in size (Fig. 12.1-68).[390]

MRI: Simple SCs are high signal on T2 imaging and low signal on T1 sequences, usually present below the external angle of the ventricle near caudate or posterior to the foramen of Monro at the caudothalamic groove (Fig. 12.1-67B).[387,392] Hemorrhage may be suggested by high T1 signal, low T2 signal, and susceptibility artifact on gradient echo imaging. If the wall of the cyst is very thin or the lesion is less than 5 mm, the cyst may not be apparent.[388] SSFP or heavily weighted T2 imaging may be considered in the presence of an US abnormality. MRI is helpful to confirm the topography of the cyst and exclude additional cerebral pathology.[390]

Associated Anomalies: Associated anomalies depend on etiology, though many SCs are isolated.

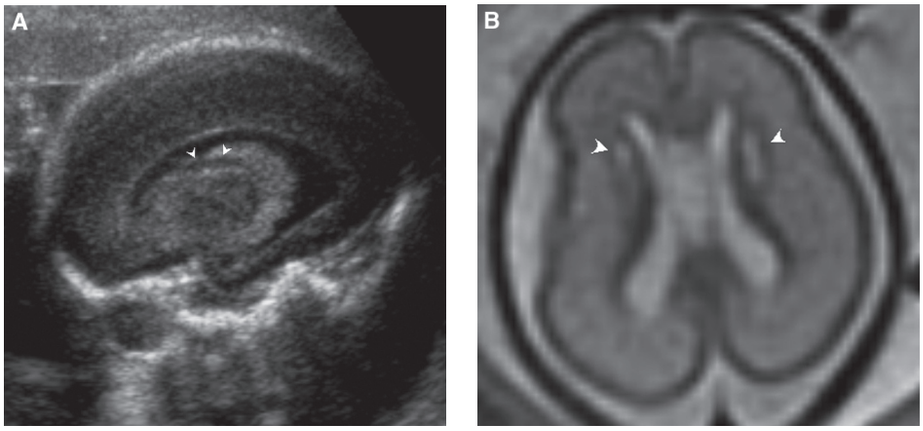

FIGURE 12.1-67: Fetus at 36 weeks with bilateral subependymal cysts. **A:** Sagittal US demonstrates teardrop cystic structures at the caudothalamic groove *(arrowheads)*. **B:** Axial T2 image demonstrates small bilateral cysts *(arrowheads)* adjacent to the caudate heads.

Differential Diagnosis: SCs should be differentiated from choroid plexus cysts that are intraventricular in location. There are three additional cystic lesions that can lie by the ventricle: coarctation, cystic white matter disease, and porencephaly (Fig. 12.1-69). Coarctation of the lateral ventricle manifests as a cystic area anterior to the foramen of Monro and adjacent to the superolateral margin of the body and frontal horn of the lateral ventricles. These cystic areas represent approximation of the walls of the ventricle and are a normal variant.[392] Injury in the white matter may become cystic and simulate a SC. However, cystic degeneration in the white matter is above the angle of the ventricle; whereas a SC is below.[392] A porencephalic cyst typically communicates with the ventricle and extends into the adjacent white matter.

Prognosis: When isolated, 93.5% of SCs regress spontaneously within 1 to 12 months after birth, and in absence of abnormal CMV titers, normal neurologic outcome is expected.[393] In the presence of a positive CMV titer and SC, 50% have neurologic deficit.[389] Atypical cysts are more guarded in outcome, usually dependent on the etiology and associated anomalies.[387,390] In the presence of a history of IUGR, fetal infection, malformation, and chromosomal anomalies, or if the cyst does not resolve postnatally, there is a higher risk of neurodevelopmental impairment.[393]

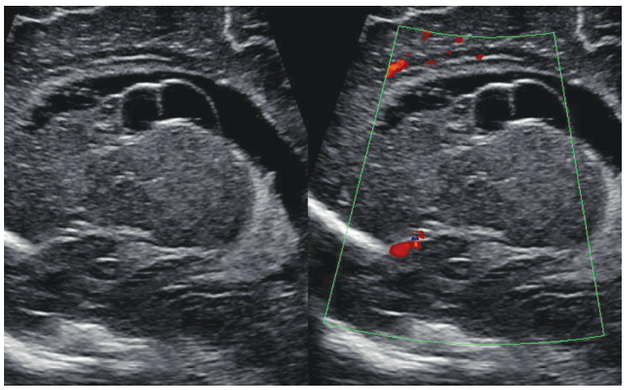

FIGURE 12.1-68: Neonatal US showing complex cysts at the caudothalamic groove. The child had positive CMV titers.

Management: Infection titers or genetic testing may be considered based on the presence of associated anomalies. If the lesion is isolated, no intervention is necessary.

Recurrence: There is no risk of recurrence for isolated SC.

Hypoxic Ischemic Injury

Incidence: The incidence of perinatal stroke, defined as injury between 28 weeks gestation and 28 days postnatal, is reported to occur in 1 in 4,000 live births.[398] The incidence for fetal intracranial hemorrhage and stroke is not clearly known but has been suggested in 1 per 10,000 pregnancies.[399] Many patients remain undiagnosed perinatally as symptomatology is not evident until the first year of life.[398]

Pathogenesis: The severity, type, and distribution of the injury depend on numerous factors that include the duration of the hypoperfusion and the fetal gestational age. In contrast to the neonate, an acute response to hypoxia in the fetus is not common. Most fetal hypoxic injuries are chronic. Therefore, chronic imaging findings or a combination of acute and chronic insults may be observed.[400,401] Acute injury to the basal ganglia and cortex are uncommon in the fetus due to greater resistance of neurons to hypoxia earlier in gestation and also the less acute in utero event.[401] White matter injury is also less common in the fetus when compared to the neonate.[401] Germinal matrix hemorrhage, however, is widely described.

Ischemic and hemorrhagic parenchymal injuries are often mixed as after ischemia, reperfusion of a lesion may result in hemorrhage. Hemorrhage can occur anywhere in the fetal brain: germinal matrix, ventricles, cortex, subarachnoid, or subdural spaces. Approximately 80% to 90% of cases of hypoxic ischemic disease cause intracerebral hemorrhage and the remaining 20% subdural hemorrhage.[402,403] In the presence of intracerebral hemorrhage, nearly 90% are supratentorial, and the remaining infratentorial.[398] Germinal matrix hemorrhage is more common than intraparenchymal bleed.[399]

Etiology: Injury in the fetal brain may be due to hemorrhage, ischemia, or thrombosis. In the majority of cases of fetal brain injury, there is no identified etiology.[398] A cause may

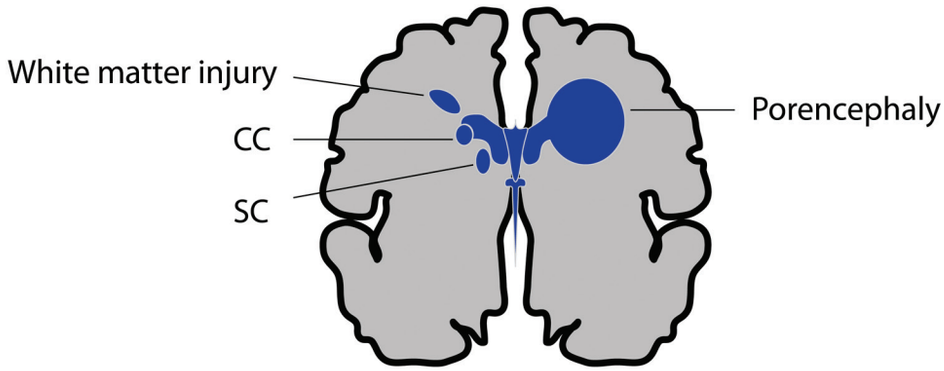

FIGURE 12.1-69: Diagram of different types of cysts and their locations: white matter injury, coarctation cyst *(CC)*, subependymal cyst *(SC)*, and porencephaly.

be detected in to 45% of cases, with many etiologies listed in Table 12.1-17.[398,402] The most frequently identified factors are hematologic or maternal trauma.[398,402] Of those with a cause, hemorrhage due to alloimmune thrombocytopenia has been cited in up to 15% of cases.[402] Fetomaternal alloimmune thrombocytopenia (FAT) occurs in 1 to 2 of 50,000 pregnancies, can affect the first born child, and results from maternal fetal platelet antigen incompatibility, the most common being the Pl(A1).[404,405] Fetal platelets carrying specific paternal derived antigens gain access to the maternal system through the placenta, causing alloimmunization. After sensitization, maternal IGG platelet-specific antibody is produced, which then crosses the placenta and results in fetal platelet destruction. The risk of intracranial hemorrhage with this disorder is 10% to 30%, with 25% to 50% of hemorrhages occurring in utero.[404,405]

Other causes for bleeding include drugs such as warfarin and fetal inherited and acquired coagulopathies. Maternal trauma is another leading cause, often secondary to placental hemorrhage and abruption.[403] Placental thrombosis or vasculopathy in the presence of infection is noted in 11% of case.[403] Intrauterine hypoxia and fetal anemia may result in antenatal hemorrhage, especially in monochorionic twin gestations.[402,403] Fetal anemia is believed to cause ischemia and hemorrhage by disruption of vessels due to hyperdynamic circulation. Metabolic disorders can be as high as 22% of cases and include pyruvate carboxylase deficiency, postulated to cause chronic ischemia due to metabolite depletion in the germinal matrix.[403]

Diagnosis

Ultrasound: Ultrasound criteria for fetal hypoxia include intrauterine growth restriction, abnormal Dopplers, especially umbilical artery and cerebral, and later a bad biophysical profile score which reflects abnormalities in fetal heart rate, amniotic fluid volume, fetal breathing, gross body movements, and fetal tone.[406] Imaging may be initiated by decreased fetal movements and low amniotic fluid.[407] Fetal heart changes including smooth baseline variability and late decelerations with sinusoidal pattern may represent the first sign of brain injury.[398,408] In some cases, fetal anemia may be detected by elevated peak systolic velocity in the middle cerebral artery (MCA).[398] Increased resistance in the MCA may be a sign of increase in intracranial pressure related to a hemorrhage.[404] Absent or reversed diastolic flow in the MCA has been associated with poor outcome.[408–410]

Table 12.1-17 Predisposing Factors for Antenatal Fetal Intracranial Hemorrhage/Ischemia

Maternal
Alloimmune thrombocytopenia
Idiopathic thrombocytopenia purpura
Von Willebrand disease
Vitamin K deficiency
Rh alloimmunization
Drugs including warfarin, cholestyramine, and antiepileptic medications
Toxic exposure alcohol, cocaine, carbon monoxide
Trauma
Iatrogenic—amniocentesis, cordocentesis, blood sampling
Hypoxia related to stroke, hemorrhage, seizure, preeclampsia, or cardiac arrest
Cholestasis of pregnancy
Febrile disease
Diabetic ketoacidosis

Pregnancy
Chorioamnionitis
Prolonged rupture of membranes
Placenta previa
Placental hemorrhage
Placental thrombosis
Abruptio placenta
Monochorionic vascular anastomosis
Twin-to-twin transfusion syndrome
Demise of the cotwin
Cord accident

Fetal
Fetal alloimmune thrombocytopenia
Congenital factor V deficiency
Congenital factor X deficiency
Metabolic disorders—mitochondrial, pyruvate carboxylase deficiency, non-ketotic hyperglycemia, amino acid metabolism, and peroxisomal disorders
Protein C deficiency
Infection—TORCH and non-A, non-B hepatitis
Space-occupying lesions—tumors and cysts

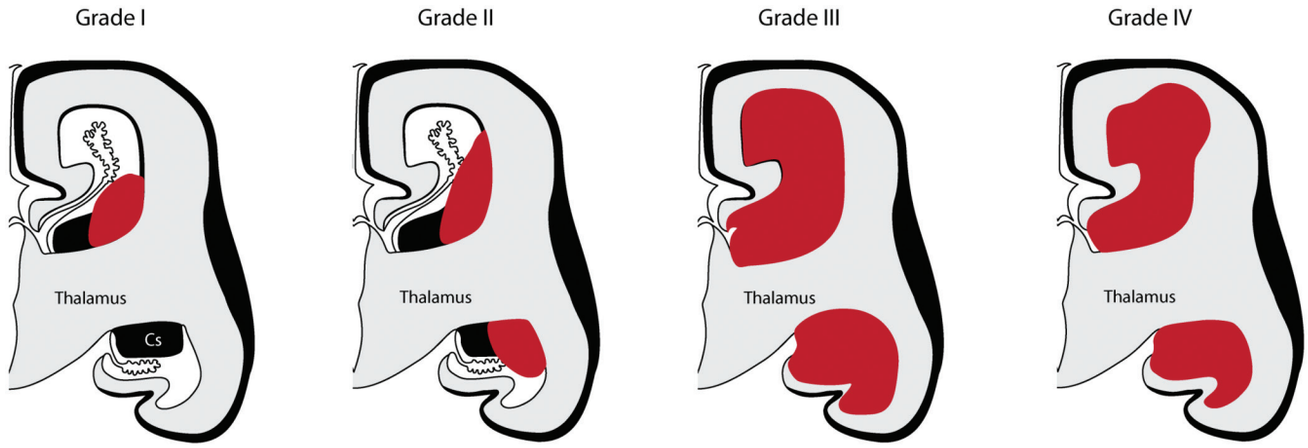

FIGURE 12.1-70: The grade of the germinal matrix hemorrhages.

MRI: MRI is valuable to confirm the presence of hemorrhage or ischemia and to evaluate for parenchymal abnormalities that may not be apparent via US.[411] In utero hypoxia tends to depict chronic imaging finding of injury (67%) rather than acute (33%).[401] MRI may define cerebral abnormalities in up to 67% of cases of hypoxic ischemic injury. The most common findings are ventricular dilatation (77%), hemorrhage (15%), or brain destruction (35%).[401]

Germinal Matrix Hemorrhage

Between 24 and 32 weeks, the germinal matrix is highly proliferative and metabolically active, and contains a thin multilayer, highly vascular network which is particularly sensitive to variations in blood pressure, hypoxia, acidosis, and anoxia. Germinal matrix hemorrhages occur due to sudden changes in the cerebral blood pressure and hypoxia which cause bleeding in the fragile premature capillary bed, likely due to a hypoperfusion–reperfusion cycle.[398] Rupture of the ependyma may then result in intraventricular hemorrhage.

A modified grading system denoted by Burstein and Papile can be used to stage fetal germinal matrix injuries (Fig. 12.1-70, Table 12.1-18).[398,402,412]

Periventricular hemorrhagic infarction or Grade IV has been shown to occur as the result of a venous infarct that develops if a large intraventricular hemorrhage compresses or obstructs terminal veins along the surface of the ventricle.[413] Hydrocephalus may develop if the intraventricular hemorrhage incites an inflammatory ependymitis or obstructs the aqueduct of Sylvius or fourth ventricle with clot. Cerebellar hemorrhage has also been described prenatally and is likely the result of germinal matrix hemorrhage in the cells of the external granular layer.

Before 20 to 21 weeks, insults in the brain result in parenchymal necrosis without gliosis, with the most common appearance being a porencephalic cavity. After 26 weeks, there is astrocyte proliferation, and glial septated cavities, known as cystic encephalomalacia, develop. Later in gestation, the insult will usually result in pure gliosis with no cyst.[414]

Ultrasound: Most cases of intracranial hemorrhage are detected between 26 and 33 weeks, but cases have been described as early as 20 weeks.[408] Intracranial hemorrhage appears different, depending on the time of imaging after the initial insult. Acutely in the first 3 to 8 days, the clot is hyperechoic (Fig. 12.1-71A). If there is significant intraventricular component, the choroid plexus may appear large and irregular.[411] Choroid plexus is not present anterior to the foramen of Monro, and therefore in the presence of echogenic tissue in the frontal horns, hemorrhage should be suspected.[411] After 3 to 8 days, the liquefying clot appears heterogeneous in echotecture, often with an external echogenic lining and an internal echolucent core (Fig. 12.1-71B). From 7 to 28 days, the clot has completely liquefied, begins to decrease in size, and appears as a cystic hypoechoic mass (Fig. 12.1-71C).[408]

Unilateral hemorrahge is more likely to occur in the left than right hemisphere, possibly because of less susceptibility of right hemisphere vessels to hypoperfusion.[398] Echogenicity of the ventriclular wall due to ventriculitis may be noted. With complete resolution, the brain and ventricles may be normal.[408] Sometimes, a transient ventriculomegaly occurs, which resolves over time as the blood products degrade, relieving obstruction at the foramen of Monro.[402] In grade III and IV, ventricular dilatation is more likely to develop and persist (Fig. 12.1-71D).[415] Ventriculomegaly has been detected in as high as 60%, and some may progress to hydrocephalus due to aqueductal stenosis or ventricular obstruction.[402,403]

Intraparenchymal hemorrhage is seen acutely as a densely echogenic mass, frequently extending from the subependymal layer of the ventricle (Fig. 12.1-71E).[402] As the clot degrades, these lesions often become hypoechoic and then progress to a

Table 12.1-18 Burstein and Papile Modified Grading System to Stage Fetal Germinal Matrix Injuries[402,412]

Grade	Description
I	Subependymal hemorrhage
II	Intraventricular hemorrhage, filling less than 50% of the ventricle with ventricle size 15 mm or less
III	Intraventricular with more than 50% of the ventricle with ventriculomegaly >15 mm
IV	I–III with intraparenchymal periventricular hemorrhage

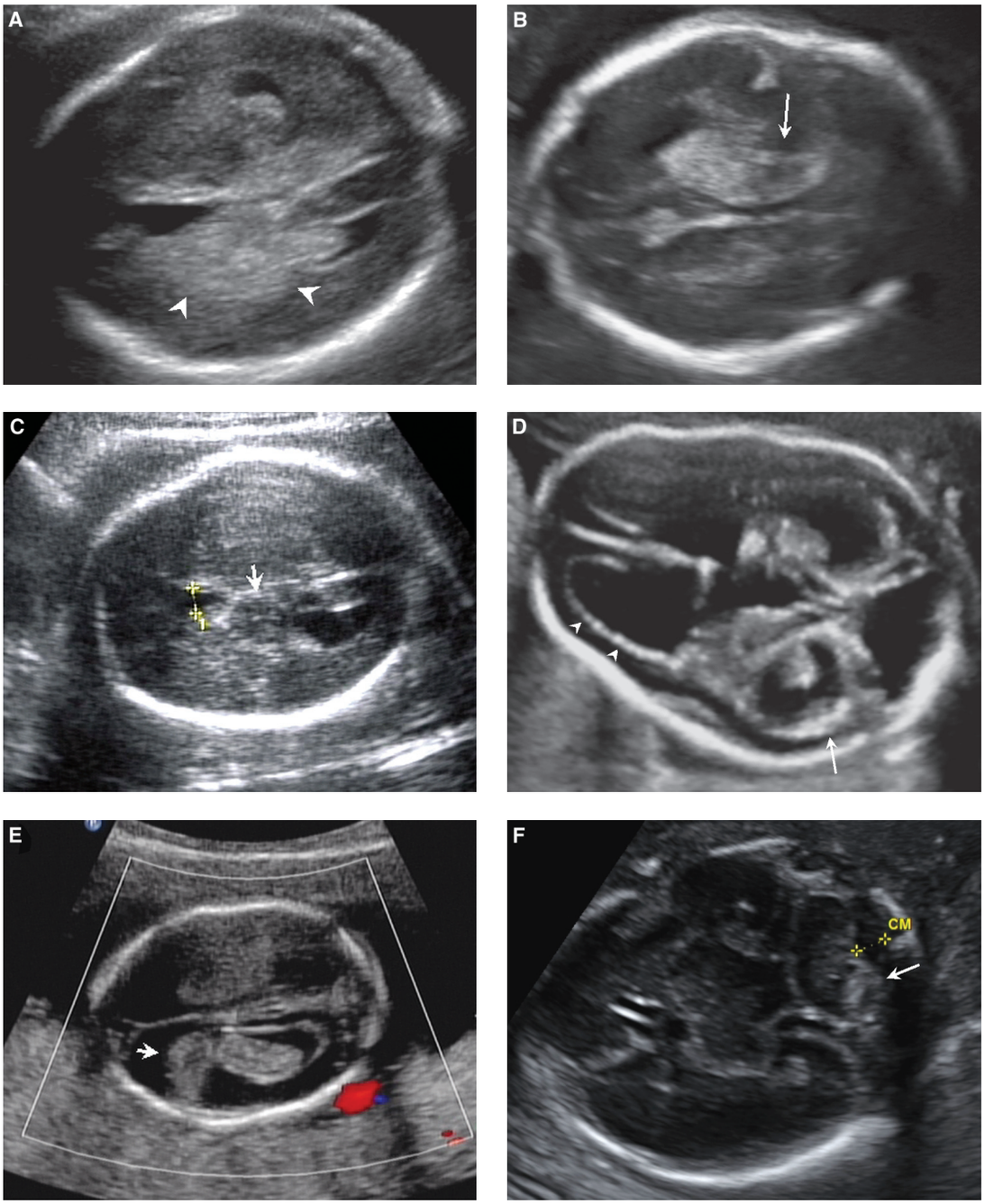

FIGURE 12.1-71: Intracranial hemorrhage on US. **A:** Axial image demonstrates large echogenic choroid, lack of visualization of ventricular wall and abnormal echogenicity extending into the adjacent brain parenchyma *(arrowheads)*, consistent with an acute Grade IV hemorrhage. **B:** Evolving subacute hemorrhage depicted by a large heterogeneous choroid with internal echolucent area *(arrow)*. **C:** Axial ultrasound of same fetus in **A** 2 weeks later. There is a hypoechoic cystic structure *(arrow)* in the area of the choroid and lateral ventricle consistent with chronic clot. Calipers represent septum pellucidum. **D:** Axial image in a fetus diagnosed previously with bilateral Grade III hemorrhages. There is significant ventriculomegaly and residual layering blood in the lateral ventricle *(arrow)*. Increased echogenicity of the ependymal surface *(arrowheads)* is consistent with ventriculitis. **E:** Axial view of focal hemorrhage in the frontal lobe *(arrow)*. Notice lack of color flow. The choroid is large, and there is increased echogenicity along the ventricular wall. **F:** Axial view of posterior fossa demonstrates abnormal echogenicity *(arrow)* in the left cerebellum proven to represent hemorrhage. Calipers denote cisterna magna (CM).

porencephalic cyst.[402] Cerebellar hemorrhages have similar imaging, but clues to the presence include an irregular cerebellum and obliterated cistern magna (Fig. 12.1-71F).[416] Because of limited contrast resolution of US in solid tissues, small clots within the cerebral and cerebellar parenchyma may be missed.[416]

MRI: The appearance of hemorrhage changes on MRI with degradation of the clot; however, signal changes via hemorrhage age have not been fully studied in the fetus. In general, acute hemorrhage is intermediate on T1 and hypointense on T2, subacute blood is hyperintense on T1 and hypointense on

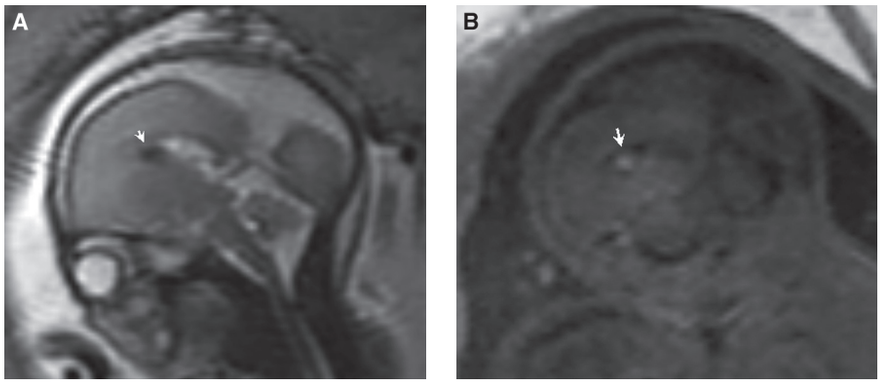

FIGURE 12.1-72: Germinal matrix hemorrhage on MRI at 20 weeks in a monochorionic twin gestation. **A:** Sagittal T2 demonstrates a focal area of decreased signal *(arrow)* at the caudothalamic groove. **B:** Sagittal T1 image confirms small bleed by demonstrating high T1 signal *(arrow)*.

T2, and chronic hemorrhage is heterogeneous but with areas of hypointense signal on T1 and T2 (Fig. 12.1-72). The grade of germinal matrix hemorrhage is defined by identifying hemorrhage along the ventricular wall, intraventricular or parenchymal (Fig. 12.1-73).[398,400] As hemorrhage has the same signal as the germinal matrix, symmetry of the brain and knowledge of normal is imperative. Hemorrhages tend to be larger and more irregular than the germinal matrix, often with ventricular enlargement. Gradient echo imaging can aid in defining hemorrhage by demonstrating susceptibility artifact (Fig. 12.1-74).[400]

MRI is more accurate than US with regard to grading germinal matrix hemorrhages and is more sensitive in the detection of either acute or small ischemic lesions.[398,403] Gradient echo and T1-weighted images are helpful in depiction of calcifications.[414] In the presence of ventriculomegaly, evaluation of the aqueduct is important to exclude obstruction.[417]

Hemorrhage and edema may be transient and resolve. However, chronic changes of volume loss, which include unilateral or bilateral large, sometimes distorted ventricles with enlarged subarachnoid spaces, can be noted when injury is permanent.[400]

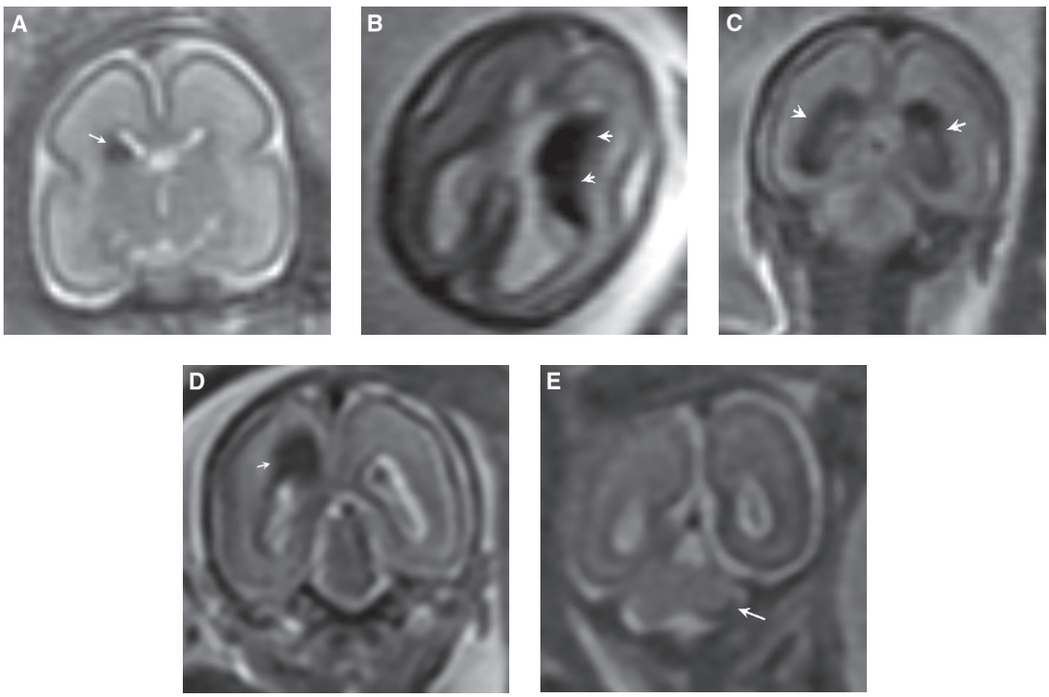

FIGURE 12.1-73: Grades of germinal matrix hemorrhages on fetal MRI in twin monochorionic gestations. **A:** Grade I: Coronal image shows small focus of low signal (*arrow*) along the right caudothalamic groove. **B:** Grade II: Axial image shows abnormal dark signal along the wall of the left lateral ventricle *(arrows)*. **C:** Grade III: Coronal image shows abnormal dark signal *(arrows)*, distending the posterior horns of the lateral ventricles. **D:** Grade IV: Coronal image demonstrates abnormal dark signal extending into the right parietal white matter *(arrow)*. **E:** Cerebellar germinal matrix in a fetus with anhydramnios. Coronal image demonstrates crescentic abnormal low signal in the left cerebellum peripherally *(arrow)*.

Kline9781451175837-ch012.1.indd 408 08/08/14 9:58 AM

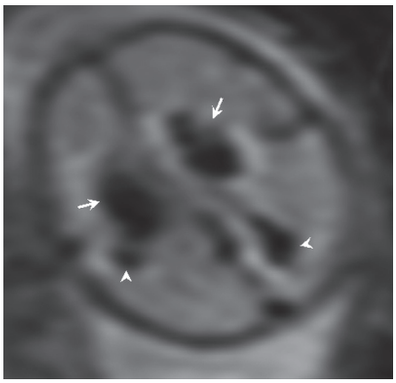

FIGURE 12.1-74: Fetus with bilateral grade IV hemorrhages. Gradient echo imaging confirms hemorrhage with susceptibility artifact in the lateral ventricles *(arrows)* and in the adjacent brain *(arrowheads)*.

Irregularity of the ventricular wall or premature loss of the germinal matrix is consistent with germinal matrix injury (Fig. 12.1-75).[417] Parenchymal defects, some appearing cystic or septated, can develop. Supependymal cysts may be seen. Laminar necrosis refers to selective destruction of distinct cortical layers, being most susceptible beginning at 28 weeks. Calcification with laminar necrosis appears as a linear cortical signal abnormality that is hyperintense signal on T1 and hypointense on gradient echo imaging.[414,417] The corpus callosum may be thin or deficient. The sulcation is often abnormal, with PMG developing in 2% of hypoxia cases.[401]

Extra-axial Hemorrhage

Subdural and, less commonly, epidural hemorrhage have been described in the fetus, occurring most commonly over the cerebral convexity but also in the posterior fossa.[409] Subdural hemorrhages typically develop from tearing of loose draining veins. Epidural and subdural hemorrhages tend to be related to maternal trauma, maternal coagulopathy, or rarely hypoxic ischemic injury.[409,410,416]

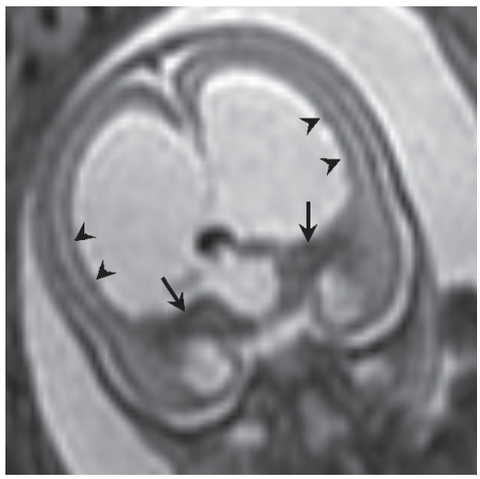

FIGURE 12.1-75: Coronal T2 image of a fetus with ventriculomegaly after germinal matrix hemorrhage. There is irregularity of the germinal matrix *(arrowheads)* and dark heterogeneous signal along the basal ganglia *(arrows)*.

Ultrasound: Subdural hematomas appear as echogenic, heterogenous, or hypoechoic collections that displace the brain parenchyma away from the calvarium, usually over the hemispheres, though posterior fossa tentorial collections have also been described (Fig. 12.1-76A).[404,410,418] With organization of the clot, there may be echogenic layering debris in a cyst, an echogenic rim, or development of new collections over time.[418] Macrocephaly is often present. Cerebral edema may result in acoustic enhancement adjacent to the collection.[419]

MRI: This technique is excellent at defining extra-axial hemorrhage in the subdural or epidural space (Fig. 12.1-76B). Even small collections of hemorrhage are easily identified.[418] MRI also can depict mass effect and injury to the adjacent brain.

White Matter Injury/Parenchymal Ischemia

White matter injury is most common below 32 weeks. The pathogenesis is suggested to be due to incomplete development of the vascular supply in the white matter, lack of regulation in blood flow early in gestation, and immaturity of the oligodendrocyte cell, especially when exposed to glutamate. In the presence of neuronal hypoxia, subsequent cell death results in release of glutamate, which has cytoxic effects on neurons.[420] Microglial cells present in the white matter aggravate the process with inflammatory cytokines. Astrocytes attempt to repair the injury and reduce glutamate which eventually leads to cell membrane swelling and cytotoxic edema. Eventually, there is lysis of the cell membrane and increase in water in the extracellular space with loss of blood-brain barrier and vasogenic edema.

Ischemic infarcts have rarely been noted in the fetus, with most occurring secondary to abnormalities of the middle cerebral artery or venous thrombosis.[420]

Ultrasound: White matter injury is more difficult to detect on US but has been described in the presence of periventricular echodensities that result in loss of normal brain parenchymal lamination.[421] If followed over greater than 2 weeks, cystic areas may become apparent in the periventricular white matter.[404] In the presence of diffuse injury, multiple cystic spaces consistent with multicystic encephalomalacia may be seen.

MRI: In the fetus, white matter injury is different than postnatal. Most cases show increased T2 and decreased T1 signal in the subcortical white matter rather than areas of T1 high and dark T2 in the periventricular area (Fig. 12.1-77).[401] Injury in the white matter will cause loss of normal laminar pattern, especially in the intermediate zone.[400] Sometimes, these lesions are harder to detect on fetal MRI due to lower signal to noise and the high water content of the brain. In general, MRI is more accurate in the detection of small focal lesions than diffuse white matter abnormalities.[414] In some cases diffusion imaging may be helpful by identifying restricted diffusion, though care should be made to ensure delineation from the normal germinal matrix.[417] In the presence of vasogenic edema and astrogylosis, the apparent diffusion coefficient (ADC) value is increased, which can confirm white matter injury.[420]

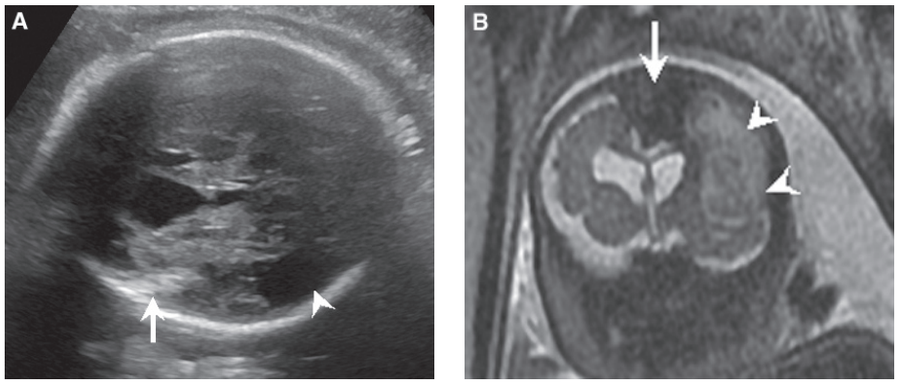

FIGURE 12.1-76: Subdural in a fetus with venous thrombosis. **A:** Axial US demonstrates heterogeneous tissue in the extraaxial space displacing the adjacent brain. More anterior, the subdural is echogenic *(arrow)* and posterior hypoechoic *(arrowhead)*. **B:** Coronal T2 MR image shows heterogeneous T2 hyperintense subdural along the left hemisphere *(arrowheads)*. The sagittal sinus is enlarged and heterogeneous *(arrow)* consistent with venous congestion. (Courtesy of Dorothy Bulas, MD.)

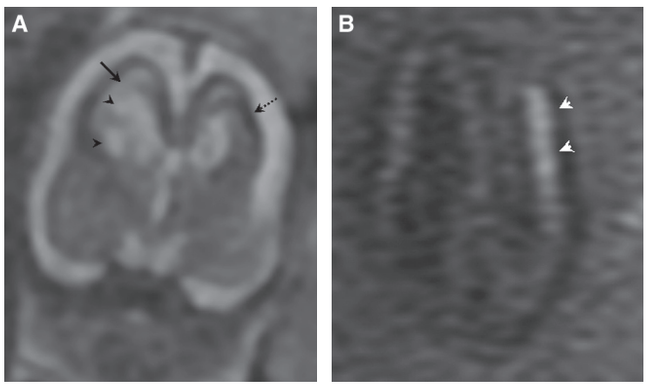

FIGURE 12.1-77: White matter injury and laminar necrosis in a fetus at 28 weeks with anhydrmanios. **A:** Coronal T2 image shows white matter hyperintense signal *(solid arrow)* and small cystic areas of degeneration *(arrowheads)*. Notice that the cortex is thin and extremely dark T2 signal *(dashed arrow)*. There is lack of normal lamination of the brain. **B:** Axial T1 image shows linear hyperintense signal in the cortex of the left hemisphere *(arrows)* and, to a lesser extent, the right hemisphere. Findings are consistent with lamninar necrosis.

Parenchymal ischemic lesions cause edema which tends to be dark on T1 and high signal on T2 (Fig. 12.1-78A). There may be loss of the normal lamination of the brain.[417] In the presence of acute ischemia, restricted diffusion is noted as high signal on the T2 trace and low on the ADC map (Fig. 12.1-78B).[417] Acute response in the fetal brain is not common, so many of these areas of signal abnormality will not show diffusion restriction.[401] Proton spectroscopy may have a role in the future for evaluation of ischemic lesions, though it is technically more difficult in the fetus.[401,417]

Associated Anomalies: Extracerebral findings may be seen in the presence of hypoxic ischemic disease. The most common is intrauterine growth restriction.[417] Infection and ischemia may affect the kidneys, liver, and heart. Fetal hydrops may be present. Evaluation of the placenta for pathology may yield important clues to the cause of intracranial injury.

Differential Diagnosis: Tumor should be considered in the presence of a heterogeneous echogenic mass, but unlike a hemorrhage, which decreases in size, a tumor will remain stable or grow. Hemorrhage may result from vascular malformations such as vein of Galen, dural sinus malformations, or cavernoma. In late stages, hemorrhage liquefies and appears cystic. Differential would include cystic lesions such as choroid plexus cyst, arachnoid cyst and if in the posterior fossa, malformations of Blake pouch may be considered.

Prognosis: Neurodevelopmental outcome can range from normal to neurologic deficits such as seizure, mental retardation, psychomotor delays, and cerebral palsy. Extreme cases may result in fetal or neonatal death.[398] Prognosis is dependent on the etiology and extent and location of the hemorrhage. In prenatally diagnosed intracranial hemorrhages, 40% to 55% of fetuses die in utero or within the 1st month of life.[402,403] Among survivors, approximately 45% to 50% can be expected to be neurologically normal.[402]

In the presence of a germinal matrix hemorrhage, perinatal mortality and neurologic outcome are dependent on the grade of injury.[402] Lower grade of germinal matrix hemorrhage and those bleeds that disappear are associated with a better outcome.[398]

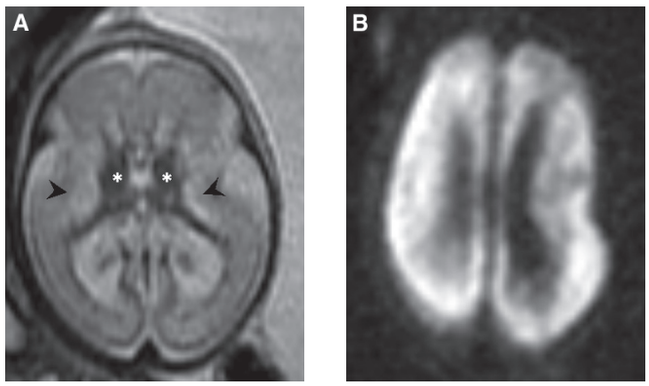

FIGURE 12.1-78: Severe hypoxic ischemic injury secondary to twin-to-twin transfusion syndrome. **A:** Axial T2 image demonstrates abnormal hyperintense signal in the white matter *(arrowheads)*, but the basal ganglia also demonstrated abnormal dark T2 signal *(astericks)* similar to ischemic disease in the newborn. **B:** Axial T2 trace shows diffuse hyperintense signal consistent with diffuse ischemia.

Kline9781451175837-ch012.1.indd 410 08/08/14 9:58 AM

Intrauterine progression of a bleed is associated with a worse neurological outcome.[398] Grade III–IV hemorrhages are associated with a poorer postnatal status.[398] Up to 60% of surviving infants will develop hydrocephalus requiring CSF diversion.[403]

Subdural hemorrhage may be fatal or may resolve completely without therapy, though some require surgical intervention.[418] About two-thirds of fetuses with subdural lesions have normal neurologic outcome.[402] Poor prognosis is more likely if the subdural is in the presence of hydrocephalus, cerebral infarction, or cerebral atrophy leading to microcephaly.[419]

White matter injury may lead to significant neurologic deficits, but prognosis is dependent on the extent and persistent area of abnormality.[416] Associated anomalies or genetic syndromes have a more guarded outcome.[398]

Management: Laboratory testing for fetal platelet disorder may be considered. Treatment of alloimmune thrombocytopenia is debatable.[402] However, if there is concern for recurrent thrombocytopenia, fetal blood sampling at 20 weeks may be performed to evaluate fetal platelet phenotype and platelet count. If the fetus is positive for alloimmune thrombocytopienia, maternal treatment with high-dose intravenous immunoglobuluin weekly and oral corticosteroids may be considered.[405,422] Second blood sampling at 24 weeks may be obtained to evaluate for efficacy of treatment. Platelet transfusion may be necessary in the presence of low counts; however, transfusion alone is difficult as the life span for a platelet is only 8 to 10 days, and repeat fetal blood sampling is also associated with increased risk for hemorrhage and exsanguination.[405] Near delivery, fetal sampling may help determine the mode of delivery. If above 50,000 per μL, vaginal delivery is considered safe. Below this level, intrauterine transfusion prior to vaginal delivery or cesarean section may be considered.[405]

Depending on severity of the lesion, termination or supportive care may be solely provided.[402] In the presence of a subdural collection or large hematoma, close monitoring intrauterine is recommended to check for increase in bleeding, hydrocephalus, or hydrops secondary to fetal anemia. The optimum mode of delivery is uncertain and likely case-dependent.[402]

Some infants require surgical evacuation of hematoma postnatally.[418] Hydrocephalus can develop from obstruction at the aqueduct of Sylvius or as a result of mass effect from a large hematoma. In those children, ventricular shunting may be required.

Recurrence: The risk of recurrence is low, being between 3% and 5%.[402] With a history of alloimmune thrombocytopenia, the recurrence risk is 75% to 100%, with increased severity of symptoms with sequential pregnancies.[404,419]

Porencephaly

Porencephaly represents a cavitary fluid-filled area within the brain that usually communicates with the ventricles, subarachnoid spaces, or both.

Incidence: Porencephaly is found in 1 per 9,000 births.[416]

Pathogenesis: Porencephaly is a cystic lesion replacing cerebral substance, which is smooth and lacks adjacent glial reaction, as the inciting event occurs typically before 27 weeks, prior to the acquisition of mature astroglial response.[414] Two types of porencephaly have been described. Type I or encephaloclastic porencephaly is the most common. These cases are usually related to a venous medullary infarct or less likely, an arterial insult.[423,424] Type II or developmental porencephaly is believed to arise because of a primary defect in the germinal matrix with abnormal migration of neurons.[425]

Etiology: The most common cause for porencephaly is an intraparenchymal hemorrhage occurring between 24 and 32 weeks secondary to medullary vein thrombosis in the presence of an intraventricular hemorrhage.[426] Hereditary porencephaly with hemiplegia has been described in families, usually presenting with frontal porencephaly, hemiparesis, and seizures.[423,427]

Diagnosis

Ultrasound: Initially, an echogenic clot is identified usually periventricular arising from the germinal matrix. As the clot retracts, the hyperechoic area is replaced by a lesion that is centrally anechoic but with a peripheral echogenic border. Up to 6 weeks later, the area of porencephaly becomes completely anechoic and usually communicates with the lateral ventricle.[426] Coronal and sagittal imaging is often helpful. Sometimes, the septum pellucidum may be partially or completely absent.[426] The cleft of the porencephalic cavity chronically is lined by white matter, and therefore when mature, should not have an echogenic lining. Asymmetrical enlargement of the lateral ventricle with midline shift to the affected side is common (Fig. 12.1-79A).[426] There is no blood flow within the lesion.[425] Microcephaly or macrocephaly may be present.

MRI: Centrally, CSF signal on T1- and T2-weighted images extends from the white matter typically in continuity with the ventricle (Fig. 12.1-79B). MRI will often demonstrate evolving hemorrhage or hemosiderin staining along the defect (Fig. 12.1-79C).[416]

Associated Anomalies: In the presence of an associated syndrome, intracranial and extracranial anomalies may be noted. Hippocampal and amygdala volume loss are often present.[428]

Differential Diagnosis: The main differential diagnosis is schizencephaly. In schizencephaly, the malformation extends form the ventricle to the subarachnoid space and is lined by gray matter. Porencephaly is lined by white matter. In addition, schizencephaly is often bilateral, whereas porencephaly tends to be unilateral.

Prognosis: Outcome is related to underlying etiology, timing of the insult, lesion size, and location.[426] Neurologic deficits are typical.[424] The child may have spastic hemi- or quadiparesis and infantile spasms.[423] Many children with porencephaly suffer from epilepsy and cognitive deficits. Seizures tend to correlate with abnormalities in the temporal lobes rather than the porencephalic defect.[428]

Management: Epilepsy is treated with antiepileptic drugs, though some children may become refractory to the drugs and require surgical resection.[416]

Recurrence: In the absence of genetic syndrome, the risk of recurrence is low.

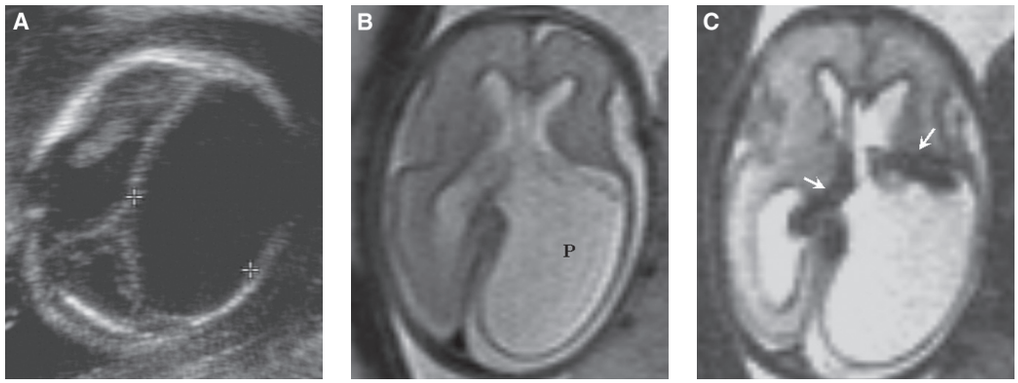

FIGURE 12.1-79: Fetus at 26 weeks with diagnosis of porencephaly. **A:** Coronal ultrasound demonstrated asymmetric severe dilatation *(calipers)* of the posterior horn of the left lateral ventricle. **B:** Axial T2 image demonstrates posterior horn of the lateral ventricle contiguous with porcencephalic cyst *(P)* replacing most of the left posterior hemisphere. **C:** Gradient echo axial image demonstrates susceptibility artifact *(arrows)* consistent with hemosiderin staining along the defect.

Hydranencephaly

Hydanencephaly is characterized by complete or near complete absence of cerebral cortex.

Incidence: Nearly all cases of hydranencephaly are sporadic, with an incidence of approximately 1 in 5,000 continuing pregnancies or 1 in 10,000 births.[429,430]

Pathogenesis: Hydranencephaly occurs when there is a liquefaction necrosis and resorption of most of the cerebral brain. There is complete or near complete absence of the cerebral cortex in the location of the anterior circulation, with most of the brain replaced by large CSF fluid collections. Cortical layers are not present, and the empty CSF spaces are covered by leptomeninges, connective tissue and a layer of ectopic glioneuronal tissue.[423] The occipital and small portions of the frontal and temporal lobes are often present because of collateral flow from the posterior circulations.[431] The basal ganglia and thalami are hypoplastic but present. The cerebellum and brainstem are intact but often are hypoplastic. Rarely, cerebellar hemisphere liquefaction has been noted.[430] Choroid plexus is present but freely floating as the lateral ventricles are destroyed. The falx is usually present but may be partially or completely absent. Hydrocephalus may develop due to aqueduct stenosis or poor CSF absorption.[423]

Etiology: The etiology is heterogeneous but destructive. The most commonly proposed mechanism is bilateral occlusion of the internal carotid arteries probably between late first to second trimester, after the brain and ventricles have been formed but before glial response is present.[432,433] However, in hydranencephaly cases, normal and hypoplastic anterior cerebral circulation has been detected. Thus, hydranencephaly is likely due to a nonspecific devastating hypoperfusion, thromboembolic or vascular insult in the area of the anterior circulation, which leads to diffuse extensive intracranial hemorrhage and necrosis.[433–435] Numerous prenatal cases have been described in association with monochorionic twin gestations, fetal infection, ischemia, hemorrhage, or vasculopathies.[434,435] Infrequently, hydranencephaly has been associated with chromosomal aberrations, including trisomy 13 and triploidy.[433,436]

Fowler syndrome, also known as proliferative vasculopathy and hydranencephaly–hydrocephaly or encephaloclastic proliferative vasculopathy, is a genetic syndrome that results in a glomeruloid vascular proliferation which impedes development of the neocortex during the first trimester at the time of vascular invasion of the cerebral mantle.[423] The result is ischemic lesions and progressive destruction of the nervous tissue. Brain injury most commonly presents as hydrocephalus, though hydranencephaly is also possible.[437] The syndrome has an autosomal recessive inheritance.[437,438]

Diagnosis

Ultrasound: Diagnosis of hydranencephaly has been made in both early and late gestation, but usually between 12 and 30 weeks.[431,439] In hydranencephaly, a cerebral falx, although at times partially or rarely absent, is typically identified, and though the supratentorial brain is abnormal, there is usually a brainstem and cerebellum with measurements small owing to hypoplasia.[439,440] The US appearance is dependent on etiology and the stage of evolution. In the phase of vascular insult, homogeneous hyperechoic or diffuse uniform low level echogenic material may replace the supratentorial brain, and no ventricles or cortical structures can be defined. The abnormal echotecture likely represents liquefied brain and hemorrhage (Fig. 12.1-80).[440] In the second phase, the echogenic material

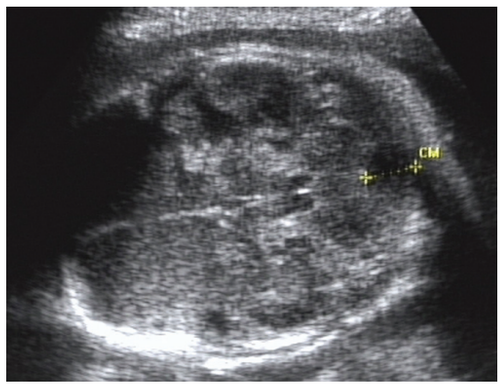

FIGURE 12.1-80: Fetus with hydranencephaly at 24 weeks. The supratentorial brain demonstrates diffuse low-level echogenicity.

becomes more hypoechoic with identification of falx and thalami. The final phase demonstrate anechoic fluid surrounding the thalami and midbrain, absence of cortical tissue, and enlargement of the cranial vault (Fig. 12.1-81A,B).[434,439] The head size may be normal, large or small, depending on the development of hydrocephalus. Color Doppler of the circle of Willis is often normal.[440] Usually, polyhydramnios is present because of lack of fetal swallowing.

In Fowler syndrome, fetal akinesia deformation sequence may be detected in the first trimester. In conjunction with hydrocephalus or hydranencephaly, there is often arthrogryposis, pterygia, cystic hygroma, and polyhydramnios.[434,437,438,441] Calcification and necrosis of the white matter, basal ganglia, brainstem, and cerebellum may be present.[437]

MRI: There is complete or near complete absence of the cerebral hemispheres with remnants of occipital, temporal and frontal lobes and basal ganglia, and preservation of the thalami, brainstem, and cerebellum (Fig. 12.1-81C,D).[442] Hemorrhage may be detected by high signal on T1, dark signal on T2, or susceptibility artifact on gradient echo images.

Associated Anomalies: With Fowler syndrome, additional anomalies may be apparent as described above.

Differential Diagnosis: The presence of the falx in hydranencephaly is important to differentiate it from HPE. HPE also usually demonstrates persistent tissue in the frontal lobe region, which is commonly fused. Facial abnormalities in HPE may also help secure the diagnosis. Hydrocephalus should also be considered, but the presence of cerebral tissue, though sometimes quite thin, should help differentiate. In the presence of a dilated third ventricle, aqueductal stenosis should be considered. Severe porencephaly or schizencephaly may be considered, but these cases can be distinguished by areas of preserved supratentorial brain.

Prognosis: Although rare cases of prolonged survival have been recorded, prognosis is typically poor with reduced life expectancy, most being either stillborn or dying within the first few weeks of life.[429] Severe retardation is uniform among survivors.[429,443] Survival is possible but complicated by spastic quadriplegia, impossibility of oral feeding, and episodic

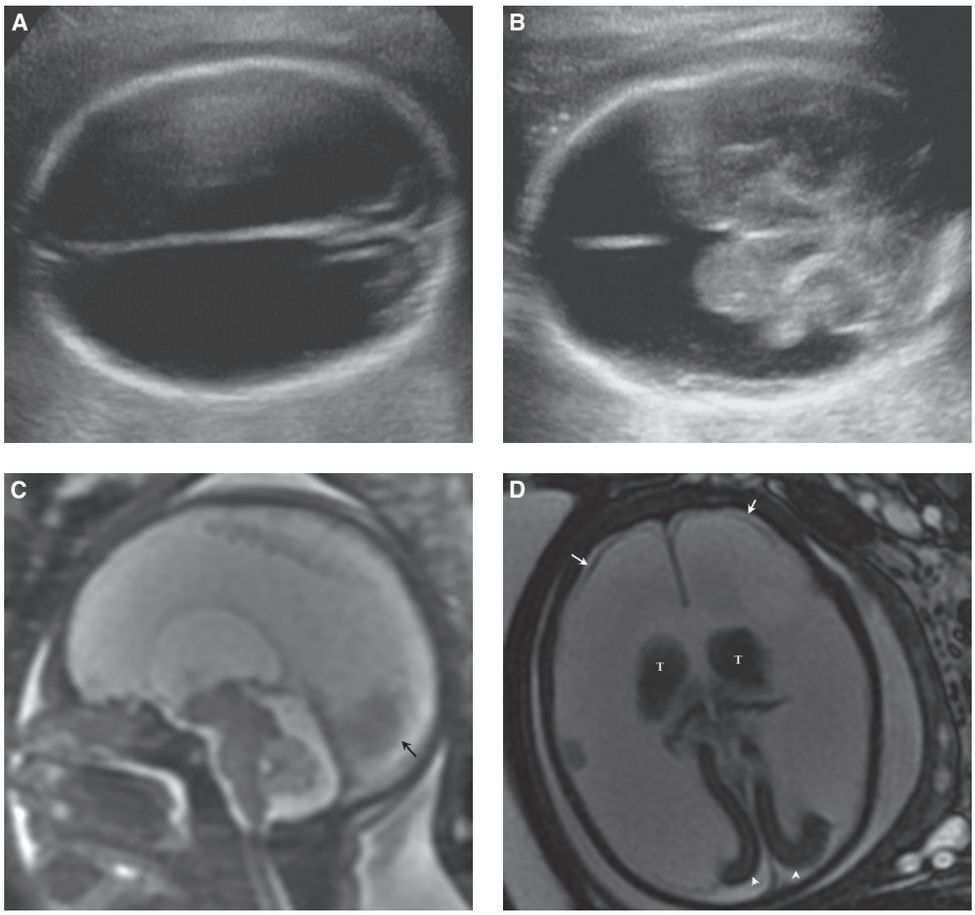

FIGURE 12.1-81: Fetus at 25 weeks with hydranencephaly. **A:** Axial US demonstrates persistence of the falx but lack of visualization of normal brain parenchyma. **B:** Axial transthalamic image shows presence of thalami and posterior fossa structures. **C:** Sagittal T2 MR shows lack of supratentorial brain other than small remnants of the occipital lobe *(arrow)*. The posterior fossa anatomy is normal. **D:** Axial SSFP image demonstrates thin remnants of frontal lobe brain mantle *(arrows)*. Small occipital lobes are present *(arrowheads)*, and thalami *(T)* are small but present.

dysthermoregulation.[423] Some consciousness, mainly auditory, is possible.[423] Seizures are common and pituitary dysfunction can occur. Fowler syndrome is lethal.[438,441]

Management: Termination of pregnancy may be discussed given poor outcome. At birth, supportive care may be provided. Some children with hydranencephaly develop hydrocephalus, and shunting may be considered.

Recurrence: In the absence of genetic anomalies, the recurrence risk is negligible.

Dural Sinus Thrombosis

Incidence: Dural venous sinus thrombosis is rare.[444]

Pathogenesis: During the 3rd gestational month, the dural venous sinuses and galenic sinuses begin to develop. The sagittal sinus forms via fusion of bilateral marginal sinuses, which initially are separate, draining into each respective transverse sinus. From the 4th to the 5th month, there is ballooning of the occipital sinus, and from the 4th to the 6th month, the lateral then medial transverse and sometimes the posterior sagittal sinus dilate.[445] In the 6th fetal month, with fusion of the marginal sinuses, the venous confluence or torcula develops with its many variations in anatomy. In the 7th month, the ballooning of the sinuses resolves. At birth, the torcula typically demonstrates a plexiform pattern.[446] The venous drainage further develops after birth as a result of further differentiation of the jugular and cavernous sinuses.[446]

Ectasia of the venous sinus is therefore a variant of dural sinus development. It is hypothesized that if a dilated disorganized sinus persists after the time of expected reduction, two secondary events may occur which include development of an AV shunt and/or disruption of the venous drainage, leading to thrombosis.[447] With persistent ballooning of the sinus, it is suspected that the dilated sinus causes elevated venous pressure and secondary dural fistulae, resulting in a dural venous malformation (DVM).[448] In the presence of both or either of these mechanisms, a dilated sinus with altered flow, immaturity of the venous channel, and changes in the endothelial wall may then incite thrombosis.[446,448] Most cases of thrombosis on prenatal imaging are in the area of the torcula Herophili or venous confluence.[444,448] The majority of cases of dural venous thrombosis and ectasia resolve spontaneously, possibly because of the presence of multiple anastomotic channels. However, when there are limited anastomoses or spontaneous thrombosis of a giant sinus, cerebral ischemia, hemorrhage, and hydrocephalus can occur owing to venous hypertension.[446,448,449]

Etiology: Unlike the neonate in which common causes for thrombosis include prothrombotic states such as dehydration, shock, hypoxia, polycythemia, leukemia, and congenital deficiency of anticoagulants, the cause of dural venous sinus thrombosis in the fetus is unknown.[444,450] In some cases of venous thrombosis, only ectasia of the veins is identified with the dural lake usually located in the transverse sinus, superior sagittal sinus, or torcular herophili. In other lesions, DVM are detected in association with clot.

DVM are classified into two types: midline giant pouches involving the torcula, transverse sinuses, and posterior sagittal sinus with a more guarded prognosis, or lateral, involving the jugular bulbs, with a benign course and good outcome.[451] Arteriovenous shunting in a DVM is typically via multiple feeding vessels in the wall of the sinus, suspected to be a secondary event. However, dilated veins have been noted to develop after an AV fistula is identified.[452] These arteriovenous shunts are characterized by low flow, rarely causing systemic hemodynamic complications, though disruption in the venous drainage may result in venous thrombosis and intracranial venous hypertension.[453] The thrombus can cause maturation of the sinus with favorable outcome, or the clot may extend into normal cerebral veins causing cerebral injury.[453]

Diagnosis

Ultrasound: Thrombosis tends to be detected in the second trimester, as early as 18 weeks.[448] Imaging findings are variable depending on the size and stage of the thrombus.[446,448] Typical imaging includes a well-defined triangular or rounded anechoic collection above the cerebellum between the cerebral hemispheres containing an echogenic structure, consistent with acute clot (Fig. 12.1-82A).[450,454] As the clot matures, the lesion becomes more heterogeneous with concentric rings (Fig. 12.1-83A).[446,450] The clot may extend into one or both transverse sinuses. 2D with 3D and transvaginal imaging may be helpful to define clot location.[455]

Color Doppler is excellent at assessing the intracranial venous system with a more continuous waveform noted in vein of Galen and straight sinus, whereas triphasic pulsatile flow is normally noted in the transverse and sagittal.[456] In most cases with ectatic veins, with or without dural thrombus, due to low-flow velocity, color Doppler confirms lack of blood flow centrally even in the presence of AV shunting (Fig. 12.1-82A).[44,448,450,457] Flow around thrombus is rarely apparent on color Doppler.[454] Pulsatile venous flow before thrombus development has been described.[446] In some cases of AV shunting, high-velocity arterial flow may be identified along the periphery of the dilated veins.[450,453,458]

The brain should be evaluated for hemorrhage, infarct, and ventriculomegaly. Macracrania may develop. Most clots show a slow and late decrease in size with stasis around the clot. There may be recanalization of the clot, best depicted on color Doppler before birth.[444] Serial US and color Doppler at intervals of 4 weeks should be obtained to monitor biparietal diameter and decreasing thrombus size.

MRI: MRI is useful in the evaluation of dural venous sinus thrombosis because it is able to confirm venous sinus pathology, exclude other masses, and identify acute and subacute thrombus.[448] MRI will detect a well-defined rounded or triangular lesion in the extra-axial space, conforming to a dilated venous confluence with variable extension into other dural sinuses (Figs. 12.1-82B and 12.1-83B).[448] The sinus is typically isointense to hypointense to gray matter containing eccentric areas of low T2 signal that are T1 hyperintense, likely reflecting acute–subacute thrombus (Fig. 12.1-83C).[444,448–450] With progression, the signal becomes progressively more heterogeneous often with a rim of T2 hyper- or hypointensity, and T1 hyperintensity.[446,449] On diffusion imaging, the intralesional thrombus can demonstrate hyperintense trace and dark ADC signal.[459] MRI can define the location, size, number, and extent of thrombi.[444]

There is usually mass effect and displacement of the adjacent brain. MRI is extremely helpful to exclude brain parenchymal findings including infarction, hemorrhage, or gyration abnormalities.[444] Diffusion imaging can also assist in exclusion of brain

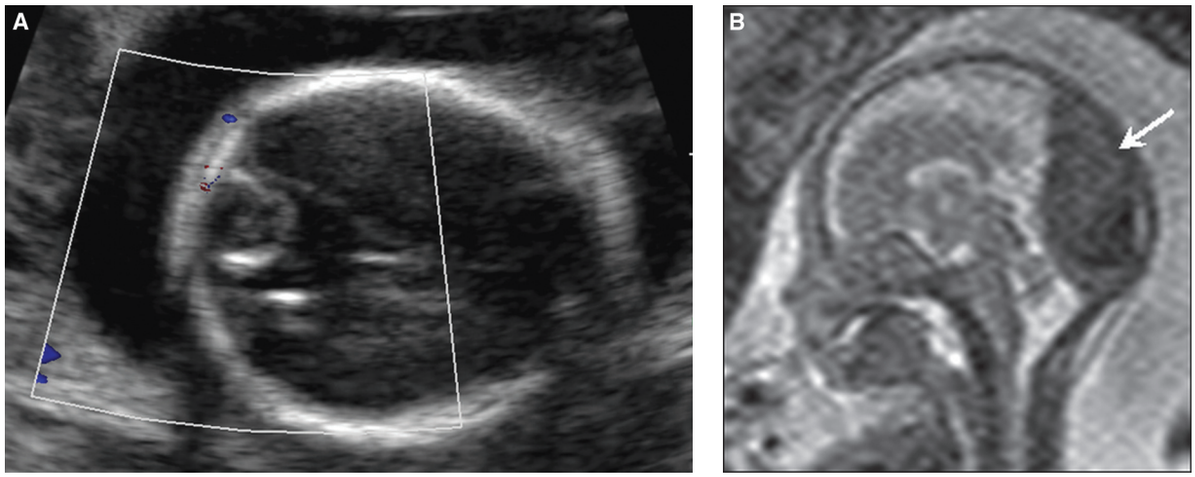

FIGURE 12.1-82: Fetus with dural ectasia and venous thrombosis. **A:** Axial US with color Doppler demonstrates avascular triangular structure posteriorly containing a heterogeneous round lesion with peripheral increased echogenicity, consistent with clot. **B:** Sagittal T2 MR image shows enlargement of the torcular and posterior sagittal sinus *(arrow)*. Notice that the sinus has heterogeneous signal. (Courtesy of Chris Cassady.)

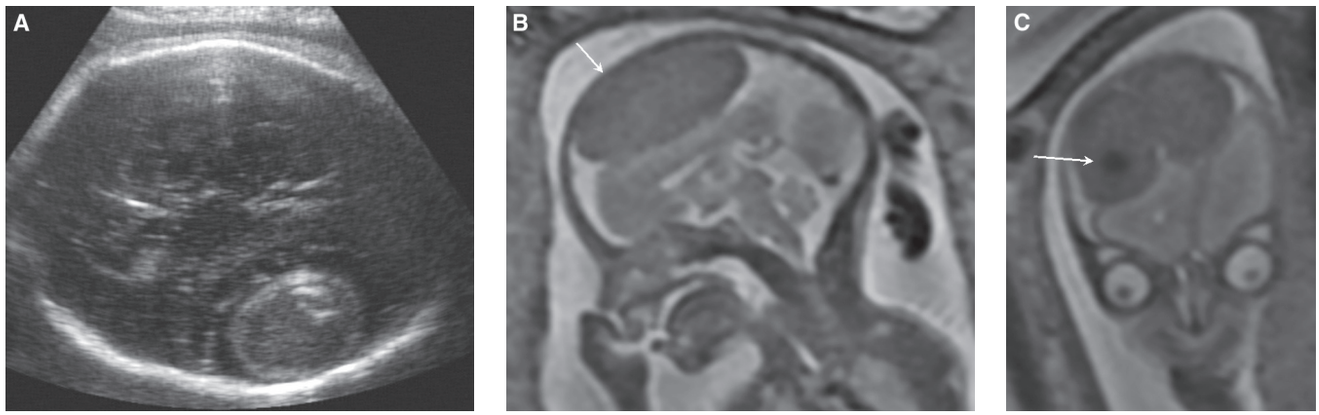

FIGURE 12.1-83: Fetus at 22 weeks with dural venous sinus malformation and clot. **A:** Axial US demonstrates echogenic area containing concentric rings consistent with clot. **B:** Sagittal T2 image of the same fetus shows abnormal enlargement and isointense signal of the anterior sagittal sinus *(arrow)*. **C:** Coronal T2 image shows a focal area of decreased T2 signal *(arrow)* in the dilated vein corresponding to the echogenic clot seen in **A**. Note mass effect on the adjacent frontal lobe. The child did well postnatally, with spontaneous resolution of the defect.

ischemia.[448,459] After diagnosis, follow-up MRI may be considered to exclude development of intraparenchymal hemorrhage or infarction and monitor resolution of the thrombus.[444,448]

Associated Anomalies: Edema and parenchymal hemorrhages may occur due to venous infarctions. Hydrocephalus may also develop in the presence of venous hypertension and poorly developed arachnoid villi in the fetus. Rarely, a DVM may cause cardiac failure.

Differential Diagnosis: The most common mimicking lesions include tumors, cystic lesions such as arachnoid, glioependymal or dermoid cysts, and malformations of the posterior fossa. Tumors are heterogeneous intraparenchymal lesions, whereas cysts tend to be fluid attenuated in the extra-axial space. Other differentials include subdural or large intraparenchymal hematomas that should be differentiated by location. Vein of Galen malformations demonstrate an oblong midline lesion with turbulent flow.

Prognosis: Prognosis ranges from normal outcome to mental retardation and death.[61] Review of a small number of cases in the literature show a good neurological outcome in up to 70% to 80% of antenatal detected cases.[446,450,451] If the fetus has a normal biparietal diameter and the malformation undergoes spontaneous regression in utero (55%), a better outcome has been noted.[446,450,460] Prognosis is not dependent on size of the clot, venous dilatation, or number of thrombi.[444] Often the torcula demonstrates thrombosis but with good outcome, likely because of fetal anastomoses which allow redirection of venous blood flow.[444] Outcome is most dependent on lack of other fetal anomalies and the presence of a normal brain.[444] Associated cerebral findings such as hemorrhage, infarct, hydrocephalus, distortion of cerebral anatomy, increasing size of thrombus, or clinical factors such as prematurity, thrombosis due to preexisting conditions, and signs of cardiac decompensation are poor prognostic factors.[64] A fetus with thrombosis and these complications may have intrauterine or postnatal demise or neurologic deficits.[449]

Management: Management is variable and includes termination of pregnancy, surgical intervention after birth, or expectant management in hopes of spontaneous regression with favorable outcome. Vaginal delivery does not seem to be contraindicated with normal head size.[453] After birth, the child should be evaluated for cardiac failure, anemia, and coagulopathy with appropriate medical management.[447] Imaging should include an MRI and MR venogram to assess venous ectasia, thrombus, DVM, and brain parenchymal injury. An arteriogram at 4 to 5 months of age is indicated, especially if spontaneous resolution has not occurred.[451,460] Surgery is not recommended because of risk of bleeding and the high likelihood of spontaneous regression.[461] Embolization or hematoma evacuation may be required in some cases.[450,451]

Recurrence: Dural thrombosis and dural venous malformations are sporadic conditions with no known risk for recurrence.[444,449]

REFERENCES

1. Huisman TAGM. Fetal magnetic resonance imaging of the brain: is ventriculomegaly the tip of the syndromal iceberg? *Semin Ultrasound CT MR*. 2011;32:491–509.
2. Nyberg DA. Recommendations for obstetric sonography in the evaluation of the fetal cranium. *Radiology*. 1989;172:309–311.
3. Filly RA, Cardoza JD, Goldstein RB, et al. Detection of fetal central nervous system anomalies: a practical level of effort for a routine sonogram. *Radiology*. 1989;172:403–408.
4. Levine D, Feldman HA, Kazam Tannus JF, et al. Frequency and cause of disagreements in diagnoses for fetuses referred for ventriculomegaly. *Radiology*. 2008;247:515–527.
5. Whitby EH, Paley MNJ, Sprigg A, et al. Comparison of ultrasound magnetic resonance imaging in 100 singleton pregnancies with suspected brain abnormalities. *BJOG*. 2004;111:784–792.
6. Levine D, Barnes PD, Robertson RR, et al. Fast MR imaging of fetal central nervous system abnormalities. *Radiology*. 2003;229:51–61.
7. Sonigo PC, Rypens FF, Carteret M, et al. MR imaging of fetal cerebral anomalies. *Pediatr Radiol*. 1998;28:212–222.
8. Simon EM, Goldstein RB, Coakley FV, et al. Fast MR imaging of fetal CNS anomalies in utero. *AJNR Am J Neuroradiol*. 2000;21:1688–1698.
9. D'Addario V, Rossi AC. Neuroimaging of ventriculomegaly in the fetal period. *Semin Fetal Neonatal Med*. 2012;17:310–318.
10. Garel C, Luton D, Oury JF, et al. Ventricular dilatations. *Childs Nerv Syst*. 2003;19:517–523.
11. Zimmerman RA, Bilaniuk LT. Magnetic resonance evaluation of fetal ventriculomegaly-associated congenital malformations and lesions. *Semin Fetal Neonatal Med*. 2005;10:429–443.
12. Salomon LJ, Bernard JP, Ville Y. Reference ranges for fetal ventricular width: a non-normal approach. *Ultrasound Obstet Gynecol*. 2007;30:61–66.
13. Achiron R, Schimmel M, Achiron A, et al. Fetal mild idiopathic lateral ventriculomegaly: is there a correlation with fetal trisomy? *Ultrasound Obstet Gynecol*. 1993;3:89–92.
14. Goldstein RB, Pidus AS, Filly RA, et al. Mild lateral cerebral ventricular dilatation in utero: clinical significance and prognosis. *Radiology*. 1990;176:237–242.
15. Filly RA, Goldstein RB, Callen PW. Fetal ventricle: importance in routine obstetric sonography. *Radiology*. 1991;181:1–7.
16. Weichert J, Hartge D, Krapp M, et al. Prevalence, characteristics and perinatal outcome of fetal ventriculomegaly in 29,000 pregnancies followed at a single institution. *Fetal Diagn Ther*. 2010;27:142–148.
17. D'Addario V, Pinto V, Di Cagno L, et al. Sonographic diagnosis of fetal cerebral ventriculomegaly: an update. *J Matern Fetal Neonatal Med*. 2007;20:7–14.
18. Nyberg DA, Mack LA, Hirsch J, et al. Fetal hydrocephalus: sonographic detection and clinical significance of associated anomalies. *Radiology*. 1987;163:187–191.
19. Brodbelt A, Stoodley M. CSF pathways: a review. *Br J Neurosurg*. 2007;21:510–520.
20. Oi S, Di Rocco C. Proposal of "evolution theory in cerebrospinal fluid dynamics" and minor pathway hydrocephalus in developing immature brain. *Childs Nerv Syst*. 2006;22:662–669.
21. Gaglioti P, Oberto M, Todros T. The significance of fetal ventriculomegaly: etiology, short- and long-term outcomes. *Prenat Diagn*. 2009;29:381–388.
22. Kelly EN, Allen VM, Seaward G, et al. Mild ventriculomegaly in the fetus, natural history, associated findings and outcome of isolated mild ventriculomegaly: a literature review. *Prenat Diagn*. 2001;21:697–700.
23. Yamaski M, Nonaka M, Bamba Y, et al. Diagnosis, treatment, and long-term outcomes of fetal hydrocephalus. *Semin Fetal Neonatal Med*. 2012;17:330–335.
24. Melchiorre K, Bhide A, Gika AD, et al. Counseling in isolated mild fetal ventriculomegaly. *Ultrasound Obstet Gynecol*. 2009;34:212–224.
25. Cardoza JD, Goldstein RB, Filly RA. Exclusion of fetal ventriculomegaly with a single measurement: the width of the lateral ventricular atrium. *Radiology*. 1988;169:711–714.
26. Alagappan R, Browning PD, Laorr A, et al. Distal lateral ventricular atrium: reevaluation of normal range. *Radiology*. 1994;193:405–408.
27. Paladini D, Malinger G, Monteagudo A, et al. Sonographic examination of the fetal central nervous system: guidelines for performing the "basic examination" and the "fetal neurosonogram." *Ultrasound Obstet Gynecol*. 2007;29:109–116.
28. Heiserman J, Filly RA, Goldstein RB. Effect of measurement errors on sonographic evaluation of ventriculomegaly. *J Ultrasound Med*. 1991;10:121–124.
29. Achiron R, Yagel S, Rotstein Z, et al. Cerebral lateral ventricular asymmetry: is this a normal ultrasonographic findings in the fetal brain? *Obstet Gynecol*. 1997;89:233–237.
30. Sadan S, Malinger G, Schweiger A, et al. Neuropsychological outcome of children with asymmetric ventricles or unilateral mild ventriculomegaly identified in utero. *BJOG*. 2007;114:596–602.
31. Guibaud L. Fetal cerebral ventricular measurement and ventriculomegaly: time for procedure standardization. *Ultrasound Obstet Gynecol*. 2009;34:127–130.
32. Mahony BS, Nyberg DA, Hirsch JH, et al. Mild idiopathic lateral cerebral ventricular dilatation in utero: sonographic evaluation. *Radiology*. 1988;169:715–721.
33. Cardoza JD, Filly RA, Podrasky AE. The dangling choroid plexus: a sonographic observation of value in excluding ventriculomegaly. *AJR Am J Roentgenol*. 1988;151:767–770.
34. Hertzberg BS, Lile R, Foosaner DE, et al. Choroid plexus-ventricular wall separation in fetuses with normal-sized cerebral ventricles at sonography: postnatal outcome. *AJR Am J Roentgenol*. 1994;163:405–410.
35. Gaglioti P, Danelon D, Bontempo S, et al. Fetal cerebral ventriculomegaly: outcome in 176 cases. *Ultrasound Obstet Gynecol*. 2005;25:372–377.
36. Grandjean H, Larroque D, Levi S; and the Eurofetus Study Group. The performance of routine ultrasonographic screening of pregnancies in the Eurofetus study. *Am J Obstet Gynecol*. 1999;181:446–454.
37. Martinez-Zamora MA, Borrell A, Borobio V, et al. False positives in the prenatal ultrasound screening of fetal structural anomalies. *Prenat Diagn*. 2007;27:18–22.
38. Richmond S, Atkins J. A population-based study of the prenatal diagnosis of congenital malformation over 16 years. *BJOG*. 2005;112:1349–1357.
39. Timor-Tritsch IE, Monteagudo A. Transvaginal fetal neurosonography: standardization of the planes and sections by anatomic landmarks. *Ultrasound Obstet Gynecol*. 1996;8:42–47.
40. Malinger G, Ben-Sira L, Lev D, et al. Fetal brain imaging: a comparison between magnetic resonance imaging and dedicated neurosonography. *Ultrasound Obstet Gynecol*. 2004;23:333–340.
41. D'Addario V, Pinto V, Di Cagno L, et al. The midsagittal view of the fetal brain: a useful landmark in recognizing the cause of fetal cerebral ventriculomegaly. *J Perinatal Med*. 2005;33:423–427.
42. Monteagudo A, Timor-Tritsch IE, Moomjy M. Nomograms of the fetal lateral ventricles using transvaginal sonography. *J Ultrasound Med*. 1993;5:265–269.
43. Rickard S, Morris J, Paley M, et al. In utero magnetic resonance of the non-isolated ventriculomegaly: does ventricular size or morphology reflect pathology. *Clin Radiol*. 2006;61:844–853.
44. Schrander-Stumpel C, Fryns JP. Congenital hydrocephalus: nosology and guidelines for clinical approach and genetic counseling. *Eur J Pediatr*. 1998;157:355–362.
45. Morris JE, Rickard S, Paley MNJ, et al. The value of in-utero magnetic resonance imaging in ultrasound diagnosed foetal isolated cerebral ventriculomegaly. *Clin Radiol*. 2007;62:140–144.
46. Li Y, Estroff JA, Mehta TS, et al. Ultrasound and MRI of fetuses with ventriculomegaly: can cortical development be used to predict postnatal outcome. *AJR Am J Roentgenol*. 2011;196:1457–1467.
47. Mehta TS, Levine D. Imaging of fetal cerebral ventriculomegaly: a guide to management and outcome. *Semin Fetal Neonatal Med*. 2005;10:421–428.
48. Griffiths PD, Reeves MJ, Morris JE, et al. A prospective study of fetuses with isolated ventriculomegaly investigated by antenatal sonography and in utero MR imaging. *AJNR Am J Neuroradiol*. 2010;31:106–111.
49. Levine D, Trop I, Mehta TS, et al. MR imaging appearance of fetal cerebral ventricular morphology. *Radiology*. 2002;223:652–660.
50. Manganaro L, Savelli S, Francioso A, et al. Role of fetal MRI in the diagnosis of cerebral ventriculomegaly assessed by ultrasonography. *Radiol Med*. 2009;114:1013–1023.
51. Levine D, Barnes PD. Cortical maturation in normal and abnormal fetuses as assessed with prenatal MR imaging. *Radiology*. 1999;210:751–758.
52. Nicolaides KH, Berry S, Snijders RJM, et al. Fetal lateral cerebral ventriculomegaly: associated malformations and chromosomal defects. *Fetal Diagn Ther*. 1990;5:5–14.
53. Lee SB, Hong SH, Wang KY, et al. Fetal ventriculomegaly: prognosis in cases in which prenatal neurosurgical consultation was sought. *J Neurosurg*. 2006;105:265–270.
54. Quahba J, Luton D, Vuillard E, et al. Prenatal isolated mild ventriculomegaly: outcome in 167 cases. *BJOG*. 2006;113:1072–1079.

55. Wax JR, Bookman L, Cartin A, et al. Mild fetal cerebral ventriculomegaly: diagnosis, clinical associations, and outcomes. *Obstet Gynecol Surv*. 2003;58:407–414.
56. Vergani P, Locatelli A, Strobelt N, et al. Clinical outcome of mild fetal ventriculomegaly. *Am J Obstet Gynecol*. 1998;178:218–222.
57. Parilla BV, Endres LK, Dinsmoor MJ, et al. In utero progression of mild fetal ventriculomegaly. *Int J Gynaecol Obstet*. 2006;93:106–109.
58. Pilu G, Hobbins JC. Sonography of fetal cerebrospinal anomalies. *Prenat Diagn*. 2002;22:321–330.
59. Falip C, Blanc N, Maes E, et al. Postnatal clinical and imaging follow-up of infants with prenatal isolated mild ventriculomegaly: a series of 101 cases. *Pediatr Radiol*. 2007;37:981–989.
60. Durfee SM, Kim FM, Benson CB. Postnatal outcome of fetuses with the prenatal diagnosis of asymmetric hydrocephalus. *J Ultrasound Med*. 2001;20:263–268.
61. Devaseelan P, Cardwell C, Bell B, et al. Prognosis of isolated mild to moderate fetal cerebral ventriculomegaly: a systematic review. *J Perinat Med*. 2010;38:401–409.
62. Davis GH. Fetal hydrocephalus. *Clin Perinatol*. 2003;30:531–539.
63. Chervenak FA, Berkowitz RL, Romero R, et al. The diagnosis of fetal hydrocephalus. *Am J Obstet Gynecol*. 1983;147:703–716.
64. Kinzler WL, Smulian JC, McLean DA, et al. Outcome of prenatally diagnosed mild unilateral cerebral ventriculomegaly. *J Ultrasound Med*. 2001;20:257–262.
65. Breeze ACG, Dey PK, Lees CC, et al. Obstetric and neonatal outcomes in apparently isolated mild fetal ventriculomegaly. *J Perinat Med*. 2005;33:236–240.
66. Patel MD, Goldstein RB, Tung S, et al. Fetal cerebral ventricular atrium: difference in size according to sex. *Radiology*. 1995;194:713–715.
67. Nadel AS, Benacerraf BR. Lateral ventricular atrium: larger in male than female fetuses. *Int J Gynaecol Obstet*. 1995;51:123–126.
68. Almog B, Gamzu R, Achiron R, et al. Fetal lateral ventricular width: what should be its upper limit? A prospective cohort study and reanalysis of the current and previous data. *J Ultrasound Med*. 2003;22:39–43.
69. Snijders RJM, Nicolaides KH. Fetal biometry at 14–40 weeks' gestation. *Ultrasound Obstet Gynecol*. 1994;4:34–48.
70. Bronsteen R, Lee W, Vettraino I, et al. Isolated choroid plexus separation on second-trimester sonography: natural history and postnatal importance. *J Ultrasound Med*. 2006;25:343–347.
71. Patel MD, Filly AL, Hersh DR, et al. Isolated mild fetal cerebral ventriculomegaly: clinical course and outcome. *Radiology*. 1994;192:759–764.
72. Pilu G, Falco P, Gabrielli S, et al. The clinical significance of fetal isolated cerebral borderline ventriculomegaly: report of 31 cases and review of the literature. *Ultrasound Obstet Gynecol*. 1999;14:320–326.
73. Senat MV, Bernard JP, Schwarzler P, et al. Prenatal diagnosis and follow-up of 14 cases of unilateral ventriculomegaly. *Ultrasound Obstet Gynecol*. 1999;14:327–332.
74. Wyldes M, Watkinson M. Isolated mild fetal ventriculomegaly. *Arch Dis Child Fetal Neonatal ED*. 2004;89:F9–F13.
75. Griffiths PD, Reeves MJ, Morris JE, et al. A prospective study of fetuses with isolated ventriculomegaly investigated by antenatal sonography and in utero MR imaging. *AJNR Am J Neuroradiol*. 2010;31:106–111.
76. Parazzini C, Righini A, Doneda C, et al. Is fetal magnetic resonance imaging indicated when ultrasound isolated mild ventriculomegaly is present in pregnancies with no risk factors. *Prenat Diagn*. 2012;32:752–757.
77. Salomon LJ, Ouahba J, Delezoide AL, et al. Third-trimester fetal MRI in isolated 10- to 12-mm ventriculomegaly: is it worth it? *BJOG*. 2006;113:942–947.
78. Signorelli M, Tiberti A, Valseriath D, et al. Width of the fetal lateral ventricular atrium between 10 and 12 mm: a simple variation of the norm? *Ultrasound Obstet Gynecol*. 2004;23:14–18.
79. Leitner Y, Stolar O, Rotstein M, et al. The neurocognitive outcome of mild isolated fetal ventriculomegaly verified by prenatal magnetic resonance imaging. *Am J Obstet Gynecol*. 2009;201:215.e1–215.e6.
80. Lipitz S, Yagel S, Malinger G, et al. Outcome of fetuses with isolated borderline unilateral ventriculomegaly diagnosed at mid-gestation. *Ultrasound Obstet Gynecol*. 1998;12:23–26.
81. Gilmore JH, Smith LC, Wolfe HM, et al. Prenatal mild ventriculomegaly predicts abnormal development of the neonatal brain. *Biol Psychiatry*. 2008;64:1069–1076.
82. Bloom SL, Bloom DD, Dellanebbia C, et al. The developmental outcome of children with antenatal mild isolated ventriculomegaly. *Obstet Gynecol*. 1997;90:93–97.
83. Gomez-Arriaga P, Herraiz I, Puente JM, et al. Mid-term neurodevelopmental outcome in isolated mild ventriculomegaly diagnosed in fetal life. *Fetal Diagn Ther*. 2012;31:12–18.
84. Verhagen WIM, Bartels RHAM, Fransen E, et al. Familial congenital hydrocephalus and aqueduct stenosis with probably autosomal dominant inheritance and variable expression. *J Neurol Sci*. 1998;158:101–105.
85. Kenwrick S, Jouet M, Donnai D. X-linked hydrocephalus and MASA syndrome. *J Med Genet*. 1996;33:59–65.
86. Weller S, Gartner J. Genetic and clinical aspects of x-linked hydrocephalus (L1 disease): mutations in the L1CAM gene. *Hum Mutat*. 2001;18:1–12.
87. Humphreys P, Muzumdar DP, Sly LE, et al. Focal cerebral mantle disruption in fetal hydrocephalus. *Pediatr Neurol*. 2007;36:236–243.
88. Ishak GE, Dempsey JC, Shaw DWW, et al. Rhombencephalosynapsis: a hindbrain malformation associated with incomplete separation of midbrain and forebrain hydrocephalus and a broad spectrum of severity. *Brain*. 2012;135:1370–1386.
89. Oi S, Honda U, Hidaka M, et al. Intrauterine high resolution magnetic resonance imaging in fetal hydrocephalus and prenatal estimation of postnatal outcomes with "perspective classification." *J Neurosurg*. 1998;88:685–694.
90. Rieley MB, Kline-Fath BM, Peach EE, et al. Aqueductal stenosis diagnosed with fetal MRI: etiology, medical and developmental outcomes The David Smith Workshop on Dysmorphology and Morphogenesis, Montremblant, Canada August 2008.
91. Varadi V, Csecsei K, Szeifert GT, et al. Prenatal diagnosis of X linked hydrocephalus without aqueductal stenosis. *J Med Genet*. 1987;24:207–209.
92. Breeze ACG, Alexander PMA, Murdoch EM, et al. Obstetric and neonatal outcomes in severe fetal ventriculomegaly. *Prenat Diagn*. 2007;27:124–129.
93. Levitsky DB, Mack LA, Nyberg DA, et al. Fetal aqueductal stenosis diagnosed sonographically: how grave is the prognosis? *AJR Am J Roentgenol*. 1995;164:725–730.
94. Holmes LB, Nash A, ZuRhein GM, et al. X-linked aqueductal stenosis: clinical and neuropathological findings in two families. *Pediatrics*. 1973;51:697–704.
95. Kennelly MM, Cooley SM, McFarland PJ. Natural history of apparently isolated severe fetal ventriculomegaly: perinatal survival and neurodevelopmental outcomes. *Prenat Diagn*. 2009;29:1135–1140.
96. Cavalheiro S, Fernandes Moron A, Zymberg ST, et al. Fetal hydrocephalus—prenatal treatment. *Childs Nerv Syst*. 2003;19:561–573.
97. Orioli IM, Castilla EE. Epidemiology of holoprosencephaly: prevalence and risk factors. *Am J Med Genet C Semin Med Genet*. 2010;154C:13–21.
98. Wenghoefer M, Ettema AM, Sina F, et al. Prenatal ultrasound diagnosis in 51 cases of holoprosencephaly: craniofacial anatomy, associated malformations, and genetics. *Cleft Palate Craniofac J*. 2010;47:15–21.
99. Joo GJ, Beke A, Papp C, et al. Prenatal diagnosis, phenotypic and obstetric characteristics of holoprosencephaly. *Fetal Diagn Ther*. 2005;20:161–166.
100. Simon EM, Barkovich AJ. Holoprosencephaly: new concepts. *Magn Reson Imaging Clin N Am*. 2001;9:149–164.
101. Volpe P, Campobasso G, De Robertis V, et al. Disorders of prosencephalic development. *Prenat Diagn*. 2009;29:340–354.
102. Hahn JS, Plawner LL. Evaluation and management of children with holoprosencephaly. *Pediatr Neurol*. 2004;31:79–88.
103. Nyberg DA, Mack LA, Bronstein A, et al. Holoprosencephaly: prenatal sonographic diagnosis. *AJR Am J Roentgenol*. 1987;149:1051–1058.
104. Filly RA, Chinn DH, Callen PW. Alobar holoprosencephaly: ultrasonographic prenatal diagnosis. *Radiology*. 1984;151:455–459.
105. Barkovich AJ, Quint DJ. Middle interhemispheric fusion: an unusual variant of holoprosencephaly. *AJNR Am J Neuroradiol*. 1993;14:431–440.
106. Simon EM, Hevner RF, Pinter JD, et al. The middle interphemispheric variant of holoprosencephaly. *AJNR Am J Neuroradiol*. 2002;23:151–155.
107. Dubourg C, Bendavid C, Pasquier L, et al. Holoprosencephaly. *Orphanet J Rare Dis*. 2007;2:1–14.
108. Bullen PJ, Rankin JM, Robson SC. Investigation of the epidemiology and prenatal diagnosis of holoprosencephaly in the north of England. *Am J Obstet Gynecol*. 2001;184:1256–1262.
109. Yamada S. Embryonic holoprosencephaly: pathology and phenotypic variability. *Congenit Anom*. 2006;46:164–171.
110. DeMyer W, Zeman W, Palmer CG. The face predicts the brain: diagnostic significance of median facial anomalies for holoprosencephaly (arhinencephaly). *Pediatrics*. 1964;34:256–263.
111. Johnson CY, Rasmusen SA. Non-genetic risk factors for holoprosencephaly. *Am J Med Genet C Semin Med Genet*. 2010;154C:73–85.
112. Solomon BD, Gropman A, Muenke M. Holoprosencephaly overview. In: Pagon RA, Adam MP, Bird TD, et al, eds. *GeneReviews*™ [Internet]. Seattle, WA: University of Washington; 1993–2013, December 27, 2000. [Updated November 3, 2011].
113. Huang J, Wah IY, Pooh RK, et al. Molecular genetics in fetal neurology. *Semin Fetal Neonatal Med*. 2012;17:341–346.
114. Berry SM, Gosden C, Snijders RJM, et al. Fetal holoprosencephaly: associated malformations and chromosomal defects. *Fetal Diagn Ther*. 1990;5:92–99.
115. Bianchi D, Crombleholme T, D'Alton M, et al. *Fetology: Diagnosis and Management of the Fetal Patient*. 2nd ed. New York, NY: McGraw-Hill Medical; 2010:121–129.
116. Sepulveda W, Dezerega V, Be C. First-trimester sonographic diagnosis of holoprosencephaly: value of the "Butterfly" sign. *J Ultrasound Med*. 2004;23:761–765.
117. Hahn JS, Barnes PD. Neuroimaging advances in holoprosencephaly: refining the spectrum of the midline malformation. *Am J Med Genet C Semin Med Genet*. 2010;154C:120–132.
118. Cayea PD, Balcar I, Alberti O Jr, et al. Prenatal diagnosis of semilobar holoprosencephaly. *AJR Am J Roentgenol*. 1984;142:401–402.
119. Pilu G, Sandri F, Perolo A, et al. Prenatal diagnosis of lobar holoprosencephaly. *Ultrasound Obstet Gynecol*. 1992;2:88–94.
120. Pilu G, Ambrosetto P, Sandri F, et al. Intraventricular fused fornices: a specific sign of fetal lobar holoprosencephaly. *Ultrasound Obstet Gynecol*. 1994;4:65–67.
121. Bernard JP, Drummond CL, Zaarour P, et al. A new clue to the prenatal diagnosis of lobar holoprosencephaly: the abnormal pathway of the anterior cerebral artery crawling under the skull. *Ultrasound Obstet Gynecol*. 2002;19:605–607.

122. Wong HS, Lam YH, Tang MHY, et al. First-trimester ultrasound diagnosis of holoprosencephaly: three case reports. *Ultrasound Obstet Gynecol*. 1999;13:356–359.
123. Tongsong T, Wanapirak C, Chanprapaph P, et al. First trimester sonographic diagnosis of holoprosencephaly. *Int J Gynaecol Obstet*. 1999;66:165–169.
124. McGahan JP, Nyberg DA, Mack LA. Sonography of facial features of alobar and semilobar holoprosencephaly. *AJR Am J Roetgenol*. 1990;154:143–148.
125. Chen CP, Shih JC, Hsu CY, et al. Prenatal three-dimensional/four dimensional sonographic demonstration of facial dysmorphisms associated with holoprosencephaly. *J Clin Ultrasound*. 2005;33:312–318.
126. Lee YY, Lin MT, Lee MS, et al. Holoprosencephaly and cyclopia visualized by two- and three-dimensional prenatal ultrasound. *Chang Gung Med J*. 2002;25:207–210.
127. Plawner LL, Delgado MR, Miller VS, et al. Neuroanatomy of holoprosencephaly as predictor of function, beyond the face predicting the brain. *Neurology*. 2002;59:1058–1066.
128. Wong AMC, Bilaniuk LT, Ng KK, et al. Lobar holoprosencephaly: prenatal MR diagnosis with postnatal MR correlation. *Prenat Diagn*. 2005;25:295–299.
129. Johnson N, Windrim R, Chong K, et al. Prenatal diagnosis of solitary median maxillary central incisor syndrome by magnetic resonance imaging. *Ultrasound Obstet Gynecol*. 2008;32:120–122.
130. Hahn JS, Barkovich AJ, Stashinko EE, et al. Factor analysis of neuroanatomical and clinical characteristics of holoprosencephaly. *Brain Dev*. 2006;28: 413–419.
131. Simon EM, Hevner R, Pinter JD, et al. Assessment of the deep gray nuclei in holoprosencephaly. *AJNR Am J Neuroradiol*. 2000;21:1955–1961.
132. Hahn JS, Barnes PD, Clegg NJ, et al. Septopreoptic holoprosencephaly: a mild subtype associated with midline craniofacial anomalies. *AJNR Am J Neuroradiol*. 2010;31:1596–1601.
133. Koob M, Weingertner AS, Gasser B, et al. Thick corpus callosum: a clue to the diagnosis of fetal septopreoptic holoprosencephaly? *Pediatr Radiol*. 2012;42:886–890.
134. Pulitzer SB, Simon EM, Crombleholme TM, et al. Prenatal MR findings of the middle interhemispheric variant of holoprosencephaly. *AJNR Am J Neuroradiol*. 2004;25:1034–1036.
135. Barkovich AJ, Simon EM, Clegg NJ, et al. Analysis of the cerebral cortex in holoprosencephaly with attention to the Sylvian fissures. *AJNR Am J Neuroradiol*. 2002;23:143–150.
136. Cohen MM Jr. Holoprosencephaly: clinical, anatomic and molecular dimensions. *Birth Defects Res A Clin Mol Teratol*. 2006;76:658–673.
137. Raam MS, Solomon BD, Muenke M. Holoprosencephaly: a guide to diagnosis and clinical management. *Indian Pediatr*. 2011;48:457–466.
138. David AL, Gowda V, Turnbull C, et al. The risk of recurrence of holoprosencephaly in euploid fetuses. *Obstet Gynecol*. 2007;110:658–662.
139. Dill P, Poretti A, Boltshauser E, et al. Fetal magnetic resonance imaging in midline malformations of the central nervous system and review of the literature. *J Neuroradiol*. 2009;36:138–146.
140. Li Y, Estroff JA, Khwaja O, et al. Callosal dysgenesis in fetuses with ventriculomegaly: levels of agreement between imaging modalities and postnatal outcome. *Ultrasound Obstet Gynecol*. 2012;40:522–529.
141. Glass HC, Shaw GM, Ma C, et al. Agenesis of the corpus callosum in California 1983–2003: a population-based study. *Am J Med Genet*. 2008;146A: 2495–2500.
142. Szabo N, Gergev G, Kobor J, et al. Corpus callosum anomalies: birth prevalence and clinical spectrum in Hungary. *Pediatr Neurol*. 2011;44:420–426.
143. Fratelli N, Papageorghiou AT, Prefuno F, et al. Outcome of prenatally diagnosed agenesis of the corpus callosum. *Prenat Diagn*. 2007;27:512–517.
144. Vasudevan C, McKechnie L, Levene M. Long-term outcome of antenatally diagnosed agenesis of the corpus callosum and cerebellar malformations. *Semin Fetal Neonatal Med*. 2012;17:292–300.
145. Raybaud C. The corpus callosum, the other great forebrain commissures, and the septum pellucidum: anatomy, development and malformation. *Neuroradiology*. 2010;52:447–477.
146. Dobyns WB. Absence makes the search grow longer. *Am J Hum Genet*. 1996;58:7–16.
147. Barkovich AJ, Norman D. Anomalies of the corpus callosum: correlation with further anomalies of the brain. *AJR Am J Roentgenol*. 1988;151:171–179.
148. Atlas SW, Zimmerman RA, Bilaniuk LT, et al. Corpus callosum and limbic system: neuroanatomic MR evaluation of developmental anomalies. *Radiology*. 1986;160:355–362.
149. Hetts SW, Sherr EH, Chao S, et al. Anomalies of the corpus callosum: an MR analysis of the phenotypic spectrum of associated malformations. *AJR Am J Roentgenol*. 2006;187:1343–1348.
150. Barkovich AJ, Simon EM, Walsh CA. Callosal agenesis with cyst: a better understanding and new classification. *Neurology*. 2001;56:220–227.
151. Ickowitz V, Eurin D, Rypens F, et al. Prenatal diagnosis and postnatal follow-up of pericallosal lipoma: report of seven new cases. *AJNR Am J Neuroradiol*. 2001;22:767–772.
152. Shevell MI. Clinical and diagnostic profile of agenesis of the corpus callosum. *J Child Neurol*. 2002;17:895–899.
153. Bedeschi MF, Bonaglia MC, Grasso R, et al. Agenesis of the corpus callosum: clinical and genetic study in 63 young patients. *Pediatr Neurol*. 2006;34:186–193.
154. Gupta JK, Lilford RJ. Assessment and management of fetal agenesis of the corpus callosum. *Prenat Diagn*. 1995;15:301–312.
155. Aicardi J. Aicardi syndrome. *Brain Dev*. 2005;27:164–171.
156. Diaz-Guerrero L, Giugni-Chalbaud G, Sosa-Olavarria A. Assessment of pericallosal arteries by color Doppler ultrasonography at 11–14 weeks: an early marker of fetal corpus callosum development in normal fetuses and agenesis in cases with chromosomal anomalies. *Fetal Diagn Ther*. 2013;34:85–89.
157. Lachmann R, Sodre D, Barmpas M, et al. Midbrain and falx in fetuses with absent corpus callosum at 11–13 weeks. *Fetal Diagn Ther*. 2013;33:41–46.
158. Pilu G, Sandri F, Perolo A, et al. Sonography of fetal agenesis of the corpus callosum: a survey of 35 cases. *Ultrasound Obstet Gynecol*. 1993;3:318–329.
159. Bennett GL, Bromley B, Benacerraf BR. Agenesis of the corpus callosum: prenatal detection usually is not possible before 22 weeks of gestation. *Radiology*. 1996;199:447–450.
160. Blum A, Andre M, Droulle P, et al. Prenatal echographic diagnosis of the corpus callosum agenesis: the Nancy experience 1982–1989. *Genet Couns*. 1990;38:115–126.
161. Manfredi R, Tognolini A, Bruno C, et al. Agenesis of the corpus callosum in fetuses with mild ventriculomegaly: role of MR imaging. *Radiol Med*. 2010;115:301–312.
162. Bertino RE, Nyberg DA, Cyr DR, et al. Prenatal diagnosis of agenesis of the corpus callosum. *J Ultrasound Med*. 1988;7:251–260.
163. Blaicher W, Prayer D, Mittermayer C, et al. Magnetic resonance imaging in fetuses with bilateral moderate ventriculomegaly and suspected anomaly of the corpus callosum on ultrasound scan. *Ultraschall Med*. 2003;24:255–260.
164. Volpe P, Paladini D, Resta M, et al. Characteristics, associations and outcome of partial agenesis of the corpus callosum in the fetus. *Ultrasound Obstet Gynecol*. 2006;27:509–516.
165. Griffiiths PD, Batty R, Connolly DAJ, et al. Effects of failed commissuration on the septum pellucidum and fornix: implications for fetal imaging. *Neuroradiology*. 2009;51:347–356.
166. Ghi T, Carletti A, Contro E, et al. Prenatal diagnosis and outcome of partial agenesis and hypoplasia of the corpus callosum. *Ultrasound Obstet Gynecol*. 2010;35:35–41.
167. Harreld JH, Bhore R, Chason DP, et al. Corpus callosum length by gestational age as evaluated by fetal MR imaging. *AJNR Am J Neuroradiol*. 2011;32: 490–494.
168. Glenn OA. MR imaging of the fetal brain. *Pediatr Radiol*. 2010;40:68–81.
169. Glenn OA, Goldstein RB, Li KC, et al. Fetal magnetic resonance imaging in the evaluation of fetuses referred for sonographically suspected abnormalities of the corpus callosum. *J Ultrasound Med*. 2005;24:791–804.
170. Tang PH, Bartha AI, Norton ME, et al. Agenesis of the corpus callosum: an MR imaging analysis of associated abnormalities in the fetus. *AJNR Am J Neuroradiol*. 2009;30:257–263.
171. Warren DJ, Connolly DJA, Griffiths PD. Assessment of sulcation of the fetal brain in cases of isolated agenesis of the corpus callosum using in utero MR imaging. *AJNR Am J Neuroradiol*. 2010;31:1085–1090.
172. Parrish ML, Roessmann U, Livinsohn MW. Agenesis of the corpus callosum: a study of the frequency of associated malformations. *Ann Neurol*. 1979;6:349–354.
173. Goodyear PWA, Bannister CM, Russell S, et al. Outcome in prenatally diagnosed fetal agenesis of the corpus callosum. *Fetal Diagn Ther*. 2001;16: 139–145.
174. Rosser TL, Acosta MT, Packer RJ. Aicardi syndrome: spectrum of disease and long-term prognosis in 77 females. *Pediatr Neurol*. 2002;27:343–346.
175. Paul LK, Brown WS, Adolphs R, et al. Agenesis of the corpus callosum: genetic, developmental and functional aspects of connectivity. *Neuroscience*. 2007;8:287–299.
176. Moes P, Schilmoeller K, Schmilmoeller G. Physical, motor, sensory and developmental features associated with agenesis of the corpus callosum. *Child Care Health Dev*. 2009;35:656–672.
177. Doherty D, Tu S, Schilmoeller K, et al. Health-related issues in individuals with agenesis of the corpus callosum. *Child Care Health Dev*. 2006;32:333–342.
178. Mangione R, Fries N, Godard P, et al. Neurodevelopmental outcome following prenatal diagnosis of an isolated anomaly of the corpus callosum. *Ultrasound Obstet Gynecol*. 2011;37:290–295.
179. Patel L, McNally RJQ, Harrison E, et al. Geographical distribution of optic nerve hypoplasia and septo-optic dysplasia in Northwest England. *J Pediatr*. 2006;148:85–88.
180. Atapattu N, Ainsworth J, Willshaw H, et al. Septo-optic dysplasia: antenatal risk factors and clinical features in a regional study. *Horm Res Paediatr*. 2012;78:81–87.
181. Brodsky MC, Glasier CM. Optic nerve hypoplasia: clinical significance of associated central nervous system abnormalities on magnetic resonance imaging. *Arch Ophthalmol*. 1993;111:66–74.
182. Birkebaek NH, Patel L, Wright NB, et al. Endocrine status in patients with optic nerve hypoplasia: relationship to midline central nervous system abnormalities and appearance of the hypothalamic-pituitary axis on magnetic resonance imaging. *J Clin Endocrinol Metab*. 2003;88:5281–5286.
183. Kelberman D, Dattani MT. Septo-optic dysplasia—novel insights into the aetiology. *Horm Res*. 2008;69:257–265.
184. Stevens CA, Dobyns WB. Septo-optic dysplasia and amniotic bands: further evidence for a vascular pathogenesis. *Am J Med Genet*. 2004;125A:12–16.

Kline9781451175837-ch012.1.indd 418 08/08/14 9:59 AM

185. Polizzi A, Pavone P, Iannetti P, et al. Septo-optic dysplasia complex: a heterogeneous malformation syndrome. *Pediatr Neurol*. 2006;34:66–71.
186. Raybaud C, Girard N, Levrier O, et al. Schizencephaly: correlation between the lobar topography of the cleft(s) and absence of the septum pellucidum. *Childs Nerv Syst*. 2001;17:217–222.
187. Leonhardt EE, Tann-Sinn PA. Septo-optic dysplasia: a neurosonographic review. *J Diagn Med Sonogr*. 2005;21:479–486.
188. Barkovich AJ, Fram EK, Norman D. Sept-optic dysplasia: MR imaging. *Radiology*. 1989;171:189–192.
189. McCabe MJ, Alatzoglou KS, Dattani MT. Septo-optic dysplasia and other midline defects: the role of transcription factors: HESX1 and beyond. *Best Pract Res Clin Endocrinol Metab*. 2011;25:115–124.
190. Falco P, Gabrielli S, Visentin A, et al. Transabdominal sonography of the cavum septum pellucidum in normal fetuses in the second and third trimesters of pregnancy. *Ultrasound Obstet Gynecol*. 2000;16:549–553.
191. Pilu G, Tani G, Carletti A, et al. Difficult early sonographic diagnosis of absence of the fetal septum pellucidum. *Ultrasound Obstet Gynecol*. 2005;25:70–72.
192. Callen PW, Callen AL, Glenn OA, et al. Columns of the fornix, not be mistaken for the cavum septi pellucidi on prenatal sonography. *J Ultrasound Med*. 2008;27:25–31.
193. Lepinard C, Coutant R, Boussion F, et al. Prenatal diagnosis of absence of the septum pellucidum associated with septo-optic dysplaia. *Ultrasound Obstet Gynecol*. 2005;25:73–75.
194. Katorza E, Bault JP, Gilboa Y, et al. Prenatal visualization of the pituitary gland using 2- and 3-dimensional sonography: comparison to prenatal magnetic resonance imaging. *J Ultrasound Med*. 2012;31:1675–1680.
195. Bault JP, Salomon LJ, Guibaud L, et al. Role of three-dimensional ultrasound measurement of the optic tract in fetuses with agenesis of the septum pellucidum. *Ultrasound Obstet Gynecol*. 2011;37:570–575.
196. Li Y, Sansgiri R, Estroff JA, et al. Outcome of fetuses with cerebral ventriculomegaly and septum pellucidum leaflet abnormalities. *AJR Am J Roentgenol*. 2011;196:W83–W92.
197. Barkovich AJ, Norman D. Absence of the septum pellucidum: a useful sign in the diagnosis of congenital brain malformations. *AJR Am J Roentgenol*. 1989;152:353–360.
198. Levine LM, Bhatti MT, Mancuso AA. Septo-optic dysplasia with olfactory tract and bulb hypoplasia. *J AAPOS*. 2001;5:398–399.
199. Pilu G, Sandri F, Cerisoli M, et al. Sonographic findings in septo-optic dysplasia in the fetus and newborn infant. *Am J Perinatol*. 1990;7:337–339.
200. Belhocine O, Andre C, Kalifa G, et al. Does asymptomatic septal agenesis exist? A review of 34 cases. *Pediatr Radiol*. 2005;35:410–418.
201. Antonini SRR, Filho AG, Elias LLK, et al. Cerebral midline developmental anomalies: endocrine, neuroradiographic and opthalmological features. *J Pediatr Endocrinol Metab*. 2002;15:1525–1530.
202. Wales JKH, Quarrell OWJ. Evidence for possible Mendelian inheritance of septo-optic dysplasia. *Acta Paediatr*. 1996;85:391–392.
203. Barkovich AJ, Guerrini R, Kuzniecky RI, et al. A developmental and genetic classification for malformations of cortical development: update 2012. *Brain*. 2012;135(5):1348–1369.
204. Razek AAKA, Kandell AY, Elsorogy LG, et al. Disorders of cortical formation: MR imaging features. *AJNR Am J Neuroradiol*. 2009;30:4–11.
205. Manoranjan B, Provias JP. Hemimegalencephaly: a fetal case with neuropathological confirmation and review of the literature. *Acta Neuropathol*. 2010;120:117–130.
206. Tinkle BT, Schorry EK, Franz DN, et al. Epidemiology of hemimegalencephaly: a case series and review. *Am J Med Genet*. 2005;139A:204–211.
207. Flores-Sarnat L. Hemimegalencepahy, part I: genetic, clinical and imaging aspects. *J Child Neurol*. 2002;17:373–384.
208. Flores-Sarnat L, Sarnat HB, Davila-Gutierrez G, et al. Hemimegalencepahy, part 2: neuropathology suggests a disorder of cellular lineage. *J Child Neurol*. 2003;18:776–785.
209. Sasaki M, Hashimoto T, Furushima W, et al. Clinical aspects of hemimegalencephaly by means of a nationwide survey. *J Child Neurol*. 2005;20:337–341.
210. Baek ST, Gibbs EM, Gleeson JG, et al. *Curr Opin Neurol*. 2013;26:122–127.
211. Alvarez RM, Garcia-Diaz L, Marquez J, et al. Hemimegalencephaly: prenatal diagnosis and outcome. *Fetal Diagn Ther*. 2011;30:234–238.
212. Hafner E, Bock W, Zoder G, et al. Prenatal diagnosis of unilateral megalencephaly by 2D and 3D ultrasound: a case report. *Prenat Diagn*. 1999;19:159–162.
213. Barkovich AJ, Chuang SH. Unilateral megalencephaly: correlation of MR imaging and pathologic characteristics. *AJNR Am J Neuroradiol*. 1990;11: 523–531.
214. Di Rocco C, Battaglia D, Pietrini D, et al. Hemimegalencephaly: clinical implications and surgical treatment. *Childs Nerv Syst*. 2006;22:852–866.
215. Agid R, Liberman S, Nadjari M, et al. Prenatal MR diffusion-weighted imaging in a fetus with hemimegalencephaly. *Pediatr Radiol*. 2006;36:138–140.
216. Sato N, Yagishita A, Oba H, et al. Hemimegalencephaly: a study of abnormalities occurring outside the involved hemisphere. *AJNR Am J Neuroradiol*. 2007;28:678–682.
217. Milunsky A, Ito M, Maher TA, et al. Prenatal molecular diagnosis of tuberous sclerosis complex. *Am J Obstet Gynecol*. 2009;200:321.e1–321.e6.
218. Baskin HJ Jr. The pathogenesis and imaging of the tuberous sclerosis complex. *Pediatr Radiol*. 2008;38:936–952.
219. Gusman M, Servaes S, Feygin T, et al. Multimodal imaging in the prenatal diagnosis of tuberous sclerosis complex. *Case Rep Pediatr*. 2012;2012:925646.
220. Curatiolo P, Bombardieri R, Jozwiak S. Tuberous sclerosis. *Lancet*. 2008;372:657–668.
221. King JA, Stamilio DM. Maternal and fetal tuberous sclerosis complicating pregnancy: a case report and overview of the literature. *Am J Perinatol*. 2005;22:103–108.
222. Saada J, Rabia SH, Fermont L, et al. Prenatal diagnosis of cardiac rhabdomyomas: incidence of associated cerebral lesions of tuberous sclerosis complex. *Ultrasound Obstet Gynecol*. 2009;34:155–159.
223. Gedikbasi A, Oztarhan K, Ulker V, et al. Prenatal sonographic diagnosis of tuberous sclerosis complex. *J Clin Ultrasound*. 2011;39:427–430.
224. Bader RS, Chitayat D, Kelly E, et al. Fetal rhabdomyoma: prenatal diagnosis, clinical outcome, and incidence of associated tuberous sclerosis complex. *J Pediatr*. 2003;143:620–624.
225. Muhler MR, Rake A, Schwabe M, et al. Value of fetal cerebral MRI in sonographically proven cardiac rhabdomyoma. *Pediatr Radiol*. 2007;37:467–474.
226. Werner H Jr, Mirleese V, Jacquemard F, et al. Prenatal diagnosis of tuberous sclerosis use of magnetic resonance imaging and its implications for prognosis. *Prenat Diagn*. 1994;14:1151–1154.
227. Sgro M, Barozzimo T, Toi A, et al. Prenatal detection of cerebral lesions in a fetus with tuberous sclerosis. *Ultrasound Obstet Gynecol*. 1999;14:356–359.
228. Zhang YX, Meng H, Zhong DR, et al. Cardiac rhabdomymoma and renal cyst in a fetus: early onset of tuberous sclerosis with renal cystic disease. *J Ultrasound Med*. 2008;27:979–982.
229. Sonigo P, Elmaleh A, Fermont L, et al. Prenatal MRI diagnosis of fetal cerebral tuberous sclerosis. *Pediatr Radiol*. 1996;26:1–4.
230. Baron Y, Barkovich A. MR imaging of tuberous sclerosis in neonates and young infants. *AJNR Am J Neuroradiol*. 1999;20:907–916.
231. Rosser T, Panigrahy A, McClintock W. The diverse clinical manifestations of tuberous sclerosis complex: a review. *Semin Pediatr Neurol*. 2006;13:27–36.
232. Jansen FE, Vincken KL, Algra A, et al. Cognitive impairment in tuberous sclerosis complex is a multifactorial condition. *Neurology*. 2008;70:916–923.
233. Malinger G, Lev D, Lerman-Sagie T. Assessment of fetal intracranial pathologies first demonstrated late in pregnancy: cell proliferation disorders [review]. *Reprod Biol Endocrinol*. 2003;14(1):110.
234. Szabo N, Pap C, Kobor J, et al. Primary microcephaly in Hungary: epidemiology and clinical features. *Acta Paediatr*. 2010;99:690–693.
235. Goldstein I, Reece A, Pilu G, et al. Sonographic assessment of the fetal frontal lobe: a potential tool for prenatal diagnosis of microcephaly. *Am J Obstet Gynecol*. 1988;158:1057–1062.
236. Sztriha L, Dawodu A, Gururaj A, et al. Microcephaly associated with abnormal gyral pattern. *Neuropediatrics*. 2004;35:346–352.
237. Adachi Y, Poduri A, Kawaguch A, et al. Congenital microcephaly with a simplified gyral pattern: associated findings and their significance. *AJNR Am J Neuroradiol*. 2011;32:1123–1129.
238. Dobyns WB. Primary microcephaly: new approaches for an old disorder. *Am J Med Genet*. 2002;112:315–317.
239. Jaffe M, Tirosh E, Oren S. The dilemma in prenatal diagnosis of idiopathic microcephaly. *Dev Med Child Neurol*. 1987;29:187–189.
240. Den Hollander NS, Wessel MW, Los FJ, et al. Congenital microcephaly detected by prenatal ultrasound: genetic aspects and clinical significance. *Ultrasound Obstet Gynecol*. 2000;15:282–287.
241. Dahlgren L, Wilson RD. Prenatally diagnosed microcephaly: a review of etiologies. *Fetal Diagn Ther*. 2001;16:323–326.
242. Malinger G, Lerman-Sagie T, Watemberg N, et al. A normal second-trimester ultrasound does not exclude intracranial structural pathology. *Ultrasound Obstet Gynecol*. 2002;20:51–56.
243. Bromley B, Benacerraf BR. Difficulties in the prenatal diagnosis of microcephaly. *J Ultrasound Med*. 1995;14:303–305.
244. Stoler-Poria S, Lev D, Schweiger A, et al. Developmental outcome of the isolated fetal microcephaly. *Ultrasound Obstet Gynecol*. 2010;36:154–158.
245. Pilu G, Falco P, Milano V, et al. Prenatal diagnosis of microcephaly assisted by vaginal sonography and power Doppler. *Ultrasound Obstet Gynecol*. 1998;11:357–360.
246. Persutte WH, Coury A, Hobbins JC. Correlation of fetal frontal lobe transcerebellar diameter measurements: the utility of a new prenatal sonographic technique. *Ultrasound Obstet Gynecol*. 1997;10:94–97.
247. Verloes A. Microcephalia vera and microcephaly with simplified gyral pattern. *Orphanet Encyclopedia*. 2004;1–5. http://www.orpha.net/data/patho/GB/uk-MVMSG.pdf.
248. Tao G, Yew DT. Magnetic resonance imaging of fetal brain abnormalities. *Neuroembryol Aging*. 2008;5:49–55.
249. Fogliarini C, Chaumoitre K, Chapon F, et al. Assessment of cortical maturation with prenatal MRI, part II: abnormalities of cortical maturation. *Eur Radiol*. 2005;15:1781–1789.
250. Abuelo D. Microcephaly syndromes. *Semin Pediatr Neurol*. 2007;14:118–127.
251. Biran-Gol Y, Malinger G, Cohen H, et al. Developmental outcome of isolated fetal macrocephaly. *Ultrasound Obstet Gynecol*. 2010;36:147–153.
252. Malinger G, Lev D, Ben-Sira L, et al. Can syndromic macrocephaly be diagnosed in utero? *Ultrasound Obstet Gynecol*. 2011;37:72–81.
253. Toi A, Chitayat D, Blaser S. Abnormalities of the foetal cerebral cortex. *Prenat Diagn*. 2009;29:355–371.

254. Saleh-Gargari S, Omrani MD, Hantoushzadeh S. Prenatal diagnosis of benign familial fetal macrocephaly. *Ultrasound Obstet Gynecol*. 2007;30:547–653.
255. Lerman-Sagie T, Ben-Sira L, Achiron R, et al. Thick fetal corpus callosum: an ominous gin? *Ultra Obstet Gynecol*. 2009;34:55–61.
256. Mallerio C, Marignier S, Roth P, et al. Prenatal cerebral ultrasound and MRI findings in glutaric aciduria Type 1: a de novo case. *Ultrasound Obstet Gynecol*. 2008;31:712–714.
257. Williams CA. Macrocephaly syndromes. In: Stalker HJ, ed. *RC Philips Research and Education Unit Newsletter*. 2008;20(1). http://www.peds.ufl.edu/divisions/genetics/newsletters/macrocephaly.pdf.
258. Isaacs H Jr. I: perinatal brain tumors: a review of 250 cases. *Pediatr Neurol*. 2002;27:249–261.
259. Isaacs H Jr. Fetal brain tumors: a review of 154 cases. *Am J Perinatol*. 2009;26:453–466.
260. Woodward PJ, Sohaey R, Kennedy A, et al. From the archives of the AFIP: a comprehensive review of fetal tumors with pathologic correlation. *Radiographics*. 2005;25:215–242.
261. Schlembach D, Bornemann A, Rupprecht T, et al. Fetal intracranial tumors detected by ultrasound: a report of two cases and review of the literature. *Ultrasound Obstet Gynecol*. 1999;14:407–418.
262. Rickert CH. Neuropathology and prognosis of foetal brain tumours. *Acta Neuropathol*. 1999;98:567–576.
263. Cavalheiro S, Moron AF, Hisaba W, et al. Fetal brain tumors. *Childs Nerv Syst*. 2003;19:529–536.
264. D'Addario V, Pinto V, Meo F, et al. The specificity of ultrasound in the detection of fetal intracranial tumors. *J Perinat Med*. 1998;26:480–485.
265. Cassart M, Bosson N, Garel C, et al. Fetal intracranial tumors: a review of 27 cases. *Eur Radiol*. 2008;18:2060–2066.
266. Vazquez E, Castellote A, Mayolas N, et al. Congenital tumours involving the head, neck and central nervous system. *Pediatr Radiol*. 2009;39:1158–1172.
267. DiPietro JA, Cristofalo EA, Voegtline KM, et al. Isolated prenatal choroid plexus cysts do not affect child development. *Prenat Diagn*. 2011;31:745–749.
268. Achiron R, Barkai G, Katznelson BM, et al. Fetal lateral ventricle choroid plexus cysts: the dilemma of amniocentesis. *Obstet Gynecol*. 1991;78:815–818.
269. Kraus I, Jirasek JE. Some observations of the structure of the choroid plexus and its cysts. *Prenat Diagn*. 2002;22:1223–1228.
270. Zafar HM, Ankola A, Coleman B. Ultrasound pitfalls and artifacts related to six common fetal findings. *Ultrasound Q*. 2012;28:105–124.
271. Turner SR, Samei E, Hertzberg BS, et al. Sonography of fetal choroid plexus cysts. *J Ultrasound Med*. 2003;22:1219–1227.
272. Morcos CL, Platt LD, Carlson DE, et al. The isolated choroid plexus cyst. *Obstet Gynecol*. 1998;92:232–236.
273. Sullivan A, Giudice T, Vavelidis F, et al. Choroid plexus cysts: is biochemical testing a valuable adjunct to targeted ultrasonography. *Am J Obstet Gynecol*. 1999;181:260–265.
274. Lopez JA, Reich D. Choroid plexus cysts. *J Am Board Fam Med*. 2006;19:422–425.
275. Ghidini A, Strobelt N, Locatelli A, et al. Isolated fetal choroid plexus cysts: role of ultrasonography in establishment of the risk of trisomy 18. *Am J Obstet Gynecol*. 2000;812:972–977.
276. Becker S, Niemann G, Schoning M, et al. Clinically significant persistence and enlargement of an antenatally diagnosed isolated choroid plexus cyst. *Ultrasound Obstet Gynecol*. 2002;20:620–622.
277. Norton KI, Rai B, Desai H, et al. Prevalence of choroid plexus cysts in term and near-term infants with congenital heart disease. *AJR Am J Roentgenol*. 2011;196:W326–W329.
278. Bernier FP, Crawford SG, Dewey D. Developmental outcome of children who had choroid plexus cysts detected prenatally. *Prenat Diagn*. 2005;25:322–326.
279. Gupta JK, Cave M, Lilford RJ, et al. Clinical significance of fetal choroid plexus cysts. *Lancet*. 1995;346:724–729.
280. Reinsch RC. Choroid plexus cysts—association with trisomy: prospective review of 16,059 patients. *Am J Obstet Gynecol*. 1997;176:1381–1383.
281. Chen CP. Prenatal diagnosis of arachnoid cysts. *Taiwan J Obstet Gynecol*. 2007;46:187–198.
282. Pradilla G, Jallo G. Arachnoid cysts: case series and review of the literature. *Neurosurg Focus*. 2007;22:1–4.
283. Pierre-Kahn A, Hanlo P, Sonigo P, et al. The contribution of prenatal diagnosis to the understanding of malformative intracranial cysts: state of the art. *Child Nerv Syst*. 2000;16:618–626.
284. Pilu G, Falco P, Perolo A, et al. Differential diagnosis and outcome of fetal intracranial hypoechoic lesions: report of 21 cases. *Ultrasound Obstet Gynecol*. 1997;9:229–236.
285. Gedikbasi A, Palabiyik F, Oztarhan A, et al. Prenatal diagnosis of a suprasellar arachnoid cyst with 2- and 3-dimensional sonography and fetal magnetic resonane imaging: difficulties in management and review of the literature. *J Ultrasound Med*. 2010;29:1487–1493.
286. Blaicher W, Prayer D, Kuhle S, et al. Combined prenatal ultrasound and magnetic resonance imaging in two fetuses with suspected arachnoid cysts. *Ultrasound Obstet Gynecol*. 2001;18:166–168.
287. Booth TN, Timmons C, Shapiro K, et al. Pre- and postnatal MR imaging of hypothalamic hamartomas associated with arachnoid cysts. *AJNR Am J Neuroradiol*. 2004;25:1283–1285.
288. Blasi I, Henrich W, Argento C, et al. Prenatal diagnosis of a cavum veli interpositi. *J Ultrasound Med*. 2009;28:683–687.
289. Barjot P, von Theobald P, Refahi N, et al. Diagnosis of arachnoid cysts on prenatal ultrasound. *Fetal Diagn Ther*. 1999;14:306–309.
290. Hayward R. Postnatal management and outcome for fetal-diagnosed intracerebral cystic masses and tumours. *Prenat Diagn*. 2009;29:396–401.
291. Borha A, Ponte KF, Emery E. Cavum septum pellucidum cyst in children: a case-based update. *Childs Nerv Syst*. 2012;28:813–819.
292. Scoffings DJ, Kurian KM. Congenital and acquired lesions of the septum pellucidum. *Clin Radiol*. 2008;63:210–219.
293. Sarwar M. The septum pellucidum: normal and abnormal. *AJNR Am J Neuroradiol*. 1989;10:989–1005.
294. Mott SH, Bodensteiner JB, Allan WC. The cavum septi pellucidi in term and preterm newborn infants. *J Child Neurol*. 1992;7:35–38.
295. Hicdonmez T, Suslu HT, Butuc R, et al. Treatment of a large and symptomatic septum pellicidum cyst with endoscopic fenestration in a child: case report and review of the literature. *Clin Neurol Neurosurg*. 2012;114:1052–1056.
296. Bronshtein M, Weiner Z. Prenatal diagnosis of dilated cava septi pellucidi et vergae: associated anomalies, differential diagnosis, and pregnancy outome. *Obstet Gynecol*. 1992;80:838–842.
297. Vergani P, Locatelli A, Piccoli MG, et al. Ultrasonographic differential diagnosis of fetal intracranial interhemispheric cysts. *Am J Obstet Gynecol*. 1999;180:423–428.
298. Osborn AG, Preece MT. Intracranial cysts: radiologic-pathologic correlation and imaging approach. *Radiology*. 2006;239:650–664.
299. Tange Y, Aoki A, Mori K, et al. Interhemispheric glioependymal cyst associated with agenesis of the corpus callosum, case report. *Neurol Med Chir (Tokyo)*. 2000;40:536–542.
300. Moriyama E, Nishida A, Sonobe H. Interhemispheric multilocated ependymal cyst with dysgenesis of the corpus callosum: a case in a preterm fetus. *Childs Nerv Syst*. 2007;23:807–813.
301. Muhler MR, Hartmann C, Werner W, et al. Fetal MRI demonstrates glioependymal cyst in a case of sonographic unilateral ventriculomegaly. *Pediatr Radiol*. 2007;37:391–395.
302. Uematsu Y, Kubo K, Nishibayashi T, et al. Interhemispheric neuroepithelial cyst associated with agenesis of the corpus callosum. *Pediatr Neurosurg*. 2000;33:31–36.
303. Pelkey TJ, Ferguson JE, Veille JC, et al. Giant glioependymal cyst resembling holoprosencephaly on prenatal ultrasound: case report and review of the literature. *Ultrasound Obstet Gynecol*. 1997;9:200–203.
304. Deloison B, Chalouhi GE, Sonigo P, et al. Hidden mortality of prenatally diagnosed vein of Galen aneurysmal malformation: retrospective study and review of the literature. *Ultrasound Obstet Gynecol*. 2012;40:652–658.
305. Brunelle F. Arteriovenous malformation of the vein of Galen malformation in children. *Pediatr Radiol*. 1997;27:501–513.
306. Alvarez H, Garcia Monaco R, Rodesch G, et al. Vein of Galen aneurysmal malformation. *Neuroimaging Clin N Am*. 2007;17:189–206.
307. Lasjaunias PL, Chng SM, Sachet M, et al. The management of Vein of Galen aneurysmal malformation. *Neurosurgery*. 2006;59(5)(suppl 3):S184–S194.
308. Barbosa M, Mahadevan J, Weon YC, et al. Dural sinus malformations (DSM) with giant lakes, in neonates and infants, review of 30 consecutive cases. *Interv Neuroradiol*. 2003;9:407–424.
309. Komiyama M, Ishiguro T, Kitano S, et al. Serial antenatal sonographic observation of cerebra dural sinus malformation. *AJNR Am J Neuroradiol*. 2004;25:1446–1448.
310. Garel C, Azarian M, Lasajaunias P, et al. Pial arteriovenous fistulas: dilemmas in prenatal diagnosis, counseling and postnatal treatment. Report of three cases. *Ultrasound Obstet Gynecol*. 2005;26:293–296.
311. Sepulveda W, Platt CC, Fisk NM. Prenatal diagnosis of cerebra arteriovenous malformation using color Doppler ultrasonography: case report and review of the literature. *Ultrasound Obstet Gynecol*. 1995;6:282–286.
312. Heling KS, Chaoui R, Bollmann R. Prenatal diagnosis of an aneurysm of the vein of Galen with three-dimensional color power angiography. *Ultrasound Obstet Gynecol*. 2000;15:333–336.
313. Ruano R, Benachi A, Aubry MC, et al. Perinatal three-dimensional color power Doppler ultrasonography of vein of Galen of aneurysms. *J Ultrasound Med*. 2003;22:1357–1362.
314. Lee TH, Shih JC, Peng SSF, et al. Prenatal depiction of angioarchitecture of an aneurysm of the vein of Galen with three-dimensional color power angiography. *Ultrasound Obstet Gynecol*. 2000;15:337–340.
315. Yuval Y, Lerner A, Lipitz S, et al. Prenatal diagnosis of vein of Galen aneurysmal malformation: report of two cases with proposal for prognostic indices. *Prenat Diagn*. 1997;17:972–977.
316. Patermoster DM, Manganelli F, Moroder W, et al. Prenatal diagnosis of vein of Galen aneurysmal malformations. *Fetal Diagn Ther*. 2003;18:408–411.
317. Kosla K, Majos M, Polguj M, et al. Prenatal diagnosis of a vein of Galen aneurysmal malformation with MR imaging, report of two cases. *Pol J Radiol*. 2013;78:88–92.
318. Heuer GG, Gabel B, Beslow LA, et al. Diagnosis and treatment of vein of Galen aneurysmal malformations. *Childs Nerv Syst*. 2010;26:879–887.
319. Kurihara N, Tokieda K, Ikeda K, et al. Prenatal MR findings in a case of aneurysm of the vein of Galen. *Pediatr Radiol*. 2001;31:160–162.

320. Rodesch G, Hui F, Alvarez H, et al. Prognosis of antenatally diagnosed vein of Galen aneurysmal malformations. *Childs Nerv Syst*. 1994;10:79–83.
321. Kush ML, Weiner CP, Harman CR, et al. Lethal progression of a fetal intracranial arteriovenous malformation. *J Ultrasound Med*. 2003;22:645–648.
322. Mitchell PJ, Rosenfeld JV, Dargaville P, et al. Endovascular management of vein of Galen aneurysmal malformations presenting in the neonatal period. *AJNR Am J Neuroradiol*. 2001;22:1403–1409.
323. Huang J, Wah IYM, Pooh RK, et al. Molecular genetics in fetal neurology. *Semin Fetal Neonatal Med*. 2012;17:341–346.
324. Ghai S, Fong KW, Toi A, et al. Prenatal US and MR imaging findings of lissencephaly: review of fetal cerebral sulcal development. *Radiographics*. 2006;26:389–405.
325. Barkovich AJ, Chuang SH, Norman D. MR of neuronal migration anomalies. *AJR Am J Roentgenol*. 1988;150:179–187.
326. Dobyns WB, Das S. LIS1-associated lissencephaly/subcortical band heterotopia. In: Pagon RA, Adam MP, Bird TD, et al, eds. *GeneReviews®* [Internet]. Seattle, WA: University of Washington; 1993–2014.
327. Haverfield EV, Whited AJ, Petras KS, et al. Intragenic deletions and duplications of the LIS1 and DCX genes: a major disease-causing mechanism in lissencephaly and subcortical band heterotopia. *Eur J Hum Genet*. 2009;17:911–918.
328. Abdel Razek AAK, Kandell AY, et al. Disorders of cortical formation: MR imaging features. *AJNR Am J Neuroradiol*. 2009;30:4–11.
329. Chen C-P, Chang T-Y, Guo W-Y, et al. Chromosome 17p13.3 deletion syndrome: aCGH characterization, prenatal findings and diagnosis, and literature review. *Gene*. 2013;532:152–159.
330. Fong KW, Ghai S, Toi A, et al. Prenatal ultrasound findings of lissencephaly associated with Miller-Dieker syndrome and comparison with pre- and postnatal magnetic resonance imaging. *Ultrasound Obstet Gynecol*. 2004;24:716–723.
331. Rolo LC, Araujo E Jr, Nardozza LMM, et al. Development of fetal brain sulci and gyri: assessment through two and three-dimensional ultrasound and magnetic resonance imaging. *Arch Gynecol Obstet*. 2011;283:149–158.
332. Pugash D, Hendson G, Dunham CP, et al. Sonographic assessment of normal and abnormal patterns of fetal cerebral lamination. *Ultrasound Obstet Gynecol*. 2012;40:642–651.
333. Malinger G, Kidron D, Schreiber L, et al. Prenatal diagnosis of malformations of cortical development by dedicated neurosonography. *Ultrasound Obstet Gynecol*. 2007;29:178–191.
334. Righini A, Frassoni C, Inverardi F, et al. Bilateral cavitations of ganglionic eminence: a fetal MR imaging sign of halted brain development. *AJNR Am J Neuroradiol*. 2013;34:1841–1845.
335. Barkovich AJ, Koch TK, Carrol CL. The spectrum of lissencephaly: report of ten patients analyzed by magnetic resonance imaging. *Ann Neurol*. 1991;30:139–146.
336. Guibaud L, Selleret L, Larroche JC, et al. Abnormal Sylvian fissure on prenatal cerebral imaging: significance and correlation with neuropathological and postnatal data. *Ultrasound Obstet Gynecol*. 2008;32:50–60.
337. Bloundiaux E, Sileo C, Nahama-Allouche C, et al. Periventricular nodular heterotopia on prenatal ultrasound and magnetic resonance imaging. *Ultrasound Obstet Gynecol*. 2013;42:149–155.
338. Gonzalez G, Vedolin L, Barry B, et al. Location of periventricular nodular heterotopia is related to the malformation phenotype on MRI. *AJNR Am J Neuroradiol*. 2013;34:877–889.
339. Manganaro L, Saldari M, Bernardo S, et al. Bilateral subependymal heterotopia, ventriculomegaly and cerebellar asymmetry: fetal MRI findings of a rare association of brain anomalieis. *J Radiol Case Rep*. 2013;7:38–45.
340. Barkovich AJ, Kuzniecky RI. Gray matter heterotopia. *Neurology*. 2000;55:1603–1608.
341. Barkovich AJ. Morphologic characteristics of subcortical heterotopia: MR imaging study. *AJNR Am J Neuroradiol*. 2000;21:290–295.
342. Parrini E, Ramazzotti A, Dobyns WB, et al. Periventricular heterotopia: phenotypic heterogeneity and correlation with Filamin A mutations. *Brain*. 2006;129:1892–1906.
343. Poussaint TY, Fox JW, Dobyns WB, et al. Periventricular nodular heterotopia in patients with filamin-1 gene mutations: neuroimaging findings. *Pediatr Radiol*. 2000;30:748–755.
344. Mitchell LA, Simon EM, Filly RA, et al. Antenatal diagnosis of subependymal heterotopia. *AJNR Am J Neuroradiol*. 2000;21:296–300.
345. Glenn OA, Cuneo AA, Barkovich AJ, et al. Malformations of cortical development: diagnostic accuracy of fetal MR imaging. *Radiology*. 2012;263:843–855.
346. Vajsar J, Schacter H. Walker-Warburg syndrome. *Orphanet J Rare Dis*. 2006;1:29–33.
347. Devisme L, Bouchet C, Gonzales M, et al. Cobblestone lissencephaly: neuropathological subtypes and correlations with genes of dystroglycanopathies. *Brain*. 2012;135:469–482.
348. Barkovich AJ. Neuroimaging manifestations and classification of congenital muscular dystrophies. *AJNR Am J Neuroradiol*. 1998;19:1389–1396.
349. Brasseur-Daudruy M, Vivier PH, Ickowicz V, et al. Walker-Warburg syndrome diagnosed by findings of typical ocular abnormalities on prenatal ultrasound. *Pediatr Radiol*. 2012;42:488–490.
350. Dobyns WB, Pagon RA, Armstrong D, et al. Diagnostic criteria for Walker-Warburg syndrome. *Am J Med Genet*. 1989;32:195–210.
351. Stroustrup Smith A, Levine D, Barnes PD, et al. Magnetic resonance imaging of the kinked fetal brain stem, a sign of severe dysgenesis. *J Ultrasound Med*. 2005;24:1697–1709.
352. Pabuscu Y, Baulakbasy N, Kocaoglu M, et al. Walker-Warburg syndrome variant. *Comput Med Imaging Graph*. 2002;26:453–458.
353. Low ASC, Lee SL, Tan ASA, et al. Difficulties with prenatal diagnosis of the Walker-Warburg syndrome. *Acta Radiol*. 2005;46:645–651.
354. Widjaja E, Geibprasert S, Blaser S, et al. Abnormal fetal cerebral laminar organization in cobblestone complex as seen on post-mortem MRI and DTI. *Pediatr Radiol*. 2009;39:860–864.
355. Strigini F, Valleriani A, Cecchi M, et al. Prenatal ultrasound and magnetic resonance imaging features in a fetus with Walker-Warburg syndrome [letter]. *Ultrasound Obstet Gynecol*. 2009;33:363–368.
356. Monteagudo A, Alayon A, Mayberry P. Walker-Warburg syndrome: case report and review of the literature. *J Ultrasound Med*. 2001;20:419–426.
357. Jansen A, Andermann E. Genetics of the polymicrogyria syndromes. *J Med Genet*. 2005;42:369–378.
358. Hayashi N, Tsutsumi Y, Barkovich AJ. Polymicrogyria without porencephaly/schizencephaly: MRI analysis of the spectrum and the prevalence of macroscopic findings in the clinical population. *Neuroradiology*. 2002;44:647–655.
359. Barkovich AJ. Current concepts of polymicrogyria. *Neuroradiology*. 2010;52:479–487.
360. Glenn OA, Norton ME, Goldstein RB, et al. Prenatal diagnosis of polymicrogyria by fetal magnetic resonance imaging in monochorionic co-twin death. *J Ultrasound Med*. 2005;24:711–716.
361. Simonazzi G, Segata M, Ghi T, et al. Accurate neurosonographic prediction of a brain injury in the surviving fetus after the death of a monochorionic co-twin. *Ultrasound Obstet Gynecol*. 2006;27:517–521.
362. Barkovich AJ. Magnetic resonance imaging: role in the understanding of cerebral malformations. *Brain Dev*. 2002;24:2–12.
363. Wieck G, Leventer RJ, Squier WM, et al. Periventricular nodular heterotopia with overlying polymicrogyria. *Brain*. 2005;128:2811–2821.
364. Cagneaux M, Paoli V, Blanchard G, et al. Pre- and postnatal imaging of early cerebral damage in Sturge-Weber syndrome. *Pediatr Radiol*. 2013;43:1536–1539.
365. Fink AM, Hingston T, Sampson A, et al. Malformation of the fetal brain in thanatophoric dysplasia: US and MRI findings. *Pediatr Radiol*. 2010;40(suppl 1):S134–S137.
366. Barkovich AJ, Peck WW. MR of Zellweger syndrome. *AJNR Am J Neuroradiol*. 1997;18:1163–1170.
367. Mochel F, Grebille AG, Benachi A, et al. Contribution of fetal MR imaging in the prenatal diagnosis of Zellweger syndrome. *AJNR Am J Neuroradiol*. 2006;27:333–336.
368. Dhombres F, Nahama-Allouche C, Gelot A, et al. Prenatal ultrasonographic diagnosis of polymicrogyria. *Ultrasound Obstet Gynecol*. 2008;32:951–954.
369. Urban LABD, Righini A, Rustico M, et al. Prenatal ultrasound detection of bilateral focal polymicrogyria. *Prenat Diagn*. 2004;24:808–811.
370. Righini A, Parazzini C, Doneda C, et al. Early formative stage of human focal cortical gyration anomalies: fetal MRI. *AJR Am J Roentgenol*. 2012;198:439–447.
371. Righini A, Zirpoli S, Mrakic F, et al. Early prenatal MR imaging diagnosis of polymicrogyria. *AJNR Am J Neuroradiol*. 2004;25:343–346.
372. Barkovich AJ, Hevner R, Guerrini R. Syndromes of bilateral symmetrical polymicrogyria. *AJNR Am J Neuroradiol*. 1999;20:1814–1821.
373. Yakovlev PI, Wadsworth RC. Schizencephalies: a study of the congenital clefts in the cerebral mantle, II: clefts with hydrocephalus and lips separated. *J Neuropathol Exp Neurol*. 1946;5(3):169–206.
374. Curry CJ, Lammer EJ, Nelson V, et al. Schizencephaly: heterogeneous etiologies in a population of 4 million California births. *Am J Med Genet*. 2005;137A:181–189.
375. Howe DT, Rankin J, Draper ES. Schizencephaly prevalence, prenatal diagnosis and clues to etiology: a register-based study. *Ultrasound Obstet Gynecol*. 2012;39:75–82.
376. Barkovich AJ, Kjos BO. Schizencephaly: correlation of clinical findings with MR characteristics. *AJNR Am J Neuroradiol*. 1992;13:85–94.
377. Hayashi N, Tsutsumi Y, Barkovich AJ. Morphological features and associated anomalies of schizencephaly in the clinical population: detailed analysis of MR images. *Neuroradiology*. 2002;44:418–427.
378. Oh KY, Kennedy AM, Frias AE Jr, et al. Fetal schizencephaly: pre- and postnatal imaging with a review of the clinical manifestations. *Radiographics*. 2005;25:647–657.
379. Nabavizadeh SA, Zarnow D, Bilaniuk LT, et al. Correlation of prenatal and postnatal MRI findings in schizencephaly. *AJNR Am J Neuroradiol*. 2014. doi:10.3174/ajnr.A3872.
380. Lee W, Comstock CH, Kazmierczak C, et al. Prenatal diagnostic challenges and pitfalls for schizencephaly. *J Ultrasound Med*. 2009;28:1379–1384.
381. Denis D, Maugey-Laulom B, Carles D, et al. Prenatal diagnosis of schizencephaly by fetal magnetic resonance imaging. *Fetal Diagn Ther*. 2001;16:354–359.
382. Edris F, Kielar A, Fung KFK, et al. Ultrasound and MRI in the antenatal diagnosis of schizencephaly. *J Obstet Gynaecol Can*. 2005;27:864–868.
383. Rios LTM Jr, Araujo E, Nardozza LMM, et al. Prenatal and postnatal schizencephaly findings by 2D and 3D ultrasound: pictorial essay. *J Clin Imaging Sci*. 2012;2:30.

Kline9781451175837-ch012.1.indd 421 08/08/14 9:59 AM

384. Poretti A, Leventer RJ, Cowan FM, et al. Cerebellar cleft: a form of prenatal cerebellar disruption. *Neuropediatrics*. 2008;39:106–112.
385. Raybaud C, Girard N, Levrier O, et al. Schizencephaly: correlation between the lobar topography of the cleft(s) and absence of the septum pellucidum. *Childs Nerv Syst*. 2001;17:217–222.
386. Hung J-H, Shen S-H, Guo W-Y, et al. Prenatal diagnosis of schizencephaly with septo-optic dysplasia by ultrasound and magnetic resonance imaging. *J Obstet Gynaecol Res*. 2008;34:674–679.
387. Bats AS, Molho M, Senat MV, et al. Subependymal pseudocysts in the fetal brain: prenatal diagnosis of two cases and review of the literature. *Ultrasound Obstet Gynecol*. 2002;20:502–505.
388. Malinger G, Lev D, Sira LB, et al. Congenital periventricular pseudocysts: prenatal sonographic appearance and clinical implications. *Ultrasound Obstet Gynecol*. 2002;20:447–451.
389. Cevey-Macherel M, Forcada M, Bickle Graz M, et al. Neurodevelopment outcome of newborns with cerebral subependymal pseudocysts at 18 and 46 months: a prospective study. *Arch Dis Child*. 2013;98:497–502.
390. Correa F, Lara C, Carreras E, et al. Evolution of fetal subependymal cysts throughout gestation. *Fetal Diagn Ther*. 2013;34:127–130.
391. Shackelford GD, Fulling KH, Glasier CM. Cysts of the subependymal germinal matrix: sonographic demonstration with pathologic correlation. *Radiology*. 1983;149:117–121.
392. Epelman M, Daneman A, Blaser SI, et al. Differential diagnosis of intracranial cystic lesions at head US: correlation with CT and MR imaging. *Radiographics*. 2006;26:173–196.
393. Makhoul IR, Zmora O, Tamir A, et al. Congenital subependymal pseudocysts: own data and meta-analysis of the literature. *Isr Med Assoc J*. 2001;3:178–183.
394. Fernandez Alvarez JR, Arness PN, et al. Diagnostic value of subependymal pseudocysts and choroid plexus cysts on neonatal cerebral ultrasound: a meta-analysis. *Arch Dis Child Fetal Neonatal Ed*. 2009;94:F443–F446.
395. Larcos G, Gruenewald SM, Lui K. Neonatal subependymal cysts detected by sonography: prevalence, sonographic findings, and clinical significance. *AJR Am J Roentgenol*. 1994;162:953–956.
396. Rossler L, Ludwig-Seibold C, Thiels CH, et al. Aicardi-Goutieres syndrome with emphasis on sonographic features of infancy. *Pediatr Radiol*. 2012;42:932–940.
397. Ramenghi LA, Domizio S, Quartulli L, et al. Prenatal pseudocysts of the germinal matrix in preterm infants. *J Clin Ultrasound*. 1997;25:169–173.
398. Elchalal U, Yagel S, Gomori JM, et al. Fetal intracranial hemorrhage (fetal stroke): does grade matter. *Ultrasound Obstet Gynecol*. 2005;26:233–243.
399. Vergani P, Strobelt N, Locatelli A, et al. Clinical significance of fetal intracranial hemorrhage. *Am J Obstet Gynecol*. 1996;175:536–543.
400. Brunel H, Girard N, Confort-Gouny S, et al. Fetal brain injury. *J Neuroradiol*. 2004;31:123–137.
401. Girard N, Gire C, Sigaudy S, et al. MR imaging of acquired fetal brain disorders. *Childs Nerv Syst*. 2003;19:490–500.
402. Ghi T, Simonazzi G, Perolo A, et al. Outcome of antenatally diagnosed intracranial hemorrhage: case series and review of the literature. *Ultrasound Obstet Gynecol*. 2003;22:121–130.
403. Ozduman K, Pober BR, Barnes P, et al. Fetal stroke. *Pediatr Neurol*. 2004;30:151–162.
404. Sherer DM, Anyaebunam A, Onyeije C. Antepartum fetal intracranial hemorrhage, predisposing factors and prenatal sonography: a review. *Am J Perinatol*. 1998;15:431–441.
405. Sharif I, Kuban K. Prenatal intracranial hemorrhage and neurologic complications in alloimmune thrombocytopenia. *J Child Neurol*. 2001;16:838–842.
406. Dubinsky T, Lau M, Powell F, et al. Predicting poor neonatal outcome: a comparative study of noninvasive antenatal testing methods. *AJR Am J Roentgenol*. 1997;168:827–831.
407. de Laveaucoupet J, Audibert F, Guis F, et al. Fetal magnetic resonance imaging (MRI) of ischemic brain injury. *Prenat Diagn*. 2001;21:729–736.
408. Huang Y-F, Chen W-C, Tseng J-J, et al. Fetal intracranial hemorrhage (fetal stroke): report of four antenatally diagnosed cases and review of the literature. *Taiwan J Obstet Gynecol*. 2006;45:135–141.
409. Muench MV, Zheng M, Bilica PM, et al. Prenatal diagnosis of a fetal epidural hematoma using 2- and 3-dimensional sonography and magnetic resonance imaging. *J Ultrasound Med*. 2008;27:1369–1373.
410. De Spirlet M, Goffinet F, Philippe HJ, et al. Prenatal diagnosis of a subdual hematoma associated with reverse flow in the middle cerebral artery: case report and literature review. *Ultrasound Obstet Gynecol*. 2000;16:72–76.
411. Hines N, Mehta T, Romero J, et al. What is the clinical importance of echogenic material in the fetal frontal horns? *J Ultrasound Med*. 2009;28:1629–1637.
412. Burstein J, Papile L-A, Burstein R. Intraventricular hemorrhage and hydrocephalus in premature newborns: a prospective study with CT. *AJR Am J Roentgenol*. 1979;132:621–635.
413. Groothuis AMC, de Kleine MJK, Guid Oei S. Intraventricular haemorrhage in utero: a case report and review of the literature. *Eur J Obstet Gynecol Reprod Biol*. 2000;89:207–211.
414. Garel C, Delezoide A-L, Elmaleh-Berges M, et al. Contribution of fetal MR imaging in the evaluation of cerebral ischemic lesions. *AJNR Am J Neuroradiol*. 2004;25:1563–1568.
415. Fleischer AC, Hutchison AA, Bundy AL, et al. Serial sonography of posthemorrhagic ventricular dilatation and porencephaly after intracranial hemorrhage in the preterm neonate. *AJNR Am J Neuroradiol*. 1983;4:971–975.
416. Lituania M, Passamonti U. Prenatal ultrasound: brain. In: Raybaud C, Paolo T-D, Rossi A, eds. *Pediatric Neuroradiology*. Heidelberg, Germany: Springer Berlin; 2005:1157–1218.
417. Prayer D, Brugger PC, Kasprian G, et al. MRI of fetal acquired brain lesions. *Eur J Radiol*. 2006;57:233–249.
418. Folkerth RD, McLaughlin ME, Levine D. Organizing posterior fossa hematomas simulating developmental cysts on prenatal imaging, report of three cases. *J Ultrasound Med*. 2001;20:1233–1240.
419. Rios LTM, Araujo E Jr, Nardozza LMM, et al. Hidden maternal autoimmune thrombocytopenia complicated by fetal subdural hematoma, case report and review of the literature. *Childs Nerv Syst*. 2012;28:1113–1116.
420. Guimiot F, Garel C, Fallet-Bianco C, et al. Contribution of diffusion-weighted imaging in the evaluation of diffuse white matter ischemic lesions in fetuses: correlation with fetopathologic findings. *AJNR Am J Neuroradiol*. 2008;29:110–115.
421. Strigini FAL, Cioni G, Canapicchi R, et al. Fetal intracranial hemorrhage: is minor maternal trauma a possible pathogenetic factor? *Ultrasound Obstet Gynecol*. 2001;18:335–342.
422. Bussel JB, Berkowitz RL, McFarland JG, et al. Antenatal treatment of neonatal alloimmune thrombocytopenia. *N Engl J Med*. 1988;319:1374–1378.
423. Govaert P. Prenatal stroke. *Semin Fetal Neonatal Med*. 2009;14:250–266.
424. Grant EG, Kerner M, Schellinger D, et al. Evolution of porencephalic cysts from intraparenchymal hemorrhage in neonates: sonographic evidence. *AJR Am J Roentgenol*. 1982;138:467–470.
425. Gul A, Gungorduk K, Yildirm G, et al. Prenatal diagnosis of porencephaly secondary to maternal carbon monoxide poisoning. *Arch Gynecol Obstet*. 2009;279:697–700.
426. Eiler KM, Kuller JA. Fetal porencephaly: a review of the etiology, diagnosis and prognosis. *Obstet Gynecol Surv*. 1995;50:684–687.
427. Berg RA, Aleck KA, Kaplan AM. Familial porencephaly. *Arch Neurol*. 1983;40:567–569.
428. Ho SS, Kuzniecky RI, Gilliam F, et al. Congenital porencephaly: MR features and relationship to hippocampal sclerosis. *AJNR Am J Neuroradiol*. 1998;19:135–141.
429. Quek Y-W, Su P-H, Tsao T-F, et al. Hydranencephaly associated with interruption of bilateral internal carotid arteries. *Pediatr Neonatol*. 2008;49:43–47.
430. Taori KB, Sargar KM, Disawal A, et al. Hydranencephaly associated with cerebellar involvement and bilateral microphthalmia and colobomas. *Pediatr Radiol*. 2011;41:270–273.
431. Byers BD, Barth WH, Stewart TL, et al. Ultrasound and MRI appearance and evolution of hydranencephaly in utero. *J Reprod Med*. 2005;50:53–56.
432. Myers RE. Brain pathology following fetal vascular occlusion: an experimental study. *Invest Ophthalmol*. 1969;8:41–50.
433. Cecchetto G, Milanese L, Giordano R, et al. Looking at the missing brain: hydranencephaly case series and literature review. *Pediatr Neurol*. 2013;48:152–158.
434. Greene MF, Benacerraf B, Crawford JM. Hydranencephaly: US appearance during in utero evolution. *Radiology*. 1985;156:779–780.
435. Edmondson SR, Hallak M, Carpenter RJ Jr, et al. Evolution of hydranencephaly following intracerebral hemorrhage. *Obstet Gynecol*. 1992;79:870–871.
436. Dixon A. Hydranencephaly. *Radiography*. 1998;54:12–13.
437. Williams D, Patel C, Fallet-Bianco C, et al. Fowler syndrome: a clinical, radiological, and pathological study of 14 cases. *Am J Med Genet Am*. 2009;152A:153–160.
438. Laurichesse-Delmas H, Beaufrere AM, Martin A, et al. First-trimester features of Fowler syndrome (hydrocephaly-hydranencephaly proliferative vasculopathy). *Ultrasound Obstet Gynecol*. 2002;20:612–615.
439. Lam YH, Tang HY. Serial sonographic features of a fetus with hydranencephaly from 11 weeks to term. *Ultrasound Obstet Gynecol*. 2000;16:77–79.
440. Sepulveda W, Cortes-Yepes H, Wong AE, et al. Prenatal sonography in hydranencephaly, findings during the early stages of disease. *J Ultrasound Med*. 2012;31:799–804.
441. Usta IM, AbuMusa AA, Khoury NG, et al. Early ultrasonographic changes in Fowler syndrome features and review of the literature. *Prenat Diagn*. 2005;25:1019–1023.
442. Aguirre Vila-Coro A, Dominguez R. Intrauterine diagnosis of hydranencephaly by magnetic resonance. *Magn Reson Imaging*. 1989;7:105–107.
443. Merker B. Editorial: life expectancy in hydranencephaly. *Clin Neurol Neurosurg*. 2008;110:213–214.
444. Laurichesse Delmas H, Winer N, Gallot D, et al. Prenatal diagnosis of thrombosis of the dural sinuses: report of six cases, review of the literature and suggested management. *Ultrasound Obstet Gynecol*. 2008;32:188–198.
445. Okudera T, Peng Huang Y, Ohta T, et al. Development of posterior fossa dural sinuses, emissary veins, and jugular bulb: morphological and radiologic study. *AJNR Am J Neuroradiol*. 1994;15:1871–1883.
446. Merzoug V, Flunder S, Drissi C, et al. Dural sinus malformation (DSM) in fetuses: diagnostic value of prenatal MRI and followup. *Eur Radiol*. 2008;18:692–699.
447. Pandey V, Dummula K, Parimi P. Antenatal thrombosis of torcular herophili presenting with anemia, consumption coagulopathy and high-output cardiac failure in a preterm infant. *J Perinatol*. 2013;32:728–730.

448. Fanou EM, Reeves MJ, Howe DT, et al. In utero magnetic resonance imaging for diagnosis of dural venous sinus ectasia with thrombosis in the fetus. *Pediatr Radiol*. 2013;43:1591–1598.
449. Byrd S, Abramowicz J, Kent P, et al. Fetal MR imaging of posterior intracranial dural sinus thrombosis: a report of three cases with variable outcomes. *Pediatr Radiol*. 2012;42:536–543.
450. Has R, Esmer AC, Kalelioglu I, et al. Prenatal diagnosis of torcular herophili thrombosis, report of two cases and review of the literature. *J Ultrasound Med*. 2013;32:2205–2211.
451. Barbosa M, Mahadevan J, Weon YC, et al. Dural sinus malformations (DSM) with giant lakes, in neonates and infants, review of 30 consecutive cases. *Interv Neuroradiol*. 2003;9:407–424.
452. McInnes M, Fong K, Grin A, et al. Malformations of the fetal dural sinuses. *Can J Neurol Sci*. 2009;36:72–77.
453. Legendre G, Picone O, Levaillant JM, et al. Prenatal diagnosis of a spontaneous dural sinus thrombosis. *Prenat Diagn*. 2009;29:808–813.
454. Grange G, LeTohic A, Merzoug V, et al. Prenatal demonstration of afferent vessels and progressive thrombosis in a torcular malformation. *Prenat Diagn*. 2007;27:670–673.
455. Schwartz N, Monteagudo A, Bornstein E, et al. Thrombosis of an ectatic torcular herophili: anatomic localization using fetal neurosonography [letter]. *J Ultrasound Med*. 2008;27:989–992.
456. Laurichesse-Delmas Grimaud O, Moscoso G, Ville Y. Color Doppler study of the venous circulation in the fetal brain and hemodynamic study of the cerebral transverse sinus. *Ultrasound Obstet Gynecol*. 1999;13:34–42.
457. Visentin A, Falco P, Pilu G, et al. Prenatal diagnosis of thrombosis of the dural sinuses with real-time and color Doppler ultrasound. *Ultrasound Obstet Gynecol*. 2001;17:322–325.
458. Rossi A, De Biasio P, Scarso E, et al. Prenatal MR imaging of dural sinus malformation: a case report. *Prenat Diagn*. 2006;26:11–16.
459. Ebert M, Esenkaya A, Huisman T, et al. Multimodality, anatomical and diffusion weighted fetal imaging of a spontaneously thrombosing congenital dural sinus malformation. *Neuropediatrics*. 2012;43:279–282.
460. Spampinato MV, Hardin V, Davis M, et al. Thrombosed fetal dural sinus malformation diagnosed with magnetic resonance imaging. *Obstet Gynecol*. 2008;111:569–572.
461. Jenny B, Zerah M, Swift D, et al. Giant dural venous sinus ectasia in neonates, report of four cases. *J Neurosurg Pediatr*. 2010;5:523–528.